NOVEL METHODS FOR THE MODULATION OF WOUND HEALING AFTER GLAUCOMA FILTRATION SURGERY

STYLIANOS D. GEORGOULAS

Department of Pharmaceutics
School of Pharmacy
University of London

and

Ocular Repair and Regeneration Biology Research Unit
UCL Institute of Ophthalmology and Moorfields Eye Hospital

University of London
February 2010

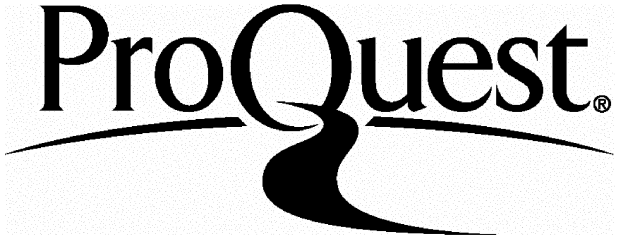

Για την επιστροφή των Μαρμάρων του Παρθενώνα στο χώρο καταγωγής τους, την Αθήνα.

ΚΙΚΗ ΔΗΜΟΥΛΑ 'ΕΡΕΒΟΣ'

Στην ψυχρή του Μουσείου αίθουσα
την κλεμμένη, ωραία, κοιτώ
μοναχή Καρυάτιδα.
Το σκοτεινό γλυκύ της βλέμμα επίμονα εστραμμένο έχει
στο σφριγηλό του Διονύσου σώμα
(σε στάση ηδυπαθείας σμιλευμένο)
που δυό βήματα μόνον απέχει.
Το βλέμμα το δικό του έχει πέσει
στη δυνατή της κόρης μέση.
Πολυετές ειδύλλιον υποπτεύομαι
τους δυό αυτούς να 'χει ενώσει.
Κι έτσι, όταν το βράδυ η αίθουσα αδειάζει
απ' τους πολλούς, τους θορυβώδεις επισκέπτες,
τον Διόνυσο φαντάζομαι
προσεκτικά απ' τη θέση του να εγείρεται
των διπλανών γλυπτών και αγαλμάτων
την υποψία μην κινήσει
κι όλος παλμό να σύρεται
τη συστολή της Καρυάτιδας
με οίνον και με χάδια να λυγίσει.
Δεν αποκλείεται όμως έξω να 'χω πέσει.
Μιάν άλλη σχέση ίσως να τους δένει,
πιο δυνατή, πιο πονεμένη
Τις χειμωνιάτικες βραδιές
και τις εξαίσιες του Αυγούστου νύχτες
τους βλέπω,
απ' τα ψηλά να κατεβαίνουν βάθρα τους,
της μέρας αποβάλλοντας το τυπικό τους ύφος,
με νοσταλγίας στεναγμούς και δάκρυα
τους Παρθενώνες και τα Ερεχθεία που στερήθηκαν
στη μνήμη τους με πάθος ν' ανεγείρουν.

To my parents, Malamatenia and Dimitris

To my grandparents, Dimitra and Stelios

ACKNOWLEDGEMENTS

It is a pleasure to thank all those who made this thesis possible.

It is very difficult to overstate my gratitude to my Ph.D. supervisors, Professors Steve Brocchini and Peng Tee Khaw, whose encouragement, guidance and support from the initial to the final step enabled me to develop an understanding of wound healing and ocular pharmaceutics. With their enthusiasm, inspiration, great ideas, teaching, amazing company, and by making themselves available whenever I needed help, they made my PhD studies fun for me and they taught me important life lessons. I feel very lucky that I had the opportunity to work with them, and without their help, some of my dreams would not have come true.

Words will never be enough to thank Peggy Khaw, who treated me during all these years as a member of her family and has made available her support to me in every possible way. Peggy taught me how to write protocols, corrected my English in all the documents I produced during this PhD, helped me deal with the bureaucracy of finding accommodation when I moved to London from the US and overcome every obstacle that I faced during my life in London. Peggy constantly fed me and tried to convince me to sleep, helped me to clean the BRU after long and demanding experiments, cheered me up when I was very stressed out, and supported me significantly during my London School of Economics studies. And these are only few of the things that Peggy did for me. In every way, Peggy made me feel all these years that I have a second mother in the UK and that whatever happens I can count on her. Without her, my life in London and at the Institute of Ophthalmology would have been much harder. Peggy, it is a complete privilege to know you. Thank you for everything.

I recognise that this research would not have been possible without the financial assistance of the School of Pharmacy and the A.G. Leventis Foundation, which awarded to me Ph.D. scholarships, and of Professor Khaw and Brocchini, who paid the laboratory expenses for my work.

I wish to thank Dr Dimitri Monos for his contribution to enabling me to undertake this PhD post at the University of London School of Pharmacy and at the UCL Institute of

Ophthalmology UCL and at the School of Pharmacy, University of London; To Dr Santa Ono for introducing me to Professor Khaw and for his very important support and friendship until today. To my New York Eye and Ear Infirmary Research supervisors before commencing this PhD, Dr Thomas Muldoon and Dr Richard Rosen, who showed me how exciting a career in Ophthalmology can be.

I wish to thank Rosalind Hart for teaching me all the histological methods that I used in this thesis and for being such a unique human being, Professor Phil Luthert and Dr Caroline Thaung, who helped me with the analysis of my histological samples, and Heidi Barnes and Christine Gaughan for the good company that kept me during the endless hours of cutting sections in the histology lab.

I am grateful to the BRU staff of the UCL Institute of Ophthalmology for their invaluable help and their unique professionalism during the many *in vivo* experiments that this PhD involved.

I would like to thank Sudershana Dave, Jenny Murray, Rachel Joseph and Rebecca Fenby for their courtesy and help.

I am grateful to Debbie Heattlie and Desta Bokre for being good company during my endless hours in the library of the UCL Institute of Ophthalmology, my second home during this PhD, and for their invaluable help with the bibliography that I needed from the British Library.

I would like to thank Karen Bonstein and Liz Hurst for helping me deal with the Home Office obligations, and Karen Mason, for making me understand the importance of the strict regulations in research.

I am very grateful to Debbie Bryant for her vital contribution on several fronts during the course of this PhD and to Louise Halfhide for her very important help during my ST application process.

Special thanks to Jonathan Clarke for being such a good teacher in clinical Ophthalmology; To Rania Fragkouli, for teaching me direct Ophthalmoscopy and helping me succeed

during the Ophthalmology ST interviews process; To Maria Papadopoulos, for all her encouragement during the Ophthalmology ST application process.

To Qian Ru, for being such a good colleague and helping me survive at the School of Pharmacy; To John Frost for the manufacturing of the rigs, without whose help the tablet experiments would have been much harder; To Hardyal Gill for teaching me High Potency Liquid Chromatography, a very difficult method for a doctor like me with limited knowledge of pharmacoanalysis; To Kostas Kalousis, who 'saved' me many times with his SPSS expertise.

I wish to thank Maria Notara, James Ellis, Bhairavi Bhatia, Ashkan Khalili, Daniel Paul, Shweta Singhal, Ásbjörg Geirsdóttir, Joanne Gilfillan Daniels, Abeer Mohamed-Ahmed, Tan Dinh, Laurence Dufaur, Maria Dawson and Lux Fatihamas for being very good friends and colleagues and for being good company during lunch breaks and outside the Institute and the School of Pharmacy.

I wish to thank Peter Marshall for being such a great friend the last 4 years that I worked at the Institute of Ophthalmology; David Daniel, George Bradley and Merv Davies for the very interesting discussions and their help with practical things during this PhD.

I would like to express my gratitude to my brother Ilias Georgoulas who is the most important person in my life; to my best friend in London, Helen Manolatou, for her constant and unlimited support and for standing always by me; to my great friends during my medical studies, and my amazing friends from Greece, UK, LSE and the rest of the world who, by constantly calling and visiting me, helped me get through the difficult times, and for all the emotional support, entertainment and care they provided. I wish I could mention each individually, but I would need many pages. I feel very lucky to have all of them in my life.

I am indebted to my grandparents, Dimitra and Stelios, who I miss very much. I feel guilty that, because of my focus on my career, I did not spend as much time as I wanted with them. They taught me what a unique thing it is to unconditionally love people and that being a good human being is the most important thing on planet earth. I owe who I am to them and to my parents, and consider them the most important gift God gave me.

Lastly, and most importantly, I wish to thank my parents, Malamatenia and Dimitris Georgoulas. They bore me, raised me, supported me, taught me, and loved me. I dedicate to them and to my grandparents this thesis.

PUBLICATIONS PRODUCED DURING THE COURSE OF THIS PhD

1. Georgoulas S, Dahlmann-Noor A, Brocchini S, Khaw PT. Modulation of wound healing during and after glaucoma surgery. Prog Brain Res. 2008;173:237-54. PMID: 18929113.

2. Khaw PT, Georgoulas S, Dahlmann AH, Mireskandari K, Bailly M, Daniels J, Limb GA and Brocchini S. Chapter 15: Tissue Repair and Regeneration. Book: Ocular Therapeutics Eye on New Discoveries 2008, Pages 333-366 doi:10.1016/B978-012370585-3.50017-0

3. Khaw PT, Georgoulas S, Dahlmann A, Ru Q, Martin Martin B, Brocchinin S. 'Future Strategies in Wound Healing Modification' in Textbook of Glaucoma. Eds Sharaawy T Hitchings RA Sherwood MB Crowston J Elsevier 2009

4. Georgoulas S, Dahlmann-Noor A, Brocchini S, Khaw PT. Chapter 28: Wound healing responses to glaucoma surgery in Ocular Disease: Mechanisms and Management. Eds: Levin and Albert Elsevier 2008

5. Georgoulas S, Limb GA, Bailly M, Brocchini S, Khaw PT. Wound Healing Modification during and after glaucoma surgery - the state of the art. Chapter 9. p 65-81 in Glaucoma: State of the Art Therapy Eds: Grieshaber Orgul Flammer Elsevier 2008 ISBN 97B 3 9523474 0 9

6. Georgoulas S, Paull D, Ru Q, Dhingra S, Khalili A, Ellis J, Brocchini S, Khaw PT. The use of a pentraxin protein after trabeculectomy to increase bleb survival in a fibrotic model. In preparation

7. Georgoulas S, Ru Q, Paull D, Murray L, Brocchini S, and Khaw PT. The Effects of Serum Amyloid P on Experimental Glaucoma Filtration Surgery. Presentation at the ARVO World Ophthalmology Research Meeting 2009. E-3908.

8. Georgoulas SD, Ru Q, Brocchini S, and Khaw PT. A novel slow release MMP inhibitor tablet against scarring after glaucoma filtration surgery. In preparation.

9. Georgoulas SD, Limb A, Brocchini S, and Khaw PT. MMPs in the eye. Manuscript in preparation.

10. Georgoulas SD, Ru Q, Brocchini S, and Khaw PT. A Novel Single Application Prolonged Release MMP Inhibitor Is Superior to Mitomycin in Preventing Scarring After Experimental Glaucoma Surgery. Presentation at the ARVO World Ophthalmology Research Meeting 2009. E-3178.

11. Ru Q, Georgoulas S, Li CT, Brocchini S, and Khaw PT. Modelling Prolonged *in vitro* Release of 5-Fluorouracil From Tablets Using a Flow Chamber. Presentation at the ARVO World Ophthalmology Research Meeting 2009. E-4538.

NON-PLAGIARISM STATEMENT

By this statement I declare that I have written this thesis completely by myself, and that I have used no other sources or resources than the ones mentioned.

The sources used have been stated in accordance with the rules and regulations that are applied by the University of London. I have indicated all quotes and citations that were literally taken from publications, or that were in close accordance with the meaning of those publications, as such.

Moreover I have not handed in a thesis with similar contents elsewhere. All sources and other resources used are stated in the bibliography.

Name: Stylianos Georgoulas

Place: University of London

Date: 29/07/2010

Signature: 

ABSTRACT

Scarring is known to be the leading cause of trabeculectomy failure. Anti-metabolic drugs (5-FU and MMC) are currently used in an attempt to inhibit scarring after glaucoma filtration surgery (GFS), but they are only effective in a limited number of patients in the long term and can cause severe side effects. There is a clinical need for better therapies to ensure that the healing process can be better mediated after GFS.

Serum Amyloid P (SAP) was examined to determine if it has potential to inhibit scarring after GFS. It has been shown that non-activated, bone-marrow derived peripheral monocyte precursor CD14+ fibrocytes circulating in the blood participate in scarring and that myofibroblasts may not originate from tissue fibroblasts, but from this bone-marrow-derived precursor. SAP is a protein that belongs in the pentraxin family of proteins and is a potent modulator of monocyte differentiation *in vitro* and *in vivo.* It has been suggested that SAP may also have broad anti-fibrotic activity in many tissues, organs and species. It was found that administration of SAP by injection to the bleb significantly prolonged bleb survival as well as maintained normal IOP (with no post-surgical hypotony) in a clinically validated *in vivo* rabbit model of GFS. There was decreased local collagen deposition and cell number in the treated eyes. These results suggest that the circulating monocytes transformed into fibroblasts in the bleb area after GFS may participate in the scarring process after GFS and that SAP may have potential for development as a therapeutic agent to prevent fibrosis following GFS.

Another class of potentially less toxic but relevant molecules that could serve to inhibit fibrosis are matrix metalloproteinase (MMP) inhibitors. Our group had previously found that multiple injections of a MMP inhibitor called ilomastat could inhibit fibrosis *in vitro* and *in vivo.* As with both SAP and with the currently used cytotoxic agents, the pharmacokinetics of multiple subconjunctival injections to control fibrosis is not optimal. Such injections are uncomfortable to the patient and carry some risk of infection. Upon injection into the bleb, there is rapid clearance of the medicine leading to dose dumping, resulting in the need to use high doses in the hope of administering enough of the medicine to provide clinical benefit. The strategy to down regulate an undesirable mediator using siRNA to treat disease has recently been shown to have potential. Since the activated fibrotic cells in the bleb may have a longer local residence time than that of an injected drug, it was thought it may be possible to use siRNA to stop the production of MMPs. *In*

vitro experiments confirmed that while collagen contraction was inhibited using siRNA, unfortunately it was not possible to decrease bleb failure *in vivo*.

Noting that ilomastat was used as an excellent positive control during the experiments with SAP and siRNA, it was felt that if a prolonged therapeutic concentration of ilomastat could be maintained in the bleb, then multiple injections could be avoided. Furthermore, a prolonged therapeutic concentration of ilomastat might result in better overall healing. Since the subconjunctiva is open during GFS surgery, it was decided to formulate a new single application prolonged release ilomastat tissue tablet that could be left in the bleb at the time of surgery. Since it is known that the first 30 days post surgery is a very critical period for the scarring process after GFS, it was hypothesised that an ilomastat tablet designed to last 30 days in the bleb would serve to inhibit fibrosis. Since ilomastat is poorly soluble (0.038 mg/ml), it was hypothesised that a tablet comprised entirely of ilomastat without excipients would be dissolved at a low rate since the volume and flow in the bleb are at non-sink conditions for such a poorly soluble molecule.

Release studies of the tablet *in vitro* showed that the excipient free ilomastat tissue tablets achieved a constant release of active ilomastat in a concentration significantly higher than the therapeutic dose for at least 30 days. HPLC analysis confirmed that ilomastat did not degrade and remained active after sterilization and after incubation in an aqueous environment for 30 days at 37°C. Ilomastat released from the tablets significantly inhibited contraction of HTF collagen I gels *in vitro*. *In vivo*, the survival of the blebs treated with the ilomastat tablet was found to be significantly superior to the sterile water group (negative control) and with the MMC group (positive control). An inert tablet comprised of only ethyl cellulose, a common excipient, did not result in bleb survival beyond the negative control. Histological analysis showed that the ilomastat treatment group had significantly less subconjunctival scarring compared to the negative and the positive controls. No ilomastat was detectable in serum or in the ocular tissues.

This work in this thesis has served to increase our understanding about the potential benefit of prolonging the local pharmacokinetics of a medicine in the bleb. This may mediate the healing process after GFS and leads the way to a possible improved treatment for scarring after glaucoma surgery and other situations when scarring is a problem.

1. INTRODUCTION

Wound healing occurs through a series of overlapping processes, which include haemostasis, inflammation, proliferation and remodelling. The work presented in this thesis aimed to formulate and test potential therapies to prevent scarring after glaucoma filtration surgery. This scarring causes the failure of the surgery, leading to the increase of intraocular pressure (IOP) and the progression of glaucoma. The control of scarring after glaucoma filtration surgery is a key tool in the management of glaucoma patients and the prevention of visual loss because of glaucoma.

In this section of the thesis, the two dominant wound healing theories are described. The theoretical and scientific background to wound healing informs the experimental strategies followed during the course of this PhD. The first theory analysed is a fairly recent one, which suggests that scarring is mainly generated by circulating monocytes that express fibroblastic markers and are transformed into fibroblasts in the wound area, cleaving extracellular matrix and depositing new scarring tissue. The second is a more established and extensively studied theory, which suggests that local fibrocytes are transformed to fibroblasts by released chemokines and cytokines from neutrophils and macrophages. The fibroblasts then cleave extracellular matrix, remodel the matrix and deposit new scarring tissue.

The therapeutic attempts based on the first theory focus on how to inhibit the recruitment of the monocytes in the wound area and their transformation to fibroblasts. It is believed that control of this transformation will reduce the amount of scarring. Serum Amyloid P, a protein produced in the human body, has been shown to block the circulating monocytes from being transformed into fibroblasts in the wound area. A decrease in the level of Serum Amyloid P in tissues, as is the case in a traumatised area, is considered to be the main stimulus for the recruitment of monocytes and their transformation to fibroblasts.

Following on from the second theory, therapeutic attempts are focused on how to block activation of local fibroblasts and degradation of the extracellular matrix (ECM) that takes place by the proteolytic enzymes produced by the activated fibroblasts. In this case, not Serum Amyloid P, but cytokines and chemokines have been suggested to play a dominant role. Our work was focused on the Matrix Metalloproteinases (MMPs), which have been shown to be involved in pathways for the activation and elongation of local fibrocytes to fibroblasts, as well as degrading extracellular matrix and boosting angiogenesis. Their role in many eye pathologies is discussed in detail below.

The development of a treatment that effectively blocks matrix metalloproteinases (MMP) will not only benefit the inhibition of scarring after GFS but could also improve the

management of many other pathological processes in the human eye and body. In this thesis, we used MMP inhibitors and SiRNAs to block the activity of MMPs and subsequently inhibit scarring

The two suggested mechanisms of scarring could work together at the same time and one does not exclude the other. In other words, both local fibrocytes and circulating monocytes may be transformed into activated fibroblasts and participate in the scarring processes. The lack of Serum Amyloid P, as well as well as the presence cytokines and chemokines, may play an important role in the transformation of cells to activated fibroblasts and the deposition of scarring. The two mechanisms are described separately below.

1.1. Circulating monocytes and the role of Serum Amyloid P in scarring

A decade ago it was postulated for the first time that during the wound healing processes, non-activated fibroblasts (fibrocytes) circulating in the blood participate in and lead to scarring (Bucala *et al.* 1994). Supporting this theory, later studies provided evidence that myofibroblasts do not originate from tissue fibroblasts, but from a bone-marrow-derived precursor (Brittan *et al.* 2002; Direkze *et al.* 2003). It has been found that these cells have CD14+ peripheral monocyte-precursor origin and, apart from stromal cell markers (pro-Collagen I, fibronectin, pro-Collagen III), these fibrocytes express hemopoietic markers as CD45, CD13, MHC class II and CD34 (Bucala *et al* 1994; Chesney *et al* 1998). These cells obtain the characteristic fibroblastic (spindle-shaped) morphology when cultured *in vitro* (Bucala *et al* 1994). Additionally, Bucala *et al* (1994) found that these cells, apart from collagen and CD34, express vimentin, indicative of their fibroblastic properties. In tissue damage, it was hypothesised that these cells enter the wound area and, by expressing cytokines and chemokines, cleave the existing ECM, promoting angiogenesis, to produce new ECM and to promote contraction (Pilling *et al* 2003). In addition to the *in vitro* studies, these cells were found to be involved in the promotion of fibrosis in an *in vivo* pulmonary fibrosis model (Phillips *et al* 2004). It is believed that fibroblasts may participate in several fibrotic disorders, such as liver cirrhosis

(Friedman *et al.* 2003; Bataller & Brennen, 2005), and in autoimmune diseases (Johnson *et al.* 2002). Subsequently, there has been evidence that these circulating fibrocytes are involved in the scarring development (Pilling *et al* 2003).

Lately, the role of the Serum Amyloid P, a protein that belongs in the Pentraxin family, has been discussed for its ability to control the transformation of the circulating fibrocytes to myofibroblasts. Pentraxins are a protein superfamily that took their name from the presence of a 200 amino acid pentraxin domain in their carboxy-terminal domain. The first described and most well known member of the family is the C Reactive Protein (CRP). The Serum Amyloid P (SAP), which consists of the protein that we studied, is a highly concerved plasma glycoprotein that has been found to share a 51% sequence homology with CRP (Garlanda *et al.* 2005). CPR is known as the acute phase protein, which increases in serum levels following infection. Only smaller changes in SAP are, however, observed in the levels of SAP as a result of infections (Pilling *et al* 2003). CRP is specialised in binding small nuclear ribonucleoprotein particles, whilst SAP binds chromatin and free DNA (Du Clos, 1989; Bickerstaff *et al* 1999). The two molecules, CRP and SAP have differences to their binding ability to FcγRs (FcγRI, FcγRII, and FcγRIII are found on human mononuclear phagocytes and function in the clearance of immune complexes and opsonized pathogens); in the case of CRP, a high affinity binding is achieved with FcγRII, lower with FcγRI and no binding with FcγRIII. SAP binds all the three FcγRs, but with higher affinity the FcγRI and the FcγRII. The aforementioned differences, together with different links of the two molecules with apoptotic material, as Pilling *et al* (2003) suggested, are indicative of the different roles of CRP and SAP *in vivo*. In particular the differences in the binding of FcγRs have been suggested as the reason why SAP and not CRP inhibits the differentiation of circulating monocytes to fibrocytes, although the entire mechanism is not yet understood. The binding of the SAP to the FcγR was lately found to play a significant role in the inhibition of kidney fibrosis through local expression of IL-10 (Castaño *et al.* 2009).

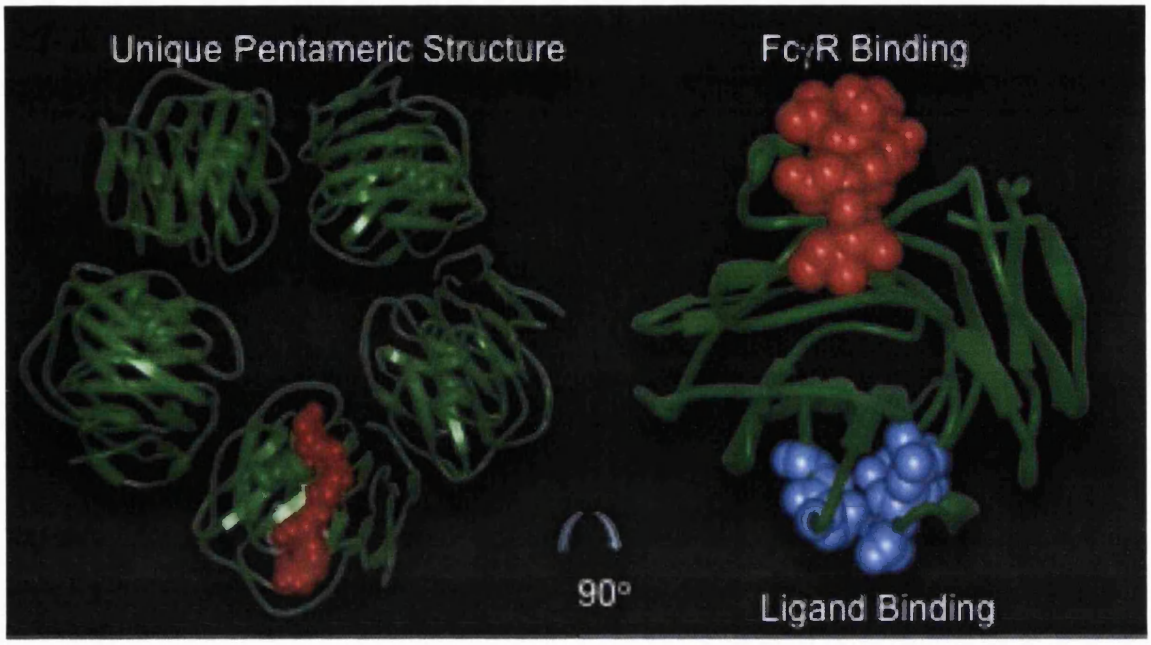

Figure 1: The Serum Amyloid P pentameric structure and its high affinity FcγR binding.

It has also been suggested that by the presence in tissues of SAP, which is connected with several ECM proteins, SAP functions like an inhibitory-regulatory mechanism that blocks the transformation of the circulating monocytes in fibrocytes (Zahedi *et al* 1996; Zahedi *et al* 1997). Abe *et al* (2001) and Bucala *et al* (1994) pointed out that the rapid recruitment of fibrocytes to the wound is indicative of the lack or inactivity of SAP in which may allow the transformation of circulating monocytes to fibrocytes. The lack of SAP or its inactivity in the wound area can be attributed to the fact that the remodeling and regeneration of the area changes the composition of the ECM (Pilling, 2003). SAP levels are reduced due to the remodeling that takes place in the area and the proteins bound with SAP in the wounded tissue are cleaved and replaced. Subsequently, lack of SAP cannot inhibit the transformation of monocytes to fibroblasts. In other words, reduction of the SAP levels in a specific tissues may serve as an injury signal so that circulating monocytes, transformed into fibrocytes, are 'sent' to the specific tissue in order to repair the wound.

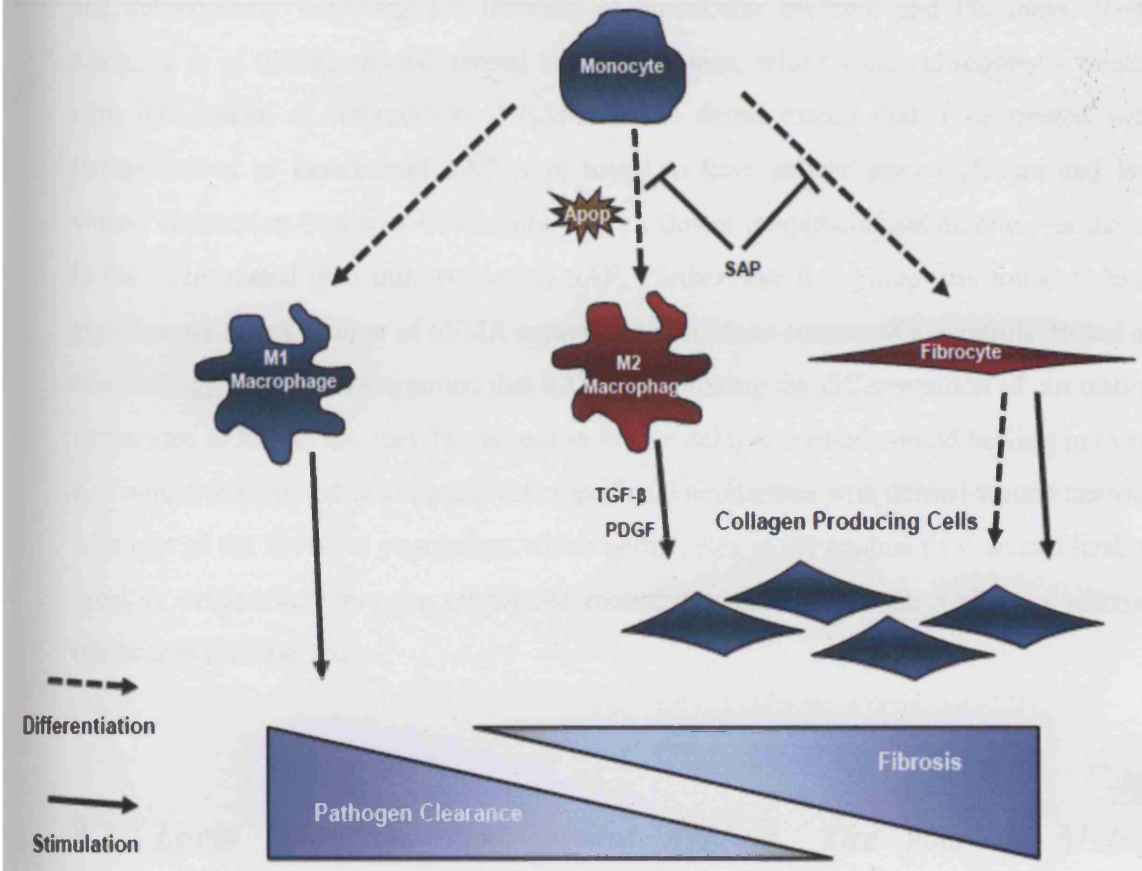

Figure 2: Serum Amyloid P inhibits the inhibits the differentiation of Monocytes to M2 Macrophages and to fibrocytes and the further differentiation of these cells to collagen producing cells that participate in the scarring process.

The lack of SAP in SAP -/- transgenic mice has been linked to antinuclear autoimmunity and glumeronephritis, which are pathological findings in the systemic lupus erythromatosus (SLE). Physiological SAP levels in the human serum are 32±7 μg/ml in men and 24±8 μg/ml in women (Nelson *et al* 1991). SAP levels are reduced in patients with autoimmune diseases including scleroderma (Pilling *et al* 2003), rheumatoid arthritis (Seemayer *et al* 2001) and mixed connective tissue disease. This finding, together with the observation that circulating fibrocytes participate in the pathological mechanisms of autoimmune diseases, indicates that SAP could be involved in the inhibition of fibrosis and, more specifically, in the inhibition of the differentiation of peripheral mononuclear precursor populations to fibrocytes (Pilling *et al* 2003). These research outcomes lead to the conclusion that SAP administration may inhibit scarring in many eye diseases as well as after glaucoma filtration surgery, extending the survival of the bleb created after surgery

and subsequently inhibiting the increase of intraocular pressure and blindness. Naik-Mathuria *et al* (2008) created dermal wounds in mice, which were subsequently treated with intradermal or intraperitoneal SAP. It was demonstrated that mice treated with intraperitoneal or intradermal SAP were found to have slower wound closure and less wound contraction than controls. Additionally, a slower re-epithelialisation rate was shown in the mice treated with intra-peritoneal SAP. Furthermore this group was found to have significantly lower number of αSMA expressing fibroblasts compared to controls. Based on this finding, the authors suggested that SAP, by inhibiting the differentiation of circulating monocytes to fibrocytes, may be the reason for the delayed normal wound healing in mice. As conjunctival wound healing presents significant similarities with dermal wound healing, with part of the fibrocyte population, which participates in the conjunctival wound healing possibly originating from the circulating monocytes, the role of the SAP as a scarring inhibitor is investigated.

1.2. Local fibrocytes and wound healing. The role of Matrix Metalloproteinases (MMPs).

The formation of fibrin clots developed after trauma involves activation of the clotting cascade and leads to the degradation of fibrinogen from thrombin. Many cytokine mediators such as PDGF, TGF-β and vascular endothelial growth factor (VEGF) are released locally by leucocytes and play an important role in the induction of inflammation and the accumulation of neutrophils and macrophages at the site of injury. TGF-β1 is produced in its latent form by platelets and is mostly responsible in its active form for the rapid attraction of neutrophils and macrophages. Neutrophils are the first migratory cells to arrive at the wound site (peak 24-48 hours post wounding), targeting dead tissues, bacteria and foreign materials with phagocytosis, in order to protect the organism from any possible infection. They also secrete TNF-α and IL-1, which attract and activate keratinocytes and fibroblasts. At a later stage, macrophages are recruited to the wound site after the neutrophils and gradually replace them. In addition to cytokines and growth factors, degraded components of ECM promote macrophage migration to the wound site, where, upon binding through their integrin receptors to ECM components, they acquire the

phenotype of tissue macrophages. Apart from their scavenger role at the site of the wound, they also secrete inducers of the proliferative phase, such as TNF-α, TGF-β, IL-1, IL-6, PDGFs, IGF-1.

The proliferative phase of wound healing comprises re-epithelialisation and the formation of granulation tissue and involves migration of fibroblasts, keratinocytes and vascular endothelial cells to the wound region from neighbouring tissues. Re-epithelialisation in dermal wounds is characterized by migration of keratinocytes from the basement membrane, just under the clot and in contact with the dermal matrix. During re-epithelialisation in both acute and chronic burn wounds, migrating keratinocytes at the migration front that are not in contact with the basement membrane express MMP-1 (Steffensen, Hakkinen, & Larjava 2001). In contrast, proliferative keratinocytes that are in contact with the basement membrane do not seem to express MMP-1 (Steffensen, Hakkinen, & Larjava 2001). MMP-1 is only secreted from keratinocytes in culture that are in contact with collagen I (Pilcher *et al.* 1998). Activated keratinocytes express transmembrane receptors known as integrins. One of the integrin receptors, the α2β1, recognises collagen type I and is essential for the migration of keratinocytes on collagen I under the influence of MMP-1 activity (Pilcher *et al.* 1998). The close connection between collagen I, α2β1 and MMP1 helps the migration of keratinocytes with local and controlled proteolysis (Steffensen, Hakkinen, & Larjava 2001). In addition, at the site of migrating keratinocytes, MMP-10 (stromelysin-2) is expressed in contrast to stromelysin-1 (MMP-3), which is expressed at the site of proliferative keratinocytes. These are located behind the migrating front and are in contact with the basal lamina. MMP-26 is also found in migrating keratinocytes (Ahokas *et al.* 2005), and it has been reported that MMP-28 is present together with MMP-3 at the site of proliferating keratinocytes (Lohi *et al.* 2001;Saarialho-Kere *et al.* 2002). MMP-9, by its natural ability to degrade collagen IV, the main component of the basement membrane, facilitates the detachment of basal keratinocytes and their migration to the wound site during the early stages of wound healing (Hartlapp *et al.* 2001;Lohi *et al.* 2001). The role of MMP-9 in wound healing is strengthened by its capability to cleave collagen VII, found in the structure of the dermal-epidermal anchoring fibrils. Migratory keratinocytes are also characterised by the expression of TIMP-1 molecules, instead of the proliferative keratinocytes, in which both TIMP-1 and TIMP-3 are found. Recent experiments in normal and chronic wounds have shown that TIMP-1 and -3 are found only in normally healing wounds and not in chronic

ulcers. The formation of granulation tissue is characterised by the replacement of the fibrin clot and the deposition of ECM at the wound region that includes mainly tenascin, fibronectin, collagen III and I. A percentage of the fibroblasts that migrate to the wound differentiate to myofibroblasts (Moulin *et al.* 1998). PDGF released from degranulated platelets and TGF-β and FGFs released from macrophages recruit fibroblasts to the wound site, which exhibits features of smooth muscle cells, because they produce smooth muscle actin, responsible for their contractile phenotype. Fibroblasts and myofibroblasts play a significant role in the deposition of ECM, a process known as fibroplasia.

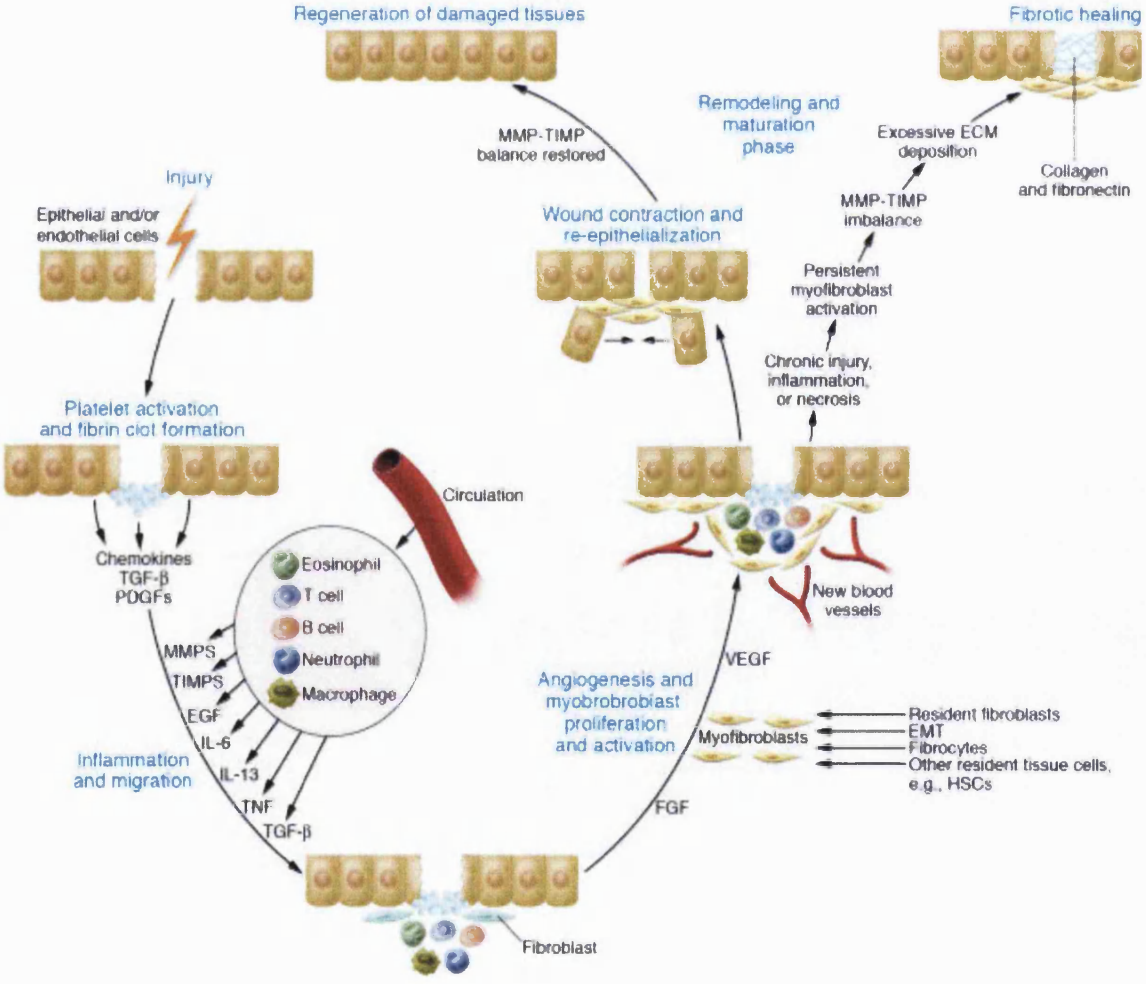

Figure 3: Phases of wound healing, the involvement of local cells in the mechanisms of wound healing and the role of MMPs. Figure attributed by Wynn (2007).

During the formation of granulation tissue *in vivo*, fibroblasts express MMP-1 and MMP-2 near the wound front. This facilitates the organisation of the newly synthesised ECM. At this stage, the balance between MMPs and TIMPs favours the ECM formation instead of the remodelling phase where the matrix degradation dominates. During the remodelling phase, the stromal cells, including fibroblasts, keratinocytes, endothelial and inflammatory cells, populate the granulation tissue and are believed to continue their expression of MMP-1,-2,-3,-9,-11,-12 and -14 (Steffensen, Hakkinen, & Larjava 2001). As a new basal lamina is formed at the wound site, MMP-1 expression is reduced and the basement membrane-keratinocytes interactions through hemidesmosomes are stabilised. Hemidesmosomes, formed within keratinocytes, bind them to anchoring fibrils of the subtending dermis. In conclusion, when the cells finish the process of wound healing, a stop signal decreases MMP expression and gradually the MMP levels approach the levels of normal tissues (Sudbeck *et al.* 1997).

Having described how the MMPs are involved in the general wound healing process, it is important to get a better understanding about the structure and the function of these enzymes as well as specifically their role in eye pathologies and in wound healing after glaucoma filtration surgery.

1.2.1. Matrix Metalloproteinases

1.2.1.1. The extracellular matrix

The extracellular matrix (ECM) is a dynamic structure that contains a complex mixture of molecules, including elastin, collagens, laminins, fibronectin, proteoglycans and other insoluble molecules. The ECM not only provides a structural framework to support cells and divide tissues (Klein *et al.* 2004a; Mott & Werb 2004), but also acts as a reservoir for biologically active molecules, such as cytokines, chemokines, growth factors and apoptotic ligands. The specific structure and composition of the ECM meets the demands of specialized tissues (Klein *et al.* 2004a). Upon interaction with cells through receptor-mediating signaling induced by growth factors, cytokines and other cell adhesion receptors, the ECM controls cell behavior and creates an influential cellular environment (Brew,

Dinakarpandian, & Nagase 2000; Massova *et al.* 1998). These ECM-cell interactions are crucial for the normal development and function of the organism. To maintain homeostasis, the remodeling of ECM is highly regulated. It is modulated through proteolytic systems that control the hydrolytic degradation of a variety of ECM molecules. By regulating the composition of the ECM structure, these proteolytic systems play a significant role in the control of signals sent by the ECM components. This affects cell migration, proliferation, differentiation and death. Uncontrolled proteolysis is an important pathogenic mechanism observed in a variety of diseases (Massova *et al.* 1998). The function of these proteolytic systems is very complex, as more than 500 genes encoding proteases or protease-like proteins exist in the human genome (Puente *et al.* 2003).

The majority of endopeptidases are divided into four different groups: 1) serine proteases, 2) cysteine proteases, 3) aspartic proteases and 4) metalloproteinases. The metalloproteinases are further divided into five subgroups that include the Metzincin superfamily and the gluzincin, inuzincin, carboxypeptidase and DD carboxypeptidase subgroups. The Metzincin superfamily includes five multigene families, the serralysins, the pappalysins, the astacins, the adamalysins (or ADAMs) and the matrix metalloproteinases (MMPs) (Sternlicht & Werb 2001). The MMPs are also known as matrixins and are the main enzymes responsible for the ECM degradation resulting in ECM turnover. The first MMP was described 45 years ago in experiments designed to explain how a metamorphosing tadpole lost its collagen-rich tail, leading to normal maturation to the frog (Gross & Lapiere 1962). This enzyme was shown to be important for the normal degradation of connective tissue in the tadpole tail. Following that discovery, MMPs were found to be present in all living organisms, from the simplest bacteria to the most complex systems in mammals. The physiological role of MMPs has been proven by experimental work using transgenes encoding MMPs, Tissue Inhibitors of Metalloproteinases (TIMPs), mutagenesis for specific MMPs or TIMPs genes (Vu & Werb 2000). These molecules take part in homeostatic mechanisms, such as tissue restoration, remodeling and repair, which are important in normal biological processes, such as fetal tissue development, organ morphogenesis, blastocyst implantation, ovulation, cervical dilation, post-partum uterine involution, endometrial remodeling, hair follicle cycling, bone remodeling and wound healing. Uncontrolled ECM degradation as a result of disruption of the balance between MMPs and their inhibitors is observed in many pathological conditions, such as in osteoarthritis, rheumatoid arthritis, cancer, atherosclerosis, aneurysms, nephritis, tissue

ulcers, fibrosis, heart failure, pulmonary emphysema, CNS diseases, fibrotic lung disease, liver fibrosis, otolaryngological disease and eye diseases.

1.2.1.2. The MMP family

MMPs constitute a family of 24 known Zn^{+2} and Ca^{+2} dependent proteases (hence the name metallo-), active at neutral pH. They have overlapping enzymatic activities with regard to ECM (Newby 2006) and non-matrix (Massova *et al.* 1998) proteins, as well as overlapping chromosomal regions based most likely on gene duplication. Although the MMP nomenclature has reached number 29 (MMP-29), the actual number of enzymes is smaller, since MMP-4, MMP-5, MMP-6, MMP-22 and MMP-29 have been removed from the MMPs list as a result of duplication (Somerville, Oblander, & Apte 2003). Additionally, the human proteinase first published as MMP-18 is now known as MMP-19, and the nomenclature MMP-18 refers to a Xenopus laevis collagenase (Somerville, Oblander, & Apte 2003).

With several exceptions, MMPs share common characteristics, which are:

1) They are extracellular proteins that hydrolyze protein or proteoglycan components of the ECM. Recent studies have identified that MMP-1 (Galt *et al.* 2002), MMP-2 (Kwan *et al.* 2004) and MMP-11 (Luo *et al.* 2002) are also found intracellularly and that they may degrade intracellular proteins (Nagase, Visse, & Murphy 2006).

2) They all have an active catalytic region that contains the zinc-binding active site.

3) They are activated by "cleavage" of the pro-domain.

4) They all have a "pre" domain-signal domain, which directs MMPs to the secretory pathway.

5) They all have a "pro" domain that maintains latency in the MMP molecule by occupying the active zinc site, making the catalytic site inaccessible to substrates.

6) A hemopexin (or else C-terminal) domain is present in all MMPs, except for MMP-7, MMP-23, MMP-26.

7) A hinge domain is found in all MMPs, except for MMP-7, MMP-21, MMP-23 and MMP-26.

8) Matrix metalloproteinases are mainly secreted in a zymogen-latent form, except in MT-MMPs and MMP-11, MMP-21, MMP-28, which contain furin-like recognition domains in

their pro-domains and can be activated intracellularly in the trans-Golgi network by serine proteases of the subtilisin family (Velasco *et al.* 1999).

9) Their enzymatic activity is inhibited by endogenous tissue inhibitors (TIMPs).

10) Specific sequences of aminoacids characterise each family member. The sequence homology with collagenase 1 (MMP-1), the VAAHExGHxxGxxH sequence at the catalytic domain and the PRCGxPD sequence at the prodomain are very important criteria for the categorization of a proteinase within the MMP family.

11) Activation is accompanied by a loss of MW of about 10.000 (Woessner, Jr. 1991). In MMP-12 and MMP-20, the loss is greater (Hernandez-Barrantes *et al.* 2001).

1.2.1.3. The MMP subfamilies

MMPs are divided into discrete categories according to: 1) their ability to degrade different substrates and 2) their structural domains.

Based on substrate specificity, MMPs are grouped in six categories: the collagenases (MMP-1, MMP-8, MMP-13 and MMP-18 in Xenopus laevis), the gelatinases (MMP-2 and MMP-9), the stromelysins (MMP-3, MMP-10 and MMP-11), the matrilysins (MMP-7 and MMP-26), the membrane-type matrix metalloproteinases (MT-MMPs) (MMP-14, MMP-15, MMP-16, MMP-17, MMP-24, MMP-25) and others that are not grouped in the aforementioned categories (MMP-12, MMP-19, MMP-20, MMP-21, MMP-23, MMP-27, MMP-28 (Nagase, Visse, & Murphy 2006).

The collagenases (MMP-1, MMP-8, MMP-13) form a subgroup that degrades interstitial collagens I (found in the bones, the ligaments, the tendons, the skin, the eye and the internal organs), II (found in the cartilage, the intervertebral disc, the notochord and the vitreous body of the eye) and III (found in the skin, the blood vessels and the internal organs) at their specific site Gly-Ile/Leu bond in the α chains, three fourths of the way from the N terminus, cutting the collagens in two fragments (3/4 and 1/4). The cleavage products denature to form gelatin at physiologic temperature, which is then degraded by a different MMP subgroup: the gelatinases (Nagase & Woessner, Jr. 1999). Native collagen types IV and V cannot be degraded by collagenases (Billinghurst *et al.* 1997;Sakai & Gross 1967;Welgus *et al.* 1982). Collagenases are capable of using, apart from collagens, other ECM and non-ECM components as substrates, and recent studies have shown that MMP-1 activates the PAR1 (the protease-activated receptor, by cleaving the same bond between arginine and serine, as thrombins do, which promotes breast cancer and the invasion of the

carcinoma cells in other tissues (Boire *et al.* 2005). MMP-8 is the only interstitial collagenase that can be stored within neutrophil granules, instead of being synthesised and released upon demand (Jeffrey 1998). When compared with MMP-1, MMP-8, which can be highly glycosylated, degrades collagens I and II at a higher rate and collagen III at a lower rate (Jeffrey 1998). MMP-13 is mainly produced from cartilage and bone during development and from chondrocytes in osteoarthritis (Velasco *et al.* 2000).

Gelatinase A (72 KD gelatinase, MMP-2) and Gelatinase B (92 KD gelatinase, MMP-9) denature interstitial collagen (gelatins) and elastin (Berton *et al.* 2000; Mecham *et al.* 1997; Shipley *et al.* 1996) as well as collagen IV, which constitutes a major constituent of mature basal lamellae (Klein *et al.* 2004a). MMP-2 is present both in tumours, inflamed and non-inflamed healthy tissue (Polette *et al.* 2004), and in addition to gelatin, it digests a wide range of substrates. MMP-2, but not MMP-9, is capable of degrading collagens I, II and III (Allan *et al.* 1995). MMP-9 has the largest molecular weight within the MMP family due to the fibronectin-like domain and the collagen V-like domain. Normally, it is present in trophoblasts, osteoclasts, neutrophils and macrophages (Vu & Werb 1998), and its synthesis is increased in conditions that require tissue remodelling, such as wound healing, tissue development, angiogenesis and tumour invasion (Polette *et al.* 2004).

Stromelysins are another group of MMPs (MMP-3, MMP-10 and MMP-11). They were named after the first member of the subgroup MMP-3 because of its stromal cell origin, where it was first identified (Nagase 1998). Their main role is to cleave proteins such as fibronectin, proteoglycans and laminin. Stromelysins -1 and -2 have the same structural homology as collagenases (Nagase 1998), and unlike other MMPs that act in neutral pH, MMP-3 has an acidic pH activity range. MMP-10 is like MMP-3 in terms of molecular weight and in proteoglycanase and collagenase activity (Mannello *et al.* 2006), although its catalytic ability, is lower than MMP-3 (Visse & Nagase 2003).

MMP-7 and MMP-26 form the subgroup of matrilysins. MMP-7 is mostly expressed in glandular epithelial cells in the pancreas, the renal mesangium, the endometrium, the skin and the uterus and is characterised by a wide substrate specificity for various ECM and non-ECM components (Woessner 1998). It is more active than other MMPs against versican, a chondroitin sulphate proteoglycan found in atherosclerotic plaque, and cleaves many stromelysin substrates (Imai, Shikata, & Okada 1995;Quantin, Murphy, & Breathnach 1989). MMP-26 is expressed in the endometrium and other normal cells, as well as in some carcinomas. Its activity includes several ECM molecules and is largely stored intracellularly (Marchenko *et al.* 2004). MMP-11 has a minor activity in

degrading ECM components, but it cleaves serine proteinases inhibitors (serpins) like other MMPs, which have higher affinities for other ECM substrates. MMP-11 is unique among the other stromelysins as it is released as an active enzyme in the extracellular space, because of the intracellular activation by the pro-hormone convertases furin (Pei & Weiss 1995) (Marchenko *et al.* 2004).

MT-MMPs are anchored to the plasma membrane and can be actively focussed by the cell to degrade their substrates. Six MT-MMPs have been identified, and, in addition to their degrading role, they also activate latent MMPs (Egeblad & Werb, 2002). They are highly expressed in fibroblasts and various tumour cells (Seiki 1998) and play a major role in modifying the pericellular environment and tumour cell behaviour, as well as in inducing cell migration, invasion and angiogenesis. As with MMP-11, MT-MMPs are activated intracellularly by furin-like protein convertases as they are translocated to the plasma membrane (Brinckerhoff & Matrisian 2002;Egeblad & Werb 2002;).

Macrophage metallo-elastase (MMP-12) is expressed in lung macrophages and in tumours. Its main function is thought to be the degradation of elastin, but it is also effective against type IV collagen, fibronectin and laminin. MMP-19 has been found in the liver by c-DNA cloning and in patients with Rheumatoid Arthritis as a T-cell derived autoantigen (Kolb *et al.* 1997; Pendas *et al.* 1997), whilst MMP-20 (enamelysin) is primarily located within newly formed tooth enamel (hence its name) and has been shown to cleave amelogenin (Li *et al.* 2001b). MMP-22 has been found in chicken fibroblasts, and, although a human homolog has been found on the basis of EST sequences, the function of this enzyme remains unknown (Billinghurst *et al.* 1997).

Based on the structural domains, MMPs are divided into nine different groups which are shown in Figure 4. MMP-7 and MMP-26 are the matrix metalloproteinases with the smallest number of domains. They only consist of the signal, the prodomain and the catalytic domain. The typical structure consisting of signal domain, propeptide, catalytic, hinge and hemopexin domains is present in MMP-1, MMP-3, MMP-8, MMP-10, MMP-12, MMP-13, MMP-19, MMP-20 and MMP-27. MMP-2 additionally has a fibronectin domain of three type II repeats, and MMP-9 has a fibronectin domain like MMP-2 plus an insert within its hinge region similar to collagen V (the collagen V-like domain). MMP-11 and MMP-28, apart from the four main domains, have a furin-susceptible site. This domain is also present in MMP-21, that was initially found in Xenopus (Yang, Murray, & Kurkinen 1997) and recently in mice and humans (Marchenko, Marchenko, & Strongin 2003). The human ortholog lacks the hinge domain, and, in addition to the furin, it also has a 20-amino

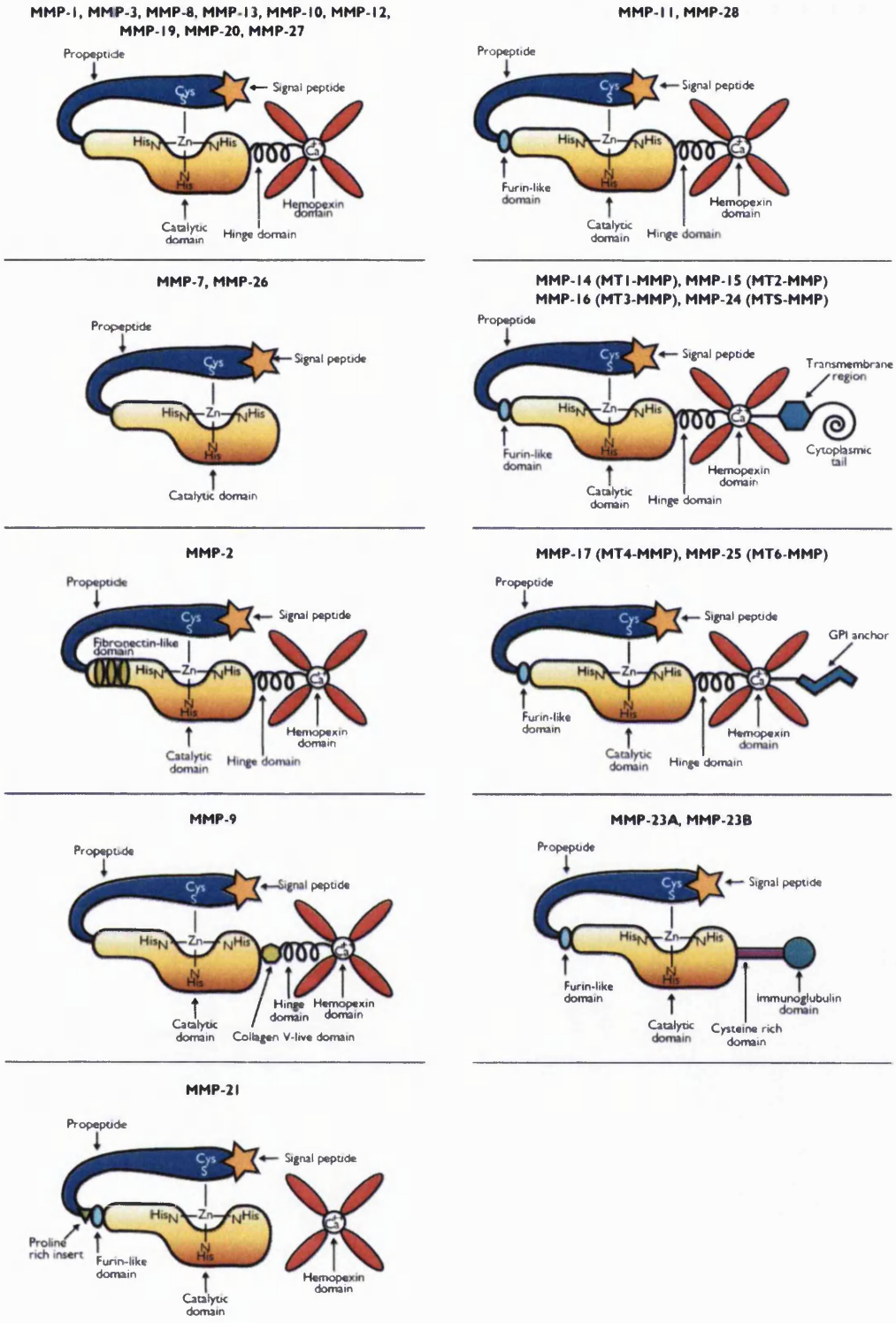

Figure 4: Domains participating in the structure of MMPs.

residue unconserved proline-rich insert in the pro-domain (Ahokas *et al.* 2002). With regard to MT-MMPs, they are divided into two groups, according to their domains. The members of the first MT-MMP group, MMP-14, MMP-15, MMP-16 and MMP-24, have a transmembrane region and a short cytoplasmic tail in their molecules (Jiang *et al.* 2001; Uekita *et al.* 2001; Valtanen *et al.* 2000). The members of the second MT-MMP group, MMP-17 and MMP-25, exhibit a glycophosphatidylinositol anchor (GPI-anchor) containing a short hydrophobic signal that anchors to GPI (Itoh *et al.* 1999; Jiang *et al.* 2001; Kojima *et al.* 2000; Sounni & Noel 2005). The catalytic domain of MT-MMPs includes an 8-aminoacid insertion between βII and βIII strands known as the MT-loop. In the MT1-MMP molecule, the role of the MT loop is known, as it creates a pocket in the catalytic domain of this enzyme that interacts with the αβ loop of TIMP-2 (English *et al.* 2001). MMP-23 lacks a recognizable signal sequence and contains a short prodomain with a single cysteine residue, which is believed to be part of the cysteine-switch mechanism that controls the latency of this enzyme. This cysteine residue is located in the sequence A-L-C-L-L-P-A, which is different from the sequence P-R-C-G-P-D that is present in the other MMPs (Velasco *et al.* 1999). Moreover, MMP-23 has a unique C-terminal cysteine-rich domain followed by an immunoglobulin domain. It was initially proposed to be categorized as a type II membrane MMP due to the transmembrane domain at the N-terminal of the propeptide. However, since it has a furin-recognition motif in its propeptide, it is cleaved in the Golgi apparatus by a proprotein convertase (Pei, Kang, & Qi 2000;Visse & Nagase 2003), and MMP-23 is, therefore, activated at the extracellular space without the N terminal signal anchor (Pei, Kang, & Qi 2000).

1.2.1.4. MMP domains

The prodomain is bound with its round side to the active cleft site of the catalytic domain. The propeptide domain of the MMPs (about 80 aminoacids) interacts with features of the active site cleft. It has a unique PRCG (V/N) PD sequence, common to the MMP family. The Cys (C) within the aforementioned sequence interacts with the Zn^{+2} in the active site, and this interaction maintains the latency of proMMPs (Kleifeld *et al.* 2000;Van Wart & Birkedal-Hansen 1990). Specifically, the cysteine residue plays a significant role as a fourth inactivating ligand for the catalytic zinc atom, and as a result, water cannot reach the active region of the catalytic domain to activate the enzyme, and so it is kept in latent

form (Boire *et al.* 2005). This mechanism is known as the "cysteine switch". For activation to take place, the cysteine-to-zinc switch must be disrupted by proteolysis of the propeptide or by ectopic perturbation of the cysteine-zinc interaction (Van Wart & Birkedal-Hansen 1990). Following this process, the thiol group is replaced by a water molecule, which hydrolyses its propeptide to complete its activation and degrade its substrate by attacking the peptide bonds (Somerville, Oblander, & Apte 2003; Vu & Werb 2000).

The catalytic domain (about 170 aminoacids) contains a conserved zinc-binding motif with three histidines linked to a conserved methionine, which forms a unique "Met-turn structure" ([VAIT]-[AG]-[ATV]-H-E-[FLIV]-G-H-[ALMSV]-[LIM]-G-[LM]-X-H-[SITV]-X-X-X-X-X-[LAFIV]-M, where X is any aminoacid (Becker *et al.* 1995; Bode *et al.* 1996; Massova *et al.* 1998; Springman *et al.* 1990). The three histidines bind the active zinc, and the methionine residue is located underneath the cavity created by the three histidines, resulting in high hydrophobicity in the area, which increases the binding ability of histidines (Bode *et al.* 1996; Massova *et al.* 1998). The catalytic domain of MMPs contains an additional structural zinc ion and at least one calcium ion, which are important for the enzymatic activity and structural stability of the MMP molecules. The distance between the zinc in the active site and the structural zinc is 12 A^0.

The C-terminal hemopexin-like domain (about 210 aminoacids) contains a four-bladed β-propeller (each composed of four antiparallel β strands connected in a W-like topology, which is strongly twisted) (Jenne & Stanley 1987; Massova *et al.* 1998), forming a gap in the middle of the structure resembling a propeller, which is filled with a calcium ion. In the fibronectin domain, each fibronectin repeat contains a hydrophobic pocket that binds the gelatin, acting as an exosite for the binding of collagenous substrates. Through their fibronectin II-like domain, proMMP-2 and proMMP-9 are able to bind the insoluble elastin, and, after the formation of that complex, they are not cleaved from other proteolytic systems. When proMMP-2 is attached to insoluble elastin, it is autocleaved to a 62-kDa active form (Shipley *et al.* 1996).

1.2.1.5. Transcription and regulation of MMP activity

MMP expression and activation is a step-by-step process that involves gene transcription, synthesis of inactive MMPs, secretion of MMPs onto the extracellular matrix or, in the case of MT-MMPs, display on the plasma membrane and activation of the zymogens, making MMPs capable of degrading their substrates.

With the exception of MMP-8 and MMP-9, which are stored in neutrophil and eosinophil granules (Kahari & Saarialho-Kere 1999), MMPs are produced when ECM degradation and remodelling are necessary. The signal for MMP transcription comes from soluble factors such as cytokines, growth factors and hormones. Factors that have been identified to induce MMP upregulation include both forms of interleukin 1 (IL-1a, IL-1b), tumour necrosis factor (TNFα), transforming growth factor-β (TGF-β) (Johnatty *et al.* 1997), epidermal growth factor (EGF), basic fibroblast growth factor (bFGF), platelet-derived growth factor (PDGF) (Uzui *et al.* 2002), Chlamydia pneumoniae heat shock protein 60 for MMP-9 (Bode *et al.* 1999), CD40 ligand for MMP-1,-3 and -8 (Bode *et al.* 1999;Mach *et al.* 1997) and many others. These factors activate MMP transcription via activation of proto-oncogene proteins that bind to cis-acting elements at the promoter site of MMP genes. The most well known regulatory elements are activating protein 1 (AP-1), activating protein 2 (AP-2), polyoma enhancer A binding protein-3 (PEA-3), the NF-kB binding site, the osteoblastic cis-acting element and the TATA box. AP-1 and PEA-3 interact with members of the Jun (c-Jun, Jun B, Jun D), Fos (c-Fos, Fra-1, Fra-2 and FosB) and E26 (Ets) families respectively. Jun and Fos proteins form homodimers and heterodimers, and Ets transcription factors are helix-turn-helix protein molecules that identify the purine rich element A of PEA3 –CGGA[A/T]. They act alone or, as in the case of Ets molecules, they form complexes with other transcription factors (Clark *et al.* 2008).

In addition to soluble factors, cell-cell and cell-matrix interactions also induce MMP expression. TNFα and IL-1 as well as ultraviolet B irradiation (Brenneisen *et al.* 1998) activate the mitogen activated protein kinase (MAPK) path and other kinases, which regulate intracellular signals from membrane receptors as well as from cell-cell and cell-matrix interactions. It is worthwhile that three parallel MAP kinase pathways have been described; the p44-p42 or Erk ½ path, the c-Jun N terminal kinase/ stress activated protein kinase path and the p38 Map kinase pathway. Other factors, like IL-4 and corticosteroids suppress MMP expression (Damas *et al.* 2002; Siwik, Chang, & Colucci 2000).

1.2.1.6. MMP activation *in vitro* and *in vivo*

Several agents, such as thiol-modifying agents, organomercurials, reactive oxygen radicals, a variety of denaturing agents as well as conditions of low pH and high temperature can lead to MMP activation *in vitro* (Nagase 1997).

In vivo, enzymes that are secreted as proenzymes form enzyme cascades, in which each enzyme is activated by the one that precedes it, and upon activation, activates the enzyme that follows it. MMPs and members of the serine proteases like plasmin, urokinase plasminogen activator (u-PA), and tissue plasminogen activator (t-PA) act together in a cascade. The activation of plasminogen to plasmin is mediated by a tissue-type plasminogen activator (t-PA) bound to fibrin or by a urokinase plasminogen activator bound to a high-affinity cellular receptor (u-PAR) (Visse & Nagase 2003). The binding of u-PA with u-PAR leads to rapid generation of plasmin (Ellis *et al.* 1999; Miles *et al.* 1991; Ritchie *et al.* 1999; Vassalli, Sappino, & Belin 1991). Plasmin activates proMMP-3, and both enzymes in combination activate pro-MMP-1 (Nagase *et al.* 1991). Plasmin has also been found to activate pro-MMP-7, pro-MMP-9, pro-MMP-10 and pro-MMP-13 (Lijnen 2001), whilst in another cascade, the coagulation factors, thrombin and factor Xa, have been reported to activate pro-MMP-2 (Galis *et al.* 1997; Rauch *et al.* 2002; Zucker *et al.* 1995).

Several MMPs are able to initiate the stepwise activation of pro-MMP-2. The most well-known mechanism of pro-MMP-2 activation takes place at the cell surface, where pro-MMP-2 forms a complex with MT1-MMP and TIMP-2, and a neighbouring MT1-MMP cleaves the prodomain of pro-MMP-2 to activate this molecule (Ellerbroek *et al.* 2001). The activation of proMMP-2 is also mediated by other MT-MMP molecules, except MT4-MMP. In addition to pro-MMP-2, MT1-MMP activates proMMP-13, a process that is facilitated by the presence of active MMP-2 and independent from TIMP-2 (Knauper *et al.* 2002; Knauper *et al.* 1996).

MMP-3 is able to activate the latent form of MMP-1, MMP-7, MMP-8, MMP-9 and MMP-13. As part of the cascade, the activated MMP-7 is also capable of activating pro-MMP-1, pro-MMP-9 and pro MMP-13. In the same way, MMP-2 activates pro-MMP-9 and MMP-12 activates pro-MMP-2 and MMP-3 (Knauper *et al.* 2002).

As indicated above, MT-MMPs, MMP-11, MMP-21 (Jones, Sane, & Herrington 2003), MMP-23 and MMP-28- possess a furin-like domain recognition sequence allowing the intracellular activation by furin-like proprotein convertases in the trans-Golgi network during the transfer of MMPs from the endoplasmic reticulum to the plasma membrane (MT-MMPs) and to the extracellular space (MMP-11,-21,-23,-28) (Hotary *et al.* 2002; Lohi *et al.* 2001; Pei & Weiss 1995; Zucker *et al.* 2003). The furin-recognition motif is located between the propeptide and the catalytic domain and it is RXKR in MMP-11 and MT-MMPs, except for the MT-MMP-4, RRRR in MT-MMP-4 (Pei & Weiss 1995; Santavicca

et al. 1996; Sato *et al.* 1996) and MMP-23 (Ohnishi *et al.* 2001), RSRR in MMP-21 (Ahokas *et al.* 2002) and RKKR in MMP-28 (Illman *et al.* 2003; Marchenko & Strongin 2001).

1.2.1.7. Control of MMP activity

Inhibition of MMPs occurs naturally as a mechanism to control excessive matrix degradation and tissue remodelling. This is exerted by natural inhibitors, known as the tissue inhibitors of metalloproteinases (TIMPs), and by non-specific enzyme inhibitors present in tissues. TIMPs are a family of four known, 20-30 kDa secreted proteins (Massova *et al.* 1998; Sternlicht & Werb 2001), consisting of an aminoterminal (about 125 aminoacids) and C-terminal (about 65 aminoacids) domain (Murphy *et al.* 1991; Williamson *et al.* 1990). TIMP-1,-2 and -4 can be found in soluble form, whilst TIMP-3 predominantly binds to the ECM (Mannello & Gazzanelli 2001). TIMPs inhibit the enzymatic activity of MMPs by forming high-affinity, non-covalent 1:1 complexes with activated MMPs. Although originally it was thought that TIMPs inhibit all the MMPs non-specifically, it has now been shown that MT-MMPs are less effectively inhibited by TIMP-1 (Baker *et al.* 2002). The inhibitory activity of TIMP-3 is not restricted to MMPs; it also inhibits ADAM-17,-10,-12 and aggrecanases (Amour *et al.* 1998) (Amour *et al.* 2000).

Several other factors have been shown to play a significant role in MMP inhibition. A GPI-anchored reversion-inducing cysteine-rich protein with Kazal motifs (known as RECK) inhibits the post-transcriptional secretion and activation of MMP-2,-9 and MT1-MMP (Oh *et al.* 2001). It is believed that α_2 macroglobulin acts through the low-density lipoprotein receptor-related protein (LDL-RP), inducing the endocytosis of MMPs (Baker, Edwards, & Murphy 2002).

MMPs are activated in several pathological conditions. In the clinical setting, it is important to identify selective inhibitors that can be used therapeutically to control MMP activity. The use of the natural TIMP inhibitors has disadvantages, such as their high molecular weight, their poor oral bioavailability and their potentially harmful effects on cellular function, which prevent their clinical use. In addition, it has been shown that although TIMPs may improve the prognosis of some categories of tumours, there are paradigms, such as in gastric tumors, renal, bladder, colorectal and breast cancer, where TIMPs are involved in more aggressive cancer progress (Glasspool & Twelves 2001; de

Mingo *et al.* 2007). To overcome these difficulties, synthetic inhibitors of MMPs (MMPIs) have been developed. The most well-known MMPIs are batimastat (BB-94), marimastat (BB-2516), Prinomastat (AG3340) and Tanomastat (BAY12-9566) (Glasspool & Twelves 2001), all of which bind reversibly to the active site of MMPs. Most of the potent inhibitors designed to date bind to theright-side of the zinc of the active site cleft, because left-side binding is much weaker, possibly due to its natural ability to prevent the carboxylate product of substrate cleavage from becoming a potent inhibitor of the enzyme (Skiles, Gonnella, & Jeng 2001).

1.2.1.8. Additional MMP functions

In addition to their role in degrading the ECM to create paths for cell migration during development and tissue repair and regeneration, MMPs take part in enzyme cascades that lead to the activation of the latent forms of several chemoattractants, chemokines, cytokines, growth factors and other enzymes, which act synergistically with MMPs to change the cell behaviour and the extracellular environment. Because of these functions, MMPs are believed to be key enzymes in the mechanisms of tissue morphogenesis. This is supported by observations that MMP activity is present in the embryo from the very first stages. For implantation to take place, trophoblasts need to invade into the maternal residue. Whilst investigating the role of MMP-9 in implantation, anti-MMP-9 antibody has been used in human trophoblast cultures, resulting in inhibition of the invading function of trophoblasts. Additionally, anti-MMP-9 antibody added to cultures of embryonic kidney explants inhibited the uteric bud development (Lelongt *et al.* 1997). It is now known that MT1-MMP and TIMP-2 are also very important in branching morphogenesis (Kanwar *et al.* 1999). With regard to mammary development, misregulation of MMP-3 expression in transgenic mice leads to abnormal gland morphology (Witty, Wright, & Matrisian 1995). Additionally, *in vitro* inhibition of MMP-2 in the embryonic pancreatic islet epithelial cells prevents their normal organization into islets of Langerhans without affecting their differentiation (Miralles *et al.* 1998). MMP-2 and MMP-9 synthesised in *in vitro* human skeletal muscle satellite cells may participate in myogenesis and skeletal muscle regeneration (Murphy *et al.* 1980). MMP-3 is produced in large quantities during chondrocyte-mediated cartilage remodelling, and MMP-13 and MMP-14 are considered to participate in the induction of bone replacement of cartilage during

various developmental stages (Jimenez *et al.* 2001). MMP-9 is also involved in the development of many neural structures, like the hypophysis, the gagglion cell layer of the retina, the uveal tract (Canete *et al.* 1995) and also in the regulation of the cell microenvironment in the cerebellum (Lijnen 2001).

1.2.1.9. MMPs and neoplasia

Due to their ability to cleave components of the basement membrane, MMPs play a significant role in invasion and metastasis. Through proteolysis of the basement membrane, tumours can spread locally and distantly (Canete *et al.* 1995; Chang & Werb 2001; Nelson *et al.* 2000). In the case of metastatic cancers, by degrading the basement membrane, cells escape from the tumour at the primary location and, through the blood or lymphatic circulation, are anchored to distant organs, where by degradation of the basement membrane and proliferation and formation of new blood vessels create secondary tumours. The role of basement membrane degradation in tumour metastasis was initially suggested in 1980 by studies which indicated that MMP secretion from a melanoma cell line was responsible for degrading basement membrane collagen (Canete, Gui, Linask, & Muschel 1995; Nelson, Fingleton, Rothenberg, & Matrisian 2000a). This has been further confirmed by several clinical and research studies in lung, brain, head and neck, colon, breast, thyroid, ovarian, prostate, and gastric carcinomas (Canete *et al.* 1995; Johansson, Ahonen, & Kahari 2000; Nelson *et al.* 2000; Stetler-Stevenson, Aznavoorian, & Liotta 1993).

The thought that inhibition of MMPs could be used as a tool for cancer treatment has led to the development of pharmaceutical compounds to block MMP activities. Batimastat (BB94), a pseudopeptide with structural similarity to collagen that inhibits MMP-1,-2,-3,-7, and -9 (Canete *et al.* 1995; Hoekstra, Eskens, & Verweij 2001), was the first synthetic inhibitor of MMPs tested in clinical trials. Because of its low oral bioavailability due to poor solubility, intraperitoneal administration was used. Side effects including abdominal pain, fever, asymptomatic elevation of liver enzymes, pain at the site of injection when administered intrapleurally, as well as no significant clinical responses led British Biotech to replace it with another, orally administered MMPi: Marimastat. Clinical trials with Marimastat (BB-2516) did not have significant differences compared to chemotherapy (gencitabine) treatment, but further analysis revealed that patients with pancreatic and gastric cancer lacking distant metastases, who have already been treated

with chemotherapy, may benefit from Marimastat (Glasspool & Twelves 2001). Additionally, Marimastat seems to increase survival and delay disease progression in patients with advanced gastric cancer (Bramhall *et al.* 2002; Lelongt *et al.* 1997). Musculoskeletal pain is its most important side effect. Today, non-peptido mimetics like BMS-275291, which is assessed for lung, prostate cancer and Kaposi's sarcoma (Lockhart *et al.* 2003), and non-peptidic chemicals like tetracyclines (Kwan *et al.* 2004) are being tested in humans.

1.2.2. Role of MMPs in eye diseases and scarring pathologies in the eye

1.2.2.1. Glaucoma

Glaucoma is a very common cause of irreversible visual loss that affects millions of people worldwide. It is categorized in the following groups; Primary angle closure glaucoma, Primary open angle glaucoma, Paediatric glaucoma and secondary glaucoma (Iridocorneal Endothelial Syndrome (ICE), Inflammatory Glaucoma, Neovascular Glaucoma, Pigmentary Glaucoma, Pseudoexfoliative Glaucoma, Traumatic Glaucoma). In this section we will outline the important role that MMPs play in the pathogenesis of this condition, as well as the potential use of pharmacological MMP inhibition in preventing scar formation following trabeculectomy to promote aqueous humour outflow and reduction of intra-ocular pressure. This is of prime importance, as aberrant wound healing is the leading cause of trabeculectomy failure.

1.2.2.1.1. Aqueous humour outflow

The aqueous humour is produced by the inner non-pigmented epithelial cells of the ciliary processes upon stimulation by circadian rhythms and it is secreted into the posterior chamber. Outflow of the aqueous humour occurs by two different pathways; 85-95% is cleared through the anterior chamber-trabecular meshwork-Schlemm's canal-episcleral veins route and is pressure dependent, whilst 5-15% is cleared through the anterior chamber-ciliary muscle-supraciliary and suprachoroidal space route (uveoscleral outflow) and is pressure independent.

1.2.2.1.2. The association of trabecular meshwork outflow with glaucoma and the role of MMPs.

Studies in cultured human trabecular meshwork (TM) cells have shown that these cells synthesize a wide range of ECM molecules including Collagen I, II, IV, V and VI, proteoglycans, fibronectin, laminin and thrombospondin (Hernandez *et al.* 1987;Polansky *et al.* 1984;Schachtschabel *et al.* 1982;Tripathi *et al.* 1991;Worthen & Cleveland 1982). In Primary Open Angle Glaucoma (POAG), elevated intraocular pressure (IOP) is one of the major risk factors leading to ganglion cell death. Elevated pressure has been ascribed to changes in the trabecular, and more specifically in the juxtacanalicular meshwork, the site with the highest aqueous humour outflow resistance (Rohen 1983). From all the trabecular ECM components, the highly charged glycosaminoglycans (GAGs) are believed to play a significant role in the outflow resistance and subsequently in the elevation of the IOP and in the development of glaucoma. The TM GAGs have been found to be synthesized and degraded more rapidly than those present in cornea and sclera, and to have an average half-life of approximately 1.5 days (Acott *et al.* 1985; Acott *et al.* 1988). The strict regulation of the trabecular ECM is very important, as excessive ECM synthesis or reduced degradation can lead to increased resistance of outflow (or even to obstruction of the intratrabecular outflow channels) (Shields 1992). It has been therefore suggested that proteolytic enzymes such as MMPs are important to maintain normal aqueous circulation through the TM channels (Park *et al.* 1987; Polansky *et al.* 1984; Shuman *et al.* 1988). Human and bovine trabecular meshwork cells have been shown to produce four members of the MMP family, the MMP-1, -2, -3 and -9, which through their proteolytic role may control cleavage of trabecular ECM. They also produce TIMP-1, suggesting that release of this inhibitor may balance MMP activity within the TM (Alexander *et al.* 1991). The basal expression of MMPs is significantly increased after stimulation of the TM cells with TPA, a broad-spectrum phorbol mitogen. Based on these observations it has been proposed that MMPs and their inhibitors may constitute an important part of the homeostatic mechanism that controls the aqueous humour outflow *in vivo*. In normal bovine aqueous humor, with the methods of zymography and Western blot analysis, MMP-2 and -9 and two TIMP members – the TIMP-1 and -2 - have been detected. Moreover gelatinolytic bands representing probably MMP-1 and -7 and an additional gelatinolytic band at ~ 100 kDa have been observed (Huang *et al.* 1996). Kee C *et al* investigated in aqueous humor collected during surgery from patients with POAG, NTG, CACG and cataract the differences in the total

protein concentration and in MMP-2 activity (Kee, Son, & Ahn 1999). They observed double total protein concentration in POAG aqueous samples compared to the NTG, CACG and cataract ones. Additionally, the levels of MMP-2 protein and activity were significantly increased in the aqueous humour of patients with POAG when compared with specimens from patients with cataract (control), CACG and NTG. This increased MMP-2 activity could not be ascribed to tissue reaction to elevated pressure, as patients with CACG and POAG had similar IOP, nor to breakdown of the blood-aqueous barrier, because of the use of pilocarpine. The study suggested that although MMP-2 may have a short-term increasing effect in the aqueous humour outflow by cleaving TM ECM molecules, in a long term it may degrade the basal lamina of TM cells causing TM cell apoptosis and glaucoma. This may be of significance as a reduced number of TM cells has been thought to lead to the pathogenesis of glaucoma. (Kimpel & Johnson 1992;Tschumper & Johnson 1990). In contrast to the above findings, two different studies found significantly reduced MMP-2 activity in aqueous samples from patients with POAG. This supports more reasonably the theory that decreased ECM degradation may facilitate the development of POAG (Maatta *et al.* 2005; Schlotzer-Schrehardt *et al.* 2003).

Using an organ culture model of human anterior segment, Bradley *et al* (1998) observed that addition of activated MMP -2, -3 and -9 to perfusion media caused a 160% increase in the aqueous outflow. In addition, purified stromelysin injected in another experiment of the same study directly three times at 12 hours intervals into the perfusion channel, induced an increase of the outflow by 140%. Confirmation of the involvement of MMPs in this process was achieved by 40% reduction of the outflow when TIMP-2 was added to the perfusion media. Interestingly, extending the anterior segment exposure to MMPs caused a marked decrease in the aqueous outflow, which further demonstrates that TM ECM turnover plays a major role in regulating the aqueous outflow *in vivo* (Kee, Son, & Ahn 1999).

Balance between MMPs and TIMPs, as that seen in many other biological processes, play an important role in the regulation of the TM ECM turnover. Especially in POAG, this is demonstrated by observations that levels of TIMP-1 in the aqueous humour are significantly higher in aqueous of POAG patients than in similar specimens from CACG, CG and NVG patients and control samples (Gonzalez-Avila *et al.* 1995). Furthermore, when investigating the effect of aqueous in an *in vitro* human lung fibroblast migration and collagen production model, the samples from POAG patients decreased collagenase activity and increased collagen production. This response was not observed

with aqueous from CG, CACG and NVG patients or control specimens (Gonzalez Avila *et al.* 1995).

A modern method that is widely used to decrease IOP in glaucoma patients by increasing the aqueous humour outflow is laser trabeculoplasty. Normally, there are 200.000-300.000 TM cells per eye and due to the cell apoptosis its number declines with age, which makes the outflow harder. During the process, 50μm burns with an argon-dye laser are applied to the TM (Parshley *et al.* 1995; Van Buskirk 1989). This induces division of cells in the anterior, non-filtering region of the TM, at the site of insertion into the cornea beneath the Schwalbe's line (Acott *et al.* 1989; Bylsma *et al.* 1988). These cells, which are referred as 'stem cells', divide the first two days after the laser treatment and most of them within two weeks migrate and repopulate the burn sites at the TM (Acott *et al.* 1989).

Several studies have supported the implication of MMPs in ECM turnover following laser trabeculoplasty. Parshley *et al* (1995) after culturing anterior segment explants for seven days, applied clinical parameters of argon laser trabeculoplasty to the cultures. Examination of the culture media for protein expression revealed a significant increase in latent and active forms of MMP-9, glycosylated or unglycosylated active and latent forms of MMP-3 and TIMP-1 in the laser treated group, when compared with sham treated and untreated explants. However, levels of active and latent forms of MMP-2 remained almost unchanged in all groups (Parshley *et al.* 1995). In addition, enhanced mRNA levels coding for MMP-3, MMP-9 and TIMP-1, but not for MMP-2 and TIMP-2 were also observed in the laser treated group. Further investigation by the same group using the same *in vitro* model confirmed the increase in MMP-3 expression after laser treatment and identified that this increase occurs at the juxtacanalicular site and at the site of TM insertion into the cornea and that TM cells were the source of MMP-3 (Parshley *et al.* 1996). The authors, based a) on the hypothesis that the accumulation of glycosaminoglycans causes outflow resistance and subsequently aqueous outflow reduction that occurs in glaucoma, and b) on the fact that Laser Trabeculoplasty (LTP) increases MMP-3 levels as well as the aqueous outflow, suggest that MMP-3 has a potential therapeutic application in primary open angle glaucoma.

The possibility of using MMPs as a therapeutic tool to increase both ECM degradation in the juxtacanalicular channels and aqueous outflow has led to the investigation of molecular pathways that regulate expression of MMPs. Initially, it was found that induction of MMP expression in TM after LTP is mediated by IL-1β and TNFa

(Bradley *et al.* 2000). Unlike IL-1β and TNFα, whose production and secretion are increased by LTP, IL-1α is increased but not secreted after LTP and remains in its pro-form within the cytoplasm of TM cells (Bradley *et al.* 2000). The exact role of IL-1α after LTP is not known, but two mechanisms have been proposed; it either triggers the activation and secretion of IL-1β and/or TNFα intracellularly, or it is released at the site of the laser burn but not in sufficient levels to be detected, where it might activate IL-1β and/or TNFα, which in turn induce MMP transcription (Bradley *et al.* 2000). An important role for IL-1α on MMP stimulation has been shown by observations that following 72 hours culture of TM cells with IL-1α caused an increase in their production of MMP-3, -9 and TIMP-1, with almost no effects on the production of MMP-2 (Samples, Alexander, & Acott 1993). Other studies have also shown that TNFα upregulates MMP-1, -3, -9 and TIMP-1 expression in cultured porcine TM cells, whilst downregulating their production of TIMP-2 without affecting MMP-2 expression (Alexander & Acott 2001). This was shown to involve a cascade of activation of various factors at membrane and intracellular levels: TNF_{α} activates the TNF-R1 55-kDa membrane receptor, which then creates a complex with the TNF receptor-associated death domain (TRADD) and the TNF receptor activation factor (TRAF-2). The steps after the formation of that complex are partially understood, but it is known that c-Raf-1 is attracted to the plasma membrane, where it becomes auto-phosphorylated and activated. A cascade of events is then followed, where this factor then phosphorylates and activates Mek, which in turn phosphorylates and activates Erk. One of the functions of activated Erk is to phosphorylate and activate transcriptional activator proteins which induce the transcription and expression of various MMPs and TIMPs (Alexander & Acott 2003). Other investigations have revealed that the trabecular protein kinase C μ isoform (PKCμ) triggers MMP/TIMP transcription by activating a different pathway (Alexander & Acott 2001). This was indicated by observations that formation of the TNF-R1/TRADD/TRAF-2 complex caused PKCμ but not c-Raf-1/Mek/Erk cascade activation, as demonstrated by the fact that G06976, a PKCμ inhibitor, inhibited MMP/TIMP expression without blocking Erk phosphorylation (Alexander & Acott 2001).

Moreover, other intracellular pathways of MMP activation have been described, which involve the phosphorylation of two sites (S63 and S73) of c-Jun (Hosseini *et al.* 2006). In this pathway, JNK induces transcription through the AP-1 sites of both the MMP-3 and MMP-9 promoters (Angel & Karin 1991;Auble, Sirum-Connolly, & Brinckerhoff 1992;James *et al.* 1993). Phosphorylation of JNK usually occurs through the activated MAPK Kinases MKK4 or MKK7 or both of them (Lawler *et al.* 1998). Treatment of

porcine TM cells with TNFα, IL-1α or IL-1β resulted in increased MMP-3 and -9 production as well as enhanced phosphorylation of MKK4, JNK1/2, c-Jun and ATF-2. Involvement of this activation pathway was clearly shown by the demonstration that JNK inhibitor 2 not only prevented the increased expression of both MMP-3 and -9, but also the phosphorylation of c-Jun and ATF-2. Although ATF-2 is phosphorylated and activated through JNK, a connection between ATF-2 and MMP-3 or -9 transcription has not yet been found. The importance of activation of AP-1 sites in the MMP-3 promoter has been shown in a study performed by Pang IH *et al* 2002 (Pang *et al.* 2003). The use of an AP-1 activator - the tBHQ - in human TM cultures stimulated the expression of MMP-3, whilst pre-treatment with SR11302, an AP-1 inhibitor, prevented the increase of MMP-3 caused by tBHQ. Moreover, tBHQ raised the aqueous outflow and had a significant effect in IOP reduction both in glaucomatous and non-glaucomatous (normal) eyes when it was tested in an *in vitro* human eye perfusion organ culture model. This effect was also blocked by inhibition of AP-1 by SR11302 (Pang *et al.* 2003).

The importance of MMPs in TM ECM regulation has been further supported by studies in a steroid-induced glaucoma (SIG) model (Snyder RW *et al* 1993). The authors studied in post mortem trabecular meshwork explants and in TM cell cultures the effect of dexamethasone treatment on MMPs. Their experiments indicated that reduction occurs in the levels of secreted (extracellular) MMP-3 and MMP-9 in the TM explants while the levels of MMP-2 remained the same. In previous investigations in human SIG specimens, excessive accumulation of glycosaminoglycans (GAGs) and wall thickening in the juxtacanalicular tissue has been observed (Rohen, Linner, & Witmer 1973; Spaeth, Rodrigues, & Weinreb 1977). This accumulation of GAGs and ECM has been thought to be responsible for the elevated IOP in SIG (Francois 1984; Hernandez *et al.* 1983; Johnson, Bradley, & Acott 1990; Knepper *et al.* 1978; Knepper & McLone 1985; Steely *et al.* 1992; Ticho *et al.* 1979; Tripathi, Millard, & Tripathi 1990). They also found that the levels of tPA in the TM explants were reduced. tPA is secreted by TM cells (Shuman *et al* 1988) and is a potent activator of latent forms of MMPs. Addition of dexamethasone to the TM cell cultures caused reduction in stromelysin and tPA, in contrast to MMP-2 that, as in TM organ explants, was found almost unchanged. As in previous studies, MMP-9 was not detected in TM cultures. This is in agreement with previous findings that dexamethasone is capable of inhibiting IL-1a stimulated expression of MMPs in trabecular explant cultures (Samples, Alexander, & Acott 1993) and other tissues (Frisch & Ruley 1987; Frisch *et al.* 1987, Lefebvre *et al* 1990). Due to these findings and to the ECM degrading role of MMPs,

connection between the accumulation of ECM and the reduction of MMPs has been suggested and has been thought possibly to be responsible for the pathogenesis of SIG.

1.2.2.1.3. Exfoliation syndrome (XFS)

Exfoliation or pseudoexfoliation syndrome (XFS) is an age-related disorder characterized by deposition of fibrillar ECM in ocular and non-ocular anatomical structures, but especially in the anterior segment. This pathological condition affects approximately 30% of individuals over the age of 60 and it is often complicated by severe secondary COAG and cataract (Schlotzer-Schrehardt & Naumann 2006). The pathogenesis of XFS is not known, but it has been thought to be caused by a disorder in the basement membrane metabolism (Schlotzer-Schrehardt *et al.* 1992). It is possible that fibrillar ECM, produced in this condition, blocks the juxtacanalicular channels, causing resistance to aqueous outflow, elevation of IOP and subsequently secondary POAG. In some populations, such as the Scandinavians, XFS constitutes the main etiology of more than half of secondary POAG cases. A common sign often found in patients with XFS is the dark pigmentation of the TM. In addition, anterior to the Schwalbe's line, a pigmented streak known as Sampaolesi's line, is usually observed, due to an inferior deposition of ECM. Significant differences exist between exfoliation glaucoma and POAG. Exfoliation glaucoma is characterised by higher IOP, worse prognosis, poor response to LTP treatment and presents many postoperative complications. It often presents monocularly. A comparative study in aqueous humor samples collected from patients with primary open angle glaucoma (POAG), pseudoexfoliation syndrome (PEX), pseudoexfoliation glaucoma (PEXG) and cataract, revealed changes in MMPs and TIMPs levels, which may facilitate a better understanding of the pathological mechanisms involved in these conditions (Schlotzer-Schrehardt *et al.* 2003). In this study, high levels of the latent form of MMP-2 and latent and active MMP-12 were observed. With the use of ultrasensitive immunoassays, very low quantities of MMP-3,-7 and -9 were also found. It was of interest that both TIMP-1 and TIMP-2 were also increased and the concentration of TIMP-1 was six to eightfold higher than TIMP-2. Additionally, active MMP-2 was detected in very low levels, covering only 0.3-1.5% of the total MMP-2 protein. In a similar comparative study the differences in the expression of various MMPs and TIMPs in the same four patient groups (POAG, PEX, PEXG and controls (cataract) were tested (Maatta *et al.* 2005). MMP-14 was detected in all groups in both its soluble active and latent form, although this

molecule is usually bound to the cellular membrane. Lower levels of MMP-13 and MMP-8 were found too, mostly in their latent forms. MMP-8 was found in three out of four POAG aqueous samples in its 55-KDa less glycosylated pro and active isoforms. In contrast, the 75-KDa highly glycosilated isoform was only found in PEXG samples (Maatta *et al.* 2005). Analyses of aqueous samples of patients with PEX and PEXG have revealed increased levels of total protein in individuals with PEX, PEXG and POAG, when compared with cataract patients, only specimens from PEX and PEXG patients had significantly enhanced levels (Maatta *et al.* 2005). Furthermore, total MMP-2, -3 and TIMP-1 were increased in POAG aqueous compared to specimens from cataract patients. However, these levels were lower than in PEX and PEXG aqueous samples, in which TIMP-2 and MMP-12 were also increased. Increased TIMP-1 in PEX samples was also observed by Ho *et al.* (2005). Moreover, they detected elevated TIMP-2 levels in POAG, PEX and PEXG compared with cataract; TIMP-2/MMP-2 ratio was >1 in PEX and PEXG and 0.88 in POAG and only 0.34 in control (cataract) samples in that study. In contrast, Gartaganis *et al* 2002 observed lower TIMP-1 levels in PEX aqueous than in patients with cataract and similar TIMP-2 levels in PEX aqueous and cataract aqueous samples. It was also found that although the levels of total MMP-2 and -3 were increased, the activated form of MMP-2 was significantly decreased, especially in the aqueous collected from PEX and PEXG patients (Schlotzer-Schrehardt *et al.* 2003). More specifically, the ratio of total to activated MMP-2 increased about five times in PEX samples and about four times in POAG samples compared to cataract aqueous samples. With regards to the serum samples that the writers tested as well, only the levels of MMP-9 were significantly decreased in PEX and POAG samples in comparison to the MMP-9 cataract levels and additionally a mild TIMP-1 increase was observed in the PEX serum samples. Since the differences in the levels of MMPs and TIMPs are also found in patients that have not received any glaucoma medication or laser therapy, the authors suggested that the anterior segment tissues and not the blood-aqueous barrier breakdown or any therapeutic approaches are responsible for the concentration changes of the above mentioned molecules. Therefore, the increased levels of TIMP-1 and -2 and the reduced activity levels of MMP-2 may be responsible for the lower degradation and subsequently the accumulation of the PEX material, the resistance on the aqueous outflow, the IOP elevation and the development of secondary glaucoma. This accumulation of PEX material has been suggested to be responsible for the upregulation of the total MMP-2 and -3 as a signal to degrade PEX material. This increase can't be considered as a cause but a result of PEX and PEXG.

Decreased MMP-2 activity in aqueous from PEX is in accordance with the study of Maata M *et al*, who observed an increase in TIMP-2 (Maatta *et al.* 2005). On the contrary, Gartaganis *et al.* (2002) reported that the gelatinolytic activity in PEX samples was increased by about 60%. Based on previous studies which suggested that neovascularization occurs in PEX (Brooks & Gillies 1983; Helbig *et al.* 1994; Ringvold & Davanger 1981), the authors justified raised levels of MMP activity in the facilitation of iris neovascularization. Although there are many discrepancies between these studies, the common conclusion of all is that the increased MMPs (active or latent) are not capable of preventing the accumulation of the PEX material. In comparison with normal aqueous humor, elevated concentrations of TGF-β2 (Tripathi RC *et al.* 1994) and –β1 (Schlotzer-Schrechardt *et al.* 2001, Koliakos *et al.* 2001) have been found in aqueous humor samples from patients with POAG and PEX respectively. TGF-β1 and -2 were found to upregulate genes that were related to secreted proteins or extracellular matrix in trabecular meshwork cells (Zhao *et al.* 2004). This is of significance, as TGF-β2 has been shown to induce the accumulation of ECM, not only by stimulating production of fibronectin from TM cells and inducing irreversible ECM crosslinking, but also by increasing the plasminogen activator inhibitor 1 (PAI1), which subsequently blocks the tPA/uPA→plasmin cascade leading to MMP activation (Fuchshofer R *et al.* 2003). In this study it was shown that TGF-β2 enhancement decreased MMP-2 activity. Furthermore, both TGF-β1 and –β2 induce the expression of tissue transglutaminase in the TM, responsible for cross-linking of the ECM components. This makes the degradation harder (Welge-Lussen, May, & Lutjen-Drecoll 2000) and promotes the accumulation of ECM.

1.2.2.1.4. Uveoscleral pathway

Induction of MMP downregulation is a potential therapeutic target for treatment of most ocular diseases presenting with increased production of these enzymes. However, in uveoscleral outflow the potential target is the upregulation of MMP production for degradation of ECM in the ciliary muscle. Since the extracellular spaces of ciliary muscle form the first part of the uveoscleral outflow, ECM degradation in this region may provide free space for the uveoscleral outflow.

It is known that prostaglandins are effective in IOP reduction and it has been supported that this function is partially succeeded due to the presence of many prostaglandin receptors, mainly FP and EP_2 in the ciliary muscle (Matsuo & Cynader 1992;

Ocklind *et al.* 1996). A relationship between prostaglandin (PG) receptor activation and MMP production has been identified in ciliary muscle cells. Studies have shown that a cascade of intracellular events resulting in MMP production can be triggered by PG binding to FP and EP2 receptors present in ciliary muscle (Matsuo & Cynader 1992; Ocklind *et al.* 1996) This cascade is initiated by G-protein mediated activation of adenyl-cyclase and phospholypases, which then increase the production of cAMP and inositol 1,4,5 triphosphate (IP_3). cAMP in turn triggers the expression of c-Jun and c-Fos, which form homo-and heterodimers that bind to the AP-1 transcription promoter sites and induce expression of MMPs (Schachtschabel, Lindsey, & Weinreb 2000). This is supported by *in vitro* experiments in which human muscle ciliary cells exposed to PGF_{2a} express high intracellular levels of cAMP (Zhan *et al.* 1998), as well as by the finding of cAMP related increase of c-Fos and c-Jun (Lindsey *et al.* 1997; Lindsey, To, & Weinreb 1994). Additionally, cAMP analogues increase c-Fos and MMP-1 expression (Schachtschabel, Lindsey, & Weinreb 2000), whilst PGF2a or other PG analogues were also shown to induce upregulation of MMPs in these cells (Weinreb & Zangwill 1997).

In addition to aqueous humor, the uveoscleral extracellular space also contains several ECM components, including collagen I, III, fibronectin and elastin, whilst the basement membrane enfolding the ciliary muscle cells contains laminin and collagen IV. Topical treatment with PGF2a has been shown to induce reduction of the ciliary ECM in monkey eyes *in vivo* (Lutjen-Drecoll & Tamm 1988) and reduction in collagen I, III and IV production has been observed after addition of PGF2a to human muscle ciliary cells *in vitro* (Lindsey *et al.* 1997) as well as in monkey eyes *in vivo* (Sagara *et al.* 1999). These observations are in accordance with the demonstration that enhanced levels of MMP-1, -2, -3 and -9 may be found in culture supernatants of ciliary muscle cells treated with PGs such as PGF2a, 11-deoxy-PGE1, PhXA85 and latanoprost (Akaishi *et al.* 2004; Lindsey *et al.* 1996; Ocklind 1998; Weinreb *et al.* 1997). A further study involving exposure of human ciliary smooth cell cultures to latanoprost acid, the biological active form of latanoprost, revealed increased mRNA levels of MMP-1, -3 and -9 and a dose-dependent increase of MMP-1 mRNA. However, the levels of MMP-2 mRNA were found to be decreased, which was ascribed to the lack of AP-1 sites in the MMP-2 promoter (Weinreb & Lindsey 2002). Other investigations have suggested that lack of transcriptional elevation of MMP-2 may be associated to intracellular storing of MMP-2 into the ciliary muscle cells (Swallow, Murray, & Guillem 1996) or that PG delay MMP-2 transcription compared to the other

three MMPs (Gaton *et al.* 2001; Swallow, Murray, & Guillem 1996; Taraboletti *et al.* 2000).

In an attempt to explain the molecular mechanisms involved in MMP induction mediated by PGs, it was found that PKC-Erk1/2 dependent pathways are involved in PGF2a induced MMP-2 secretion and activation, as that seen with MMP regulation in the trabecular meshwork (Husain, Jafri, & Crosson 2005). Moreover, it was shown that mRNA and protein levels of TIMP-1 were significantly increased in cultures exposed to latanoprost for 18 and 24 h but not for 6h (Anthony, Lindsey, & Weinreb 2002). In contrast, mRNA and protein levels of TIMP-2 were only slightly elevated after 6h but not after 18h and 24h culture with this compound. Furthermore they observed a time correlation between MMP-1,-2 and TIMP-1 induction. In addition PKC was shown to be involved in the TIMP-1 increase observed after latanoprost exposure of human ciliary muscle cells (Anthony, Lindsey, & Weinreb 2002).

MMP induction by PG has also been observed *in vivo* (Gaton *et al.* 2001). Since early studies had shown that PGF2a Isopropyl Ester had an increasing effect in the uveoscleral outflow in cynomolgus monkeys (Gabelt & Kaufman 1989), the immunoreactivity of MMP-1, -2 and -3 in the uveoscleral pathway following PGF2a Isopropyl Ester treatment was examined in order a potential role of MMPs to be investigated (Gaton *et al.* 2001). They observed a significantly increased immunostaining for these three MMPs. They also observed a link between the ciliary muscle MMP-2 immunoreactivity and IOP reduction. Based on the above results, it has been suggested that by increasing MMP expression, PGs decrease the resistance of the uveoscleral outflow and subsequently reduce the IOP without affecting the trabecular ouflow (Schachtschabel, Lindsey, & Weinreb 2000). It is of interest that previous work from the same group revealed MMP-1 expression in the normal human uveoscleral pathway (ciliary muscle, iris root and sclera exterior to the ciliary muscle) (Schachtschabel, Lindsey & Weinreb 2000).

Parallel to the effect of prostanoids on the ciliary body, application of latanoprost and PGF_{2a} also increase MMP and TIMP production in the sclera (part of the uveoscleral outflow), as demonstrated by observations that enhanced immunoreactivity for MMP-1, -2 and -3 can be induced by topical application of PGF_{2a}-isopropyl ester in monkey eyes (Sagara *et al.* 1999). In addition, topical prostaglandin application resulted in increased levels of MMP-1, -2 and -3, enhanced amount of catabolised collagen and subsequently raised scleral permeability in monkeys (Weinreb 2001). Levels of MMP-1, -2 and -3 were also found to be raised in culture supernatants of scleral tissue exposed to PGF2a or

PhXA85 -the active form of latanoprost- (Kim *et al.* 2001). Further studies showed that human scleral tissue cultured with PGF2a produced significantly higher levels of MMP-1 and -9 mRNAs, whilst latanoprost increased MMP-1 mRNA. A dose dependent increase in mRNA levels of MMP-3 and -10 as well as TIMP-1, -2 and -3 was also observed following treatment of human scleral tissue with latanoprost (Weinreb *et al.* 2004). The expression of TIMPs may occur as a protective mechanism to control excessive MMP scleral ECM degradation. Although TIMP levels are elevated, these are not sufficient to balance MMP activity, which causes increased ECM degradation that facilitates the aqueous outflow through the uveoscleral pathway. Based on these findings, several prostanoids, especially FP agonists, have been used therapeutically to control IOP (Weinreb *et al.* 2004).

1.2.2.1.5. Glaucoma filtration surgery

In clinical cases in which lack of IOP control causes progressive optic neuropathy and loss of visual field despite laser trabeculoplasty and use of conventional drug therapies, glaucoma filtration surgery known as well as trabeculectomy is the treatment of choice (American Academy of Ophthalmology 2005). In trabeculectomy, a partial thickness filter formed by removing limbal tissue from beneath the scleral cup creates a new drainage channel for the aqueous humor. This procedure facilitates IOP control as it lowers the IOP without causing hypotony or other complications associated with full thickness procedures. The effects of trabeculectomy will remain as long as the drainage channel remains functional. This has been found to depend on the wound healing response and the formation of scar tissue at the subconjunctival space, which if excessive, can gradually reduce and finally block the aqueous drainage, causing again elevation of the IOP (Wong *et al.* 2002).

The wound healing process that takes place in the eye after trabeculectomy presents significant similarities with the dermal wound healing (as described above). After the incision, plasma proteins and blood cells are released into the wounded area and a fibrin clot is formed. Neutrophils and macrophages are then attracted to the area, where they degrade the clot by releasing various degrading enzymes, including MMP-8 and -9. Activation, proliferation and migration of fibroblasts is then observed (Wong *et al.* 2002). Before activation, fibroblasts are found as quiescent undifferentiated mesenchymal cells known as fibrocytes in low numbers in the subconjunctival connective tissue (Tenon's capsule) (Wong *et al.* 2002). After their activation, fibroblasts, not only produce large

amounts of ECM molecules such as collagens, glucosaminoglucans, elastin, but also various MMP molecules, which further facilitate fibroblast migration and organization of the newly formed ECM. MMP-1, MMP-2, TIMP-1 and TIMP-2 staining has been detected in the cytoplasm of fibroblasts from human subconjunctival connective tissue. Comparison between normal and healing conjunctiva specimens showed that MMP-1 and TIMP-1 were located only in the healing subconjunctival tissue and not in normal subconjunctival tissue or conjunctival epithelium (Kawashima Y *et al* 1998). Because of these findings, it has been suggested that the MMP-TIMP expression and activation alterations may play an important role in the post-operative cell proliferation and subconjunctival scarring (Kawashima *et al.* 1998). Moreover, expression of other MMPs and TIMPs, including MMP-1, -2, -3, -9, -14 and TIMP-1 and -2 has been detected in cultured human Tenon's fibroblasts (Mietz *et al.* 2003). During fibroblast migration over the fibronectin interface, traction forces are generated by fibroblasts in the underlying substrate causing wound contraction (Harris, Stopak, & Wild 1981). Fibrovascular granulation tissue is gradually formed at the site of injury, whilst part of the fibroblast population differentiates into myofibroblasts due to mechanical stress and growth factor stimulation (mainly TGF-β and PDGF). After months of continuous remodeling of the granulation tissue and apoptosis of myofibroblasts, dense collagenous subconjunctival scar tissue is formed. Extended fibrosis and tissue contraction finally block the aqueous outflow channel. This causes loss of function of the bleb with subsequent increase of IOP (Harris, Stopak, & Wild 1981).

Using an *in vitro* model of wound healing, it has been shown that inhibition of MMPs induces inhibition of contraction of collagen I lattices populated by HTF (Daniels *et al.* 2003a; Porter *et al.* 1998). Comparison between three MMP inhibitors (MMPIs) – Ilomastat, BB-94 and Cell-Tech- revealed inhibition of gel contraction with the application of all the three MMPIs in a dose-dependent manner, although ilomastat was proven to be the most effective (Daniels *et al.* 2003a). In addition to inhibiting collagen contraction, ilomastat also reduced collagen production from fibroblasts in a dose-dependent manner (Daniels *et al.* 2003a). This is of special importance, as excessive collagen production and deposition at the trabeculectomy area is responsible for bleb failure (Cordeiro *et al.* 2000; Daniels *et al.* 1998). Due to these observations, MMP inhibition has been considered to be an ideal therapeutic target to prevent excessive scarring after glaucoma filtration surgery. Application of ilomastat in an *in vivo* trabeculectomy model significantly prolonged the bleb survival and lowered the IOP effect (Wong, Mead, & Khaw 2003). Histological assessment showed reduction of scar tissue in the ilomastat treated group when compared

to the control group. In the treated group reduction of scar tissue was accompanied by decreased number of myofibroblasts and reduced apoptosis, as well as a bigger bleb area.

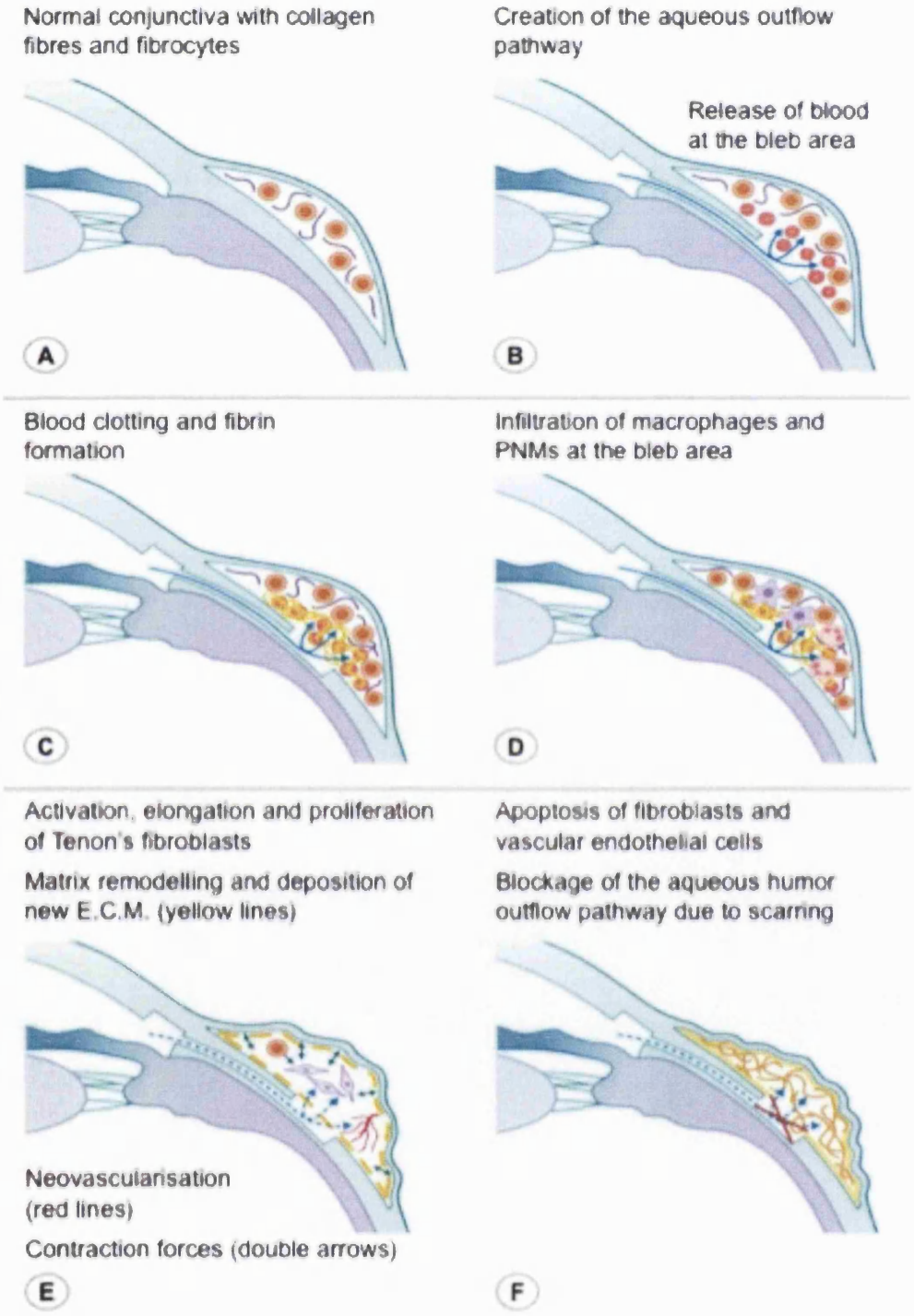

Figure 5: The wound healing process after glaucoma filtration surgery.

Comparison of the antiscarring effects of ilomastat with MMC, the main antiscarring post-trabecular therapy, showed that the ilomastat treated group had similar

prolonged bleb survival and IOP lowering results to the MMC treated group and significantly better outcome for both factors than the control group. In addition, the subconjunctival tissue morphology was normal in the ilomastat group but hypocellular in the MMC (Wong, Mead, & Khaw 2005). Although ilomastat has potential advantages for clinical application, such as lack of toxicity (based on the observations during the in vivo experiments), target specificity, possible less side effects and better tolerance than antimetabolites, several problems have to be solved before it can be used therapeutically. Determination of optimum doses and formulation of slow release drug delivery systems would facilitate the administration of ilomastat to control intraocular scarring in humans.

1.2.2.1.8. Optic nerve head (ONH)

The lamina cribrosa is a sieve-like small section of the sclera at the posterior pole that is formed by fibroelastic lamellae, the cribriform plates, which are placed in order to create channels for the exit of the non-myelinated axons of retinal ganglion cells (RGCs). These axons converge at the optic disc and after their passage from the lamina cribrosa become myelinated. In the cribriform plates, astrocytes are organized in a vertical position to the RGC axon and parallel to the optic nerve head. They are separated from the ECM components of the cribriform plates-proteoglycans, collagen and elastic fibers- by basement membranes (Agapova *et al.* 2001;Agapova *et al.* 2003;Anderson 1969).

In POAG, the cause of blindness is the progressive and irreversible loss of RGC axons. Parallel to the loss of axons, cupping of the optic disc – backward bowing- and reorganization of the cribriform plates are observed. Several studies suggest that rearrangement of the cribriform plates occurs because of increased IOP (Johnson *et al.* 1996;Pena *et al.* 2001) and damages of the nerve axons (Bellezza *et al.* 2003), which may occur as a consequence of tissue remodeling (Hernandez & Pena 1997). At the ECM level, elastotic degeneration and reduction of collagen take place at the optic disc region (Agapova *et al.* 2001;Hernandez 1992;Pena, Mello, & Hernandez 2000;Quigley, Brown, & Dorman-Pease 1991;Varela & Hernandez 1997), whilst activated astrocytes migrate from the basement membranes of the cribriform plates into the nerve beams.

MMPs and TIMPs have been shown to be implicated in the pathogenesis of glaucoma, as they play a crucial role in the remodeling of the optic disc structures and in the survival of RGCs. Staining for MMP-1, -2 and -3 has been detected in both normal and glaucomatous eyes (Yan *et al.* 2000). In normal eyes, MMP-1 was found in the cytoplasm

of a small number of laminar and postlaminar glial cells at the ONH and around the axons. In all of these regions and additionally in prelaminar RGCs, staining for MMP-2 and MMP-3 was also detected. It is worth mentioning that MMP-3 staining was observed in fewer glial cells. In glaucomatous eyes, the intensity of staining and the number of stained cells for these three MMPs were increased. In the case of NPG eyes, stronger staining for MMP-2 was revealed around pial blood vessels and axons than in POAG eyes. Staining for MMP-2 was also found at the reorganized laminar plates and at the pial septae that covers the cavernous spaces, as well as in astrocytes in these regions (Yan *et al.* 2000). Other investigations have reported low MMP-1 reactivity in the optic nerve region of normal eyes, which has been detected in astrocytes in the prelaminar, laminar and in the postlaminar optic nerve. However, in glaucomatous eyes, MMP-1 staining of reactive astrocytes in the cribriform plates and in the nerve bundles as well as in small vessels located in ONH has been observed (Agapova *et al.* 2001). In addition, MMP-14 was found to be associated in the ONH with astrocytes and blood vessels located at the lamina cribrosa in normal eyes. Enhanced MMP-14 immunoreactivity was found in glaucomatous eyes in the lamina cribrosa and the post laminar optic nerve, laminar region and post laminar optic nerve of normal eyes has also been shown (Agapova *et al.* 2001). Unlike that reported by Yan X *et al*, Agapova OA *et al* did not find quantitative differences in MMP-2 expression between normal and glaucomatous eyes (Agapova *et al.* 2001). MMP-3 was not found to be associated with astrocytes and MMP-3 staining was detected only in the blood vessels throughout the ONH region. Staining for MMP-7,-9 and -12 in normal and glaucomatous ONH was not found, but TIMP-1 and -2 staining was detected in astrocytes and RGCs axons in the prelaminar and laminar region, as well as in RGCs axons and astrocytes lining the pial septa, with no significant differences among normal and glaucomatous eyes. Based on these observations, it was suggested that increased MMP-1 expression leads to excessive degradation of collagen fibbers, the main pathological characteristic of the ECM in cribriform plates of glaucomatous eyes. This may facilitate the migration of astrocytes to the nerve beams. MMP-14 is thought to play a role in the transformation of quiescent into active astrocytes, TIMP-1 and -2 are believed that after their production at the RGCs soma in the nerve retina layer, they are transferred to the axons and one of their functions is to protect the axons from MMP-proteolysis. This was supported by studies in an experimental model of glaucoma in monkeys, in which increased levels of MMP-1 and -14 were expressed by reactive astrocytes in the glaucoma eyes, when compared with quiescent astrocytes from normal eyes. Interestingly, specific

reactive astrocytes expressing these proteolytic enzymes were migrating into the nerve bundles, suggesting that these two MMPs may have an important role in cell movement. Additionally, the astrocytes in the same study obtained reactive phenotype only in the experimental glaucoma eyes and not in eyes that experimental transection of the optic nerve was performed in order the pathological differences among the two pathological situations to be investigated. Moreover, the writers didn't observe migration of the astrocytes into the nerve bundles at the optic nerve transection eyes (Agapova *et al.* 2003). Furthermore, ECM remodelling has been shown to occur only in glaucoma and not in the case of optic transection, which can be explained by the lack of activated astrocytes and increased MMP levels (Agapova *et al.* 2003;Pena *et al.* 2001). These results, together with previous studies, suggest that the stress caused to the cells by high IOP, induces astrocytes to become reactive and subsequently to produce ECM molecules like elastin and tenascin, as well as MMPs, and to commence the remodeling process of the optic nerve head (Pena *et al.* 1999b;Varela & Hernandez 1997;Wax *et al.* 2000). It was suggested by Agapova OA *et al* that increased IOP may lead to enhanced MMP-14 expression, which upon activation of MMP-2 may facilitate the activation and migration of astrocytes. By cleaving collagen, MMP-1 may open paths for the migration of reactive astrocytes, and if not inhibited by TIMP-1, it may degrade other ECM molecules that are important for the axonal survival. It was also proposed by the authors in the same study that the destructive role of MMPs in the RGCs axons may continue even after lowering of the IOP (Agapova *et al.* 2003).

At cellular level, it has been reported that elevated IOP may affect the RGCs –brain signalling transportation by compressing the axons and affecting neurotrophin transfer. The mechanisms by which RGC apoptosis occurs is unknown, but it has been suggested that ischemia, high levels of extracellular glutamate, nitric oxide production, downregulation of glutamate transporters may play an important role in this process (Chintala 2006). Although it has been generally believed that ischemia causes accumulation of extracellular L-glutamate, which in turn induces overstimulation of glutamate ionotropic receptors (NMDA, APMA, kainate) and NMDA-mediated RGC death, recent observations have shown that glutamate and NMDA cytotoxicity do not reduce the survival of purified RGCs, but that of amacrine cells (Ullian *et al.* 2004).

From all the members of the MMP family, MMP-9 is considered to act negatively on neuronal survival. Previous studies have shown that MMP-9 deficient mice are resistant to neuronal cell apoptosis after brain injury or ischemia (Asahi *et al.* 2001; Rivera *et al.* 2002; Wang *et al.* 2000). Using an experimental model of ischemia induced by transient

ligation of the optic nerve, which presents similarities to the glaucoma pathology, increased levels of MMP-9 associated with activation of astrocytes in the retinal gagglion cell layer as well as increased gelatinolytic activity and degradation of laminin in the ILM were observed (Chintala *et al.* 2002; Zhang, Cheng, & Chintala 2004b). This is of relevance to the glaucoma pathology, as laminin is important for cell-ECM interactions and subsequently for cell survival. The increased levels of MMP-9 observed in this model may be responsible for the degradation of laminin, which triggers the apoptosis of RGCs, as suggested by observations that MMP inhibitors (GM6001) caused a reduction in RGC apoptosis. These findings lead the authors to suggest that MMP-9 also plays a crucial role in this pathogenic process (Zhang, Cheng, & Chintala 2004a). Participation of MMP-9 in pathological mechanisms involved in the development of glaucoma has been further supported by *in vivo* and *in vitro* experimental studies. Increased IOP in an experimental rat model of glaucoma was found to raise the levels of MMP-9 and TIMP-1, whilst reducing immunostaining for laminin (Guo *et al.* 2005). Although MMP-9 activity in this study was related to RGC apoptosis, the mechanisms by which this process occurred are not clear. It was suggested that either high IOP has a direct effect on MMP-9 increase, which then causes damage to the RGCs, or that increased IOP causes mechanical damage to RGC bodies at the ONH. This could possibly lead to MMP-9 upregulation and consequently to ECM changes (Guo *et al.* 2005). Upregulation of MMP-9 was suggested to be caused by hyper-stimulation of glutamate receptors on RGCs by kainic acid, a non-NMDA receptor agonist (Zhang, Cheng, & Chintala 2004a). The non-NMDA antagonists NBQX and CNQX block this increase and as glutamate accumulates extracellularly in glaucoma ischemia *in vivo*, it may trigger MMP-9 expression. In addition to inhibiting MMP-9, TIMP-1 has been shown neuroprotective activity (Tan *et al.* 2003). This suggests that increased levels of TIMP-1, observed in experimental glaucoma (Guo *et al.* 2005), apart from inhibiting MMP-9 activity, may also protect retinal neurons. Although TGF-β2 accumulation in ONH correlates with IOP exposure, it was found to be decreased in the retina of experimental induced glaucoma. Although this factor is a potent MMP-inhibitor, its reduction can probably explain the ineffective blocking and subsequently the elevated MMP-9 activity (Cordeiro 2002;Guo *et al.* 2005; Pena *et al.* 1999a).

1.2.2.2. Cornea

Several research groups have investigated the expression of MMPs in normal cornea by testing primary corneal cell cultures and corneal explants. Primary cell cultures of corneal fibroblasts only express MMP-2 as detected by zymography (Fini & Girard 1990b). This MMP can be extracted from the normal corneal stroma and endothelium in organ cultures mostly as proenzyme (Fini & Girard 1990a) and is localised extracellularly. Although it has not been possible to isolate MMP-2 from the corneal epithelium of rats and rabbits (Fini, Girard, & Matsubara 1992), with the use of a monoclonal antibody, light intracellular staining for MMP-2 has been identified in human corneal epithelial cells (Kenney *et al.* 1998). In addition, TIMP-1 has been found in normal corneal epithelium and endothelium, whilst TIMP-2 and TIMP-3 have been observed in epithelium, endothelium and keratocytes. It has been proposed that MMP-2 is important for the maintenance of the normal corneal structure because it cleaves denatured collagen molecules and possibly promotes the right orientation and positioning of new collagen fibrils (Fini & Girard 1990b). MMP-14, a membrane bound MMP molecule that has been proven to play a very vital role in the activation of MMP-2, has been mostly found in normal rat corneal stroma and seldom in corneal basal epithelial cells (Ye *et al.* 2000).

1.2.2.2.1. Corneal wound healing

During corneal injury, the wound healing process varies according to the type of corneal layers affected. If only the corneal epithelium is damaged, epithelial cells in the basal layer near the wound margin lose their hemidesmosomal attachments and flatten, their actin cytoskeleton is reformed to become a motile phenotype and migrate to the damaged area. At the site of epithelial damage, they form filopodia and lamellipodia in order to expand over the affected area. This is followed by epithelial cell proliferation and re-establishment of cellular bonds. Cells localised at the basal layer appear to have the task of re-establishing the thickness of the epithelium by moving upwards; these cells are thought to be born from stem cells located at the limbus (Daniels *et al.* 2003b; Dua & zuara-Blanco 2000; Hanna & O'Brien, 1960).

In cases where both the Bowman's layer and the epithelium are damaged, there is not restoration of the initial cellular structure, and, in the long term, epithelial cells or stromal tissue replace the Bowman's layer. When the stroma is affected, keratocytes

adjacent to the wound become activated and migrate to the wounded area beneath the newly formed epithelium, where they differentiate into myofibroblasts and then proliferate and produce ECM. The maximum fibroblast density is observed during the period of restoration of the epithelial thickness (Moller-Pedersen *et al.* 1998). This newly synthesized ECM, in contrast to the lamellae in the unwounded cornea, which run parallel to the corneal surface and are perfectly organised in order to create the corneal transparency, has a slightly different structure from the normal tissue. The collagen is increased in diameter and is embedded in random directions resulting in corneal opacity. Both the contractile ability of myofibroblasts and the embedding of the newly synthesized ECM contribute to the wound closure. The remodelling of the ECM is a continuing process that can last for months, during which the size and the arrangement of collagen fibrils promote the restoration of the normal parameters and the opacity is gradually reduced. Finally, Descemet's membrane can be replaced -in contrast to the Bowman's layer- by the endothelial cells that produce it, but damaged endothelial cells are not replaced; the endothelial cells that exist at the wound edge flatten in order to cover the gap that occurs as result of the wound.

1.2.2.2.2. Corneal wound healing and MMPs

The presence of specific MMPs seems to be an important element in the corneal wound healing process. In this chapter, we will discuss not only the role of MMPs and factors that trigger MMP production, but also therapeutic approaches to prevent extended corneal scarring, which target MMPs and factors that take part in pathways that lead to MMP synthesis and activation.

Due to the fact that corneal fibroblasts in culture exhibit similar morphological characteristics to those of activated stromal fibroblasts in the healing cornea *in situ*, they have been widely used as *in vitro* experimental models. Fini & Girard *et al* 1990b) detected different patterns of MMP expression in passaged cultures compared to primary corneal fibroblast cultures. Synthesis of MMP-1, -3 and -9, both mRNAs and proteins, which were absent in primary cultures, were observed after various cell passages *in vitro*. In addition, the use of inflammatory mediators like phorbol myristate acetate triggered activated fibroblasts in passaged cultures to produce significant higher amounts of these MMP molecules. This has led to the suggestion that inflammatory factors released at the wounded

site *in vivo* could promote the expression of MMPs by stromal cells. It was of interest that cultured corneal epithelial cells isolated from rabbit corneas, when stimulated with PMA, produce large amounts of MMP-9 and small quantities of MMP-2 (Fini *et al.* 1991).

Further observations have implicated MMPs in the corneal healing process. *In vivo* experiments using keratectomy to initiate wound healing showed increased levels of MMP-2, both in active and pro-active form, localised in the corneal stroma (Matsubara *et al.* 1991). Furthermore, pro-active and active MMP-2 have only been found at the newly formed ECM when, at the same time, no quantitive differences of MMP-2 can be found at the wound edges. Interestingly, MMP-2 does not increase immediately after wounding, but the peak of MMP-2 production coincides with the migration and proliferation of fibroblasts into the damaged tissue, the deposition of new ECM and the cleavage of the destroyed collagen. This process occurs during the first week after wounding, after which the levels of both active and pro-active MMP-2 decrease. However, after a period of seven months, MMP-2 levels remain increased in comparison to the levels found in normal cornea (Fini, Girard, & Matsubara 1992).

The pro-active form of MMP-9, which is not observed in normal cornea, has been detected in corneal epithelium, stromal and endothelium layers of wounded tissue. Unlike MMP-2, which is produced at a later stage of the healing process, MMP-9 upregulation is transient. It can be detected immediately after injury, but after a short period (2-4 weeks depending on the depth of the wound) it disappears from the injured tissue (Fini, Girard, & Matsubara 1992). Although MMP-9 is found in its pro-active form in wounded cornea, it has been shown to have significant proteinolytic activity in this state (Matsubara *et al.* 1991), possibly due to a restricted local activation of MMP-9 that occurs beneath the epithelium during initial stages of the healing process (Fini, Girard, & Matsubara 1992). Further work has shown that MMP-9 production takes place at the site of the migrating keratinocytes in the epithelial wound closure margins (Fini *et al.* 1996; Fini, Cook, & Mohan 1998) and that no MMP-9 production can be detected in wounds that affect only the epithelium and not the basement membrane. Additionally, two peaks in the expression of MMP-9 during corneal wound healing in rabbits have been observed (Sakuma, Miyachi, & Sakamoto 2000), which support the existence of two stages in the corneal wound healing: the first phase represents the re-epithelialisation process, and the second phase represents the basal membrane remodelling. Investigations using an *ex vivo* human corneal tissue wound healing model showed that staining for MMP-9 could be detected in the epithelial basal cells at the multi-layered epithelium of the healing tissue, whilst MMP-9 staining in

the stromal cells was absent (Daniels *et al.* 2003b). Using a transgenic mice model, expression of MMP-9 by basal keratinocytes during wound healing has been shown to be controlled through the expression of three specific transcription factors- AP-2, Sp-1 and NF-κB. The extensive expression of Sp-1 and AP-2 is regulated by interaction between migrating epithelial cells and fibronectin deposited from the tear film beneath the migrating epithelium. Sp-1 and AP-2, together with the presence of NF-κB binding site in the MMP-9 promoter (this binding site is not found in other MMPs), reveal the importance of these transcription factors in the differences from the other MMPs expression pattern of MMP-9 during corneal wound healing (Mohan *et al.* 1998).

Recently, a more specialised mechanism for the control of the MMP-9 promoter has been identified. It involves the transcription factor Pax6 gene, which is important for the regulation of eye development in a wide range of species (Glaser *et al.* 1994b; Glaser *et al.* 1994a; Grindley, Davidson, & Hill 1995; Halder, Callaerts, & Gehring 1995; Hill *et al.* 1991). One of the characteristics in the structure of the Pax protein family is a paired DNA –binding domain. The most frequently found Pax6 type, the p46, consists of a homeobox and a PD binding domain (Epstein *et al.* 1994; Sivak *et al.* 2004). It has been shown that Pax-6 expression correlates with MMP-9 promoter in the developing and adult eye (Sivak *et al.* 2000). Moreover, Pax-6 is upregulated together with MMP-9 promoter activity in the closing edges of the epithelium after injury, a fact which led to the hypothesis that in the re-epithelialization phase after wounding, Pax-6 could serve as the driving force for triggering MMP-9 expression (Sivak *et al.* 2000). With the use of an electrophoretic mobility shift assay, two potential binding sites for the Pax-6 PD were found in the MMP-9 promoter and, interestingly, they are located adjacent to an AP-2 or an Sp-1 site (Sivak *et al.* 2000), important in activating the MMP-9 promoter, as mentioned previously. Further studies in this field revealed that Pax-6 is directly attached to one of the two sites of the MMP-9 promoter through the PD domain and indirectly to the second with the cooperation of AP-2α, which has been detected in the basal layer of the corneal epithelium (Sivak *et al.* 2004). How unique the importance of Pax-6 is for normal wound healing and how vital the Pax 6-MMP-9 promoter interaction is have been shown in two studies using heterozygous Pax 6 *in vivo* models (mice $Pax6^{+/-}$) and corneal epithelial $Pax6^{+/-}$ cell cultures to test the effect of this genotype in corneal wound healing. The most noteworthy differences compared to the wild type were found to be the reduction of MMP-9 expression in the migrating front of corneal wounds and cell cultures, faster healing and higher rate of corneal re-epithelialization, increased inflammation, stromal cell apoptosis and enhanced deposition

of fibrin (possibly because of the MMP-9 reduction, which leads as well to the corneal opacities found in the $Pax6^{+/-}$ mice phenotype) (Ramaesh *et al.* 2006; Sivak *et al.* 2004). The molecular mechanisms behind these pathological findings seem to be the earlier increase of IL-1α and the delayed activation of Smad-2 transcription factor (Mohan *et al.* 2002). Based on these experimental results, it is possible to suggest that Pax-6, by controlling the promoter of MMP-9 and other paths and molecules, may constitute a key mechanism for the maintenance and remodelling of the adult cornea.

It is of interest that during remodelling of the epithelial basement membrane, both MMP-9 and MMP-2 participate in specific but different roles. After wounding, MMP-9 seems to degrade basement membrane as well as laminin-5, which is embedded beneath the epithelium during the epithelial resurfacing, and collagen VII fibrils, which are later deposited to replace the basement membrane (Fini, Cook, & Mohan 1998; Fini & Slaugenhaupt 2002). After downregulation of MMP-9, collagen VII fibrils become visible and accumulate between the epithelial layer and the stroma, forming a new basement membrane. This collagen VII lamellae structured basement membrane does not last for more than six months, because it is dissolved, possibly by the increased levels of MMP-2 that gradually accumulate at the stroma, and that has been found to be responsible for the remodelling of the newly deposited ECM that fills the wound gap of the corneal stroma. Although MMP-9 seems to initiate the degradation of the basement membrane, MMP-2 is the dominant gelatinase that remodels the randomly deposited collagen fibrils in the wounded area in a process that lasts for about 1.5 years (Fini, Girard, & Matsubara 1992).

Interesting findings have been recently published on observations in an experimental model of corneal burn *in vivo.* In this model, basement membrane degradation occurs just after re-epithelialization of the burned region, suggesting that corneal cells and their protein products are responsible for the damage of the basement membrane rather than the inflammatory cells or their products that accumulate at the region after the burn (Fini *et al.* 1992). The delayed restoration of the epithelial basement membrane that occurs in corneal burns has been found to be caused by excessive proteolytic degradation affecting laminin-5 and mostly collagen VII- molecules, which are destined to restructure the epithelial basement membrane. The use of cycloheximide, a protein synthesis inhibitor, blocks membrane degradation after thermal burn (Matsubara, Zieske, & Fini 1991). Comparison between the levels of gelatinases produced in experimental models *in vivo* following thermal burn and mechanical injury revealed a significantly higher production of these MMPs in the thermal burn model. Evidence that MMP-9 is responsible for the

degradation of the basement membrane was demonstrated by findings that inhibition of MMP-9 production by cycloheximide in the thermal burn model blocks degradation of the basement membrane (Fini *et al.* 1996; Fini, Cook, & Mohan 1998).

In addition to gelatinases, later studies revealed the production of other MMPs not normally produced in the intact cornea. Using primary cultures of carefully isolated corneal epithelium and stroma, Girard *et al* (1993) observed that non-glycosylated and glycosylated types of the latent MMP-1 are produced by stromal cells but not from the epithelium. It was thought that the main role of epithelial cells is the production of cytokines that induce or inhibit the activation of MMP-1 (He *et al.* 1989; Johnson-Wint 1980; Johnson-Wint 1988). Upregulation of MMP-12 mRNA and protein expression has been observed in corneal myofibroblasts of rabbits after alkali burns (Iwanami *et al* 2009).

In contrast, other studies using whole human corneas or limbal corneal rims have shown that epithelial cells at the wound edges express MMP-1 during their migration over the Bowman's Layer when no intact epithelial layer exists. However, when the epithelial monolayer is developed over the basal membrane, the epithelial cells stop expressing MMP-1. Because of this finding, it has been proposed that MMP-1 is important for the epithelial migration over collagen I, the main component of the Bowmann's Layer. However, stromal cells continue the production of MMP-1 until the development of the multilayered epithelium and then the mechanism of MMP-1 production is switched off in stromal cells as well (Daniels *et al.* 2003b). Moreover, from examination of tissue repair mechanisms using animal explant cultures, it has been found that production of latent MMP-1 from stromal cells commences at the early stages of corneal wound healing (even from the first 24h) and gradually increases to peak between 1 and 4 weeks after injury. However, the levels of production do not seem to correlate with the rate of cell proliferation and decline. Evidence that MMP-1 is not produced in intact cornea but that production of this MMP is upregulated after corneal wounding, where it persists for a long period, indicates the need for MMP-1 during collagen turnover that occurs during stromal remodelling (Girard *et al.* 1993).

The expression of MMP-1 is a multi-step process in which corneal epithelial cells, in addition to producing MMP-1, have been shown to trigger the production of this collagenase from stromal fibroblasts. Studies revealing the signalling behind the collagenase production from stromal fibroblasts during wound healing have been reported. These show that corneal epithelial cells *in vitro* produce IL-1α, which is able to stimulate MMP-1 production from stromal cells (Strissel, Rinehart, & Fini 1997), as well as TGF-β2

(Strissel, Rinehart, & Fini 1995), which inhibits collagenase production (Edwards *et al.* 1987). In addition, many inflammatory cells that infiltrate the cornea during the wound healing process have been shown to produce factors that promote MMP-1 expression (Fini, Cook, & Mohan 1998). Fini ME *et al* (1994) and West-Mays JA *et al* (1995) (Fini *et al.* 1994; West-Mays *et al.* 1995) proposed that collagenase expression triggered by PMA and cytochalasin B *in vitro* on early passage corneal fibroblast cultures is mediated by IL-1α, as the addition of an IL-1 receptor antagonist in the cultures blocks almost all the expression of the MMP-1. Furthermore, early passaged corneal fibroblasts have been found to produce IL-1α, which activates an autocrine feedback loop, leading to a continued production of collagenase without external stimuli. This mechanism is missing from freshly isolated corneal fibroblasts, which are capable of producing only a limited amount of MMP-1 under stimulation with exogenous cytokines (West-Mays *et al.* 1995). These observations highlight the importance of activation of the IL-1α loop for induction of the changes occurring in the fibroblast cytoskeleton, which give these cells their remodelling appearance (West-Mays *et al.* 1997).

In contrast to MMP-1 which is only found in latent form, zymography bands corresponding to proactive and small levels of active forms of MMP-3 were detected in corneal stroma after injury (Girard *et al.* 1993). The main role ascribed to MMP-3 by the authors was to facilitate the activation of MMP-1. Additionally, as MMP-3 is specialised in the degradation of proteoglycans, it was thought that this enzyme may be involved in the restoration of the normal ratio between decorin and lumican in the repaired cornea. The 3:2 ratio of these two proteins observed in the normal cornea is changed after injury, when decorin accumulates at higher levels. Decorin plays an important role in the correct hydration of the cornea, which is necessary for its transparency. The changed balance between these two molecules is believed to be an important factor responsible for the opacity in the damaged area of the cornea (Girard *et al.* 1993). In determining the exact location of MMP-3 expression after injury, it has been reported that staining for this MMP may not only be observed in the stroma, but also in the stromal cells that migrate over the basal layer and beneath the epithelial cells. As with MMP-1, expression of MMP-3 has not been observed in corneal samples after the creation of the multilayered epithelium. This suggests that restoration of the multilayered epithelium could serve as the stopping signal for the synthesis of these two MMPs (Daniels *et al.* 2003b). In the same study, expression of MMP-10 was observed not only in the wound edges of the corneal epithelium, but also in the epithelial cells attached to the basal membrane behind the wound margins.

Interestingly, even after the formation of the epithelial monolayer staining for MMP-10 was found and only when the cornea gained its full thickness, an end signal of MMP-10 expression was seen in half of the samples (Daniels *et al.* 2003b).

Examination of the expression of other MMPs in human cornea has shown that MMP-14 may be found in post-mortem human corneas, as detected by western blot analysis (Smine & Plantner 1997). Other investigations in a rat corneal wound model have shown that staining for MMP-14 is mainly present in the superficial stromal keratocytes and in the lower level in basal epithelial cells (Ye *et al.* 2000). MMP-14 is believed to be proangiogenic, due to its cleavage of the antiogenic function of decorin. MMP-14 may cleave this component directly, or in-directly by inducing the activation of MMP-2 (Mimura *et al.* 2009). Additionally, Onguchi *et al.* (2009) demonstrated that MMP-14 was vital for the angiogenic role of bFGF. It has been observed that the levels of both MMP-14 and bFGF are increased in corneal wound healing. This study suggested that bFGF induces the expression of MMP-14, which enhances the expression of VEGF and subsequently induces corneal neovascularisation. MMP-13 is only detected in epithelial cells of wounded corneas (Ye *et al.* 2000). TIMP-1 has been found beneath the epithelial cells monolayer formed after wound healing and deeper in the stroma creating what is thought to serve as a restriction area for MMP activity, thus allowing MMP function mainly close to the wound edges (Daniels *et al.* 2003b).

1.2.2.2.3. Wound healing after photorefractive keratectomy (PRK) and laser assisted in situ keratomileusis (LASIK).

Following excimer laser keratectomy, the wound healing process may induce different and unpredictable results in the visual outcome of individuals (Azar *et al.* 1996). Histological changes, such as transient epithelial hyperplasia and subepithelial fibroblast proliferation leading to subepithelial haze and stromal scarring (McDonald *et al.* 1990; Marshall *et al.* 1988) as well as intrastromal epithelial migration, have been observed after excimer laser keratectomy (Jain *et al.* 1996). Leucocytes appear to be generally absent from the wounded area after deep excimer laser keratectomy, as seen in mild corneal thermal burns (Matsubara, Zieske, & Fini 1991). As a result, inflammatory products released by leucocytes, mainly MMPs and cytokines, do not seem to participate in the formation of scar tissue after excimer laser keratectomy (Azar *et al.* 1996). Investigation of the expression

and role of MMPs after this surgical procedure in cornea using an *in vivo* rat model has shown the presence of latent and activated MMP-9 forms in epithelium and stroma following excimer laser keratectomy (Azar *et al.* 1996). Persistence of MMP-2 expression in the stroma after excimer laser keratectomy has been shown as well. MMP-9 was only detected during the period of wound closure and neither during the first hours after laser surgery nor after wound closure (Azar *et al.* 1996). Differences in MMPs' expressions, especially MMP-9, compared to unwounded corneas or debridement wounds indicate a potential role of MMPs in wound healing after excimer laser keratectomy. This is further supported by observations that application of the synthetic MMP inhibitor β-mercaptomethyl tripeptide resulted in significantly reduced intrastromal epithelial migration (Azar *et al.* 1996). Additionally, with the use of an anti-MMP-9 antibody and confocal microscopy, the presence of MMP-9 was identified in the outer borders of these intrastromal islets that we mentioned previously (Maeda *et al.* 1998). Other studies by the same investigators have identified the presence of mRNA and proteins coding for MMP-2, MMP-3, MMP-7, MMP-9, MMP-13, MMP-14, TIMP-1 and TIMP-2 mRNA in the healing wounds after laser keratectomy in rats (Ye & Azar 1998; Lu *et al.* 1999; Ye *et al.* 2000). MMP-9 protein was localized in epithelial basement membrane and superficial stroma (found as well by Gabison *et al.* 2003) whilst its mRNA was only observed in the migrating epithelial cells that cover the wounded epithelial gap. This supports the very important role of MMP-9 in re-epithelialization (Ye & Azar 1998). MMP-13, which is known to be involved in the MMP-9 activation *in vitro* (Knauper *et al.* 1997), has been found to be expressed during the re-epithelialization period. This MMP has been detected in the basal epithelial cells at the leading margins of the migrating epithelium a few hours after surgery and later on in the ECM of the wound area. MMP-13 has not been detected after the re-epithelialization period and has not been observed in normal unwounded corneas. In addition to its synergistical role with other MMPs in the cleavage of ECM, it has been suggested that MMP-13 may be important for MMP-9 activation (Ye *et al.* 2000). MMP-7 has been detected at the leading edge of the migrating epithelium during the re-epithelialization period after excimer laser keratectomy, as well as in the entire epithelial layer during the proliferation phase (Lu *et al.* 1999). Epithelial staining after LASIK for this MMP has been reported by Maguen *et al* (Maguen *et al.* 2002). Intense MMP-2 staining has been observed in basal regenerated epithelial cells and superficial stroma (possibly produced by activated myofibroblasts that replaced keratocytes undergoing apoptosis) at the wounded area after refractive surgery. MMP-14 has been shown to have a

similar expression pattern to MMP-2 in rat corneas after laser surgery. It is known from previous studies that MMP-14 is vital for MMP-2 activation, and it is possibly involved in this case in this biological process, as suggested by the demonstration that a soluble activated MMP-14 form captured by TIMP-2 is present in tear film of unwounded and wounded corneas after PRK (Holopainen *et al.* 2003). Increased levels of the highly glycosilated latent and activated forms of MMP-8 have also been detected in the tear fluid of the PRK group compared to controls, and it has been suggested that MT1-MMP could also be involved in MMP-8 activation *in vivo* (Holopainen *et al.* 2003). MMP-9 was first found in the deep stroma and on the newly deposited ECM in the anterior stroma but not in the epithelial cells, and it is of interest that TIMP-1 co-localizes with MMP-9 at the same time after wounding. Marked TIMP-2 staining has also been found in the basal epithelial cells of wounded rat corneas following excimer laser keratectomy (Ye & Azar 1998). Changes in the balance of MMP/TIMP expression after refractive surgery are possibly a crucial factor for tissue remodeling to take place. Excessive MMP activity has been reported to cause corneal keratolysis after PRK and topical application of diclofenac sodium 0.1%, an NSAID (Hargrave *et al.* 2002). However, in this study it was proposed that a vitamin E based solubilizer, a compound present in the drug solution, could have caused inhibition of corneal epithelial proliferation after PRK, as this has been shown to inhibit proliferation of retinal pigment epithelial cells (Sakamoto *et al.* 1996). This agent could have caused the enhancement in the levels of MMPs, which may have aided in the pathological mechanisms leading to corneal melting observed in this study (Hargrave *et al.* 2002). These observations have been supported by further studies that show that prolonged use of NSAIDS may lead to corneal melting with central perforation, increased MMP-2 and MMP-9 mRNA production and gelatinolytic activity around the perforated area (Gabison *et al.* 2003). Toxicity caused by NSAID application may cause increased MMP expression in a large corneal area, leading to the pathological changes observed. Based on the finding that MMP-9 was detected 2 months after PRK, when normally it is not detected after a month, the writers suggested that extended use of NSAIDs and conditions like diabetes mellitus may cause delayed wound closure and accumulation of MMPs in the wound margins (Gabison *et al.* 2003).

It has been suggested that MMP-9 may constitute one of the factors that control corneal re-epithelialization, due to observations that MMP-9 deficient mice show enhanced corneal wound closure (Mohan *et al.* 2002). In addition, MMP-7 has been implicated in the healing process following excimer laser keratectomy. Following this surgical procedure in

MMP-7 deficient and wild type mice, MMP-7 deficient mice corneas have been shown to develop increased neovascularization when compared to the wild type. Interestingly, new vessel formation is not accompanied by an increase in the levels of the angiogenic factors VEGF or bFGF, which could explain this finding. These observations suggest that MMP-7 may be important in the maintenance of corneal avascularity, a crucial biological process for retaining corneal transparency after corneal wound healing. However, the mechanisms of MMP-7 involvement are not yet known (Kure *et al.* 2003).

Various discrepancies regarding MMP expression following PRK have been presented by different scientific groups. This may in part be due to the use of different *in vivo* models. MMP-1, not previously found, has been observed below the basal epithelial cells at the wound edges after PRK (Mulholland, Tuft, & Khaw 2005). Additionally, although staining for MMP-2 and MMP-9 has been observed in the regenerated epithelial layer in previously mentioned studies, MMP-9 has not been detected in the leading edges of the migrating epithelium, where only MMP-1 was present. The two gelatinases were found behind the margins. The same study also reported reduced MMP expression in LASIK lesions when compared with PRK in the same *in vivo* model. In PRK, staining for MMP-1,-2,-3 and -9 in the stromal interface was observed, whilst in LASIK only MMP-2 was detected in the intrastromal interface, and the other MMPs were absent. The reduced MMP expression in LASIK compared to PRK could be responsible for the faster healing and visual recovery as well as for the decreased subepithelial scarring and haze in LASIK. These findings have been supported by other studies that showed that the number of corneas with epithelial MMP-9 expression in PRK group was significantly higher than in the LASIK group, although no significant differences in MMP-9 stromal expression were found between the two groups (Azar *et al.* 1998). A small recent study evaluating the scaring process in corneas that developed postoperative corneal ectasia (2.5 - 5 years after LASIK), observed the existence of MMP-9, in addition to changes in the collagen composition at the wound edge of the corneal flap created by LASIK. These findings suggested that both wound healing and tissue loss may take place at any time upto 5 years following LASIK surgery (Esquenazi *et al.* 2009). With regards to MMP-2, significantly lower number of LASIK corneas staining for this enzyme have been found a week after surgery, when compared with PRK (Azar *et al.* 1998). ECM turnover taking place after LASIK and involvement of MMPs in the healing process has been presented by Maguel *et al* (Maguen *et al.* 2002. In this study, dissected flap regions from two patients after complicated LASIK were tested and significant reduction of the α3-α6 type IV collagen

chains in the epithelial membrane were found. MMP-1 and MMP-2 staining was also found in the fibrous areas of the anterior stroma of LASIK -treated corneas along with epithelial staining for MMP-7. Since collagen IV is a substrate for MMP-2, these changes could partially be ascribed to this MMP.

As that observed with any other healing process, cytokines have shown to play an important role in the regulation of MMPs after laser keratectomy. IL-6 levels were found significantly enhanced in tear fluid after PRK (Malecaze *et al.* 1997). *In vitro* studies revealed that increased production of this cytokine could be possibly due to keratocyte and epithelial cell stimulation after refractive surgery. IL-6 has been shown to stimulate keratocytes *in vitro* to produce collagen I. Additionally, it was not only shown to have an inhibitory effect in MMP-2 synthesis by human keratocytes; but, it also stimulates the expression of TIMP-1 (Bugno *et al.* 1995).

1.2.2.2.5. Keratoconus

Keratoconus is a degenerative ocular disorder that affects mainly young adults of any sex and race. It is a chronic, non-inflammatory and progressive disease, mostly observed bilaterally, resulting in myopia, astigmatism and severe vision impairment. Keratoconus constitutes one of the main reasons for corneal transplantation. Central cornea in keratoconic eyes gradually acquires a conic shape, becomes thin and loses its tensile strength. Histopathologically, thinning of the epithelium and stroma, scarring of the stroma (mainly the anterior stroma), break up of the Bowman's layer and Descemet's membrane and tears in Bowmann's layer can be observed in this condition (Bron 1988; Collier, Madigan, & Penfold 2000) . Although the pathogenesis and etiology of this disorder is poorly understood, it can be observed as an independent disease, or it may be associated to connective tissue disorders (Ehlers-Danlos syndrome type IV and VI, Marfan syndrome, osteogenesis imperfecta), Down syndrome, Barlow syndrome, atopy, or contact lenses wear. In keratoconus, increased collagenolytic and gelatinolytic activity as well as increased synthesis of ECM molecules (referred in Fini, Yue, & Sugar 1992) and lower total protein than normal corneas have been observed (Yue, Sugar, & Benveniste 1984;Yue, Sugar, & Benveniste 1985). Although much effort has been placed on investigating the role of MMPs in this condition, a full understanding of the implication of these molecules in the pathogenesis of keratoconus has not yet been obtained.

In keratoconic corneas, mainly latent MMP-2 has been detected and only minimal amounts of active MMP-2 has been found (Fini, Yue, & Sugar 1992). However, the levels of MMP-2 were not found to be different between normal and keratoconic corneas. Based of this finding, the greater gelatinolytic digestion observed in keratoconus compared to normal corneas can't be a result of enhanced MMP-2 production (Fini, Yue, & Sugar 1992). It was later suggested that responsible for the increased gelatinolytic activity in keratoconus are not the changes in MMP-2 production but possibly the reduction of the protein levels of TIMPs. This was demonstrated by observations that the ratio of MMP-2/TIMP-1 (TIMP-1 is produced as well from stromal fibroblasts) is significantly increased in keratoconus (Brown *et al.* 1993; Kenney *et al.* 1994). This is of interest as TIMP-1 is capable of deactivating the active site of MMP-2 in the MMP-2-TIMP-2 complex. Whilst TIMP-1 mRNA was not found decreased in this study, other investigations showed a significant decrease in the TIMP-1 mRNA levels of keratoconus tissue when compared to normal corneas (Kenney *et al.* 2005). Further studies revealed that the gelatinolytic increase in keratoconus is not a result of genetical changes in the structure of the TIMP-1 mRNA, which would make the molecule ineffective in MMP inhibition (Opbroek, Kenney, & Brown 1993). Supportive of the possibility that lack of TIMPs may increase proteolysis in keratoconus is the finding that, contrary to normal eyes, TIMP-3 staining is absent in the stroma of keratoconus eyes in which the Bowmann's layer was degraded (Kenney *et al.* 1998). In the same study, in contrast to previous findings, it was interestingly found that TIMP-2 levels were not changed in keratocyte cultures from normal, early and scarred keratoconus tissue. Additionally, although TIMP-1 levels were unchanged in keratocyte cultures from normal and early keratoconus corneas, TIMP-1 levels were elevated in the scarred keratoconus keratocytes. The most reasonable explanation for these observations is that, as the pathogenesis of keratoconus reaches the end stage, increased production of TIMP-1 may serve as a protective mechanism against MMP-2 mediated degradation of the corneal ECM as well as of cell apoptosis and migration (Smith *et al.* 2006).

Experiments based on the ability of MMP-2 to degrade one of the main components of the human cornea, Collagen VI, that accounts for the ¼ of the dry weight of human cornea, revealed that gelatinase A has the ability to cleave this collagen molecule. It is likely that this process plays a significant role not only in the maintenance of the corneal transparency, but also in the generation of keratoconus and other corneal disorders (Myint *et al.* 1996). Cleavage of collagen VI was parallel observed in *in vitro* cultures of keratoconus keratocytes, probably due to increased MMP-2 activity (Chwa *et al.* 1996).

Expression of MT1-MMP but not of MMP-2 in keratoconus corneas has been reported to be significantly increased in the epithelium and stroma of keratoconus corneas when compared with normal corneas and it has been suggested that MT1-MMP may be important for the activation of MMP-2 (Collier, Madigan, & Penfold 2000). In contrast, other studies have not found increased MT1-MMP levels in keratoconus compared to the normal corneas (Kenney *et al.* 2005). Although the aforementioned studies have not demonstrated excessive expression of MMP-2 in keratoconus, in a later study increased production of the ~ MW 62000 MMP-2 type in cultures of keratocytes isolated from early-phase clear keratoconic and scarred keratoconic corneas has been reported (Smith *et al.* 2006). Keratoconic keratocytes have been linked with the production of a 61 kDa metalloproteinase. This MMP band activity could not be detected in the media from normal keratinocyte cultures (Smith *et al.* 1995). However, different opinions have been given on the 62 kDa form of MMP-2. It has been suggested that this MMP may be found together with the 65 kDa MMP-2 proactive form of MMP-2 and that it is easily transformed by autocatalysis into the activated enzyme (Smith *et al.* 2001; Smith & Easty 2000). It has also been suggested that it constitutes an activated enzyme in which the N-terminal domain, that inhibits the activation of the enzyme- has been cut from the structure of the molecule (referred in Smith *et al.* 2001). In a following study it has been proposed that PDGF possibly plays a crucial role in the production pathway of this 62 kDa pro-MMP-2 (Parkin, Smith, & Easty 2000).

An interesting study has been recently published about the role of MMP-1 and of EMMPRIN, a known potent MMP inducer, in keratoconus (Seppala *et al.* 2006). In this study the authors found enhanced staining for both MMP-1 and EMMPRIN in keratoconus corneas, as compared to the normal corneas. They also observed that there was no regional overlap in the expression of these two molecules, as EMMPRIN expression was found in the pathologically changed places of the keratoconic corneas, in contrast to MMP-1 which was rarely present in these regions. Based on these results, the authors proposed that MMP-1 may participate in the structural maintenance of the normal cornea, whilst EMMPRIN may enhance the expression of other MMP molecules that are involved in the pathogenesis of keratoconus. The last statement is also based on the finding that pathological changes of the Descemet's membrane and endothelial corneal layer have been found in keratoconic corneas where EMMPRIN, but not MMP-1 staining, has been observed. Slight overexpression of MMP-1 in keratoconus has also been reported by others, in addition to

significant expression of MMP-13 and a slight decrease of MMP-8 (Mackiewicz *et al.* 2006).

In tear film samples from patients with keratoconus, MMP levels are close to those observed in healthy patients. Only in cases where keratoconus has been linked to atopic disease, MMP levels have been detected notably elevated (Smith, El-Rakhawy, & Easty 2001). Parallel to these findings, increased levels of MMP-9 in the tear film of keratoconus patients have been reported (Lema & Duran 2005). However, it is difficult to compare these two studies due to the unknown history of the patients participating and the different techniques used for the collection and analysis of the samples. Other groups, in contradiction, report that other proteinases different from MMPs have a key role in the pathogenesis of keratoconus (Zhou *et al.* 1998). Their studies have shown that MMP inhibitors can not reduce the increased gelatinolysis and caseinolysis of keratoconus samples observed by *in situ* zymography. However, using western blot and immunostaining analysis they found increased staining for cathepsins B and G. They also observed that inhibitors of serine and cysteine proteinases are capable of reducing the gelatinolytic and caseinolytic activity in keratoconus samples.

To summarize, research in keratoconus presents with many difficulties, due to the different etiologies of this condition, as well as the fact that the studies are performed on human specimens at the latest stages of development of this disorder (just before corneal transplantation). These factors constitute serious barriers for the exploration of the pathological paths of this disease.

1.2.2.2.6. Pseudomonal keratitis

During keratitis caused by Pseudomonas aeruginosa, enhanced corneal degradation is observed and corneal perforation may occur within the first 72h of onset if no treatment is given (Thiel, Steuhl, & Doring 1987). This may result in corneal necrosis, ulceration, scarring and subsequent blindness. The corneal melting that occurs after infection with Pseudomonas aeruginosa is believed to be a result of both the host inflammatory process (infiltration of mostly polymorphonuclear leukocytes and PMNs, production of cytokines and proteases) and proteases produced by P. aeruginosa (Steuhl *et al.* 1987; Matsumoto *et al.* 1993; Twining *et al.* 1993). P. aeruginosa virulence factors and especially alkaline protease and elastase play an important role in the corneal infection and are able to directly

cleave components of the corneal structure (Kessler, Mondino, & Brown 1977; Kreger & Gray 1978; Heck, Morihara, & Abrahamson 1986; Heck *et al.* 1986; Steuhl *et al.* 1987; Howe & Iglewski 1984; Kreger *et al.* 1986; Kernacki *et al.* 1995). It has been reported that P.aeruginosa strains, which produce at least one of these two proteases, can be infectious and can cause corneal damage (Howe 1981). However, the *in vivo* concentration of alkaline protease has been found to be very low to stimulate the production of a specialized antibody against this protease (Kernacki *et al.* 1995). Some of the factors released by P.aeruginosa, especially elastase and alkaline protease, have been thought to trigger the activation of MMPs from keratocytes (Matsumoto *et al.* 1993; Hao *et al.* 1999). Indeed, MMP-2 and MMP-9 have been shown to become activated in the presence of elastase and alkaline protease produced by P. aeruginosa (Hao *et al.* 1999; Miyajima *et al.* 2001). During *in vitro* cultures of rabbit corneal fibroblasts where MMP-2 is constitutively produced, the application of P.aeruginosa virulence factors elastase, alkaline protease and pseumomonal lipopolysaccharide resulted in increased expression of this MMP (Miyajima *et al.* 2001). Latent MMP-9 has been found only in rabbit corneal fibroblast cultures treated with pseudomonal proteases or pseudomonal lipopolysaccharide, indicating the triggering role of these factors in MMP-9 production (Miyajima *et al.* 2001). *In vivo* studies in which mice resistant and non-resistant to P. aeruginosa infection have been used, active and proactive MMP-9 were detected and it is of interest that in the mice non-resistant to inflammation, levels of both active and latent forms of MMP-9 were found enhanced when compared to mice resistant to inflammation (McClellan *et al.* 2006). Latent and active MMP-9 forms were also found to be induced after infection using an *in vivo* rabbit model (Ikema *et al.* 2006). IL-1β has been shown to play crucial role in corneal damage caused by bacterial keratitis, and P. aeruginosa strains have been found to cause enhancement in IL-1β expression (Thakur *et al.* 2002). Using an *in vivo* model, IL-1β inhibition using an anti-IL-1β ab not only reduced corneal damage and inflammation after injury induced by Pseudomonas aeruginosa infection, but also resulted in a remarkable reduction in the levels of MMP-9 (Xue *et al.* 2003). Further studies designed to find the role of MMP-9 in the regulation of cytokines in P. aeruginosa kerititis suggest that MMP-9 leads to the increase of active IL-1β after infection (McClellan *et al.* 2006). It has been, however, suggested that none of these factors exclusively triggers the production or the activation of the other, but that these two factors may interact with each other (McClellan *et al.* 2006). The implication of MMP-9 in corneal degradation after P. aeruginosa infection has been further supported by studies in the MMP-9 deficient mice or the use of an MMP-9 antibody. Lack of MMP-9

significantly reduced corneal damage, whilst addition of recombinant MMP-9 caused increased corneal degradation. Further studies designed to examine the implication of inflammation and P. aeruginosa proteases in MMP expression have involved the use of immunized and non-immunized mice against P. aeruginosa (McClellan *et al.* 2006). Zymography of the corneal protein extracts of non-immunized mice revealed increased expression of latent MMP-2 and MMP-9 as well as of alkaline protease compared to immunized mice. Furthermore, active MMP-9 band was only detected in non-immunized mice, whilst the corneal proteolysis observed in these mice was enhanced when compared to the immunized mice (Kernacki *et al.* 1997). TIMP-1 has been shown to have a protective role against BM and stromal break down after corneal degradation caused by P. aeruginosa infection (Kernacki *et al.* 2004). Moreover, delayed and weaker TIMP-1 expression compared to an earlier and stronger MMP-9 production has been thought to be responsible for the corneal degradation and ulceration observed in an *in vivo* model (Ikema *et al.* 2006). In addition to natural inhibitors, the use of ilomastat, a broad spectrum MMP inhibitor, significantly inhibited pseudomonas aeruginosa mediated collagen degradation *in vitro*, indicating the role of MMPs in corneal ulceration after infection (Hao *et al.* 1999). MT1-MMP was shown to be expressed in mice corneas after infection with P. aeruginosa, and MT2-MMP and MT3-MMP have been also detected. However, expression of these two MMPs has been shown to be lower than the expression of MT1-MMP. In addition, levels of MT-MMPs have been found increased in mice non previously immunized against P.aeruginosa, when compared with immunized animals. Histological analysis of the cornea revealed localisation of the MT1-MMP staining in the corneal epithelium and of MT2-MMP and MT3-MMP in the border between the epithelium and stroma and in the stroma itself (Dong *et al.* 2000). Since MT-MMPs are implicated in MMP activation, it has been suggested that possibly their expression in corneal infection by P. aeruginosa serves the same goal (Dong *et al.* 2000).

1.2.2.2.7. Herpetic keratitis

The pathological mechanisms behind the visual impairment and blindness observed after herpes simple virus (HSV) infection are complicated, as the participation of different cells and factors has been observed. The main characteristics of herpetic keratitis are immunoinflammatory reaction, neovascularization and corneal tissue distruction that may

be responsible for corneal melting and perforation (Streilein, Dana, & Ksander 1997), (Kumaraguru, Davis, & Rouse 1999). The neovascularization observed after HSV infection is a very important step in the scarring process and studies have been carried out to identify the molecules that promote angiogenesis. In addition to the vascular endothelial growth factor that is known to trigger angiogenesis and that has been found to be expressed after ocular HSV infection (Zheng *et al.* 2001), the presence and role of MMPs, especially of MMP-9 has been studied. Although MMP-2 levels did not change, increased expression of MMP-9 was detected by zymography in mice corneas after HSV infection when compared to controls. The production of MMP-9 presented in two peaks over time, coinciding with the two peaks of PMN infiltration observed at 2 days and a week after infection of the cornea with HSV (Thomas *et al.* 1997;Thomas & Rouse 1997). The origin of MMP-9 observed during the first peak was demonstrated by the depletion of neutrophils using a specific anti-neutrophil mAb, that resulted in significant reduction in MMP-9 levels (Lee *et al.* 2002). The second peak of MMP-9 expression was observed after herpetic keratitis had been developed (Lee *et al.* 2002). In addition to increased expression of MMP-9 on day 2 post HSV infection in mice, enhanced staining for MMP-2 and -8 in mouse corneal tissue has been reported (Yang *et al.* 2003). After day 2 until the end of the first week, the levels of MMPs were reduced, possibly due to the expression of TIMP-1 and 2 by corneal epithelial cells and superficial keratocytes, as shown in this study. At the end of the second week that, as we previously mentioned, intense infiltration of PNMs takes place, significant enhancement of MMP-2, MMP-8 and MMP-9 staining was also found in the corneal regions with ulceration and necrosis. Using zymography, MMP-2, MMP-8 and MMP-9 latent forms were detected at both day 2 and 14, but their active forms were mainly observed at day 14 (Yang *et al.* 2003). The same group later tested the transplantation of amniotic membrane in corneas with ulcerative herpes stromal keratitis on day 14 using the same *in vivo* model. Their results showed reduced expression of MMP-8 and MMP-9, enhanced localization of TIMP-1 and better clinical appearance, as compared to controls (Heiligenhaus *et al.* 2005). Amniotic membrane is known to have anti-inflammatory effects (Lee *et al.* 2003), and possibly reduction of the MMPs/TIMPs balance is one of the mechanisms by which amniotic membrane exerts its anti-inflammatory actions. Upon examination of the tear fluid of patients with herpetic keratitis, only the latent MMP-2 and MMP-9 forms were detected (Sakimoto, Shoji, & Sawa 2003). However, the small number of patients involved and the lack of clinical data from the patients used in this study justify further investigation to corroborate these findings.

The importance of MMP-9 in corneal angiogenesis after HSV infection has been further supported by studies using MMP-9 knockout mice, which present significantly reduced neovascularisation. Additionally, induction of MMP-9 inhibition in mice with the use of a plasmid DNA encoding TIMP-1 (potent inhibitor of MMP-9) also resulted in reduced angiogenesis (Lee *et al.* 2002). Impressively, MMP-9 has been shown to be involved in VEGF angiogenesis, as TIMP-1 remarkably reduced VEGF induced neovascularisation in mice eyes (Lee *et al.* 2002). An interesting recent study that examined the pathological mechanisms that take place in herpetic stromal keratitis suggested that the remaining in the tissue copies of HSV-DNA and of HSV – IgG immune complex (HSV – IC), which continue to exist even after the active replication of the virus has stopped, trigger angiogenesis and inflammation and subsequently corneal opacification. More specifically, HSV-DNA and HSV-IC triggered the expression of VEGF in corneal stromal fibroblasts and in macrophages and the expression of MMP-9 in macrophages *in vitro* (Hayashi *et al.* 2009). Knockdown of MMP-9 expression in mouse cornea after HSV infection with plasmids encoding short hairpin RNAs targeting specific MMP-9 sequences also resulted in inhibition of neovascularization and in milder herpetic keratitis (Azkur *et al.* 2005).

1.2.2.2.8. Fungal keratitis

Treatment of fungal keratitis constitutes a difficult problem for clinicians, as there is a big variety of fungal species that can cause corneal lesions and keratitis. The clinical appearance of these lesions is characteristic of each fungal species and the virulence of these micro-organisms depends on their ability to produce molecules that facilitate their invasion into tissues by ECM degradation. Studies that have been carried out to investigate the role of MMPs in the pathology of fungal keratitis have provided an important insight into the possible pathogenic mechanisms responsible for tissue degradation in this condition. Using zymography, MMP-2 and -9 have been detected in rabbit corneas with fungus infection. Moreover, positive correlation between MMP-9 expression and the amount of PMNs detected in the infected corneas has been observed after infection with two corneal fungal pathogens: A.flavus and Fusarium solani (Gopinathan *et al.* 2001). Positive significant correlation of MMP-9 levels with the virulence of the tested fungal species and the degree of inflammation after infection has also been found (Dong *et al.*

2005). In addition to MMP-9, MMP-8 has been found in fungal kerititis tissues, where significant PMN infiltration has been observed. On this basis, it has been suggested that MMP-8 and MMP-9 may be released by PMN granules, which, by degrading ECM and initiating inflammation, trigger the release of cytokines that can activate corneal cells to produce MMPs and other degrading molecules, as well as to attract more PMNs to the site of inflammation. Although the expression of TIMP-1 and TIMP-2 has been detected, the levels of these inhibitors do not appear to be sufficient to control MMP activity in fungal keratitis, which explains the active degrading role that MMPs play in this pathological condition (Rohini *et al.* 2007).

1.2.2.2.9. Dry eye

Dry eye syndrome constitutes one of the most common sources of chronic ocular irritation and discomfort. Although it mainly affects people over the age of 65, one in ten people between the ages 30 and 60 are also affected. The main characteristics of this disorder are reduced tear secretion and eye redness, and the major causes are i) lacrimal gland problems observed in conditions such as sarcoidosis, conjunctival tissue diseases and involutional changes; ii) cicatricial disease of the conjunctiva occurring in conditions such as trachoma, pemphigoid, Sjogren's syndrome and keratoconjunctiva sicca; iii) systematic diseases like rheumatoid arthritis; iv) reactions to drugs, such as diuretics, which can worsen the symptoms of the dry eye (International Ophthalmology Clinics Dry Eye 1994; Shah, Jacks, & Khaw 1999). The inflammation observed in dry eye has been thought to be caused by pathological mechanisms in which inflammatory molecules and MMPs play an important role (Suzuki & Sullivan 2005).

The observation that dry eye is a condition found mainly in women and that estrogen therapy worsens the clinical signs of dry eye, led researchers to test the effect of 17β-estradiol in human corneal epithelial cell cultures (Suzuki & Sullivan 2005). They observed that 17β-estradiol increased the expression of MMP-2, -7 and -9, as well as of members of the IL family. As isolation of dry eye tissues for experimental reasons is very difficult in humans, important attempts for the development of a dry eye animal model, in order to test the causes and pathological mechanisms in this condition, have been published.

One of these models, the Neurturin factor deficient mice, shows with reduced tear secretion due to the parasympathetic system deficiency and subsequently presents with dry eye phenotype. In this mice increased IL-1β and MMP-9 concentrations are found in tears and both molecules are expressed in the corneal epithelium (Song *et al.* 2003). Another experimental model of dry eye can be elicited by the use of an anticholinergic agent, scopolamine, in combination with low humidity conditions and the exposure to an air hood (Dursun *et al.* 2002). Under these conditions it is possible to induce the development of a dry eye syndrome in mice. This is characterized by increased expression and production of MAPKs (involved in the signalling for MMP production), increased expression and production of IL-1β in tear film and of IL-1β and TNF-α in the corneal and conjunctival epithelia. Although it is known that these two factors can activate the MAPK signalling pathway, the results of this study in the corneal and conjunctival epithelia that show earlier activation of MAPK than of IL-1β and TNF-α production, suggest a possible role for MAPK in the triggering of IL-1β and TNF-α expression. Subsequently, IL-1β and TNF-α may take part in an autocrine mechanism to further activate MAPK for not only the production of IL-1β and TNF-α, but also for the transcription and translation of MMP-9. Both MMP-9 concentration and activity were found in the same study to be increased in the ocular surface.

On the question of how the MAPK pathway is initially activated in the dry eye we could likely find a proposed answer in the study of Mott and Werb (Mott & Werb 2004). By exposing primary corneal epithelial cells in culture to high osmolarity resembling *in vivo* conditions where corneal epithelium is in contact with hyperosmolar tear film, the authors observed activation of c-Jun N-terminal kinases (JNKs)- the p-JNK-1 and p-JNK-2- (members of the big MAPK family) as well as of the direct downstream substrate of activated JNK, the p-c-Jun. Additionally, gradual enhancement of MMP-1,-3,-9 and -13 concentrations was detected in media of increased osmolarity and more specifically in an osmolarity increase dependent manner for MMP-1,-3, and -9. Non-significant difference was found in the case of MMP-2. A potential different or parallel path for MAPK activation in the corneal epithelial cells could be the increased IL-1β secretion from the lacrimal glands (Solomon *et al.* 2001). Furthermore, the use of SB202190, a p38 MAPK inhibitor that blocks activation of JNK, not only inhibited the phosphorylation and activation of p-JNK-1, p-JNK-2 and c-Jun, but also blocked the increase of MMPs. Doxycycline, an anti-inflammatory agent used in many ocular surface diseases, had similar inhibitory results to SB202190 in both the Jun and MMP molecules. These observations led

this group to suggest that these two agents act in a similar way at the molecular level. In contrast, use of a corticosteroid, Dexamethasone, caused reduction in the levels of MMP-1,-3 and -13, but appeared to function through different pathways, as it did not inhibit JNK significantly.

A later study of the same group reported similar findings (De Paiva *et al.* 2006). Using the same experimental model of dry eye in mice, they observed increased expression and activity of MMP-9 and enhanced production of IL-1α, IL-1β and TNF-α mRNA as well as increased phosphorylation of the MAPK family molecules, especially p38 and JNK. They also observed the inhibitory effect of doxycycline in MAPK pathways, but in contrast to their previous study, using another corticosteroid agent, methylprednisolone, they inhibited the phosphorylation of MAPKs. They also observed a decrease in ILs, TNF-α and MMP-9 expression and trying to explain this finding they suggested that these two therapeutic agents protect the corneal epithelial barrier disruption observed in dry eye, possibly due to their inhibitory effect in MMP-9 expression. The possibility of MMP-9 involvement in the break down of the corneal epithelial barrier has also been suggested (Pflugfelder *et al.* 2005). In this study, a dry eye condition was induced in MMP-9 knock-out and normal mice. No changes were observed in the corneal epithelial barrier permeability of the MMP-9 knock-out mice, in contrast with the normal animals, where significant increase was observed. Interestingly, local application of active MMP-9 in the knock-out mice caused disruption of the corneal epithelial barrier. In the same study, lysis of the apical corneal epithelial cells junction stroma, created in response to the dry eye condition, was shown to be due to the cleavage of its main component, the protein occludin. MMP-9 is known, too, to be one of the most potent activators of the pre-form of IL-1β. This could explain the reason for the parallel increase in the levels of mature IL-1β and active MMP-9, and a decrease in the IL-1β pre-form observed in experimental models of dry eye (Solomon *et al.* 2001).

1.2.2.2.10. Trachoma

Trachoma, the most common cause of preventable blindness worldwide, is a chronic infection caused by Chlamydia trachomatis serotypes A, B, Ba and C (Kanski 2003). It is mostly present in the third world and is mainly transmitted by the common fly. The most common clinical signs of trachoma are chronic conjunctival inflammation,

progressive conjunctival and subconjunctival scarring, limbal follicles and keratitis. Characteristic of the end-stage trachoma is the corneal opacification and subsequently blindness. Although not many studies have been published regarding the role of MMPs in the pathological mechanisms of trachoma, two scientific groups have reported a potential role of MMP-9. Zymography performed by isolating proteins from normal and active trachoma conjunctival revealed markedly increased activity of MMP-9 in trachoma samples compared to normal. In contrast, no significant differences were detected in the levels of MMP-2 in trachoma and normal conjunctiva. Analyzing the conjunctiva of trachoma patients with the method of immunohistochemistry, MMP-9 was mainly detected in macrophages and PNM cells that are present in the area due to the chronic inflammation (Abu El-Asrar, Geboes, & Missotten 2001). Furthermore, a recent study performed by Natividad A. *et al* detected a mutation that reduces the degradation ability of MMP-9. This mutation substitutes arginine with a non synonymous aminoacid – glutamine- that participates in the structure of the active site of MMP-9 and especially of one of the fibronectin-like repeats that are important in the substrate binding. This change in the MMP-9 structure was linked with reduced fibrosis after ocular Chlamydia trachomatis infection and supported further the role of MMP-9 in the pathogenesis of trachoma (Natividad *et al.* 2006)

1.2.2.2.11. Pterygia

Pterygia are a degenerative pathological condition that present at the corneo-conjunctival junction, which is believed to be caused mainly by UV-B exposure. The main pathological mechanism that leads to the development of pterygia is thought to be the migration of basal limbal epithelial cells as a layer, possibly generated by limbal basal cells. This layer is thinner at the advancing border. Some of the most common histological characteristics of pterygia are cleavage of the Bowmann's layer (BL), elastosis (denaturation of the ECM proteinic molecules), vascularization and leukocyte infiltration. Because of the proteolytic phenomena that occur during the growth of pterygia, MMPs have been thought to be involved in the pathogenesis of this condition. Histological analysis of pterygial tissue has revealed the presence of the MMP-1 mRNA and protein in the pterygial epithelial cells, in contrast to the normal conjunctival tissue where MMP-1 mRNA is absent. MMP-2 has also been found at pterygial specimens, but staining for this

protein is mostly localised at the basal pterygial epithelial cells. Intravascular neutrophils in the region predominantly express MMP-9, which may facilitate cell invasion of basement membranes, due to the MMP-9 ability to degrade collagen IV, their main component. The same pattern of staining was observed for MMP-1 and TIMP-1, none of which are normally found in conjunctival tissue, whilst TIMP-3 was mainly detected in basal epithelial cells and perivascular inflammatory cells (Di, Wakefield, & Coroneo 2000). Further analysis showed the presence of MMP-1 in pterygial epithelial cells (PECs), elastotic matrix and pterygium fibroblasts as well as in some adjacent corneal stromal fibroblasts (Di, Wakefield, & Coroneo 2000). At the leading edge, MMP-13 was localised at the basal columnar PECs over the BL and at the vascular endothelial cells. Milder immunoreactivity was also found in pterygium fibroblasts. Furthermore, MMP-2 and MMP-9 were found in the basal columnar PECs. Apart from PECs, MMP-2 was detected at the BL and at the denatured tissue, where MMP-9 was absent. MMP-9 was detected in pterygium fibroblasts, pterygium vascular endothelium and inflammatory cells, in contrast to MMP-2, that was not found in the vascular endothelium and that was only mildly expressed in the pterygium fibroblasts. TIMP-1 and -3 expressions were also observed in the pterygial epithelium and the signal was stronger nearer to the degraded BL (Di, Wakefield, & Coroneo 2000). As these MMP inhibitors are not expressed in normal conjunctiva, it has been proposed that their production in pterygia is triggered as a protective mechanism to control MMP activity.

Other studies have demonstrated the presence of MMP-14 and -15 (MT1-MMP and MT2-MMP) in pterygial tissue as well as the latent and active form of MMP-7 (Dushku *et al.* 2001). MMP-7, which has been found at the epithelial basement membrane and at the pterygial vascular endothelium, led scientists to suggest its involvement in the neovascular process observed in this disease (Di, Coroneo, & Wakefield 2001).

As suggested by the above studies, the implication of MMPs in pterygial pathology involves a multistep process. It is possible that UV-B light may cause mutations to the TP53 tumour suppressor gene in limbal epithelial cells. Further mutations may lead to the development of pterygia from limbal epithelial cells expressing p53. Through a p53-RB-TGF-β pathway, significant increase of TGF-β may occur, causing subsequently upregulation of the expression of gelatinases, as well as of MT1-MMP and MT2-MMP. MMPs may subsequently lead to degradation of their hemidesmosomal bonds, proliferation, and finally migration of limbal epithelial cells towards the cornea. The migration is believed to be facilitated by the expression of MMP-1 and MMP-3 by these

cells, which may then be followed by migration of conjunctival epithelium (Dushku *et al.* 2001). Induction of MMP-1 expression by pterygial epithelial cells is mediated by ERK1/2 activation, as supported by observations that PD98059 (an ERK1/2 inhibitor) causes a significant reduction in UV-B induced MMP-1 production by these cells in culture (Di, Coroneo, & Wakefield 2003). Apart from the pterygial limbal epithelial cells, it is suggested that fibroblasts found in pterygia participate in BL degradation by expressing MMP-1 and MMP-3. None of these fibroblasts was found to express p53. TGF-β expressed by the pterygial limbal epithelial cells probably activates fibroblasts beneath the limbus basal cells and induces them to increase their expression of MMP-1 and MMP-3 (Dushku *et al.* 2001). In conclusion, MMP-1, -3 and-13 produced by pterygial epithelial cells and fibroblasts appear to be important for cell invasion and for denaturation of BL. MMP-2 and -9 may then induce proteolysis of gelatins produced upon MMP-1 and -3 collagen degradation. MT1-MMP may also play a role in the activation of MMP-2and MMP-9 that leads to break down of basement membrane and leukocyte infiltration, whilst MMP-7 and -9 appear to play an important role in the neovascularization process that occurs in pterygia.

1.2.2.3. Lens

Although MMPs are believed to play a vital role in tissue remodelling during embryogenesis, MMP-2 immunoreactivity has not been detected in mice during all the steps of lens formation (Iamaroon *et al.* 1996). However, MT1-MMP, which is important for MMP-2 activation, was found to be expressed in this animal species (Smine & Plantner 1997). It is of interest that diversity in the existence of MMPs has been reported in normal lenses in different species. MMP-2 and -9 have been found in normal rat lenses (John *et al.* 2004), but not in normal human (Kawashima *et al.* 1998; Seomun *et al.* 2001), porcine (Tamiya *et al.* 2000) or chicken (Richiert & Ireland 1999) normal lenses.

Cataract is the most common pathological process observed in the lens, and is a major cause of reversible blindness throughout the world. The most common types of cataracts are the subcapsular, nuclear and cortical forms. After implantation of the intraocular lens (IOL), about 20-30% of cases develop posterior capsule opacification (PCO), known as after-cataract. This constitutes a wound healing process in which lens epithelial cells remaining after the formation of the capsular bag, proliferate, migrate and

produce ECM proteins, such as collagen, which is mainly found in PCO. The epithelial cell cytoskeleton is re-arranged into very long stress fibers, which aids cells to cause wrinkling of the ECM deposited on the lens capsule. This results in light scattering regions and subsequently in impaired vision. The potential MMP implication in cataract pathology and in PCO has been investigated in post mortem porcine eyes (Tamiya *et al.* 2000). Although no MMPs were found in normal lenses, gelatinolytic bands representing possibly MMP-2, MMP-9, MMP-9 and TIMP-1 complex and MMP-9 dimer were detected in the medium from cultured cupsular bags. Additionally, in the medium of lenses cultured under oxidative stress conditions (oxidative stress is known to be one of the main causes of cataract), gelatinolytic bands that possibly represent MMP-2 and the dimer of MMP-9 were found. This study indicates that stimuli like cataract surgery and oxidative stress can induce the MMP production. In contrast, it has been supported that oxidative stress conditions in cultured rat lenses have reduced expressed MMP-2 and -9. Responsible for this disagreement could be the fact that the oxidative conditions were tested in different species as well as the different protocols followed for induction of oxidation. MMP-9 activity has been shown to be significantly higher in cortical cataracts than in nuclear or posterior subcapsular cataracts. These levels are significantly higher than the background MMP-9 leveles observed as a consequence of increasing age (Alapure *et al.* 2008).

MMP involvement into the pathological conditions that occur after cataract surgery has been demonstrated by observations that following sham cataract surgery, culture supernatants of lens capsule bags cultured in gelatinase free medium contained MMP-2 and -9. This was accompanied by migration of the lens epithelial cells to the posterior capsule. Interestingly, this migration and MMP release was markedly reduced by the broad spectrum MMP inhibitor ilomastat, indicating both the participation of MMPs in the capsular wrinkling as well as the potential application of ilomastat as a therapeutic approach for PCO (Wong *et al.* 2004).

The role of TGF-β in cataract development, PCO and MMP expression in lens has also been studied. Observations that lenses cultured with TGF-β developed cataract and that TGF-β is present in vitreous, aqueous humor, lens surface and lens cells, and that it upregulates MMP expression in many tissues, have led to investigations into the effect of TGF-β1 on MMP production by lens cells (Hales, Chamberlain, & Mcavoy 1995). After culturing chicken lens annular pad cells with several growth factors, it was observed that significantly higher levels of MMP-2 and MMP-9 production were induced by TGF-β1 (Richiert & Ireland 1999). Enhanced expression was shown as well with PDGF, but in

lower levels compared to TGF-β1. Parallel to these findings, the effect of TGF-β1 was tested on human LEC cultures and it was found that TGF-β1 induced MMP-2 mRNA expression. TGF-β1 mediated induction of MMP-2 coincided with the stimulation of LECs differentiation. Since blocking of MMP-2 with an MMPi hindered LEC differentiation, it was suggested that MMP-2 may play an important role in the morphological changes observed in these cells upon stimulation with TGF-β1 (Seomun *et al.* 2001).

Endogenous active TGF-β2, matrix changes and expression of αSMA and fibronectin (transdifferentiation markers) have been detected in supernatants from post mortem human capsular bags from eyes that had received intraocular lens (Wormstone *et al.* 2002). Although MMP-2 and -9 are expressed in *ex vivo* capsular bags soon after cataract surgery and this MMP induction seems to be independent of TGF-β2, studies have revealed that without TGF-β2, the maintenance of MMP-2 and -9 expression is significantly reduced. Moreover, in rat lens cultures where development of anterior subcapsular cataracts and induction of MMP-2 and -9 was observed upon TGF-β2 treatment, the use of ilomastat or of a specific MMP-2/-9 inhibitor not only reduced the levels of these two MMPs, but also prevented lens epithelial differentiation into fibroblasts (Dwivedi *et al.* 2006).

Anterior capsule specimens taken during post-cataract surgery from patients with posterior subcapsular cataracts immunostained for MMP-1, -2, -3, -9 and TIMP-1 and -2 for up to 18 months after the first cataract operation, but no staining for these molecules was observed in specimens taken more than 18 months after IOL implantation. This indicates that MMP-mediated remodelling occurs in the first $1^1/_2$ years after the operation (Kawashima *et al.* 2000). MMP-3 is possibly involved in the differentiation of LECs in their contractile phenotype, leading to the development of the opacifications after cataract surgery (Kawashima *et al.* 2000).

In addition to PCO, MMPs have been thought to directly contribute to the genesis of other pathological conditions of the lens. The involvement of MMP-1 in cortical cataract has been supported by findings that intracellular staining for MMP-1 predominates in cortical fibers of opacified lenses, although MMP-2, -3, -9 and TIMP-1, -2, and -3 may also be found. Since human lens epithelial cells exposed to UV-B radiation in a dose dependent manner show increased expression of MMP-1, but not of TIMP-1, this may explain why UV radiation is one of the main causes of cortical cataract in humans. This findings, together with observations that strong MMP-1 staining is found in the inferonasal quadrant (the region that receives the higher light concentration), and the possibility of MMP-1

participation in crystalline aggregation present in cortical cataracts, strongly suggest that MMPs play an important role in this condition. On this basis, MMP inhibition may constitute an important therapeutic approach to treat this disorder (Sachdev *et al.* 2004).

Based on speculations that increased MMP-9 levels observed in eyes affected by inflammation and diabetes may have an effect on lens pathology, it was reported that MMP-9 is capable of breaking through the lens structure, degrade mainly crystalline βB1 and other substrates and cause cataract (Descamps *et al.* 2005). Pathological analysis of sublaxated lenses, a common characteristic of Marfan Syndrome, revealed the presence of MMP-1,-3 and -9 and lack of TIMPs. In contrast, MMP-1 and -3 were lacking in the zonules of normal lenses, whilst TIMP-1,-2 and -3 were found to exist. Furthermore, MMPs have been implicated in the sublaxation of the lens in Marfan syndrome as supported by the detection of MMP mediated fibrillin catabolization molecules (Sachdev *et al.* 2002).

1.2.2.3. Retina

During embryonic life, cell migration and proliferation play an important role in tissue development. Investigations in mice embryos have shown that staining of transcripts of MMP-9 may be found in the optic tract neurons that give rise to the retinal ganglion cell layer, but not in the pigmented layer (Canete-Soler *et al.* 1995).

TIMP-1 may be found in the inner plexiform layer (IPL) of normal bovine retina (Jones *et al.* 1994), whilst TIMP-3 is expressed *in situ* by RPE (Della, Campochiaro, & Zack 1996; Fariss *et al.* 1997; Vranka *et al.* 1997) and choroidal endothelial cells (Vranka *et al.* 1997). TIMP-2 is also expressed in the choroid and Bruch's membrane (Vranka *et al.* 1997). Brown *et al* first reported the presence of MMP-2 in normal human vitreous further experiments led the same group to identify the role of this MMP in vitreous liquefaction in mammals (Brown *et al.* 1996). In 1997 it was observed that human retinal pigment epithelial (RPE) cells in culture secrete MMP-2 and TIMP-1 and that this secretion was more significantly observed at the apical surface of the RPE (Padgett *et al.* 1997). Later investigations demonstrated the presence of MMP-1, MMP-2, MMP-3 and MMP-9 as well as of TIMP-1, -2 and -3 in the retina, RPE cells, interphotoreceptor matrix (IPM) and vitreous body of the normal human eye (Plantner, Smine, & Quinn 1998). In addition, the

presence of low levels of MT1-MMP and MMP-2 was reported in normal human retina and it was suggested that these MMPs derive from neighbor tissues, such as the vitreous body and the choroid, where they are abundant (Smine & Plantner 1997). MMP-1 was found too in the inner and outer plexiform layers and nuclear cell layers of normal cadaveric retina (Webster, Chignell, & Limb 1999). TIMP-2 was also identified in the inner and outer nuclear cell layers, whilst MMP-2 was not detected. However, MMP-2 has been shown to be constitutively expressed by human Müller cells *in vitro* and it has been suggested that expression of this MMP may play important role in the maintenance of retinal integrity *in vivo* (Limb *et al.* 2002). Based on the aforementioned studies, it is possible to conclude that balance between specific MMPs and TIMPs are important for the normal function of the vitreous and the retina. In the following sub-sections we will address the implication of MMPs and TIMPs in the control of ECM changes during pathological processes affecting the retina as well as the potential use of MMP inhibitors for therapeutic use in retinal proliferative conditions.

1.2.2.4.1. Proliferative vitreoretinopathy

Proliferative vitreoretinopathy, a wound healing process of the retina, is the most common reason for failure of retinal detachment surgery. It occurs in 5-10% of patients undergoing surgery and is characterized by formation of fibrocellular membranes on the neuroretinal surface. Upon contraction, these membranes cause further retinal detachment. Formation of retinal membranes is initiated by inflammation, which results in activation and attraction of macrophages and lymphocytes, as well as activation of inflammatory cascades that lead to production and release of cytokines and growth factors (Gilbert *et al.* 1988;Limb *et al.* 1991). This is followed by migration of epithelial cells and fibroblasts to the affected region, deposition of ECM and consequent development of epiretinal (on the inner surface) and subretinal (on the outer surface of the retina) membranes. In addition to epithelial cells and fibroblasts, glial cells (astrocytes and Müller cells), infiltrating inflammatory cells including T lymphocytes, B lymphocytes and macrophages expressing HLA-DQ and –DR in their surface are present in these membranes (Baudouin *et al.* 1990; Esser, Heimann, & Wiedemann 1993; Gilbert *et al.* 1988; Jerdan *et al.* 1989; Tang *et al.* 1992). Immunohistochemical examination of subretinal and epiretinal membranes of PVR showed intense staining for MMP-1 and MMP-2, but much lower expression of MMP-3,

MMP-9, TIMP-1 and TIMP-2 (Webster, Chignell, & Limb 1999). These observations were later confirmed by Sheridan *et al* (2001), which showed that in addition to active forms of MMP-2 and -9, the latent forms of these MMPs are also found in PVR membranes and in surrounding media. Because different patterns of MMP expression were found in PVR membranes compared with normal retina (in normal cadaveric retinas that were used as controls, only staining for MMP-1 and TIMP-2 was found), it was suggested that MMP-2, -3, -9 and TIMP-1 may have a role in the pathological formation of epiretinal membranes. In a study that 140 vitreous samples from patients with rhegmatogenous retinal detachment were examined for the presence of MMP-2 and MMP-9, mainly complicated by preoperative PVR and giant retinal tears, MMP-2 was detected in all the samples, unlike MMP-9, that was present in only 47% of the specimens investigated (Kon *et al.* 1998). Additionally, measurement of MMP-2 and MMP-9 levels in the same samples showed that there is a significant association between the levels of these two MMPs and the development of postoperative PVR. Similar observations were also reported in a study that the authors have found constitutive expression of MMP-2 without variations in the levels of this MMP in vitreous samples from eyes with rhegmatogenous retinal detachment complicated or uncomplicated with PVR and diabetic retinopathy (bu El-Asrar *et al.* 1998). In addition, the presence of MMP-9 was more often found in vitreous from eyes with PVR and especially with PDR, compared with vitreous from eyes with uncomplicated rhegmatogenous retinal detachment. Furthermore, it is worth mentioning that vitreous levels of MMP-9 were significantly higher in vitreous from eyes with diabetic retinopathy, when compared with PVR and uncomplicated retinal detachment. Partially responsible for MMP-9 expression and secretion at the vitreoretinal level are Tumor Necrosis Factor – α and Interleukin 1. They are known to induce MMP-9 production (Mohtai *et al.* 1993; Unemori, Hibbs, & Amento 1991) and are found in vitreous and epiretinal membranes from eyes with PVR and diabetic retinopathy (bu el Asrar *et al.* 1992; Limb *et al.* 1991; Limb *et al.* 1994; Limb *et al.* 1996; Mohtai *et al.* 1993; Tang *et al.* 1993). Moreover, the role of IL-1β and hepatocyte growth factor (HGF) in MMP expression and production has been reported in a rabbit model, which showed that these two cytokines increase MMP-9 expression (Liou *et al.* 2002). RPE cells have been shown to produce IL-1β (Alexander *et al.* 1990), which is released into the vitreous and subretinal fluid in PVR as well as during other conditions induced by trauma and inflammation. HGF has been detected in the initial phase of PVR which is characterized by RPE proliferation and migration. Its receptor, c-met, is expressed both in normal RPE cells and in activated RPE cells of proliferative PVR

membranes (Briggs *et al.* 2000; Lashkari, Rahimi, & Kazlauskas 1999). IL-1β and HGF are capable of activating the MAPK cascade, which as indicated above, induces expression of the oncogenes c-jun and c-fos, which in turn induce the expression of MMPs. It is of interest that in the same study, the maximal levels of MMP-9 were observed at the same time at which c-met phosphorylation reached maximal levels. HGF also activates uPA and tPA that lead to activation of plasminogen to plasmin and finally of proMMPs. These observations may therefore explain the overexpression of MMP-2 and the presence of MMP-9 in PVR membranes (Liou *et al.* 2002). MMP-9, through its ability to degrade collagen IV, assists in the detachment and migration of RPE cells, the main cellular component of PVR membranes, from the basement membrane (Liou *et al.* 2002). It also facilitates the migration of T lymphocytes (Leppert *et al.* 1995), which may explain the presence of these cells in retinal membranes. Müller cells isolated from human eyes are able to release MMP-2 and -9 but only MMP-9 expression is upregulated by TNF-α either in soluble form or bound to ECM proteins (Limb *et al.* 2002). The role of MMPs in matrix contraction has been elucidated *in vitro* using a three dimensional model of collagen gel contraction (Sheridan *et al.* 2001). In this model, cells that have fibroblastic appearance contract collagen efficiently, but cells with epithelial appearance do not exert such contraction. Inhibition of MMP activity by Ilomastat, a potent MMP inhibitor, causes inhibition of contraction, thus highlighting the important role of MMPs in collagen contraction *in vitro* and their potential role *in vivo*. This is further supported by investigations in which intravitreal injections of Prinomastat, an inhibitor of MMP-2, -9, MT-1MMP and MMP-3 activity, significantly prevented the development of PVR in a rabbit model of retinal detachment (Ozerdem *et al.* 2000).

1.2.2.4.2. Diabetic retinopathy

Proliferative diabetic retinopathy (PDR) is one of the main complications of diabetes, characterized by retinal neovascularisation (Garner 1993; Williams *et al.* 2004). In normal retina, the blood-retinal-barrier (BRB) consists a wall of firmly connected endothelial cells that separate the neural retina from the circulation. The BRB is divided into two anatomical structures; the inner BRB formed by retinal endothelial cells and the outer BRB formed by RPE cells. During early stages of diabetic retinopathy, apoptotic loss of mural pericytes from retinal capillaries occurs, leading to the breakdown of the BRB and

subsequently to changes in the morphology of retinal capillaries, appearance of microaneurysms, neovascularization and dot haemorrhages due to vascular leakage (Frank 2004). Neovascularisation is induced by growth factors found in vitreous samples of patients with DR, such as Vascular Endothelial Growth Factor (VEGF), Transforming Growth Factor beta (TGF-β), Insulin-like Growth Factor (IGF) and basic Fibroblast Growth Factor (bFGF) (Adamis *et al.* 1994;Forrester *et al.* 1993). Initial release of growth factors is thought to be induced by hypoxia, caused by vascular alterations and haemorrhage. An essential step for neovascularisation is the production of ECM, necessary for the migration of endothelial, glial, RPE, inflammatory cells and fibroblasts (Hiscott *et al.* 1993). In more severe diabetic retinopathy, the proliferating new vessels pass through the ILM to the vitreous. The ECM deposition, cell migration and development of preretinal neovascularisation leads to formation of contractile epiretinal fibrovascular tissue, causing tractional retinal detachment and vascular leakage. Fibrovascular membranes of PDR are often developed at the borders of the posterior hyaloid membrane and the internal limiting membrane (ILM). Cell migration through the ILM requires degradation of the ILM components, which mainly are collagen VI and I, fibronectin, laminin and proteoglycans (Ishizaki *et al.* 1993; Kohno *et al.* 1987; Russell, Shepherd, & Hageman 1991). This is believed to be the main involvement of MMPs in the PDR pathology, but further understanding of the role that MMPs may play in normal retina and pathological conditions affecting retina is very important and may lead to the development of promising treatments.

A significant difference in the presence of MMPs in vitreous samples between post mortem human eyes from non-diabetic and diabetic patients has been identified (Brown *et al.* 1994). Although proMMP-2 was present in both non diabetic and diabetic vitreous samples, an additional gelatinolytic activity identical to proMMP-9 was only found in diabetic vitreous. In addition, presence of TIMP-2 was found in both diabetic and non-diabetic vitreous samples (De La Paz *et al.* 1998). Moreover, active forms of MMP-2 and -9 have been also observed by other investigators in the diabetic retina and staining for pro-MMP-2 and -9 in normal retinas has been shown to be significantly lower than in diabetic epiretinal membranes, suggesting a potential role of MMPs in retinal neovascularisation (Das 1999). As supported by others, the role of MMP-2 and -9 is highlighted by observations that angiogenesis is markedly reduced in mice deficient in these two MMPs (Itoh *et al.* 1998; Vu *et al.* 1998). Differences in the activation ratio of proMMP-2 and -9 have been shown in vitreous and fibrovascular membranes of diabetic eyes (Noda *et al.* 2003). The activation ratio of proMMP-2 and proMMP-9 was found to be higher in

fibrovascular membranes than in vitreous from eyes with PDR and the activation rate of proMMP-2 elevated compared to proMMP-9. Parallel to these findings, it has been suggested that pro-MMP-9 presents some proteolytic function and without its activation to MMP-9 (Bannikov *et al.* 2002). Furthermore, Noda *et al* (2003) reported co-localization of MMP-2 and -9 in glial and endothelial cells of fibrovascular tissues, expression of MT1-MMP in fibrovascular tissue and co-localization of MMP-2, MT1-MMP and TIMP-2 in the same cells (in most of the samples), which may explain the activation mechanism of the proMMP-2 during the development of PDR.

Presence of pro-MMP-9 has been identified in 73% of vitreous samples from diabetic patients, in comparison with 8% of normal vitreous. Expression of this MMP has been shown to increase with the progression and severity of PDR (Kosano *et al.* 1999), and high levels have been associated to active progression of PDR where ECM remodeling and neovascularisation are taking place (Jin *et al.* 2001). Furthermore, increased levels of MMP-9 have been observed in rat retinas when BRB permeability is increased and in supernatants of RPE cells cultured in high glucose medium (Giebel *et al.* 2005). Since MMP-2 and -9 are capable of degrading occludin (Giebel *et al.* 2005), a protein component of tight junctions between endothelial cells of the inner BRB, increased permeability of the retinal vessels observed in these diabetic animals may be explained by reduction of this protein (Antonetti *et al.* 1998).

Moreover, the levels of MMP-9 in vitreous from eyes with PDR were significantly higher than in eyes with macular hole, but that levels of MMP-2 in both conditions were similar (Ishizaki *et al.* 2006). The most important finding of this study was the correlation of angiotensin-converting enzyme (ACE) and VEGF levels with those of MMP-9 in PDR vitreous. It was suggested that both factors upregulate MMP-9 as part of the pathophysiology observed in PDR. Furthermore, the existence of a positive feedback between VEGF and MMP-9 was found in RPE cells, with VEGF to have been reported to increase the MMP-9 expression and secretion and MMP-9 to have been found to enhance the VEGF expression. Under hypoxic conditions that VEGF expression is upregulated, this mechanism could lead to increased expression of both angiogenic molecules, VEGF and MMP-9, in RPE cells. What remains to be found is if this mechanism is initiated by the secretion of MMP-9 by inflammatory cells that infiltrate the region when hypoxia occurs (Hollborn *et al.* 2007). A recent study indicated that hypoxia induced VEGF-mediated angiogenesis, as well as the MMP-9 activity is controlled by the gene dose of Angiopoietin-2 (Ang-2). It was shown that concomitant Ang2 and MMP expression occurs

in the retina of $Ang2^{+/-}$ transgenic mice in which angiogenesis was induced through hypoxia. Reduced MMP-9 activity as well as declined pre- and intra-retinal angiogenesis was also shown in the $Ang2^{+/-}$ transgenic mice (Feng *et al.* 2009). Another possible pathway by which MMPs may play a role in angiogenesis is suggested by evidence that exposure to proteolysis of the HUIV26 site within collagen IV is critical for angiogenesis. Mice deficient in MMP-9 show reduced exposure to this site (Xu *et al.* 2001).

An earlier comparative study between PVR and PDR membranes indicated that there are no significant differences in the staining for various MMPs and TIMPs between both conditions. This suggested the existence of common pathological pathways in these disorders (Salzmann *et al.* 2000).

1.2.2.4.3. Sorby's Fundus Dystrophy

In 1949 Sorsby and co-workers described in five families a fully penetrant autosomal dominant disorder of the macula (the retinal central area specialized in colour and high resolution vision) as a 'central retinal lesion showing oedema, haemorrhage and exudates'. Sorsby's fundus dystrophy is a rare condition with its onset taken place between the third and sixth decade-usually in the fourth decade- of life (Sorsby 1949). It is characterized by Bruch's membrane (basement membrane that consists of five layers of connective tissue and anatomically separates RPE from the choriocapillaris) thickening and extracellular deposits-drusen-among the basement membrane of the RPE cells and the inner collagenous layer of Bruch's membrane (Capon *et al.* 1988; Capon *et al.* 1989). Clinically, the first symptom is night vision difficulties that occur about two decades before rapid loss of central vision takes place. The final stage is the progressive loss of peripheral vision (Capon *et al.* 1988). The pathophysiology of this blinding disorder is characterized by either initial atrophy of the choriocapillaris and subsequently the retina (Capon *et al.* 1988) or by subretinal neovascularisation and retinal detachment (Clarke *et al.* 2001; Polkinghorne *et al.* 1989).

Mutations in the TIMP-3 gene on chromosome 22q13 are responsible for Sorsby Fundus Dystrophy (Weber *et al.* 1994b). Exon five, where all the reported mutations are located, encodes the C-terminal domain of this MMP inhibitor, which has been shown to confer TIMP-3 its unique characteristic to bind to insoluble ECM (Langton, Barker, & McKie 1998; Leco *et al.* 1994). To date, nine mutations have been described in patients

with SFD; seven point mutations [Tyr168Cys, Ser181Cys (Weber *et al.* 1994a), Ser156Cys (Felbor *et al.* 1995), Gly167Cys (Felbor *et al.* 1996), Tyr172Cys (Jacobson *et al.* 2002) Gly166Cys (Felbor *et al.* 1997), 508A→T resulting in Ser170Cys (Barbazetto *et al.* 2005)], a splice site mutation-single base insertion- at the junction of intron 4 with exon 5, changing the sequence from CAG to CAAG (Langton, Barker, & McKie 1998; Tabata *et al.* 1998) and finally a point G→T mutation encoding a stop codon (Glu139Ter), resulting in non expression of most if the C-terminal domain as well as in an unpaired cysteine residue, the Cys122 (Langton *et al.* 2000). Langton *et al* have demonstrated that these mutant proteins are functional inhibitors, are expressed in lower volume than the wild type and are glycosylated and bound to ECM (Langton *et al.* 2000;Langton, Barker, & McKie 1998). Unlike wild type, the mutant proteins form dimmers by combining homotypically and heterotypically with other heterologous proteins, due to the presence of free cysteine in their molecules and the formation of disulfide bonds. In each mutation, different dimmers are formed due to the different positions of free cysteine in their molecules (Langton *et al.* 2000). Some of these mutations are related to different ocular disorders, as illustrated by the association of Glu139Ter with macular atrophy (Clarke *et al.* 2001), the Ser156Cys mutation with choroidal neovascularization and the Ser181Cys mutation with late onset of the SFD disorder (Felbor *et al.* 1995, Carrero-Valenzuela *et al.* 1996)

As previously indicated, TIMP-3 is expressed by RPE cells and the ciliary epithelium (Della, Campochiaro, & Zack 1996;Ruiz, Brett, & Bok 1996) and constitutes an important component of the Bruch's membrane (Fariss *et al.* 1997). Because TIMP-3 is an inhibitor of angiogenesis and endothelial cell migration *in vitro* and *in vivo* (nand-Apte *et al.* 1997; Takahashi *et al.* 2000), it was originally thought that a reduction in the production of the wild type of this molecule due to genetic mutations would decrease MMP inhibition and consequently promote neovascularisation. Surprisingly, it was found that patients with SFD show increased accumulation of TIMP-3 in the Bruch's membrane (Chong *et al.* 2000), as judged by increased immunoreactivity. This increased accumulation has been ascribed to either an increased production or to delayed degradation of this natural inhibitor. Chong NH *et al* suggested that the high levels of TIMP-3 observed in Bruch's membrane can not be the outcome of overexpression of TIMP-3 (Chong *et al.* 2003) and later Langton *et al* (2005) testing the Ser156Cys, Ser181Cys and Glu139Ter mutation cases, observed that high concentration of TIMP-3 is caused by its delayed cleavage by RPE cells. They also found that accumulation of TIMP-3 doesn't reduce the secretion of TIMP-3. This is in agreement with previous studies that showed that TIMP-3 expression

from RPE cells during aging is constitutive and almost unaffected (Bailey *et al.* 2001; Vranka *et al.* 1997).

At present, there is a debate of whether accumulation of TIMP-3 creates the pathological background of Sorsby's fundus dystrophy. It has been suggested that increase in TIMP-3 may inhibit ECM turnover, creating a physical barrier that affects the nutrition of the retina, consequently leading to atrophy and visual impairment (Langton *et al.* 2005). Because TIMP-3 has been found to have pro-apoptotic effects (Baker *et al.* 1998; Smith *et al.* 1997; Vranka *et al.* 1997), it may be possible that TIMP-3 have a direct effect on the induction of RPE apoptosis (Majid *et al.* 2002).

1.2.2.4.4. Age-related macular degeneration

Age-related macular degeneration is the leading cause of untreatable blindness in the developed world (Evans 2006; Klein *et al.* 2004). The etiology and precise pathogenesis of AMD have not been completely identified. However, a mutation observed in the Statgardt's disease gene, which is responsible for encoding of the photoreceptor rim protein (an ATP binding Cassette Transporter-the ABCA4-), appears to be the cause in only a small percentage of AMD cases (Allikmets *et al.* 1997).

Two types of AMD have been identified; the 'dry' or non-exudative or atrophic form and the 'wet' or exudative or neovascular form. The dry form accounts for more than 80% of the AMD cases but only for 20% of visual loss incidents, whilst wet form, that is more severe, occurs in less than 20% of the AMD patients, but accounts for more than 80% of the blindness incidents caused by AMD. The first pathological sign of AMD is the presence of deposits, known as drusen, that appear either between the basal membrane of the RPE and the inner collagenous layer of the Bruch's membrane, or between the plasma membrane of RPE and the basal membrane of RPE. Bruch's membrane consists of five layers: a) the basal membrane of RPE, b) the inner collagenous layer, c) the middle elastic layer, d) the outer collagenous layer and e) the basal membrane of the choriocapillaris. Because of the location of drusen, mainly around the RPE cells, it has been suggested that RPE cells synthesize the main components of these deposits (Amin *et al.* 2004). These deposits may be hard or soft and their presence constitute the first clinical sign of AMD. Presence of drusen and RPE and photoreceptor atrophy are regularly the pathological signs of the dry form, although it is not known whether photoreceptor atrophy is the primary

pathological sign of this disorder, or whether it is triggered by drusen deposition and cleavage of RPE and Bruch's membrane. The main characteristic of wet AMD is the presence of choroidal neovascularisation and formation of fibrovascular membranes that extend into the Bruch's membrane and end up in the subretinal space. Histological analysis of these membranes indicated the presence of RPE cells and Bruch's membrane fragments as their components.

Although there is a close similarity between Sorsby's fundus dystrophy and AMD, mutations in the TIMP-3 gene have not been found in AMD patients (Felbor *et al.* 1997). However, several studies have implicated various MMPs and TIMPs in the pathogenesis of AMD. TIMP-3 has been found in the RPE layer as well as MMP-1,-2,-3,-9. TIMPs, apart from TIMP-4, were additionally detected in the subretinal fibrovascular membranes (Steen *et al.* 1998). Using immunohistochemical methods, significant staining for TIMP-3 has been found in Bruch's membrane and in drusen from eyes with AMD (Apte, Olsen, & Murphy 1995; Fariss *et al.* 1997). In Bruch's membrane, increasing accumulation of glycosaminoglycans with age (Kliffen *et al.* 1996) can possibly explain the accumulation of TIMP-3, due to the ability of this inhibitor to bind to sulphated glycosaminoglycans(Yu *et al.* 2000). Plantner *et al* observed that in comparison with normal retinas, there is a significant increase of MMP-2 in the RPE related interphotoreceptor matrix (IPM) in AMD patients (Plantner, Smine, & Quinn 1998). Because of the known ability of RPE cells to secrete MMPs, the fact that the RPE layer is firmly connected to Bruch's membrane, and the first pathological signs of the disorder are present in the borders between these two structures, it has been suggested that changes in the secretions of MMPs by RPE cells may initiate the pathological mechanism of AMD (Plantner, Smine, & Quinn 1998). This is supported by other studies that show that increased expression of MMP-2 mRNA can be seen in experimental induced choroidal neovascularization in rats (Kvanta *et al.* 2000), and that in addition to the presence of inactive MMP-1, -2, -3 and -9 and the active form of MMP-2 only, levels of proMMP-2 and -9 increase with age (Guo *et al.* 1999). It is of interest that active MMP-2 may be found in the peripheral retina but not in the macular regions (Guo *et al.* 1999). Based on these results it was suggested that low levels or absence of active MMP-2 in the macular region could be responsible for the reduced degradation and accumulation of deposits found in AMD. Moreover it was suggested that increased levels of inactive MMPs are most likely the result of Bruch's membrane thickening and not the cause of AMD (Guo *et al.* 1999). Although MMPs are found in RPE, Bruch's membrane and fibrovascular membranes, they are absent from drusen core

and it is believed that abundance of TIMP-3 in the drusen make them resistant to proteolysis (Leu *et al.* 2002). The increased TIMP-3 levels may affect remodeling of ECM in the retina by inhibiting the activation of MMPs, therefore leading to accumulation of ECM. Subsequent deposition of ECM may reduce functionality of the 'hydraulic system' of Bruch's membrane, the circulation of nutrients and the diffusion of activated MMPs or activators of MMPs in the region. This is supported by the study of Ahir A *et al* (2002), which reported that activated forms of MMP-2 and especially of MMP-9, have been shown to increase Bruch's membrane permeability *in vitro*. This study also indicated that activated MMP-9 was produced in large quantities during the migration of the RPE cells *in vitro*. Based on these observations, it was suggested that lack of MMP-2 and MMP-9 may lead to thickening of Bruch's membrane and accumulation of debris. Migration of RPE cells is observed in eyes undergoing laser treatment for AMD, possibly as a healing response and the need to remove dead tissue by phagocytosis (Marshall & Mellerio 1971). Active MMP-9 produced by RPE cells after laser treatment could play a role in the phagocytosis of dead tissue by these cells and may also improve the permeability of Bruch's membrane.

Examination of polymorphisms in the promoter region of the gene that encodes MMP-9 and specifically the region characterized by a sequence of CA (Cysteine Adenine) repeats (from 13 to 27 times) has shown that patients with one allele with equal or higher number of 22 CA repeats have more than double risk to develop AMD. This is of special interest because CA repeats has been suggested to facilitate the opening of the double stranded DNA and its transcription (Fiotti *et al.* 2005).

Other studies have shown that MMP-7 is expressed in fibrovascular membranes of CNV and that staining for MMP-7 may be found within the basal laminar deposits (Kadonosono *et al.* 1999; Yazama *et al.* 2002). This suggests that this MMP may also play a significant role in the pathogenesis of CNV. Unlike other MMPs found in AMD eyes, MMP-7 was detected in its active form, for which the authors proposed a potential model in which MMP-7 degrades the basement membranes of RPE, choriocapillaris and Bruch's membrane, leading to the development of CNV. The authors also observed that MMP-7 is localized to the non-collagenous components of the basal laminar deposits, which are believed to derive from degenerated RPE cells.

Using a CNV model (laser-induced rupture of the Bruch's membrane) in wild mice or in mice deficient in MMP-2 or MMP-9 or both, and application of MMP-2, -9 and -14 inhibition using Batimastat or Ro 28-2653 (Lein *et al.* 2002) or by transfecting mice with recombinant adenovirus carrying the TIMP-1 and -2 human genes, it was concluded that

MMP-2 and -9 co-operate during the development of CNV and that the inhibition of only one of these MMPs is not enough to prevent it (Lambert *et al.* 2003). They also suggested that synthetic MMPi could constitute a potential therapeutic strategy. Later studies showed that carboxyamido-triazole (CAI), an inhibitor of non-voltage, ionophore and refilling channels in an *in vitro* 'wet' AMD model, inhibits RPE and choroidal endothelial cell proliferation induced by bFGF. These constitute important features in the development of choroidal neovascularisation (Hoffmann *et al.* 2005). In addition, CAI inhibited MMP-2 production, supporting what had been previously reported by Kohn EC *et al* (1994), that MMP-2 expression is dependent on the presence of extracellular calcium. Due to these observations, it may be possible to suggest that CAI may have therapeutic potential for the treatment of 'wet' AMD.

1.2.2.4.5. Uveal melanoma

Uveal melanoma is a rare malignant disease. However, it is the most common intraocular malignant tumor in the adult population (Shields 1977; Shields, Shields, & Donoso 1991). Based on cell morphology, two main types of uveal melanoma have been identified: the spindle type and the epithelioid type. The overall patient survival is approximately 6.5 years (McLean 1993), although the epithelioid type has poorer prognosis. Uveal melanoma spreads mainly via the hematogenous route as there is no lymphatic circulation in the eye (McLean 1993). It usually metastasizes into the liver (Zimmerman 1980), with about 40% of the newly diagnosed uveal melanomas spreading to the liver within 10 years of diagnosis (Shields, Shields, & Donoso 1991). Once metastasis occurs, the life expectancy is less than a year (Char 1978; Gragoudas *et al.* 1991). For metastasis to commence, a number of cells detaches from the primary tumor and binds to the ECM and the basement membrane of the vessels through adhesion molecules such as integrins, cadherins and selectins. Upon degradation of ECM by proteinases including MMPs, they are able to pass into the circulation (Elshaw *et al.* 2001; Pignatelli & Vessey 1994).

Involvement of MMPs in the pathogenesis of uveal melanoma has been demonstrated by several studies. Initially, gelatinase A and B were detected in the medium of primary cultures of uveal melanoma cells (Cottam *et al.* 1992) and in a later study MMP-2, TIMP-1 and -2 were found in the vitreous of eyes with uveal melanomas

(Vaisanen *et al.* 1999). Intracytoplasmic MMP-2 staining was also identified in all of the epithelioid type melanomas, in half of uveal melanomas comprised of both epithelioid and spindle cell types, and in a third of melanomas comprised mainly of spindle type cells. In the study of Väisänen A *et al*, it was shown that cases in which MMP-2 was present had worse prognosis than cases in which MMP-2 was absent. They suggested that MMP-2 expression could be possibly used as a marker for metastatic risk and poor prognosis (Vaisanen *et al.* 1999). Increased MMP-2 expression in uveal melanomas has been also reported (Beliveau *et al.* 2000), although the authors did not differentiate between the active and latent forms of this MMP. The answer to this question has been given by Bèrubè *et al* (2005) who found that the ratio of active to inactive MMP-2 is high in uveal melanoma and that MMP-2 activity is closely related to the progression of this malignancy. In addition to MMP-2, MMP-9 seems to play a significant role in the pathogenesis of uveal melanoma and is also associated with poor prognosis (El-Shabrawi *et al.* 2001). Indeed, it was shown that about 70% of epithelioid uveal melanomas or the epithelioid parts of the mixed uveal melanomas stained for MMP-9, in comparison with only 10% of the spindle cell type melanomas. Moreover, about 67% of MMP-9 positive melanomas developed metastases within 47.5 months, compared to only 15% of the MMP-9 negative melanomas. Previous studies had shown that tumor cells located within retinal or vortex vessels express MMP-9, suggesting a role for this enzyme in tumor invasion (Kim *et al.* 1998). That MMPs play an important role in the metastasis of uveal melanoma was further supported by observations that showed that TIMP-1 and -2 positive melanomas had much lower metastatic rate and much higher survival rate than TIMP-1 and -2 negative melanomas (El-Shabrawi *et al.* 2001). In contrast to these observations it was reported that although MMP-2 and MMP-9 were found in the majority of uveal melanoma cultures, no correlation between MMP secretion and tumor invasiveness was found (Elshaw *et al.* 2001). Based on the evidence that MMPs play a major role in uveal melanoma, studies that aimed to control tumor growth with MMP inhibitors have been published (Ozerdem *et al.* 2002). Accordingly, the authors administered prinomastat (AG3340), a potent and selective MMP inhibitor of MMP-2,-9,-13 and -14, intravitreally into the eyes of rabbits with uveal melanoma xenografts. Interestingly, only one third of the prinomastat treated eyes accepted the xenograft, in contrast with 83% of eyes in the control group. In addition, in the prinomastat treated eyes the tumour size was much smaller than in the control group and the apoptotic rate of the implanted uveal melanoma cells was much higher in prinomastat treated eyes than in the controls. The authors suggested that these results could be due to

previously reported findings that MMP inhibitors cause a decrease in the proliferation of tumor cells (Zervos *et al.* 1997; Shalinsky *et al.* 1999), or that MMP inhibition may increase the susceptibility of tumor cells to TNFα induced apoptosis (Nakamura *et al.* 2001). Another important study suggested a mechanism by which aggressive melanoma cells form vasculogenic networks in three dimensional collagen I gels *in vitro,* similar to those observed in uveal and cutaneous melanoma tissues isolated from patients (Seftor *et al.* 2002). They observed that vasculogenic-like networks were found only in cultures of aggressive melanoma cells and that these cells, compared to the poorly aggressive ones, expressed much higher levels of MMP-1, -2, -9, -14 and laminin 5 γ2 chain. The study shows that Ln-5 γ2 chain, MMP-2 and -14 cooperate in the formation of vasculogenic-like networks *in vitro*, which may resemble that observed *in vivo*. Several factors can regulate this cooperation, as demonstrated by inhibition of phosphoinositide 3 kinase (PI3K), which reduces the expression of MMP-14 and subsequently the activation of MMP-2 and the cleavage of Ln5 γ2 chain, all important for the formation of vasculogenic-like networks (Hess *et al.* 2003). Additionally, chemically modified tetracycline (COL-3) decreased vasculogenic network formation *in vitro* by inhibiting MMP release (Seftor *et al.* 2002). Furthermore, depsipeptide (DP), a histone deacetylase inhibitor (HDACI) reduces in a dose dependent manner the invasiveness of primary and metastatic uveal melanoma cells. This is due to a decreased MMP-2, -9 and -14 expression and an increase in TIMP-1 and -2 levels (Klisovic *et al.* 2005). These factors, as well as MMPis, may be used as targets of future therapies for uveal melanoma.

1.2.3. Current postoperative treatment of fibrosis after GFS

Antimetabolites such as mitomycin C (MMC) and 5-fluorouracil (5-FU) are used clinically to prevent scarring after glaucoma surgery. They have been shown to be effective in reducing the scarring after trabeculectomy (1996;Skuta *et al.* 1992). Many studies have been published from our lab that describe the increase of the functioning period of the outflow channel in the bleb. Results indicate that a single five minute application of 5-FU or mitomycin C during surgery reduces the activity of the healing response to decrease fibrotic formation. It is thought this is mainly due to suppression of fibroblast proliferation, prolonging the bleb survival (Doyle *et al.* 1993; Khaw *et al.* 1992; Khaw *et al.* 1994). Unfortunately, severe complications often occur after treatments with these metabolites.

The bleb sometimes leaks and there are lots of other effects including hypotony, endophthalmitis and excessive ocular cell apoptosis that can cause irreversible vision loss. Hence safer and more effective agents are needed to reduce scarring and to control healing after GFS.

1.2.4. Synthetic inhibitors of MMPs

Since MMPs take part in several pathological conditions, it is important to identify selective inhibitors that can be used therapeutically to control MMP activity in defined ways. The use of the natural TIMP inhibitors has significant disadvantages such as their high molecular weight and their poor oral bioavailability, which prevent their clinical use. In addition, it has been shown that although TIMPs may improve the prognosis of some categories of tumors, there are examples where TIMPs are involved in more aggressive cancer progress (Glasspool & Twelves 2001).

To overcome these difficulties, synthetic compounds to block MMP activities (MMPIs) have been designed. Some of the most well-known MMPIs are batimastat (BB-94), marimastat (BB-2516), Prinomastat (AG3340) and Tanomastat (BAY12-9566) (Glasspool & Twelves 2001). These are hydroxamic acid derivatives that bind reversibly to the zinc in the active site of MMPs. Most of the potent inhibitors designed to date are right-side binders, as left-side binding is much weaker possibly due to its natural ability to prevent the carboxylate product of substrate cleavage from becoming a potent inhibitor of the enzyme (Skiles, Gonnella, & Jeng 2001).

Batimastat is a pseudopeptide with structural similarity to collagen that inhibits MMP-1,-2,-3,-7, and -9 (Canete *et al.* 1995; Hoekstra, Eskens, & Verweij 2001), was the first synthetic inhibitor of MMPs tested in clinical trials for malignances. Because of its low oral bioavailability caused by poor solubility, intraperitoneal administration was used. Side effects included abdominal pain, fever, asymptomatic elevation of liver enzymes and pain at the site of injection. However, there were no significant clinical responses and this led British Biotech to replace it with another, orally administered MMPI, marimastat.

Although there were not important clinical differences when compared to other chemotherapy (gencitabine), further analysis revealed that patients with pancreatic and gastric cancer lacking distant metastases and already been treated with chemotherapy, may benefit from marimastat (Glasspool & Twelves 2001). Additionally, marimastat seems to

increase survival and delay disease progression in patients with advanced gastric cancer (Lelongt *et al.* 1997). Musculoskeletal pain is its most important side effect. Today non-peptido mimetics, like BMS-275291 (is being assessed for lung, prostate cancer and Kaposi's sarcoma) (Lockhart *et al.* 2003) and non-peptidic chemicals like tetracyclines (Kwan *et al.* 2004) are being tested in humans.

1.2.4.1. Ilomastat

Ilomastat (Figure 6) is a synthetic derived MMP inhibitor. This molecule is also known as GM6001 or as Galardin, named after the person who discovered it (Galardy *et al.* 1994). Studies in our lab have demonstrated that ilomastat can inhibit MMPs during subconjunctival wound healing without toxic effect. For these reasons our group is focused on Ilomastat for use for scarring inhibition after GFS.

Ilomastat (molecular formula $C_{20}H_{28}N_4O_4$, 388.47 g/mol) is a peptide analogue with the formal chemical name of N-[(2R)-2-(hydroxamidocarbonylmethyl)-4-methylpentanoyl]-L tryptophan methylamide. It is a broad spectrum hydroxamate MMP inhibitor (Galardy *et al.* 1994).

The reported Ki values are as follows: Human MMP-1 (Fibroblast collagenase): 0.4 nM, Human MMP-3 (Stromelysin): 27 nM, Human MMP-2 (72 kDa gelatinase): 0.5 nM, Human MMP-8 (Neutrophil collagenase): 0.1 nM, Human MMP-9 (92 kDa gelatinase): 0.2 nM (Galardy *et al.* 1994).

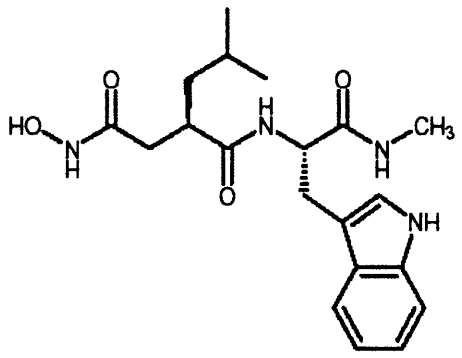

Figure 6: Ilomastat, a hydroxamic acid inhibitor. Else known as Galardin or GM6001.

Ilomastat achieves its inhibitory effect through the competitive binding of the catalytic zinc of MMP by its hydroxamic acid. Hydroxamic acid inhibitors have two

significant disadvantages; (1) short half-life due to the fast metabolism in the liver and (2) low solubility in aqueous solutions (0.03885 mg/ml) (Parker *et al.* 1999). Ilomastat is soluble in DMSO up to at least 400 mg/ml. In contrast Ilomastat is hardly soluble in water (Galardy *et al.* 1994). Relative concentrations of GM6001 in aqueous solutions may be determined by measuring the absorbance of the solution (tyrosine) at 280 nm.

Since it has been found that MMPs play a significant role in wound contraction (Daniels *et al.* 2003; Porter *et al.* 1998), their critical involvement was shown in studies where inhibition of MMPs reduced wound contraction in *in vitro* experiments using collagen I lattices as the wound contraction model (Scott, Wood, & Karran 1998). Both *in vitro* and *in vivo* studies in order to test the effect of MMPis in contraction models have been performed. Daniels *et al* (2003) tested the effect of three MMPIs – Ilomastat, BB-94 and BMS-275291 (Cell Tech) in HTF populated collagen gels. Observations revealed inhibition of the contraction of the gels with the application of all the three MMPIs in a dose-dependent manner and Ilomastat was observed to be the most effective.

The tested MMPIs were also found to have a non-toxic and reversible effect and zymography results indicated significant reduction of the proteolytic activity of the detected MMP bands after the application of the MMPIs. It was also shown that ilomastat inhibited collagen production from fibroblasts in a dose-dependent manner. This was an important finding, as excessive collagen production and deposition at the incision area is mainly responsible for the bleb failure (Cordeiro *et al.* 2000; Daniels *et al.* 1998).

Administration of ilomastat in an *in vivo* contraction model after trabeculectomy was found to significantly prolong the bleb survival in comparison to the control group as well as to have a lowering IOP effect throughout the experiment (Wong, Mead, & Khaw 2003). Histological findings showed that reduction of scar tissue formation in the ilomastat treatment group occurred with decreased cellularity compared to the control group. There was also decreased cell apoptosis (that is known from other studies to be associated to MMC), decreased myofibroblasts in the wound area (possibly because of an inhibitory effect of ilomastat in fibroblast migration) and a large bleb area compared to control group.

The necessity of comparison of the antiscarring effects of ilomastat with MMC led scientists design a new comparative *in vivo* study (Wong, Mead, & Khaw 2005). The ilomastat treated group had similar prolonged bleb survival and IOP lowering results as the MMC treated group. Importantly, this study showed that the morphology of the subconjunctival tissue was normal in the ilomastat group but hypocellular in the MMC

group. It is worth mentioning that in none of our *in vivo* experiments ilomastat damaged conjunctiva, as it can happen in the case of MMC.

1.2.5. RNA Interference

One of the ways with which we tried to inhibit MMPs to stop scarring after glaucoma filtration surgery was by using MMP RNA interference. The mechanism of RNA interference is described below in order to gain a better understanding of how this mechanism works, and how it can reduce the levels and subsequently the effects of specific enzymes, in our case MMPs.

The development of gene targeting technologies have enhanced the understanding of gene function all over the world (Aigner 2006). It is strongly believed that RNA interference (RNAi), through small interfering RNAs (SiRNA), plays a vital role in the structuring of the genome of most organisms (Sharp 2001). This natural mechanism, which is high in reliability and specificity as well as efficiency (Fire, Xu, Montgomery, Kostas, Driver, & Mello 1998; Tebes & Kruk 2005), is believed to have been created even before the divergence of animals and plants and to constitute the oldest antiviral system. Investigating the effects of RNAi in the nematode *C. Elegans*, Fire (1998) applied long double-stranded RNAs (dsRNA) containing the identical sequence to the target genes and detected post-transcriptional silencing of specific genes. This RNAi mechanism (long dsRNAs) was also successful in other organisms including Drosophila. Where vertebrates are concerned, initial efforts with RNAi were unsuccessful because dsRNAs trigger the interferon response (Hammond *et al.* 2000; Tebes & Kruk 2005).

1.2.5.1. Small interfering RNAs (SiRNAs)

siRNAs are small 19-23 nucleotide duplexes (Bernstein *et al.* 2001) with two nucleotide overhangs at each end, containing 5′-phosphates and 3′-hydroxyls, that cleave

mRNA molecules. They are generated in response to introduction of long dsRNAs into the cytoplasm. Modern methods directly transfect siRNAs to the cells (Bernstein *et al.* 2001).

1.2.5.2. Micro-RNAs (miRNAs)

RNA silencing evolved as a mechanism for eukariotic cells to defend themselves against both transposons and pathogens as well as to control their own gene expression. Attempts to detect short-RNAs with the 'interferance' function from several animal species were focused on the detection and isolation of short-RNAs formed by the host genome whose role was not to produce proteins. These RNA molecules are known as pre-miRNAs, ~70 nucleotide short hairpin molecules which fold on themselves because of their self-complementary structure. The enzyme Dicer, which is vital for the function of the siRNA mechanism is also dominant in the miRNA mechanism, as it cleaves the pre-miRNAs into 21-22 nucleotide molecules (miRNAs) (Bernstein, Caudy, Hammond, & Hannon 2001). It has been found that in humans, both *in vitro* and *in vivo*, miRNAs induce cleavage of perfectly complementary target RNAs resulting in gene silencing.

After discussing some general similarities between the siRNA and the miRNA mechanisms, the intracellular mechanism of siRNA interference is described below.

1.2.5.3. Delivery into the cell

1.2.5.3.1. Forms of nucleotides that are introduced into the cell and by which RNAi is achieved

a) *In vivo* direct application of *in vitro* synthesised 19-23 bp double stranded small interfering RNAs (siRNAs) containing 2-nt 3′ overhangs (Aigner 2006).

b) Long dsRNAs may cause a potent interferon response, which results in total post-transcriptional inhibition of gene expression (Filipowicz *et al.* 2005; Meister & Tuschl 2004). Long dsRNA, developed by viral replication or viral gene expression, may be detected through the serine-threonine kinase PKR (Katze *et al.* 1991; Meurs *et al.* 1992; Williams 2001) or the Toll-like receptor 3 (TLR3) (Alexopoulou *et al.* 2001). Expression of interferon (IFN-alpha and IFN-beta) is the result of this process,

especially in plasmocytoid dendritic cells (PDC). A multi-step and multi-factor signalling pathway is induced (Leaman *et al.* 1998) resulting in the upregulation of many interferon-induced genes and this process may cause inhibition of protein synthesis and apoptosis. Further research focusing on RNAi facilitated the overcoming this barrier. Specifically, the Dicer enzyme, an endogenous cytoplasmic RNase III-like enzyme, was found to reduce long dsRNAs into small 19-21 nucleotide duplexes (siRNAs) with two nucleotide overhangs in the 3′(Aigner 2006). It was shown that dsRNAs greater than 30 bp trigger the interferon response, but not the small siRNAs(Manche *et al.* 1992). Consequently, siRNAs could be used as a very useful RNAi tool to perform gene analysis in mammalian cells.

c) DNA encoding short hairpin RNA (shRNA) expression cassettes can be delivered to cells, through which intracellular expression of shRNAs is achieved. These shRNAs are then cut and active siRNAs are developed by the host cell. (Plasmids containing polymerase III promoters have been created by several researchers, known to synthesize small RNA, which facilitate synthesis of 50 bp-long single-strand RNA folded in 21-23 bp dsRNAs with a small hairpin at the middle (shRNAs) (Coumoul & Deng 2006). Other vectors allow synthesis of two complementary short RNA duplexes which then form a siRNA(Uprichard 2005).

1.2.5.4. Ways by which the RNAi nucleotides are transferred into the cells

There are three major strategies for delivery of siRNA into mammalian cells.

a) RNAi effectors

RNAi effectors can be delivered to cells using two different approaches:

i) siRNAs are synthesized in order to be delivered as a 'drug'(Uprichard 2005), and

ii) through a gene therapy approach, in which viruses are used to deliver DNA encoding the target siRNA into the cell nucleus. Viral mediated delivery offers efficient delivery of DNA with persistent siRNA production by the host cells(Brummelkamp, Bernards, & Agami 2002). Retroviruses, adenoviruses, lentiviruses, herpes viruses, simbis viruses and baciloviruses have all been used in gene therapy studies(Lotze & Kost 2002), but

only the first three have been shown to be efficient and to have a long-term effect. In the case of lentivirus mediated gene silencing, Abbas *et al.* suggested that this mechanism is effective within 72 hours post-infection and its function was maintained for at least 25 days. Unfortunately, although viral vectors have significant advantages for RNAi (excellent tissue-specific tropism and transduction efficiency), they are linked with risks and safety issues (Uprichard 2005). Despite the significant problems encountered in the past in gene therapy clinical trials, the RNAi benefits outweigh the risk, and adeno- and lenti-virus associated vectors are being evaluated for clinical delivery of shRNAs(Uprichard 2005).

b) Local delivery

Following successful local administration of antisense drugs to the eye, in initial clinical trials for RNAi-based treatment of age-related macular degeneration, siRNAs are administered with injections directly into the vitreous humor(Check 2005). Intranasal administration for pulmonary delivery and direct delivery into the central nervous system have been considered as additional promising routes (Uprichard 2005).

c) Systemic delivery

SiRNA stabilization, targeting of the effector to the correct tissue, and inducement of cellular uptake are required for the optimization of systemic delivery (Uprichard 2005).

1.2.5.5. Description of the mechanism of RNA interference

1.2.5.5.1. Initial step

Dicer and Drosha (Rnase III family enzymes) are important for the formation of siRNAs from dsRNAs. The importance of these two enzymes was initially shown in a Drosophila embryo extract and these RNA molecules were found to contain a 5′ phosphate and a 3′ hydroxyl terminus (Hammond 2005). It is known that these RNA properties are found when RNaseIII enzymes are involved in the cleavage process.

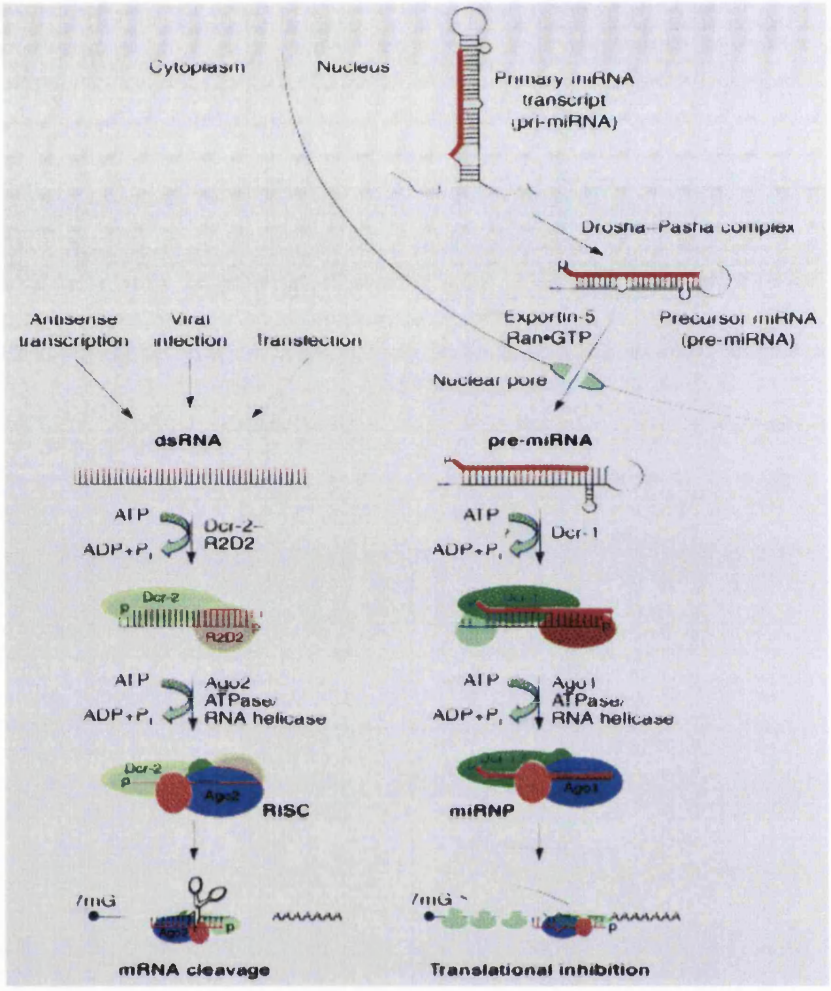

Figure 7: Genesis of siRNAs and miRNAs and how RNA silencing is achieved. This graph shows how pre-miRNAs (from the nucleus) and dsRNAs (introduced into the cells), with the help of enzymes, gradually create miRNAs and siRNAs respectively, through which the silencing of specific genes is achieved, by cleavage of the mRNA. Figure from Filipowitz *et al* (2005).

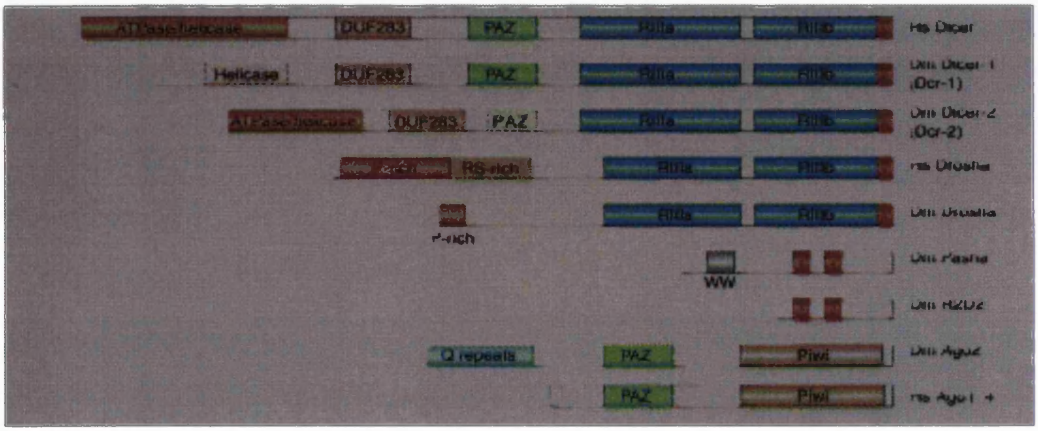

Figure 8: Domain structure of Dicers, Droshas and Argonaute proteins. Diagram from (Filipowitz *et al*, 2005).

Dicers and Droshas are structured by 2 RNase III catalytic domains (RIIIa and RIIIb) and a dsRBD located at the C-terminus.

The Droshas, which are 130-160 kDa nuclear proteins, have N-terminal proline-rich regions and the human (Hs) enzyme has a domain rich in Arg-Ser (RS) dipeptides, similar to the protein–protein interaction domains found in many splice factors (splicing factors are proteins known for their functions to cut introns and exons from the mRNAs). Drosha and Dicer work as a complex with proteins that contain dsRBDs and are known as Pasha (in Drosophila) and R2D2 or DGCR8 (in mammals) (Landthaler, Yalcin, & Tuschl 2004). They are both important for the processing of pre-miRNAs. This large complex (~650 kDa) is believed to be formed as a result of the dimerization of the different components (Filipowitz *et al*, 2005). Although WW, which contains two conserved tryptophans, is usually expected to interact with proline-rich sequences, the WW module of Pasha is not necessary for the connection with Drosha. The pre-miRNA is released by Drosha and it is transferred from the nucleus to the cytoplasm in an Exportin-5/RAN-GTPase-dependent manner. In the cytoplasm, the pre-miRNA is formed into double stranded miRNA structure by the Dicer. The 2 nucleotides 3′ overhang terminus on the pre-miRNA, formed by the Drosha, is captured by the Piwi/Argonaute/Zwille (PAZ) domain of Dicer, analogous to the recognition of dsRNA termini. Drosha and Dicers present substrate specificity (Drosha is involved in the pre-miRNA processing but not in the processing from a dsRNA terminus). It is believed that the stem–loop structure and especially its size is important for the substrate recognition of Drosha(Zeng, Yi, & Cullen 2005). Unstructured sequences located close to the stem–loop are believed to be important for processing, and possibly other proteins-enzymes, and not Drosha, may be involved in the recognition of these regions. It is possible that other factors participate as well, as it seems unlikely that Drosha recognises these sequences as they are located outside its zone of activity (Hammond 2005).

1.2.5.5.2. The role of Dicers

Dicers are large proteins (~200 kDa). They are shown to have a double role by developing miRNAs and siRNAs from pre-miRNAs and dsRNAs respectively. Differences in Dicers have been detected between species. Although vertebrates and *C. elegans* have in their genome single Dicer genes, in Drosophila and in other species. two or more Dicers are detected that present specialised functions (Hammond 2005).Dicers have an N-terminal ATPase/RNA helicase domain, followed by a DUF283 domain with unidentified role and a

PAZ domain, also found in Argonaute family proteins. The structure of the two *Drosophila* (Dm) Dicers is different: In Dcr-1, the helicase domain is smaller. The PAZ domain is the same in humans and in Dcr-1, but the PAZ of Dcr-2 is structurally different. Dicers are divided into three categories (Figure 8). Category I is mainly found in bacteria and yeast. In this category only one RNaseIII domain is detected which is bound to a dsRBD. In contrast, two Rnase III domains are present in enzymes belonging to categories II and III. Enzymes belonging in category III share a similarity with the Argonaute family proteins, as they both have in their structure a PAZ domain (Piwi/Argonaute/Zwille) (Tabara *et al.* 1999). The two Dicers expressed in Drosophilla have different roles. The role of Dcr-1 seems to be important for the generation of double stranded miRNAs from pre-miRNAs. Dcr-2, on the other hand, seems to be important in two steps in achieving RNA silencing; It is involved in the cutting of the dsRNA and the creation of the double stranded siRNA as well as in the structure of the RISC complex. For the first step, Dcr-2 interacts withR2D2, which has two dsRBDs domains (Grishok *et al.* 2001). In the case of vertebrates, which have two Dicer proteins, as well as in *C. Elegans*, where only one Dicer protein has been detected, other factors connected with the Dicer may change the activity of the enzyme. Both Dicers (Dcr-1 and Dcr-2) have been found to interact with Argonaute proteins (Figure 7 and Figure 8). In humans, this interaction is believed to be achieved through regions located at the RNase III and Piwi domains (Hutvagner *et al.* 2001).

Although it was initially suggested that Dicer works as a dimer performing four cleavage reactions, later studies indicate that it is more likely that dimers may work as monomers. This is because Dicers seem to start by capturing an already existing terminus and it is then necessary to have two (instead of four) cleavage reactions at ~21 nucleotides from the existing terminus. The existence of a terminal position from which the Dicer can start its function is believed to speed up the cleavage process. By contrast, delays happen when Dicers initiate their function with an initial internal binding, as it has been suggested that this binding is less efficient than when an end terminus exists (Hammond 2005). The most representative model of the structure and the function of the Dicer is shown in Figure 9. An active enzymatic pocket is created by the two Dicer RNaseIII domains, which come opposite one another, and the molecule functions as a pseudo-dimer. Each domain is in charge of cleaving one of the two strands of the double stranded RNA. For the calculation of the 21 nucleotide length new product, the distance between the PAZ domain and the active pocket generated by the RNase III domains is vital (Figure 9). The pseudodimer alignment also seems to be a reason for the creation of the 2 nucleotide overhang (Figure

9). The existence and function of these enzymes is vital; this was shown in experiments in which early embryonic lethality occurred in mice without Dicers. The way and the site to which the dsRBD domain binds the RNA is not yet known (Hammond 2005).

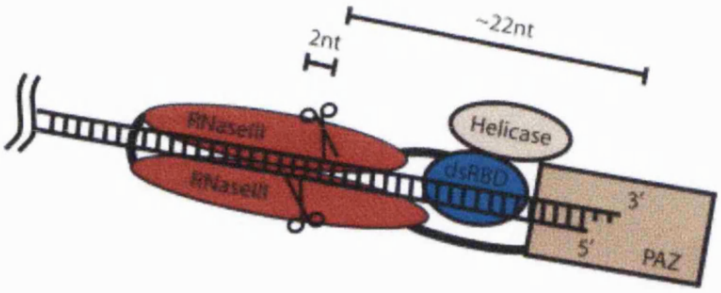

Figure 9: Structure of the Dicer and how Dicer 'captures' the dsRNA and cuts it. Figure from Hammond (2005).

1.2.5.5.3. The role of RNA-induced Silencing Complex (RISC)

It has been suggested that RISC is the last part of the chain in the RNAi process. Argonautes participate in protein complexes like RISCs and miRNPs and they are also known to be linked with Dicer Argonaute2 (Ago2), the first identified member of the family, which has in its structure the PAZ and the Piwi domains. The C-terminal Piwi domain found in the Argonautes presents structural similarities with the RNase H fold. The existence of a domain rich in glutamine is the reason why *Drosophila* Ago2 is larger than Ago1 and human Ago1–4 (Filipowicz, Jaskiewicz, Kolb, & Pillai 2005).

Many scientists have suggested that RISC seems to function differently in the case of mRNA silencing, insofar as it works by inducing suppression of translation rather than cleavage of the mRNA.

Scientists have also found additional protein components in the RISC (dFXR, RNA binding protein VIG, the Drosophila homolog of the Fragile X protein, helicase proteins), but their role has not been yet described. Further studies have shown that an oligonucleotide-binding (OB)-like fold exists in the ~130 KDa PAZ domains of Drosophila Ago1 and Ago2 (Filipowicz, Jaskiewicz, Kolb, & Pillai 2005). The model that has been suggested for the siRNA-PAZ interaction is characterised by significant asymetry. The 3' end of the strand domain interacts with PAZ along its full 9-nt length. On the other

hand, the opposite strand of the antisense interacts only with the 5'-terminal residue. In humans, four members of the Argonaute family have been detected, the Ago1-4. Although Ago1-4interact with siRNAs and microRNAs, only complexes that include endogenous or recombinant hAgo2 are capable of cleaving mRNA. Indicative of this is that RNA interference is not achieved in Ago2 negative (knock out) mice(Filipowicz, Jaskiewicz, Kolb, & Pillai 2005).

The Piwi domain has been indicated to have a role in RNase H and, for that reason, it is also known as 'Slicer' and is believed to cleave mRNA in RISCs. RNase H and Ago share a common triplet of aminoacids (DDE), which are important for the catalysis. Equivalent amino acids appear to be conserved in most eukaryotic Argonaute proteins. The importance of the two aspartates of this amino acid triplet for RNAi has been shown in studies based on mutagenesis of human Argonaute 2 protein which, as previously mentioned, is important for RNA interference (mRNA cleavage through RISC)(Khvorova, Reynolds, & Jayasena 2003). Apart from this, other studies have found similarities in the functioning of the RISC and RNA-H (both enzymes generate 5′-phosphate and 3′-OH termini) (Filipowicz, Jaskiewicz, Kolb, & Pillai 2005) which are indicative of the role of Argonaute 2 as 'Slicer'.

The Slicer catalytic model is shown in Figure 9. The SiRNA 5′ end of the siRNA guide is linked to the Piwi domain. In this link, the 5′ phosphate plays a very important role and is coordinated by four conserved residues. As shown in Figure 10, the 3′ SiRNA is linked with the PAZ domain and captures the 3′ OH terminal ends of RNA, or duplexes with a 3′ overhang (Filipowicz, Jaskiewicz, Kolb, & Pillai 2005;Hammond 2005). In microRNA/target pairs, the vital role of nucleotides 2–8 in the microRNA for the detection of the target has been indicated. It has been suggested that the first nucleotide is not important for target recognition as, when a strong base pair is located at the 5′ SiRNA terminus of the siRNA, the activity of the Piwi domain as a Slicer is reduced. As previously mentioned, the cleavage takes place at the Piwi domain as it is shown in Figure 8. It has also been indicated that the 'cutting' is measured from the 5′ SiRNA end. The product is then released without any knowledge of the mechanism by which this is achieved and the enzyme at the end of the process recycles.

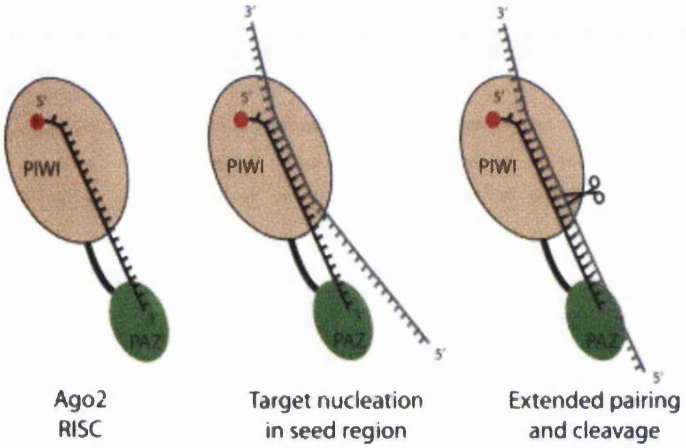

Figure 10: Structure of the Slicer. PIWI and PAZ domains are linked with the 5' and 3' ends of the siRNA and cleavage of the mRNA takes place at the PIWI domain.

1.2.5.5.4. siRNA strand selection

Studies designed to test the effectiveness of different forms of double- and single-stranded siRNAs as well as the processing of pre-miRNAs by Dicers and the sequencing of the created miRNAs by RISC showed that the strand from the dublex (created after the Dicer processing) with the less thermodynamically stable 5′ N terminus is selected as the miRNA . In Drosophila, it has been proposed that the Dcr-2–R2D2 heterodimer senses the differential stability of the duplex ends and determines which siRNA strand gets selected. Facilitated by the use of 5-iodouracil, photocross-linking applied to siRNAs at different positions showed that the less stable end is linked to Dicer and the more stable to R2D2, the siRNA end (Filipowicz, Jaskiewicz, Kolb, & Pillai 2005).

1.2.5.6. Off-target effects

Although RNAi has been suggested as a gene inhibition tool with high target specificity, off-target effects have been observed post siRNA introduction, indicating non-specific inhibition. Eight to eleven base pairs of homology of the siRNA with a single-stranded RNA were shown to lead to silencing. It is believed that siRNA presents the ability to inhibit mRNAs that are characterised by limited sequence similarity to siRNAs. In fact, in some cases, regions comprising of only 11–15 contiguous nucleotides of

sequence identity were sufficient to induce gene-silencing (Jackson *et al.* 2003). No evidence has been presented regarding the off-target siRNA effects. The prediction of these off-target activities is difficult so far, but nowadays scientists, having in their hands the 'weapon' of searchable genetic information, can in many cases avoid inadvertent off-target silencing.

1.2.5.7. Guidelines for designing siRNAs

Three main guidelines, which are an optimal length of 19–25 bp, the existence of a 3′ dinucleotide overhang, and a low Glutamine and Cytocine (G/C) content ranging between 36% and 52% have been proposed for effective RNAi (Elbashir *et al.* 2001; Elbashir *et al.* 2002; Elbashir, Lendeckel, & Tuschl 2001; Holen *et al.* 2002). More recent studies suggested that the thermodynamic flexibility of the duplex 3′-end (i.e. positions 15–19, sense strand), but not of the 5′-end, correlates with silencing efficacy and that silencing efficacy is increased by the presence of at least one Adenine/ Uracile (A/U) bp in this region, which decreases the internal stability of the 3′-end (Reynolds *et al.* 2004). Furthermore, internal repeats or palindrome sequences are not suggested as facilitating the formation of internal fold-back structures and decreasing the possibility of silencing.

Later extensive studies have suggested more specific siRNA structure guidelines for effective interference; the Glutamine and Cytocine content in the siRNA structure should be 30–52%; at least three Adenosine or Uracile nucleotides should exist in positions 15–19 of the sense strand; specific nucleotides should be located in specific positions (A at position 3, U at position 10, no G at position 13, no G at position 19, no C at position 19; A is preferred at position 19). By following these guidelines, greater siRNA efficacy is achieved (van Es & Arts 2005).

HYPOTHESIS AND AIMS

There is a clinical need for better therapies to ensure that the healing process can be better mediated after GFS. Less toxic compounds are needed than are currently used. Additionally, we hypothesise that it is necessary for the drug to reside longer in the bleb than it does by simple injection. To avoid multiple injections and dose dumping, a longer local pharmacokinetic profile is required to achieve optimal clinical benefit in mediating the healing process after GFS.

Initial work in this project focused on examining potentially less toxic drugs: SAP and siRNA. However, the issue of increasing the local pharmacokinetics within the bleb also required examination. A matrix metalloproteinase (MMP) inhibitor called ilomastat (GM6001) had previously been found to inhibit fibrosis. If SAP and siRNA do not display sufficient activity, then attention will focus on increasing the bleb pharmacokinetics of ilomastat. Many MMP inhibitors have been developed during the past two decades but all have failed clinical trials for cancer due to systemic toxicity as well as, as many scientists believe, because the patients that participated in the clinical trials had metastatic cancer. However, for use in the subconjunctival space, the dose of ilomastat would be much lower than when used systemically. A key risk however, is the potential toxicity in ocular tissue.

The two key aims of this project that are directed to minimizing fibrosis after GFS are:

1. Determine the potential of compounds that are less toxic than the cytotoxic agents that are currently used in the clinic.
2. Develop a strategy for prolonging the local bleb pharmacokinetics of the compound that has the greatest potential to inhibit fibrosis after GFS.

2. MATERIALS AND METHODS

2.1. Serum Amyloid P

2.1.1. *In vitro* collagen gel contraction study

2.1.1.1. Human Tenon's Fibroblasts (HTF)

Human Tenon's Fibroblasts (HTF) were used for *in vitro* cultures. They are the key cells involved in subconjunctival scarring. HTFs were isolated from 0.5 cm^3 tissue explants obtained from donor eyes obtained from Moorfields Hospital Eye Bank under the Tenets of the Declaration of Helsinki (1989). Explants of 0.5 cm^3 tissue were kept for two hours on 25 cm^3 flasks, with a glass coverslip placed over them. Each flask contained 5 ml of normal culture medium consisting of Dulbecco's modified Eagle's Medium (DMEM) with 10% fetal calf serum, 2 mM L-glutamine, 100 U/ml penicillin, 50 mg/ml gentamicin, 100 μg/ml streptomycin and 0.25 μg/ml amphoteracin. The flasks were placed in incubators at 37°C with 5% humidified CO_2 in air. In these primary explants the culture medium was changed every 3 days and when they became confluent – normally within one month – they were passaged in new flasks for direct experimental use or were stored in liquid nitrogen.

2.1.1.2. Passaging and maintenance of cell cultures

After the HTFs reach confluence, the culture medium was aspirated and the monolayer was washed with 1 ml of trypsin x1 (Gibco). The trypsin was subsequently aspirated after about 15 seconds. Next, 2 ml of Trypsin 1x (Gibco) were added to each flask and HTFs were detached from the flasks by incubation for 2 minutes at 37°C with 5 % humidified CO_2 in air. After confirmation by phase contrast microscopy with a Leica microscope with x10 magnification that the cells had been detached from the bottom of the flask and that they had taken on a round shape, 2 ml of cell culture medium was added to neutralize the trypsinisation. The cell suspension was transferred to a 15 ml centrifuge tube (Starlab Gmbh) and was centrifuged at 1600 rpm for 5 minutes. The cell pellet was then re-suspended in 10 ml of cell culture medium and was divided into four separate 75 cm^3 flasks (1:4 expansion). In each flask, 7.5 ml of cell culture medium were added. Flasks were placed in incubators at 37°C with 5% humidified CO_2 in air, and the culture media was

changed every three days. On average, it took 1 week to reach confluence between passages.

2.1.1.3. Imaging of fibroblast monolayers

Phase contrast microscopy was used to observe the morphology of the cells at set time points throughout the experiments. Images were captured by the use of digital camera with a microscope attachment and stored as JPEG files (Nikon Coolpix 950, Tokyo, Japan).

2.1.1.4. Preparation of collagen gels (*in vitro* contraction model)

With a Neubauer plate (Haemocytometer), 6.2 x 10^4 HTF were counted and re-suspended in 170µl FBS in a 50 ml universal tube. Concentrated medium (160 µl) was added (stock solution consisting of 3.5 ml DMEM (x10 stock)), 0.35 ml glutamine (2 mM stock) and 0.9 ml sodium bicarbonate (7.5% stock). 830 µl of First Link type I collagen solution collagen (stock 2.2 mg/ml in 0.6% acetic acid) were then added and the solution was mixed by swirling to avoid air bubbles. Rapid addition of 75-80 µl of sterile 1 M NaOH followed in order to change the acidic pH of the solution, which helped to turn the solution to pink colour without reverting back to yellow. Quickly 150 µl of the collagen gel solution was cast into the wells of Mattek dishes (Mattek Corp.) making sure, by using a pipette tip, that the gel extended to the edges of the central groove. Care was taken to ensure that air bubbles were not created when ejecting the gel from the tip; if any air bubbles were formed, they were aspirated out. Usually, from a 1.2 ml gel suspension, six gels could easily be cast. Following this process, the Mattek dishes with the gels were placed in incubator to set for at least 10-15 minutes (up to 30 minutes). Gels were detached from the edges of the central groove using yellow pipette tips and excess unpolymerised solution was aspirated off. Two millilitres of cell culture medium were added and the dishes were placed in incubators at 37°C with 5 % humidified CO_2 in air. The medium was replaced every three days (Daniels *et al.* 2003).

2.1.1.5. Description of the *in vitro* study

The efficacy of SAP in the inhibition of HTF collagen I gel contraction was tested. In this study, ilomastat (GM6001) was used as positive control and media without any

treatment was used as negative control. Three different concentrations of SAP were tested. The purpose of this experiment was to investigate whether the SAP had any effect on the HTFs that did not originate from circulating monocytes.

Treatment Plan		Concentration of media
Ilomastat (Positive control)		100 μM ilomastat
Serum Amyloid P	Part 1	20 μM SAP
	Part 2	10 μM SAP
	Part 3	5 μM SAP
Media (Negative control)		No treatment

Table 1: Testing of the efficacy of three different concentrations of Serum Amyloid P in inhibiting the Collagen I gel contraction. There were 5 gels and 2 ml of media in each one of the five treatment plans. The media was renewed on day 3.

2.1.2. *In vivo* study

2.1.2.1. Glaucoma filtration surgery in rabbits

All experiments conformed to ARVO Statement for the Use of Animals in Ophthalmic and Visual Research (ARVO Animal Policy). To anaesthetise the rabbits, Ketamine (50 mg/kg) and Xylazine (10 mg/kg) were given by intramuscular injections. Initially, a partial thickness 8-0 silk corneal traction suture (Ethicon) was used at the 12 o'clock position to gain exposure to the superior conjunctiva. A fornix based conjunctival flap was then raised and blunt dissection of subconjunctival area was performed. Following this, a partial thickness scleral tunnel was created with an MVR blade starting 2 mm behind the limbus and continuing until the blade was visible in the anterior chamber. Then a 22G/25 mm Veflon in a cannula was passed through the scleral tunnel until the cannula needle was visible in the clear cornea. During this process the cannula needle entered the anterior chamber, was advanced to the mid pupiliary area and then withdrawn. The cannula was trimmed and bevelled at its scleral end so that it protruded 1 mm from the insertion point. The tube was fixed to the scleral surface using a 10-0 nylon suture on a B/V 100/4. The conjunctival incision was closed with two interrupted sutures as well as with a central mattress type 10-0 nylon suture on a B/V 100/4 needle to form a water-tight closure. One drop of Atropine Sulphate 1% (Martindale Pharmaceuticals, Romford, UK) and Betnesol N

ointment was instilled at the end of surgery (Wong *et al.* 2003; Wong *et al.* 2005; Mead *et al.* 2005).

2.1.2.2. Experimental design

A random, one block study design was performed, with all rabbits undergoing glaucoma drainage surgery to the left eye. 24 Female New Zealand White Rabbits (Harlan UK Ltd., c. 2.0-2.5 kg, 12-14 weeks old) were used for this experiment. Animals were observed for a period of 30 days. The experiment was performed as a randomised, blind, controlled study. A single masked observer assessed the clinical data. All treatments were applied to the left eye. The right eye did not receive any treatment during the study and served as the unoperated control.

The 24 rabbits were randomly assigned into four groups (6 rabbits in each group). Randomisation was performed by a masked individual using the software available on www.randomisation.com. Randomisation was done with a Latin square crossover design. The design of the *in vivo* study is shown below.

GROUP	GLAUCOMA FILTRATION SURGERY	PHARMACEUTICAL TREATMENT	IOP MEASUREMENTS (TIME POINTS)
A (LEFT EYE)	Yes	Water injections (Negative control)	Days: 0,3,6,9,12,15,18,21,24,27,30
A (RIGHT EYE)	No	No	Days: 0,3,6,9,12,15,18,21,24,27,30
B (LEFT EYE)	Yes	MMC 0.2 mg/ml Sponge (Positive control)	Days: 0,3,6,9,12,15,18,21,24,27,30
B (RIGHT EYE)	No	No	Days: 0,3,6,9,12,15,18,21,24,27,30
C (LEFT EYE)	Yes	Serum Amyloid P: Subconjunctival injections on days 0 (post surgery), 1,2,4,6	Days: 0,3,6,9,12,15,18,21,24,27,30
C (RIGHT EYE)	No	No	Days: 0,3,6,9,12,15,18,21,24,27,30
D (LEFT EYE)	Yes	Serum Amyloid P: Subconjunctival injections & Intravenous injections on days 0 (post surgery), 1,2,4,6	Days: 0,3,6,9,12,15,18,21,24,27,30
D (RIGHT EYE)	No	No	Days: 0,3,6,9,12,15,18,21,24,27,30

Table 2: Treatment regimen for the Serum Amyloid P *in vivo* study.

2.1.2.3. Endpoints and clinical examination

Assessments of the following parameters were made every 2-3 days from day 0 to day 30:

- bleb size(width, height and length) using callipers,
- bleb capacity,
- bleb vascularity (very hyperaemic = 3, hyperaemic = 2 , normal vascularity = 1, avascular = 0)
- bleb location (top, nasal, temporal),
- anterior chamber inflammation (0 = quiet, 1 = many cells, 2 = fibrin, 3 = hypopyon),
- anterior chamber depth (deep, swallow or flat),
- corneal epitheliopathy (0 = nil, 1 = <25 %, 2 = 50 %, 3 = 75 %, 5 = up to 100%)

2.1.2.4. Measurement of IOP

Measurement of intraocular pressure in both eyes was done using a Mentor tonopen. IOP was measured after topical installation of 0.5 % Proxymetacaine HCl local anaesthetic. The tonopen was lowered perpendicularly onto the corneal surface and a recording was made. Five recordings per eye were made per time point and all the readings, and their mean, were documented.

2.1.2.5. Termination of the *in vivo* study

All animals were sacrificed after the experiment was completed with a lethal intracardial injection of pentobarbitone (4 ml), administered under a general anaesthetic.

2.1.2.6. Histology

A horizontal cut was made from the middle of the cornea to the optic nerve, dividing the eye into almost two equal parts. Only the upper part was processed. The filtration tube was not removed from the operated rabbit eyes. The upper part of each eye was placed in an appropriately sized cassette and was loaded onto the tissue processor for 48 hours. The eyes were placed in gradually increasing alcohol concentration (70 % methyl

alcohol, 80 % methyl alcohol, 95 % methyl alcohol, 100 % methyl alcohol) and were finally washed with xylene. Using this method, dehydration of the eyes was achieved. Next, the specimens were embedded in paraffin wax in a mould of an appropriate size (approximately 4 cm x 2 cm x 3 cm). The eyes were orientated before being embedded in the paraffin wax so that the scleral end of the tube was located at the top (at 12 o'clock). The moulds were kept in the cold storage area until they solidified. The paraffin blocks were then secured to a microtome. Sections were cut transversely across the globe so that the area of interest (the bleb area) was at the top of the block and in the middle of each cut section. A ribbon of 5μm sections was cut, which were then placed in warm distilled water <65°C (the melting point of paraffin wax is 65°C). The paraffin sections were collected on microscope slides and were placed in a hot place to dry. Next, in order for the specimens to be dewaxed and rehydrated, the microscope slides were placed in xylene for 5 minutes, followed by two further xylene washes for three minutes each. They were then washed with descending concentrations of methylated spirit, and finally with water. The slides were washed in tap water for 5 minutes and were rinsed in distilled water before starting the staining process.

Histological stains used for the purposes of this experiment include haematoxylin and eosin to assess the inflammatory reaction and cellularity of the bleb, and Picrocirius red to evaluate collagen deposition.

2.1.2.6.1. Eosin and Haematoxylin staining

The Eosin and Haematoxylin staining was performed with the use of two solutions, Eosin Y and Harri's haematoxylin.

Initially the sections were gradually hydrated, starting with xylene, 100 % methyl alcohol, 90 % methyl alcohol, 80 % methyl alcohol and 70 % methyl alcohol. Then the sections were placed into water and were then stained in Harris's haematoxylin for 3 minutes, then washed well with tap water. For differentiation purposes, the slides were then placed in 1% acid alcohol (1%HCl and 70% alcohol) for 5-10 seconds. Next, they are washed well with tap water for 5 minutes or less until sections were blue. The sections were then stained with 1% Eosin Y for 10 minutes, and washed in running tap water for 1-5 minutes. Then, to dehydrate the specimen, ascending concentrations of methylated spirit were used, and finally the slides are washed with xylene. A drop of Digital Picture

Exchange (DPX) mounting media was placed in the centre of a coverslip, which was pressed gently onto each slide and left to dry.

Using this method, nuclei are stained blue or black, cytoplasm is presented as varying shades of pink, muscle fibres show as dark pink-red, red blood cells are orange or red in colour and fibrin are deep pink.

2.1.2.6.2. Picrosirius Red staining

The Picrosirius Red staining was done with 100ml of a saturated picric acid solution mixed with 0.1 gm Sirius red powder.

Initially, the sections are gradually hydrated starting with xylene, 100 % methyl alcohol, 90 % methyl alcohol, 80 % methyl alcohol and 70 % methyl alcohol. Once hydrated, the sections are placed in distilled water for about 10 minutes, followed by the picrosirius red stain solution for 30 minutes and they are then washed in water. Then, in order to dehydrate the specimen, ascending concentrations of methylated spirits were used in the opposite sequence to the initial hydration, and finally the slides were washed with xylene. For each slide, a drop of DPX was placed in the centre of a coverslip and pressed gently to the slide, then left to dry.

Using polarizing microscopy, collagen type I is stained yellow, orange or red, collagen type II is stained blue or pale yellow depending upon orientation and collagen III is stained green (Junqueira *et al.* 1978).

2.1.2.6.3. A newly designed method for quantifying scarring

Previous experiments performed in the Ocular Repair and Regeneration Biology Unit used a grading system of four options (the slides were graded as 1; 2; 3 or 4) based on the amount of scarring that is deposited within the bleb area. Unlike the numerical system, this newer method uses comparative analysis to indicate which eyes are more scarred versus those less scared. A similar grading method was used to evaluate the cell number of the bleb in each picture. Attempting to quantify the scarring in the bleb area, the new histological method was designed to measure in the bleb area i) the percentage of scar tissue and ii) the number of elongated cells. The evaluation of the first parameter was performed using slides stained with Picrosirius Red.

Sections

Three sections were evaluated per operated eye. First, sections were cut at the level passing through the centre of the tip of the tube located inside the bleb. The next section was 2mm away laterally from the inferior end of the tip of the tube, and the third a further 2mm laterally. In this way not only the central, but also the peripheral areas of the bleb were evaluated for scarring.

Evaluation

High-resolution pictures were taken of the three sections from each rabbit. In printed magnified pictures, the distance between the sclera and the conjunctiva was at least 5 cm, which allowed easier measurement of the deposition of scar tissue. In each picture, two vertical axes were drawn - the first was located 2 mm posterior from the tip of the tube (or 4 mm from the corneoscleral junction – approximately equal distance) and the second located 4 mm posterior from the tip of the tube (or 6 mm from the corneoscleral junction). This method did not evaluate any points closer than 2 mm to the tip of the tube, as the material of the tube usually causes aggressive inflammatory reaction and scarring deposition in the immediate area, which can lead to confusion in evaluating the histological results.

In each section, the area of the bleb covered with scar tissue was measured, and the figure was divided by the total size of the bleb. For example, if in the axis of an evaluated picture, the size of the bleb is 5 cm in the magnified picture and 3 cm is covered with scar tissue (2 cm is 'empty'), then this is graded as 6/10. Measuring the six axes (2 axes from the three sections for each rabbit), adding the grades and dividing by six, to give an average, this number then used as the scarring grade for the bleb of the evaluated rabbit.

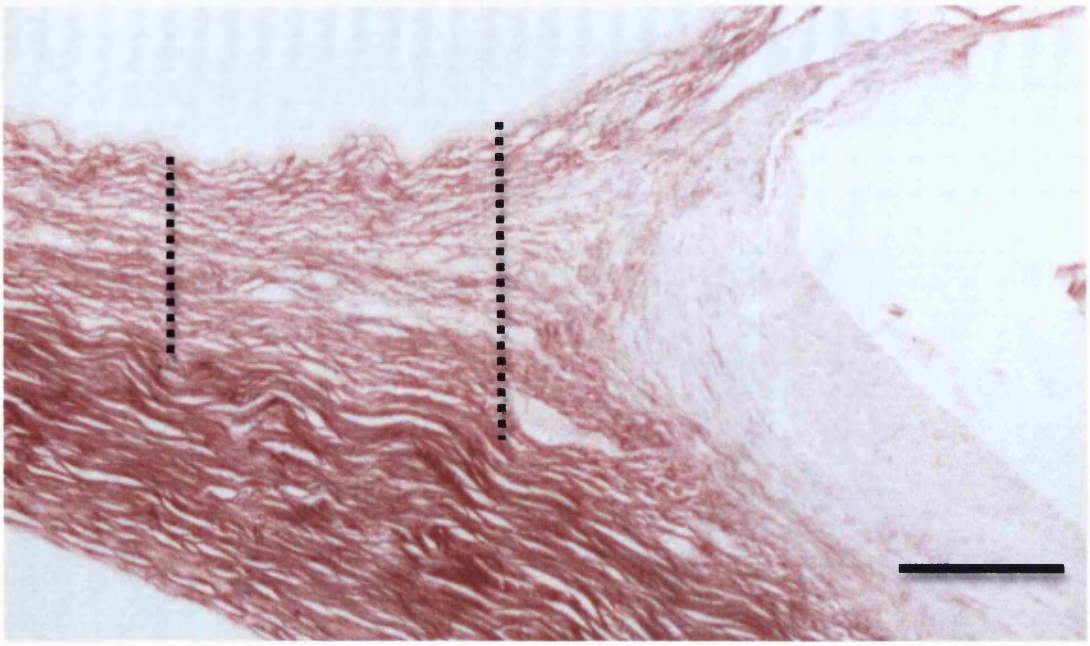

Figure 11: Picrosirius Red staining image of the subconjunctival space of a rabbit 30 days after glaucoma filtration surgery. Two vertical axes were drawn, 2 mm and 4 mm (of actual size) posterior from the tip of the tube. The scarring deposition was evaluated by measuring the percentage between the sclera and the conjunctiva that is covered with scar tissue and the percentage that is 'empty' along each one of the axes. Using this method, a quantitative analysis of the scarring deposition of the bleb between groups could be performed and a comparison made between groups. Scale 1 mm.

In addition, the number of cell nuclei located between the two axes in each picture, were also calculated. An average of the cells, in the three pictures, was taken. Eosin and Haematoxylin images were used for the measurement of cellularity of the blebs. If the number of cells was >101, the cellularity of the bleb in the evaluated rabbit was graded as 5, if it was between 76 and 100 it was marked as 4, if it was between 51 and 75 it was marked as 3, if it was between 26 and 50 it was marked as 2, and if it was between 1-25 it was marked as 1 (it was very rare for a sample to be in the last category).

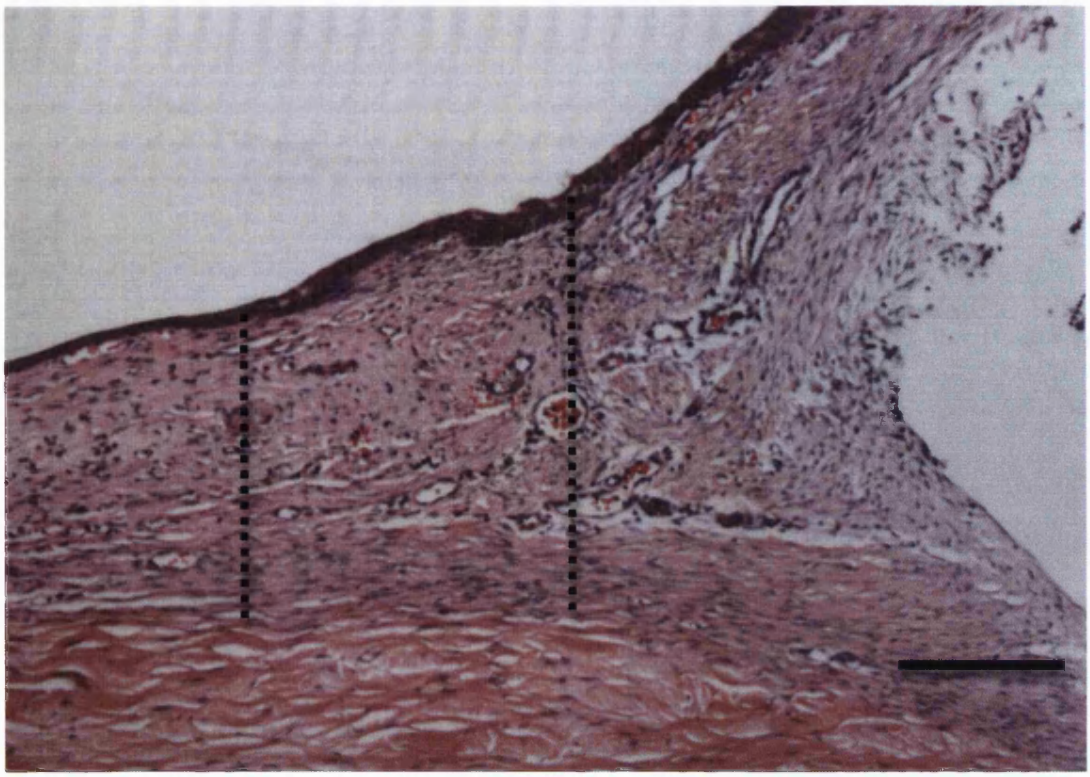

Figure 12: Eosin and Haematoxylin staining image. The nuclei of the cells located between the two axons were measured and the sample was graded based on the guidelines described in the previous figure. Scale 1 mm.

2.1.2.6.4. Immunohistochemistry

Immunohistochemistry was performed to detect α smooth muscle actin in order to identify the presence of myofibroblast transformed fibroblasts. This technique was used to analyse the specimens from the rabbits that had undergone glaucoma filtration surgery for the serum amyloid P experiment. Sections were dewaxed through xylene, 100 %, 90 % and 70 % methylated spirit, were washed in 70 % alcohol and then were placed in endogenous peroxidase blocking solution for 20 minutes. Slides were washed with Tris Buffered Saline prepared in the lab (TBS: 150 mM sodium chloride, 10 mM Tris-HCl, pH 7.6). After this step, sections were placed in normal rabbit serum for 20 minutes to block non-specific binding sites to be achieved (NRS, 1:10 dilution in TBS; DAKO A/S Denmark). The sections were then incubated with the primary antibody, Mouse anti-human α SMA (1:150 dilution in 1:100 NRS, IgG2A, Clone1A4 DAKO, A/S, Denmark) for 1 hour, washed in

TBS and incubated in the secondary antibody, biotinylated rabbit anti-mouse (1:300 in TBS, DAKO) for 45 minutes. A streptavidin AB complex / horseradish peroxidase kit was used (DAKO A/S, Demark) and finally a solution of 3,3- Diaminobenzadine (DAB, Sigma, Dorset, UK) was placed on the slides for 10 minutes. Nuclei were stained in Meyers haemotoxylin for 30 seconds, and the slides were dehydrated through alcohol and mounted in DPX. A positive control was in built in the iris and ciliary body of the eye. For negative control slides, a mouse anti-human negative control primary antibody was used (IgG2a, DAKO A/S, Demark).

2.2. Formulation, characterisation and experimental evaluation of an excipientless slow release ilomastat tablet

2.2.1. Formulation of the ilomastat tissue tablet

2.2.1.1. Flow system

To determine the release kinetics of the ilomastat tissue tablet, two flow rigs of 50 and 200 µl capacity were manufactured at the School of Pharmacy University of London, in order to mimic the bleb produced during GFS. For the purposes of determining release kinetics, one single tissue tablet was placed into each rig. A flow system was further designed to be connected to the rig to allow the simulation of the flow of aqueous fluid through the bleb. Two plastic tubes were connected to each rig. One tube was connected to a peristaltic pump to introduce the aqueous solution (model to approach the aqueous humor outflow from the anterior chamber to the subconjunctival space). The other tube was placed into a collection tube to collect the sample for HPLC analysis of Ilomastat. During initial experiments, PBS (Oxoid® Phosphate Buffered Saline Tablets, Sigma-Aldrich, UK) was prepared and buffered to pH 7.6 (to mimic the pH of the aqueous fluid). The flow rate of PBS was maintained at either 5 µl/min (for the first tablet in the 50 µl rig) or 2 µl/min (for all the other tablets, tested in the 200 µl rig). We initially aimed to test the effects of flow rate on ilomastat release. The flow rate the eye is of about ~2 µl/min (Ingram & Brubaker, 1999). In order to keep the aqueous solution at 37°C, we placed the solution in a glass flask. We put then the glass flask in an oil bath maintained at 37°C.

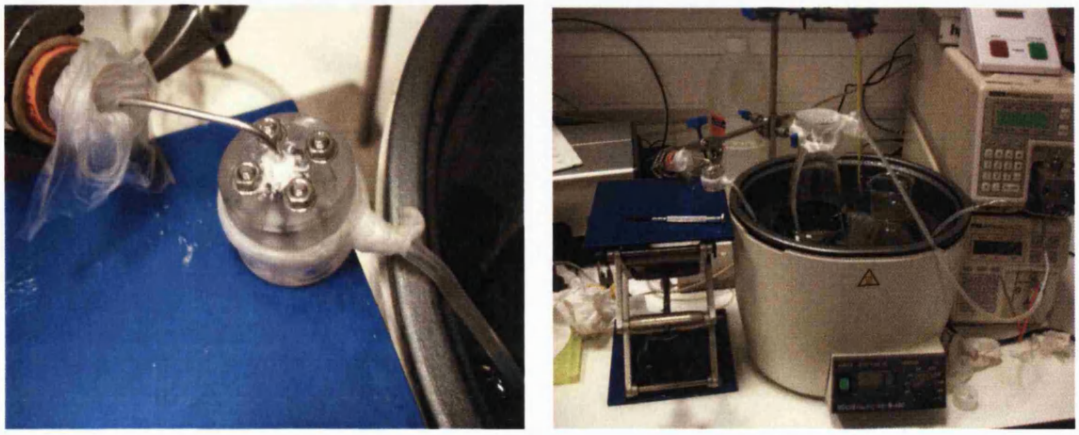

Figure 13: The flow system used for the release experiments of the ilomastat tablet. In these pictures the peristraltic pump, the oil bath, the flow rig and the collection tube are shown.

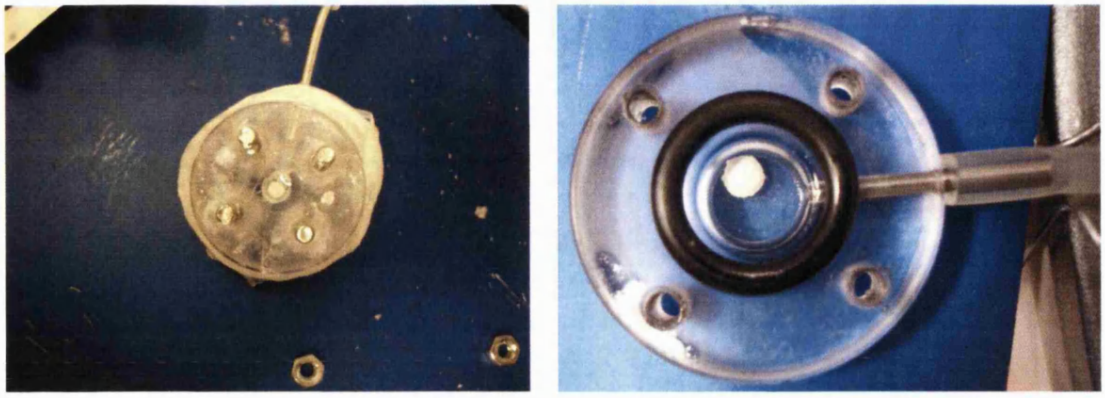

Figure 14: Ilomastat tablet placed into the 50 µl rig (left) and into the 200 µl rig (right).

In order to test the release profile of the ilomastat tablet, a calibration curve was necessary. Ilomastat powder was weighed using an accurate scale and eight different ilomastat solutions were created. The concentrations of these solutions were: 100 µM, 80 µM, 60 µM, 40 µM, 20 µM, 10 µM, 5 µM and 2.5 µM. The concentrations were measured by using two ultraviolet (UV) detectors (Perkin Elmer) and High Potency Liquid Chromatography (HPLC) methods. Because HPLC has been suggested to be a more accurate method to test the concentration of samples, we used HPLC for all the experiments and UV (together with HPLC) only for the calibration curve experiments.

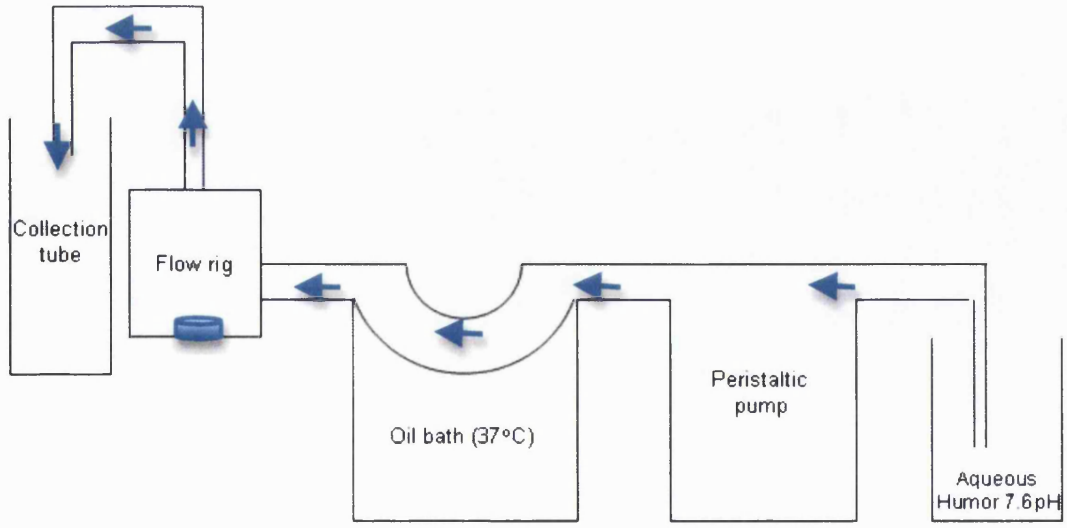

Figure 15: Diagram of the flow system. The small cylinder inside the flow rig represents the ilomastat tablet. The blue arrows represent the flow.

2.2.1.2. Tablet formulation process

Ilomastat tablets were prepared by direct compression of ilomastat powder (Caldiochem, UK) in a punch and die supplied by Dr Erdal Cehver and modified by Mr John Frost at the School of Pharmacy, London, UK. Solid ilomastat was placed in the die and the punch carefully fitted. The ilomastat powder was accurately weighed prior to being placed in the die. The punch and die were then placed into the tablet compressor and the powder was compressed at 5 bars for about ten seconds.

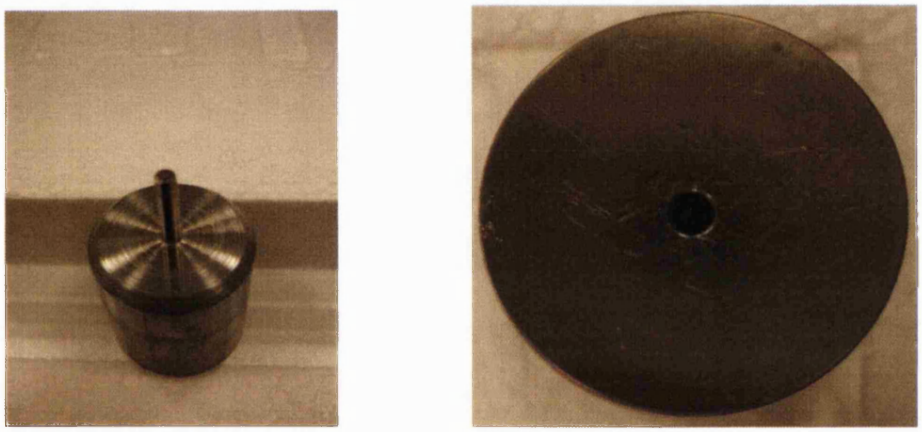

Figure 16: Punch (left) and die (right) - 3mm diameter. The ilomastat powder was placed inside the die and the punch was placed over it. The punch and die system was compressed and the powder was turned into a micro tablet.

2.2.1.3. High performance liquid chromatography method

High performance liquid chromatography (HPLC) was used to determine the concentration of ilomastat within simulated aqueous fluid following the release study experiments. To enable detection of ilomastat, reverse-phase liquid chromatography was used. Reverse phase HPLC is the method of choice for non-polar molecules such as ilomastat, as a greater retention time (the time it takes for an analyte to be eluted from a HPLC column and be detected by UV) can be achieved.

During reverse-phase HPLC, analytes possessing large hydrophobic surfaces demonstrate longer retention times due to poor or non-solvation in the aqueous mobile phase. The hydrophobic surface area of the molecule (analyte) is also critical for the

retention time. Branching of molecules also has a significant effect on retention time (reduced retention time), as the hydrophobic area of the molecule that interacts with the ligand's alkyl chain is smaller in branched molecules than in the case of linear isomers. It has also been indicated that C-C-bonds elute less rapidly than C=C or C-C-triple bond, because double or triple organic bonds have shorter length than the single bond. Attention is, additionally, needed to the size of the analytes, as when the molecules are very large they may not manage to pass through the stationary phase pores (Dong, 2006).

For stationary phase in the case of Reversed Phase HPLC, silica is usually used in the following two forms: $C_{18}H_{37}Me_2SiCl$ or $C_8H_{17}Me_2SiCl$ (C18 and C8 columns respectively) The C18 HPLC columns that were used for the ilomastat tablet experiments were washed with 100% acetonitrile solvent after each use to remove remaining buffer and ilomastat and were stored in 100% composition of solvent.

Several reverse phase columns and mobile phases were evaluated to determine optimal conditions needed for HPLC separation of ilomastat. It was found that a C-18 (company and model) and a 25% acetonitrile aqueous mobile phase gave good base line resolution. The mobile phase was prepared as follows. To make 1000 ml of buffer we used 1.54 gr ammonium acetate (Fluka), 6 ml Triethylamine 99.5 % (Sigma Aldrich), ~950 ml de-ionized water and ~ 10 ml of acetic acid 100 % (Analar BDH) to adjust the pH of the buffer to 5.0 ± 0.1. When the pH has been adjusted, de-ionized water was added in order to make the buffer volume of 1000 ml. Samples from the rig were collected more frequently during the early stages of the release studies and were more likely to have bigger fluctuations in the concentration. 0.1 ml of each sample was transferred into HPLC vials and the HPLC vials were placed in the HPLC auto-sampler. The HPLC system was manufactured by Jasco. The pump was set to 1 ml/min and the UV detector to 280 nm. Experimentally, the measurement of the concentration of an ilomastat solutions is determined by the absorbance of the solution (because of tyrosine) at 280 nm (Galardy *et al.* 1994). Three injections (10 μl each) from each time point were evaluated. A computer is connected to the UV detector and with the use of the software Chrom+ (H & A Scientific), the peak area is analyzed. The surface of the peak represents the concentration of ilomastat in the tested solution. The average of the three measurements was taken as the result; for the calculations and graphs, the programme MS Excel (Microsoft Office 2003 and 2008) was used.

2.2.1.4. Sterilisation of the tablet with gamma radiation

Both European (EUP) and American Pharmacopoeia (USP) require tissue implants to be sterile. Since the tablet fabrication was not conducted in aseptic conditions, and it was not possible to source sterile ilomastat, terminal sterilisation of the ilomastat tablet was required to meet EUP and USP requirements. Sterilization by gamma radiation is preferable for thermo-sensitive solid state drugs. This method is widely used (Engalytcheff *et al.* 2004; 2007) as has significant advantages over asepctic processing and filtration as there is a greater likelihood of sterilisation even with a relatively high bioburden. The main disadvantage of gama-irradiation is the potential change in the molecular structure of the formulation. Generally, a 25 kGy dose is needed to achieve the minimum sterility assurance level of SAL=10^{-6} (the probability of the product being non-sterile after the process being one in a million). Lower doses may be validated using appropriate sterility tests. Under the USP regulations a 25 KGy dose of radiation ensures sterilization (EUP, 2000; USP. 2000). In co-operation with Cranfield University (UK) ilomastat tablets were sterilized using a Cobalt 60 gamma source (4500 KGy per hour). The ilomastat compound was left in the Cobalt 60 panoramic chamber for about 5 hours and 35 minutes in order to obtain the 25 kGys exposure.

2.2.2. *In vitro* experiments

The HTF populated collagen I gels used in this experiment were created following the steps described in the 'Serum Amyloid P Materials and Methods'.

2.2.2.1. Preparation of cell culture media with ilomastat

In previous experiments performed at the Ocular Repair and Regeneration Biology Unit at the UCL Institute of Ophthalmology as well as in other labs around the world working with ilomastat, solid ilomastat was first diluted in DMSO before being added into the media. However, in this experiment, we attempted to dissolve solid ilomastat in the normal media without DMSO. When culture media and ilomastat (irradiated and non-irradiated) were placed in 50 ml universal tubes and with a magnet for about 5-6 hours, almost total dissolution of ilomastat was achieved. One of the experimental aims of this project was to test the ability of irradiated ilomastat to inhibit the HTF mediated

contraction of collagen I gels compared to non-irradiated ilomastat (positive control). For that reason, the concentration of the medias with irradiated and non-irradiated ilomastat had to be the same. In order to achieve that, we performed HPLC in both solutions and based on the results we dilute the solution with the higher ilomastat concentration down to the same level as the solution with the lower ilomastat concentration.

2.2.2.2. Design of *in vitro* experiment to test the inhibitory ability of irradiated ilomastat

The inhibitory effect of non-irradiated ilomastat on HTF contraction of collagen I gels is known. However the effect of gamma irradiation on the inhibitory activity of ilomastat has not previously been investigated. In order to explore this possibility, the following experiment was designed. Each experiment was repeated three times.

Three different treatment groups were used. Each treatment group had 5 collagen I gels with HTFs. The gels of the first group were treated with media without ilomastat (negative control), the gels of the second group were treated with media with non-irradiated ilomastat (positive control) and the gels of the third group were treated with media with irradiated ilomastat powder. No DMSO was used in any of the groups.

Photographs of the gels were obtained daily. The percentage contraction was determined using Image J software. The graph showing the percentage contraction was plotted using Microsoft Office Excel (2003, 2008). The media from the treated gels have been kept in -70°C for future zymographic analysis in order to test the levels of active MMPs.

2.2.3. Preliminary *in vivo* study

2.2.3.1. Experimental design

A random, one block study design was performed, with four rabbits undergoing glaucoma drainage surgery to the left eye. Animals were observed for a period of 30 days. The experiment was performed as a randomised, blind, controlled study with masked observers. One observer was used to assess clinical data.

2.2.3.2. Treatments and animals

Four Female New Zealand White Rabbits (Harlan UK Ltd; 2-2.2 kg, 12 - 14 weeks old) were used. Animals were housed in the BRU Unit of the UCL Institute of Ophthalmology and were allowed an acclimatization period of 7 days, as is normally required.

2.2.3.3. Treatment and regimen

Animals were randomly assigned to two selected groups, as shown in the Table 3. Rabbits underwent glaucoma filtration surgery (described in section 2.1.2.1.) in the left eye and the right eye was used as control. Animals in Group A received the ilomastat excipient-free tablet and Group B the ethylcellulose pellet, which is the control. Ethylcellulose is an excipient that does not swell or dissolve in aqueous solution. Subsequently we expected the size of the ethylcellulose tablet to remain unchanged during the 30-day period of the *in vivo* experiment. This control tablet was the same size as the ilomastat tablet in order to investigate if the effect of ilomastat itself and not just the placement of an external body (tablet) kept the bleb area functioning.

Group #	Treatment	Tablet characteristics	Schedule	Control eye (right)	Study End
A (3 rabbits)	Ilomastat tablet	Weight: 2.1-2.3 mg Diameter: 3mm Thickness: 0.4 mm	Placement of one pellet in the left eye during GFS	No treatment	Day 30 – all rabbit eyes to histology
B (1 rabbits)	Ethylcellulose tablet	Weight: 1.5 mg Diameter: 3mm Thickness: 0.4 mm	Placement of one pellet in the left eye during GFS	No treatment	Day 30 – all rabbit eyes to histology

Table 3: Description of a preliminary *in vivo* study in which the anti-scarring effect of an excipientless ilomastat tablet was tested.

The ilomastat and ethylcellulose pellets were placed subconjunctivally just before conjunctival closure at the end of GFS. Pellets will be placed only in the left eyes (one pellet per eye).

2.2.4. Second *in vivo* study

2.2.4.1. Experimental design

A randomized, prospective, masked-observer study with 24 NZW rabbits was conducted to evaluate the potential therapeutic effect of these tablets. The 24 NZW rabbits were divided in three different treatment groups (8 rabbits in each group) as shown in the Table 4, the ilomastat tablet treatment group, the positive control group treated with sponges with 0.2 mg/ml MMC and the negative control group treated with sponges with sterile water. Rabbits underwent glaucoma filtration surgery (described in section 2.1.2.1.) in the left eye and the right eye was used as control. As in the former *in vivo* study, the rabbits (24 Female New Zealand White Rabbits) were bought from the same provider (Harlan UK Ltd) and were of the same size and weight (2-2.2 kg, 12 - 14 weeks old).

Endpoints, clinical examination, measurement of IOP and termination of the study were performed as previously described in the 'Preliminary Ilomastat tablet *in vivo* study'.

Group #	Treatment	Tablet/ sponge characteristics	Schedule	Control eye (right)	Study End
A (8 rabbits)	Ilomastat tablet	Weight: 2.1-2.3 mg Diameter: 3mm Thickness: 0.4 mm	Placement of one pellet in the subconj. area of the left eye at the end of the GFS just before conj. closure	No treatment	Day 30 – all rabbit eyes to histology
B (8 rabbits)	0.2 mg/ml MMC sponges for 3 minutes	Sponges removed after 3 minutes	Placement of the sponge in the subconj. area of the the left eye d at the end of the GFS just before conj. closure	No treatment	Day 30 – all rabbit eyes to histology
C (8 rabbits)	Sponges with sterile water for 3 minutes	Sponges removed after 3 minutes	Placement of the sponge in the subconj. area of the the left eye d at the end of the GFS just before conj. closure	No treatment	Day 30 – all rabbit eyes to histology

Table 4: Description of the second (randomised, blind, control) study *in vivo* study in which the anti-scarring effect of the ilomastat tablet was tested.

2.2.4.2. Aqueous, vitreous and blood samples

At the end of the *in vivo* study and prior to the killing of the rabbits, samples of aqueous humor and vitreous body from the treated and untreated eyes and cardiac blood were obtained from each rabbit. Blood was obtained from the heart of the rabbits with

cardiac puncture. The bloods were placed in lithium heparin polypropylene tubes and were spun via centrifuge at 4000 rpm for 10 minutes. The plasma was collected and was placed in 15ml polypropylene tubes. The samples were tested with HPLC for ilomastat detection.

2.2.4.3. Histology

The methods for histological processing and staining (H&E and Picrosirius Red), and the method of grading for cellularity and scarring deposition were as previously described in section 2.1.2.6.

2.3. Determination of the efficacy of novel MMP Inhibitors

2.3.1. Physicochemical characteristics of the MMPi compounds

In addition to ilomastat, the effect of novel MMPis on collagen gel contraction was investigated. Four compounds (compounds 1, 2, 3 and 4) were supplied under contractual agreement with Astra Zeneca (UK). Some information regarding the structure as well as the physicochemical characteristics of the molecules were provided by Astra Zeneca (AZ) and is shown below.

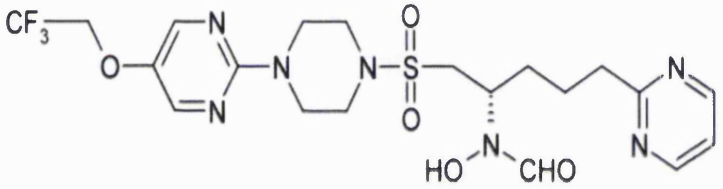

Figure 17: Structure of the Compound 4. The structure of the other compounds was not available from the company that developed the compounds.

	Compound 1	Compound 2	Compound 3	Compound 4
MMP13Hu FRET IC_{50} (nM)				0.8
HACP (nM)				32
MMP 14	13.1	14.5	46	28
MMP 2 / 8 / 9	0.17/0.4/0.2	0.35/1/0.27	1.31/0.6/44	0.1 / 0.8 / 1
MMP 15 / 16	- / -	- / -	- / -	- / -
MMP 1 / TACE	1061/105.9	1900/328	809/217.7	378 / 3939
MMP 3 / 7	18/>10000	100/>10000	68/nd	26 / 966
MMP 12 / 19	Nd/1710	nd/4900	2.47/10.1	1 / 52
ADAM 9 / 10	4650/-	3630/-	602/-	>10000 / 2538
MWt	484.0	469.0	451.5	502.5
pKa |a=acid / b=base|	8.3/-	8.2/5.4	8.2/5.0	8.2a / 2.9
ClogP / LogD (7.4)	1.29	1.72	1.60	0.62 / 1.9
Stability aq solution pH1-10				No issues
Light Stability - Hanau (t1/2)				11.6hr
Solid State Properties				Crystalline
Sol. pH 7.4 (ug/ml)	1100	41	>3000	140
Dose / solubility (uid/bid)				17 / -

Table 5: Physicochemical characteristics of the Compounds 1, 2, 3 and 4.

2.3.2. *In vitro* study

2.3.2.1. Experimental design

The positive control and each compound were prepared in the concentrations shown in Table 6.

Sample	Concentration of media	
ILOMASTAT (Positive control)	Max conc. 30 % conc. 10% conc.	100 μM 30 μM 10 μM
COMPOUND **1**	Max conc. 30 % conc. 10% conc	1100 μM 330 μM 110 μM
COMPOUND **2**	Max conc. 30 % conc. 10% conc	41 μM 12.3 μM 4.1 μM
COMPOUND **3**	Max conc. 30 % conc. 10% conc	3000 μM 900 μM 300 μM
COMPOUND **4**	Max conc. 30 % conc. 10% conc	278.61 μM 83.583 μM 27.861 μM
Negative control	Normal media without any anti-scarring agent	

Table 6: Concentration of Compounds 1, 2, 3 and 4 evaluated for effectiveness in inhibiting *in vitro* contraction. There were 5 gels and 2 ml of media in each one of the five treatment plans. The media was renewed on day 3.

2.3.2.2. Preparation of stock solutions with DMSO

Ilomastat: 0.777 mg of ilomastat was added in 100 μl of DMSO, creating a stock solution of 20 mM.

Compound 1: 10.648 mg of AZ compound 1 was added in 100 µl of DMSO, creating a solution of 220 mM.

Compound 2: 0.385 mg of AZ compound 2 was added in 100 µl of DMSO, creating a solution of 8.2 mM.

Compound 3: 27.09 mg of AZ compound 3 was added in 100 µl of DMSO, creating a stock solution of 600 mM.

Compound 4: 2.8 mg of AZ compound 4 was added in 100 µl of DMSO, creating a stock solution of 55.72 mM.

Three different concentrations were tested for each one of the molecules; the maximum aqueous solubility concentration, 30 % of the maximum aqueous solubility concentration and 10 % of the maximum aqueous solubility concentration. N (Number of gels in which the effect of the each treatment was tested) = 5 in order to increase the power of the study. Gels were placed into Mattek dishes and then 2 ml of media were added on day 0. The media was replaced on day 3.

2.3.2.3. Preparation of media with concentrations equivalent to the maximum reported aqueous solution

In order to get a concentration equivalent to the maximum reported aqueous solubility, 10 µl of each one of the AZ compounds 1, 2, 3 and 4 (stock solutions) were added to four different tubes of 1.99 ml of media. 10 µl of the ilomastat stock solution was also added to 1.99 ml of normal media. The new 2 ml solution was added to the Mattek dishes with the positive control gels. In the Mattek dishes with the negative control gels, 1.99 ml of normal media plus 10 µl of DMSO was added. No MMP inhibitors or other anti-scarring agents were added.

2.3.2.4. Preparation of media with concentration equivalent to the 30 % of the maximum reported aqueous solution

In order to get a concentration equivalent to the 30 % of the maximum reported aqueous solubility, 30 µl of AZ compound 1, 2, 3 and 4 stock solution was added to 70 µl

of DMSO. Then, 10 µl of this solution was added to 1.99 ml of normal media and was placed in the Mattek dishes. The same process was followed for ilomastat. For negative control, the negative control gels were treated with media containing 1.99 ml of normal media and 10 µl of DMSO.

2.3.2.5. Preparation of media with concentration equivalent to the 10 % of the maximum reported aqueous solution

In order to get a concentration equivalent to the 10 % of the maximum reported aqueous solubility, 10 µl of AZ compound 1, 2, 3 and 4 stock solution was added to 90 µl of DMSO. Then, 10 µl of this solution was added in 1.99 ml of normal media and was placed in the Mattek dishes. The same process was followed for ilomastat. For negative control, the negative control gels were treated with media containing 1.99 ml of normal media and 10 µl of DMSO were used.

2.3.2.6. Cells used in the *in vitro* contraction experiments

Human Tenon's fibroblasts (HTF) were used for these *in vitro* experiments. The HTFs used, belong to the same donor (Moorfields donor's ID: 5004). Cells were used from passage 6, as were the cells that were used for the ilomastat tablet *in vitro* experiments. The cells are also of the same passage.

2.3.2.7. Preparation of the collagen I gels (contraction *in vitro* model)

For the preparation of the collagen gels, the same protocol as for the Serum Amyloid P (section 2.1.1) *in vitro* experiments was used.

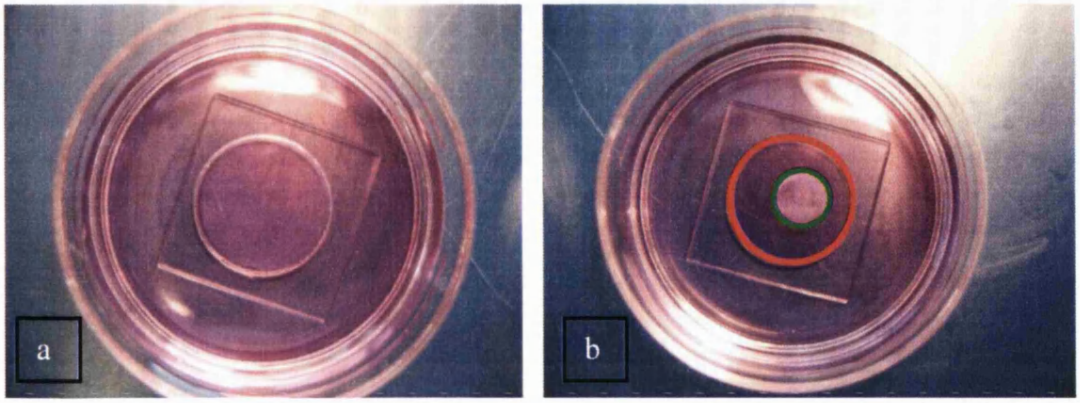

Figure 18: Examples of (a) a non- contracted gel (day 0) and (b) of a contracted gel (Day 5).

The percentage contraction was calculated with the software ImageJ and represents the percentage surface reduction of the gel at each time point (Day 1 to Day 7) based on the following mathematical formula:

$$\%\text{contraction} = \frac{\text{Surface area of the gel (inside green circle) at the tested time point (Day 5 in this case)}}{\text{Initial surface area of the gel (Surface area inside the red circle)}} \times 100$$

Graphs showing the mean percentage contraction of each treatment group, and the statistical analysis (ANOVA) were produced using SPSS version 14. The error bars at each time point were also calculated with SPSS version 14. Representative graphs and photographs of gels are shown in Figure 51 and Figure 52 in Section 3: 'RESULTS'.

2.4. Small interfering RNAs (siRNAs) against MMPs

2.4.1. Structure of the siRNAs

The five short interfering RNAs against MMP-1, -2, -3, -8 and -9 in liquid form and concentration 20mM were supplied by Quark PLC. The siRNAs against MMP-1,-2,-3,-8 and -9, patented by Quark PLC, are double-stranded siRNAs; the sense strand is designed based on the structure of a small part of the mRNA of each one of the aforementioned MMP molecules and the antisense strand is structured in order to be complementary to the antisense strand.

The provided compounds by Quark PLC follow the general structural pattern shown below:

5'$(N)_x$ – Z 3' (antisense strand)

3' Z' – $(N')_y$ 5' (sense strand)

N and N' represents a ribonucleotide.

$(N)_x$ and $(N')_y$ is an oligomer, in which the Ns are linked with covalent bonds.

x and y, in the case of the 5 MMP SiRNAs that Quark provided to us for the *in vitro* and the *in vivo* experiments, were equal to 19 nucleotides.

Z and Z' were absent in the case of the five Quark PLC MMP siRNAs that were used for the *in vitro* and *in vivo* experiments.

The oligonucleotides are non-phosphorylated at the 5′ and at the 3′ positions of both strands.

Quark PLC indicated that the five siRNAs have been found to decrease by at least 50 % the expression of the MMP genes.

Gene Name	siRNA name	Oligo Seq	
		sense	antisense
MMP1	MMP_5	GCTAATAGCTGGTTCAACT	AGTTGAACCAGCTATTAGC
MMP2	MMP_34	TTAGCAGTTTGCTTTGTAT	ATACAAAGCAAACTGCTAA
MMP3	MMP_110	TCCTGATGTTGGTCACTTC	GAAGTGACCAACATCAGGA
MMP9	MMP_80	TCTGGAGGTTCGACGTGAA	TTCACGTCGAACCTCCAGA
MMP8	MMP_131	GAGCCAGGTTATCCCAAAA	TTTTGGGATAACCTGGCTC

Figure 19: The sequences of the 5 double stranded siRNAs that inhibit MMP -1, -2, -3, -8 and -9 expression that were used in our *in vitro* and *in vivo* experiments.

The siRNA against MMP-1 targets the MMP-1 mRNA at the position 1262-1280, the siRNA against MMP-2 targets the MMP-2 mRNA at the position 2768-2786, the siRNA against MMP-3 targets the MMP-3 mRNA at the position 345-363, the siRNA against MMP-8 targets the MMP-8 mRNA at the position 1287-1305 and finally, the siRNA against MMP-9 targets the MMP-9 mRNA at the position 1914-1932.

The Quark PLC MMP siRNAs can be delivered through any of the conventional routes, but for the purposes of this thesis, only subconjunctival administration took place. The siRNA compounds were delivered in solutions ready to be injected. These solutions, based on information provided by Quark PLC, contain, apart from the 5 MMP siRNA compounds in concentration of 20 mM, "aqueous solution with or without organic solvents, aqueous or oil suspensions, emulsions with edible oils as well as similar pharmaceutical vehicles". These siRNAs, used in the preparation of a pharmaceutical composition, are admixed with a carrier in a pharmaceutically effective dose and are conjugated to a steroid or to a lipid or to another suitable molecule e.g. cholesterol. The siRNA can be delivered with viral or non-viral vectors or directly, as mentioned in the patent.

2.4.2. *In vitro* study

The effect of the MMP siRNAs against collagen embedded Human Tenon's Fibroblasts (HTF) (*in vitro* scarring model described in detail in section 2.1.1.) was assessed in the experiments shown in Table 7 and Table 8. Pre-incubation and gel formation were performed in accordance with the protocols used in our lab and described previously in the "Materials and Methods of the Ilomastat tablet *in vitro* experiments" (section 2.1.1.). We prepared 3 different gels for each group. MMP siRNAs were diluted in the media using the guidelines received from Quark PLC. Normal media without any treatment was used as negative control and media with maximum ilomastat concentration (100 μM) without DMSO was used as positive control.

2.4.2.1. 24h pre-incubation period study

TIME (DAYS)	"Negative" Control group	siRNA group 1	siRNA group 2	siRNA group 3	siRNA + lipofectamine group 1	siRNA + lipofectamine group 2	siRNA+ lipofectamine group 3	"Positive" Control Ilomastat group
FEED								
Incubate cells in culture 1 day (24h)	media without siRNA or ilomastat	100 nM siRNA	30 nM siRNA	10 nM siRNA	100 nM siRNA + lipofectamine	30 nM siRNA + lipofectamine	10 nM siRNA + lipofectamine	Media with ilomastat
FEED								
Gels day 0-day 3	media without siRNA or ilomastat	Media with 100 nM siRNA	media with 30 nM siRNA	media with 10 nM siRNA	media with 100 nM siRNA	media with 30 nM siRNA	media with 10 nM siRNA	Media with ilomastat
FEED								
Gels day 3-day 7	media without siRNA or ilomastat	Media with 100 nM siRNA	media with 30 nM siRNA	media with 10 nM siRNA	media with 100 nM siRNA	media with 30 nM siRNA	media with 10 nM siRNA	Media with ilomastat

Table 7: Description of *in vitro* contraction experiment in which HTFs were pre-incubated with the treatments for 24 hours before they populated the collagen I gels.

2.4.2.2. 48h pre-incubation period study

TIME (DAYS)	"Negative" Control group	siRNA group 1	siRNA group 2	siRNA group 3	siRNA + lipofectamine group 1	siRNA + lipofectamine group 2	siRNA+ lipofectamine group 3	"Positive" Control Ilomastat group
FEED								
Incubate cells in culture 2 day (48h)	media without siRNA or ilomastat	100 nM siRNA	30 nM siRNA	10 nM siRNA	100 nM siRNA + lipofectamine	30 nM siRNA + lipofectamine	10 nM siRNA + lipofectamine	media with ilomastat
FEED								

Gels day 0-day 3	media without siRNA or ilomastat	Media with 100 nM siRNA	media with 30 nM siRNA	media with 10 nM siRNA	media with 100 nM siRNA	media with 30 nM siRNA	media with 10 nM siRNA	media with ilomastat
FEED								
Gels day 3-day 7	media without siRNA or ilomastat	Media with 100 nM siRNA	media with 30 nM siRNA	media with 10 nM siRNA	media with 100 nM siRNA	media with 30 nM siRNA	media with 10 nM siRNA	media with ilomastat

Table 8: Description of *in vitro* contraction experiment in which HTFs were pre-incubated with the treatments for 24 hours before they populated the collagen I gels.

Photographs of the gels and the cells were taken daily in order:

a) To measure the percentage of contraction of the gels in the 16 groups each day from day 1 to day 7, and to subsequently assess the effectiveness against *in vitro* contraction. The percentage contraction was calculated with the software ImageJ and represents the percentage surface reduction of the gel at each time point.

b) To observe the morphology that the fibroblasts obtain in the gels of each group both in the pre-incubation and in the gel contraction period.

2.4.3. First *in vivo* study

In a randomized study with a masked-observer, 24 female New Zealand White Rabbits (Harlan UK Ltd, 2-2.2 kg, 12 - 14 weeks old) underwent modified glaucoma filtration surgery. The rabbits were divided in three treatment groups. Glaucoma filtration surgery was performed in the left eye of each rabbit, using our well-established model described in section 2.1.2.1. Subconjunctival 100 μl injections of MMPs siRNA, antiTGase II ab (positive) or PBS (negative control) were applied on days 0 (immediately after surgery), 1, 7, 14, and 21. Daily photographs of the bleb area were taken and the blebs were graded based on the criteria that have been analysed in the matherial and methods of the ilomastat tablet *in vivo* experiment.

Regarding the positive control used in this experiment, the TGase II ab, specialized antibody against Transglutaminase II was used, also from Quark PLC. Tissue Transglutaminases are proteins that have been linked to the generation and pathology of many diseases and biological processes. It has been suggested that crosslinking of proteins takes place in fibrosis and tissue scarring, and mediated by Tissue Translutaminase II (TGase II). Protein modification mediated by TGase II has also been indicated in diseases like cancer, neurodegenerative diseases, thrombosis, psoriasis, pathological angiogenesis etc (Aeschlimann & Thomazy, 2000). For these reasons, TGase II was considered as a potential therapeutic target for the treatment of these disorders and diseases.

The formulation provided by Quark PLC includes 'a cloned human single-chain antibody fragment (scFv), which binds to TGase II and inhibit its enzymatic activity'.

2.4.4. Second *in vivo* study

A second *in vivo* experiment was scheduled with the use of PTEN siRNA bound to the CY3 fluorescent radical to establish if the siRNA was being uptaken from the cells. For the purposes of this experiment, 6 rabbits were used and a 100 μl of a CY3PTEN siRNA formulation was administered by subconjuctival injection in the left eye of the rabbits. The rabbits were divided in three groups:

GROUP 1: 7 days before euthanasia
GROUP 2: 1 day before euthanasia
GROUP 3: 6 hours before euthanasia

The rabbits were killed with an intra-cardiac injection of phenobarbiton (4 ml) under terminal anaesthesia. The treated eyes were dissected immediately after killing and the uptake of the CY3PTEN siRNA by cells located in the subconjunctival space was assessed within 15 minutes after the death of the rabbit with confocal microscopy.

CY3 and Cyanine dyes in general are known to be brighter compared to other fluorescein dyes and to offer greater photostability. Cy3 is excited maximally at 550 nm and emits maximally in the red end of the spectrum at 570 nm. It is detected with TRITC filter sets. The LEICA TCS-SP2 AOBS (with TRITC, Texas Red Alexa 546) was used to

assess the subconjunctival tissue for detection of CY3. The subconjunctival specimens were excited at 550 nm.

3. RESULTS

3.1. Serum Amyloid P

3.1.1. *In vitro* results

The effect of three different concentrations (5, 10 and 20 μg/ml) of Serum Amyloid P (SAP) were tested against contraction in the collagen I gels populated with HTFs. Ilomastat served as positive control and normal media without any anti-scarring agent served as negative control.

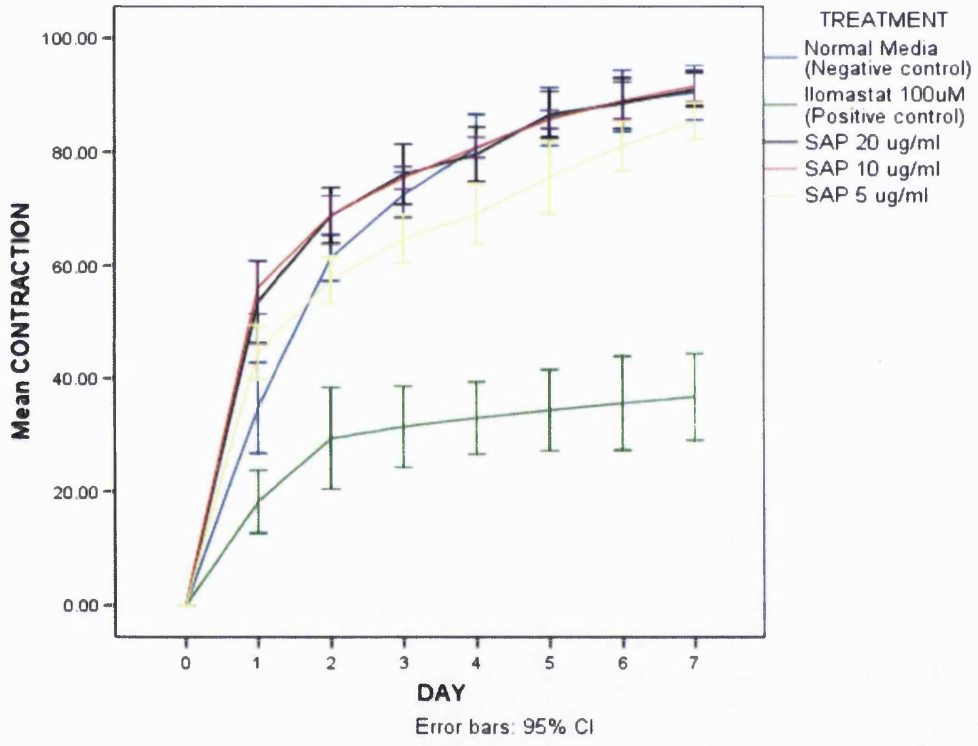

Figure 20: Percent contraction of HTF populated collagen I gels. Three different concentrations of SAP (5 μg/ml, 10 μg/ml and 20 μg/ml) of SAP were tested for their effectiveness in inhibiting the contraction of gels. SAP did not inhibit the contraction of gels in any of the tested concentrations.

SAP did not inhibit the contraction of the collagen I gels. Although SAP inhibits the transformation of circulating monocytes to fibroblasts, as indicated in the bibliography, this *in vitro* experiment showed that SAP does not inhibit the transformation of Human Tenon's Fibrocytes to elongated fibroblasts and myofibroblasts. In the gel contraction essay only Tenon's fibrocytes are used, so the observation that SAP had no effect was consistent with what is known about its biological mechanism.

3.1.2. *In vivo* results

3.1.2.1. Bleb survival results

The four treatment groups used in the *in vivo* study were: *Group A* (rabbits treated with MMC 0.2 mg/ml for 3 minutes during glaucoma filtration surgery plus five intrableb 100 μl PBS injections at time points 0, 1, 2, 4 and 7 days after glaucoma filtration surgery), *Group B* (rabbits treated with water sponge for three minutes during glaucoma filtration surgery plus five intrableb 100 μl PBS injections at time points 0, 1, 2, 4 and 7 days after glaucoma filtration surgery), *Group C* (rabbits treated with five intrableb 100 μl SAP (20 mg/ml) injections at time points 0, 1, 2, 4 and 7 days after glaucoma filtration surgery), and *Group D* (five intrableb 100 μl SAP (20mg/ml) injections on time points 0, 1, 2, 4 and 7 days after glaucoma filtration surgery plus 5 intravenous (iv) 500 μl SAP injections at the same time points). Each group was evaluated for bleb survival, bleb size and IOP.

During the post surgical observations, the rabbits that had a functioning bleb were indicated as +1 and the rabbits that had a failed bleb were recorded as 0. One rabbit assigned to Group A died after the administration of the anaesthetic drugs. In addition, one rabbit assigned to Group D died from anaphylactic shock just after the administration of the SAP intravenous injection on day 7. These two rabbits were excluded from the survival curve.

It is worth noting that the transparent fluid of the SAP injections became a cloudy white fluid when it entered the bleb immediately after each injection. It is possible that the SAP solution underwent precipitation to form a colloidal suspension upon injection into the bleb. This could have been due to the high SAP concentration in the intrableb injections. This white soft cloudiness disappeared 3-4 days after the final injection. One implication of this observation is that the local pharmacokinetics of SAP may have been different from what is expected for a homogeneous solution in the bleb. It is possible that a colloid would display longer local residence time in the bleb by adhering to tissue surfaces followed by slow dissolution of the particulates. The survival curve is shown in Figure 21. Representative images of the bleb at days 10 and 30 are shown in Figure 22 and in Figure 23.

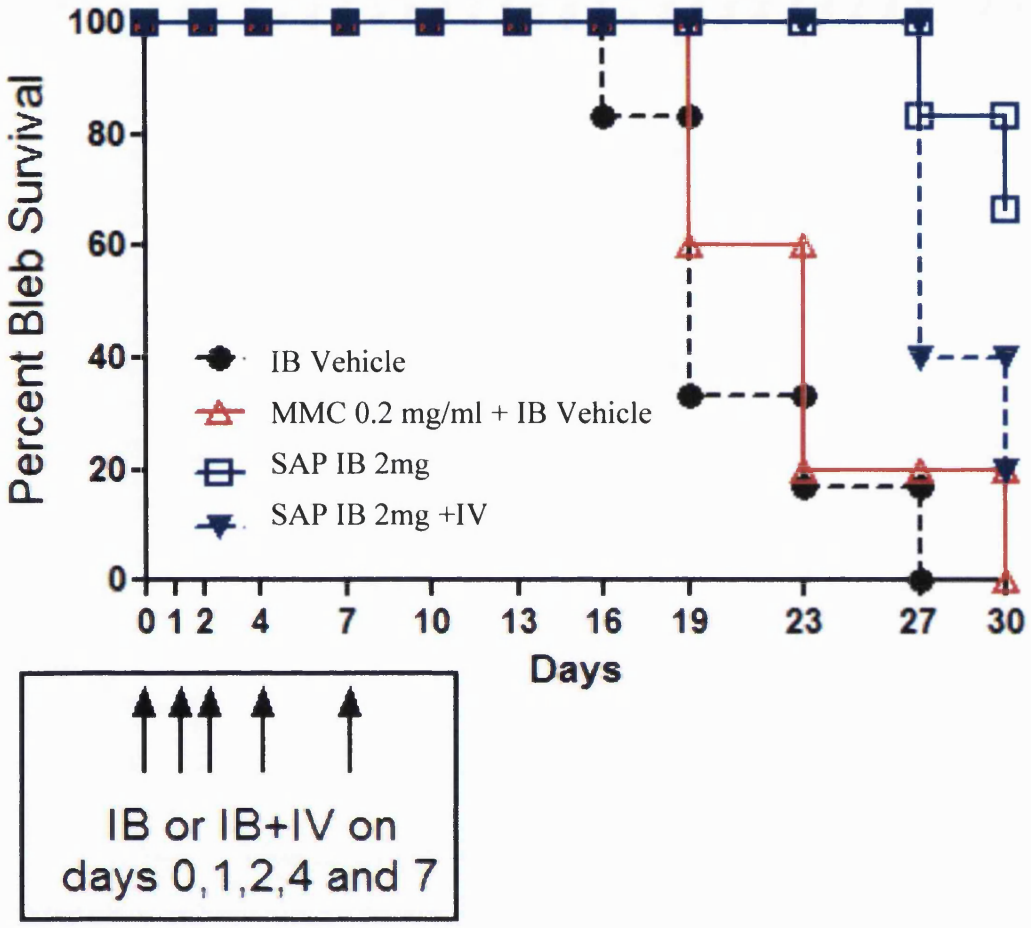

Figure 21: Red triangles represents the MMC group (positive control), solid black circles represent water sponge (negative control), blue boxes represent SAP intrableb (IB) treatment and blue triangles with blue arrows represents SAP IB and intravenous (IV) treatment. The X-axis indicates the days after GFS and the Y-axis indicates the percentage bleb survival in each group. Bleb survivals in the SAP IB and in the SAP IB+IV groups were significantly superior to the sterile water group ($P<0.001$) and the MMC group ($P<0.01$ Log Rank- confidence interval 95 %). No significant differences were found between the two SAP groups. Groups A and C had five rabbits each. Groups B and D had 6 rabbits.

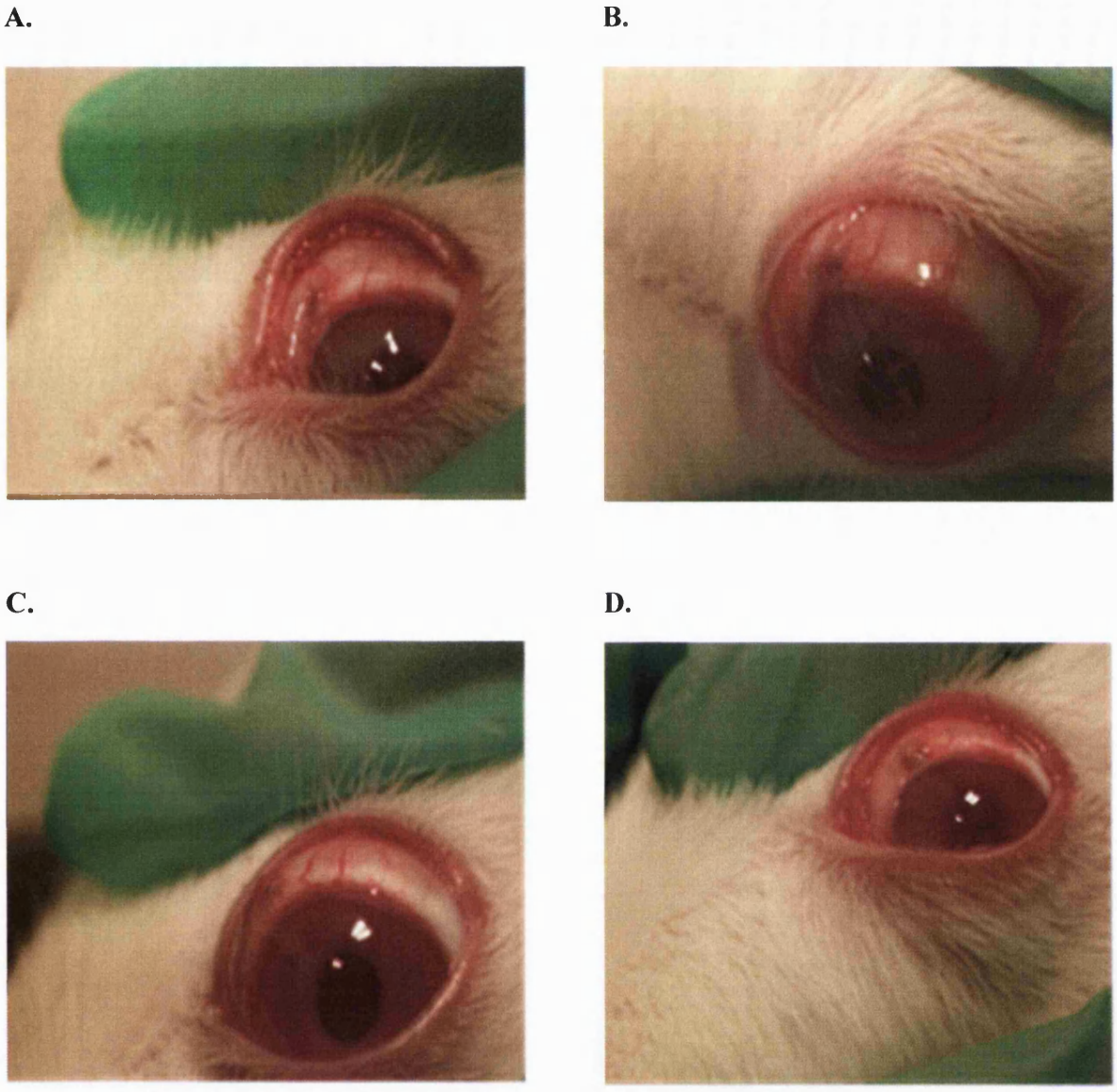

Figure 22: Images A and C: Representative photos of the bleb appearance of rabbits on day 10 and 30 respectively after glaucoma filtration surgery treated with water sponge. Image A shows a functional bleb (all the blebs treated with water sponge were functional 10 days post surgery). Image C shows a failed bleb (all the blebs treated with water sponge had failed 30 days post surgery). Images B and D: Representative photos of the bleb appearance of rabbits on day 10 and 30 respectively after glaucoma filtration surgery treated with MMC 0.2 mg/ml. Image B shows a functional bleb (all the blebs treated with MMC 0.2 mg/ml were functional 10 days post surgery). Image D shows a failed bleb (all the blebs treated with MMC 0.2 mg/ml had failed 30 days post surgery).

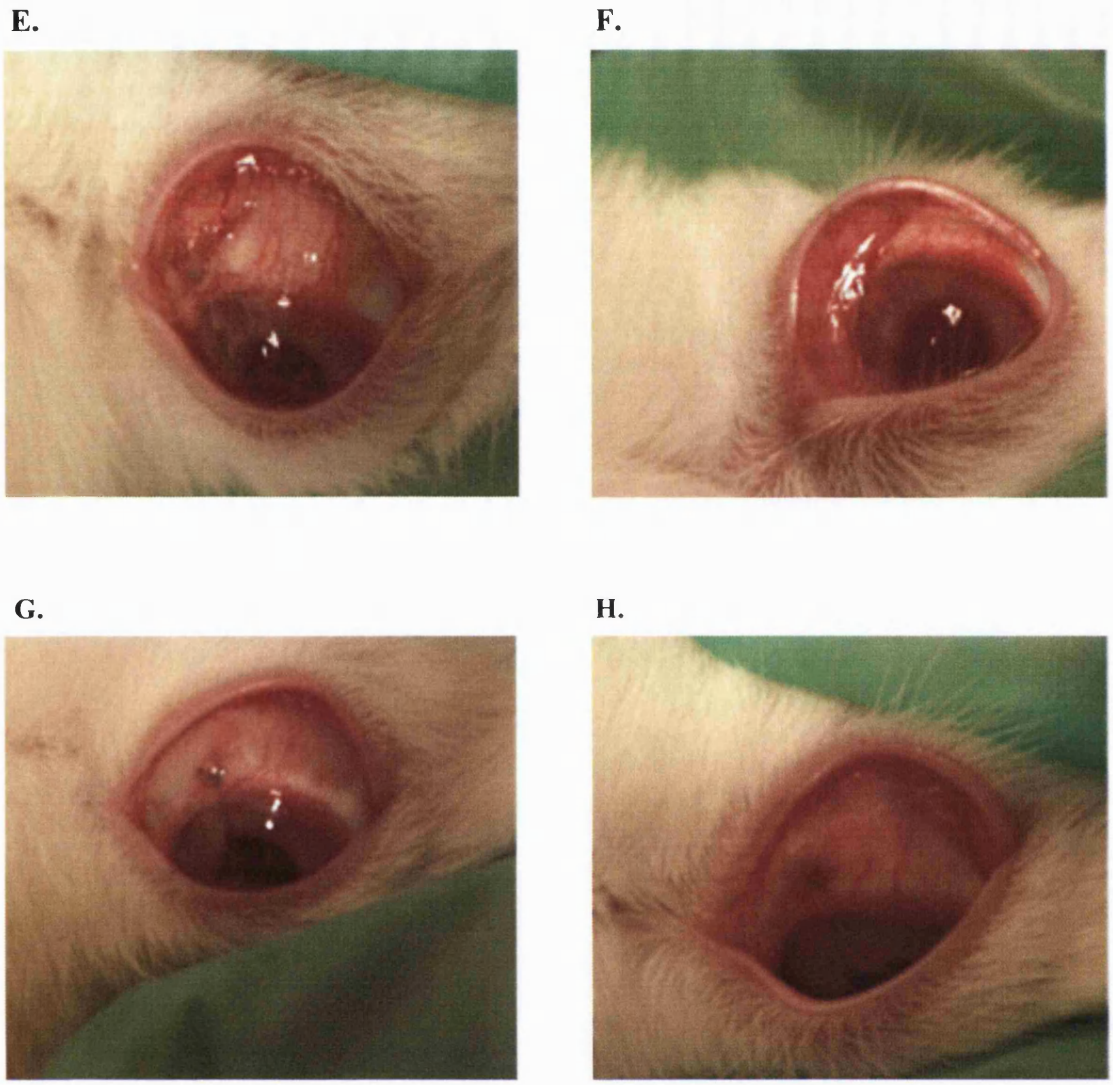

Figure 23: Images E and G: Representative photos of the bleb appearance on day 10 and 30 from rabbits treated with SAP IB&IV. Image E shows a functional bleb (all the blebs treated with SAP IB&IV were functional 10 days post surgery). In the bleb area of the operated rabbit eye shown on image E, the white soft cloudiness that had appeared after each SAP IB injection can be observed. Image G shows the only functional bleb of this group on day 30 (all but one blebs treated with SAP IB&IV had failed 30 days post surgery). The size of this bleb shown in image G is small and the bleb area is mainly limited nasally from the position of the tube. Images F and H: Representative photos of the bleb appearance of rabbits on day 10 and 30 respectively after glaucoma filtration surgery treated with SAP IB only. Image F shows a functional bleb and significantly larger bleb than the blebs of the other treatment groups (all the blebs treated with SAP IB were functional 10 days post surgery). Image H shows a functional bleb (all but two blebs treated with SAP IB were functional 30 days post surgery). The bleb is located mainly nasally from the position of the tube.

3.1.2.2. Intraocular pressure results

RABBIT	GROUP	IOP DAY 0	IOP DAY 2	IOP DAY 4	IOP DAY 7	IOP DAY 10	IOP DAY 13	IOP DAY 16	IOP DAY 19	IOP DAY 23	IOP DAY 27	IOP DAY 30
1	1	13.2	9	10.6	14	17.8	12.8	12.6	11.8	11.6	11.4	12.8
2	2	11.8	3	4.4	7.8	8.2	8.8	5.4	5	6.2	8.2	20.4
3	3	14.2	10	9.2	10.8	10.4	10	11	9.6	10.4	12.4	9.6
5	4	13.6	7.8	7.8	12.2	11.4	14.4	11	11.4	11.6	11.4	10
6	3	13.2	18	10.8	13.8	13.8	13.6	14.8	12.8	8	11.6	8.4
7	1	13	13.2	8.4	11	15	19.4	19.4	15.2	15.8	13.4	12
8	4	12.2	9.2	6	12	-1	-1	-1	-1	-1	-1	-1
9	4	12.4	7.8	6.2	10	8.8	12.8	8.6	11	7	6.4	6.4
10	2	12	5.4	11.2	11	14.6	17	15.8	13	12.4	12	10.8
11	1	12.2	7.6	9.6	13.6	15.4	12.4	14.4	15.8	13.4	14.6	11.6
12	3	13.4	7.4	11	14.2	19.8	13.8	15.4	14.8	14.6	12.4	9.6
13	2	12.2	7.2	13.8	14	15.8	14.4	16	14	12.8	14.2	13.4
14	4	11.8	6.6	10.4	10.6	15	10.2	12.8	11.2	11	11.4	10
15	3	11.6	3	8.4	7.6	11.6	13.2	12.2	12	12.4	9.8	7.8
16	1	15.2	11.8	12.8	18.8	17.6	15.4	17	14.8	16.2	15	11.8
17	1	13	11.6	10	18.4	17.6	15.2	13.8	15.4	13.4	15.6	17
18	3	12.2	9	10	11.6	11	11.6	11.4	12.2	12.6	11.2	10
19	4	11.2	9.4	10.6	8.6	13.8	10.8	14	12.6	11.8	11.8	8.6
20	2	13.8	9	11.6	13.2	14.8	14.4	12	16.6	19.6	12.8	9.6
21	4	10	10	12.6	11.6	13.4	12.6	12.2	10	11.8	8.8	10
22	3	15	8.2	13.6	12.8	17	11.2	12	12.6	13.8	14.2	10.8
23	1	12.6	11.8	9.6	11.2	12.4	11.8	16.6	12.6	14.6	12.6	11.4
24	2	15	6.4	7.4	7.8	10.6	16.4	25.6	7.6	15.4	11	14.8

Table 9: Each value at the columns 'IOP' represents the IOP of the treated eye and are the mean of five measurements with the Mentor Tonopen. Missing values after day 7 for the rabbit no8 (due to sudden death) are indicated with -1.

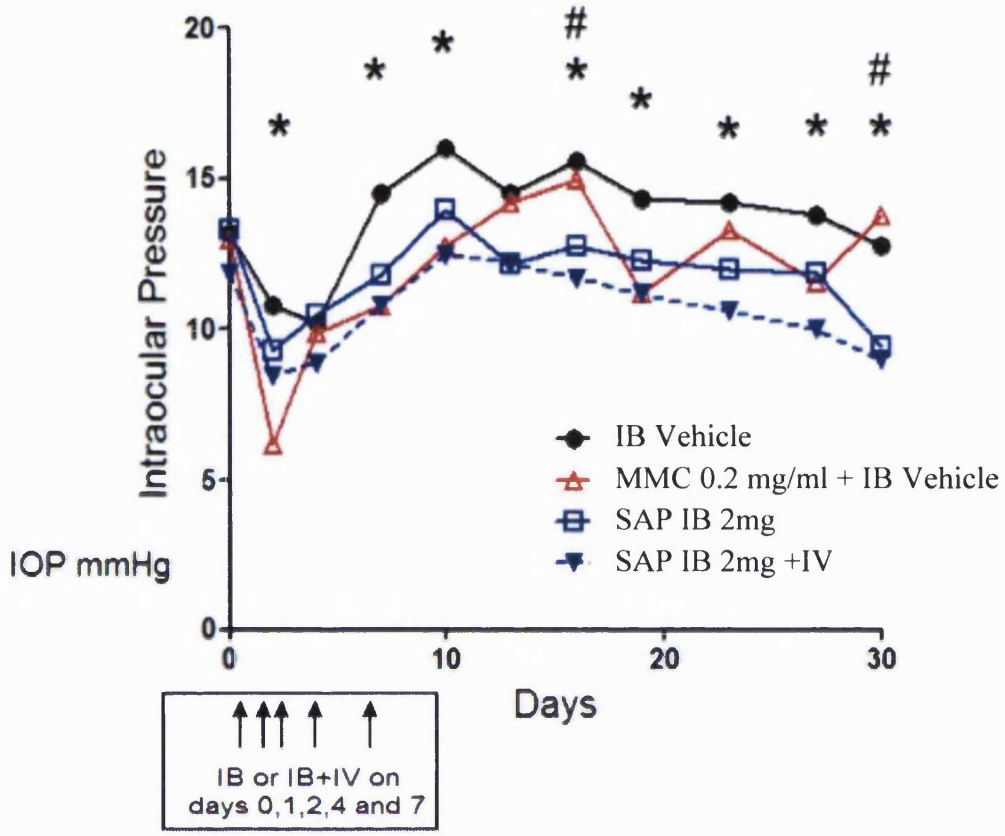

Figure 24: Comparison of intraocular pressure between the water sponge (solid black circle), MMC (red triangle), SAP IB (blue square) and SAP IB&IV groups (blue triangle). The * sign indicates statistically significant lower IOP in the SAP IB&IV group compared to the WS group and the # sign indicates statistically significant lower IOP in the SAP IB group compared to the WS group.

The changes in IOP that were observed are shown in Table 9 and in Figure 24. On day 0 post GFS, no significant differences were observed in the IOP measurements that were obtained from the four groups were detected. On day 2 post GFS, the MMC and the SAP IB&IV groups had significantly lower IOP than the water sponge (WS) group. On day 4 post GFS no significant differences in the IOP measurements obtained from the four groups were detected. On day 7 post GFS, the SAP IB&IV group had significantly lower IOP than the WS group. On day 10 post GFS, the SAP IB&IV group had significantly lower IOP than the WS group. On day 13 post GFS, no significant differences in the IOP measurements obtained from the four groups were detected. On day 16 post GFS, SAP IB

and SAP IV&IB groups had significantly lower IOP than the WS group. At day 19 post GFS the SAP IB&IV group had significantly lower IOP than the WS group. On day 23 post GFS the SAP IB&IV group had significantly lower IOP than the water sponge group. On day 27 post GFS the SAP IB&IV group had significantly lower IOP than the WS group. At day 30, the SAP IB and the SAP IB&IV groups had significantly lower IOP that the MMC and the WS groups.

Changes in bleb dimensions are shown in Figure 25 and in Figure 26.

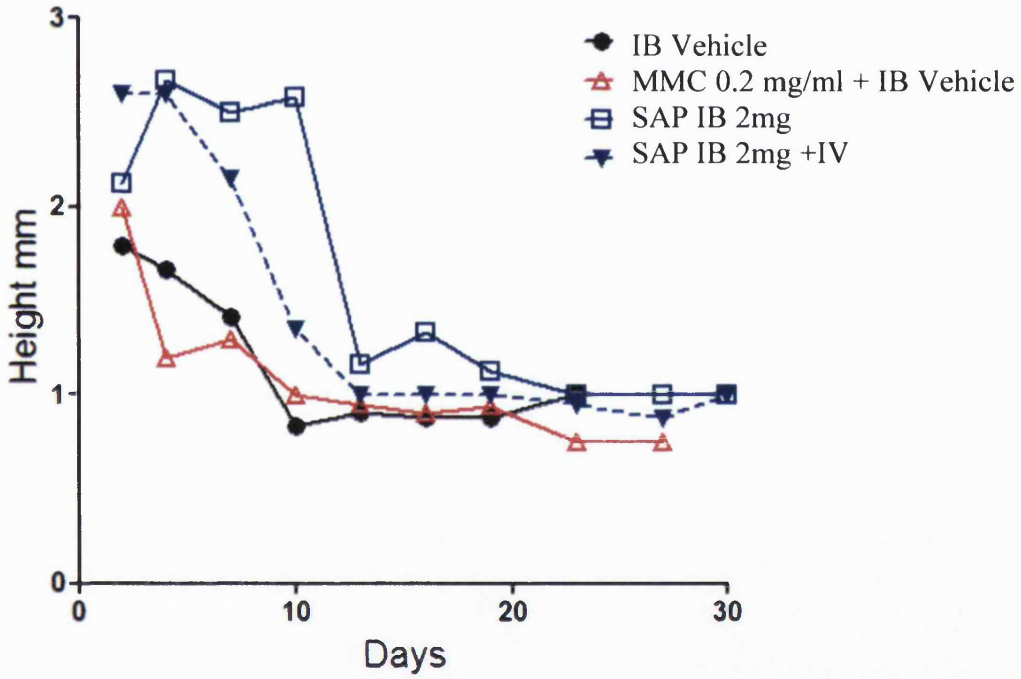

Figure 25: Comparison of bleb height between the four groups. During the first 10 days the SAP treatment groups had much higher blebs compared to the WS and MMC groups. The WS group is represented until day 23 and the MMC group is represented until day 27, as after these time points the blebs of all the rabbits in these groups had failed.

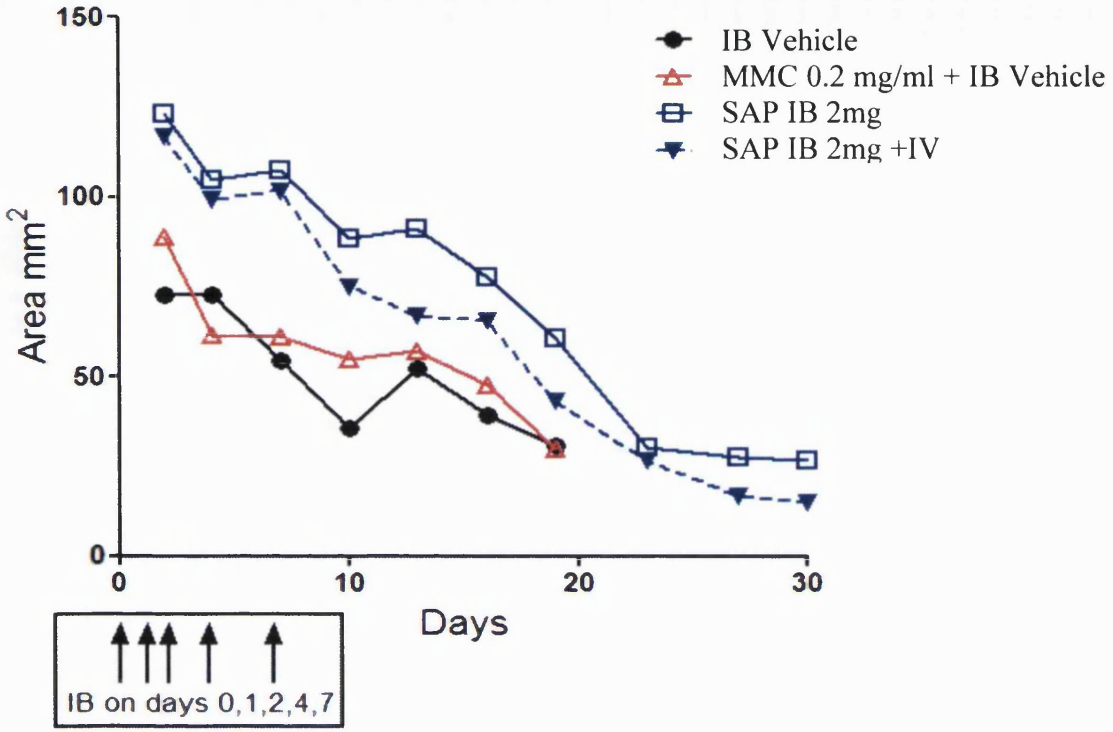

Figure 26: Comparison of bleb area between the four treatment groups. The surface areas of the WS and MMC groups are not represented after day 19, as the blebs in these groups are either failed or the bleb surface of the rabbits belonging in these groups is very small. This figure indicates that the mean bleb area of the rabbits belonging in the SAP IB & IV and SAP IB groups was larger throughout the experiment compared to the MMC (positive control) and water sponge (negative control) groups.

3.2.2.5. Histological findings

3.2.2.5.1. Number of cells in the bleb area

Analysis of the number of cells that populate the bleb area was determined histologically. The assessment of the cell number located in the blebs of the rabbits was based on images of sample sections stained with Eosin and Haematoxylin images (Figure 27). As it is shown in Figure 28, statistical analysis (t tests) indicated that the cell number located in the bleb area of the SAP IB (Group C) and the SAP IB & IV (Group D) rabbits was significantly lower ($P<0.05$) than in the MMC and the water sponge treated groups.

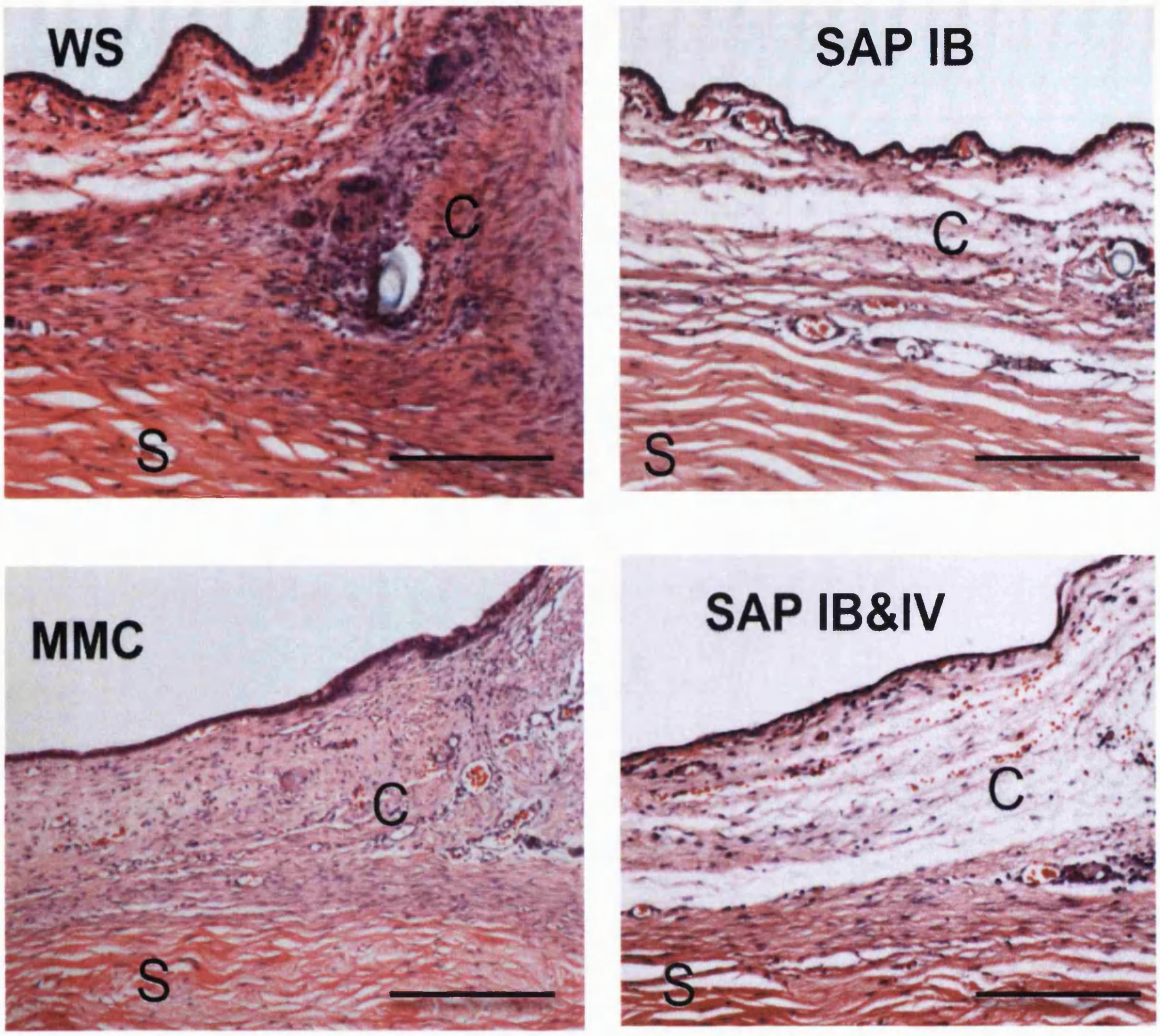

Figure 27: Representative Eosin and Haematoxylin (H & E) sections from the four groups. The nuclei of the cells are stained as dark blue with the H & E staining. The letter C indicates the subconjunctival space and the letter S indicates the sclera of the rabbit eye. Significantly lower number of cells was observed in the SAP IB and SAP IB & IV groups compared to the positive (MMC 0.2 mg/ml) and the negative control (water sponge) groups. Especially in the subconjunctival space of the WS section, a dense population of elongated fibroblasts can be observed. This finding was not observed in any of the SAP IB or the SAP IB & IV treated rabbits. In the WS and the MMC images deposition of dense collagen can be observed in the blebs. Scale 1 mm

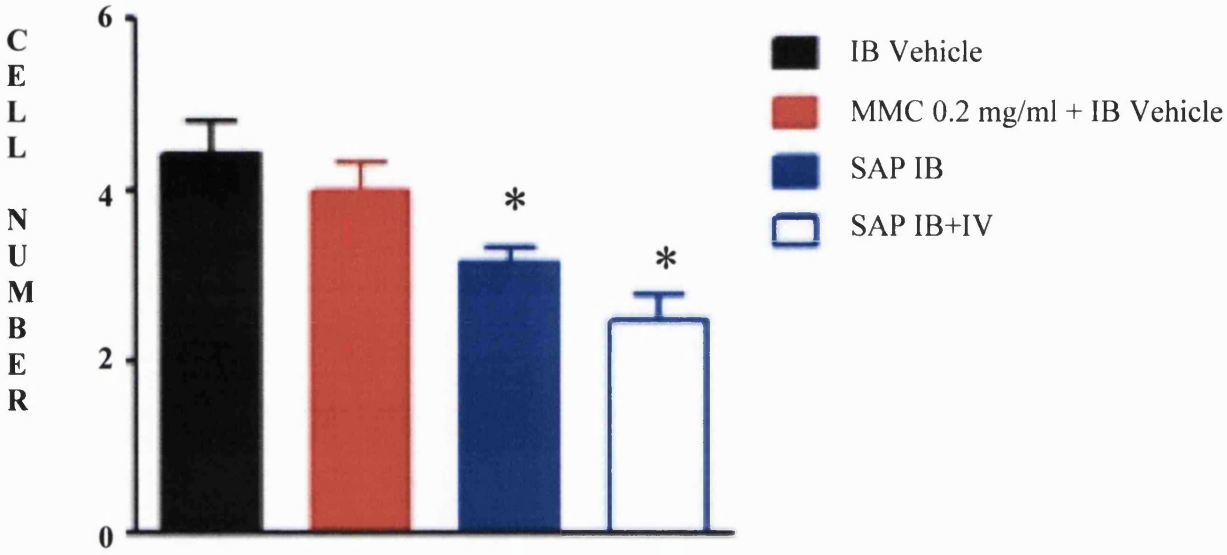

Figure 28: Graphical representation of the grading of the number of cells located in the bleb of the four treatment groups. The symbol * indicates that the number of cells in the SAP IB and the SAP IB & IV is significantly lower ($P < 0.05$, t test) compared to the WS and MMC samples.

3.2.2.5.2. Collagen deposition in the bleb area

Analysis of the deposition of collagen in the bleb area was also determined histologically. The assessment of the collagen deposition in the blebs of the rabbits was based on sample sections stained with Picrosirius Red images (Figure 29). As it is shown in Figure 30, statistical analysis (t tests) indicated that the collagen deposition in the bleb area of the SAP IB (Group C) and the SAP IB & IV (Group D) rabbits was significantly lower ($P<0.05$) than in the MMC and the water sponge treated groups. Analysis of the αSMA positive cells located in the bleb area was determined with immunohistochemistry. No statistically significant differences were detected between the four treatment groups (Figure 31).

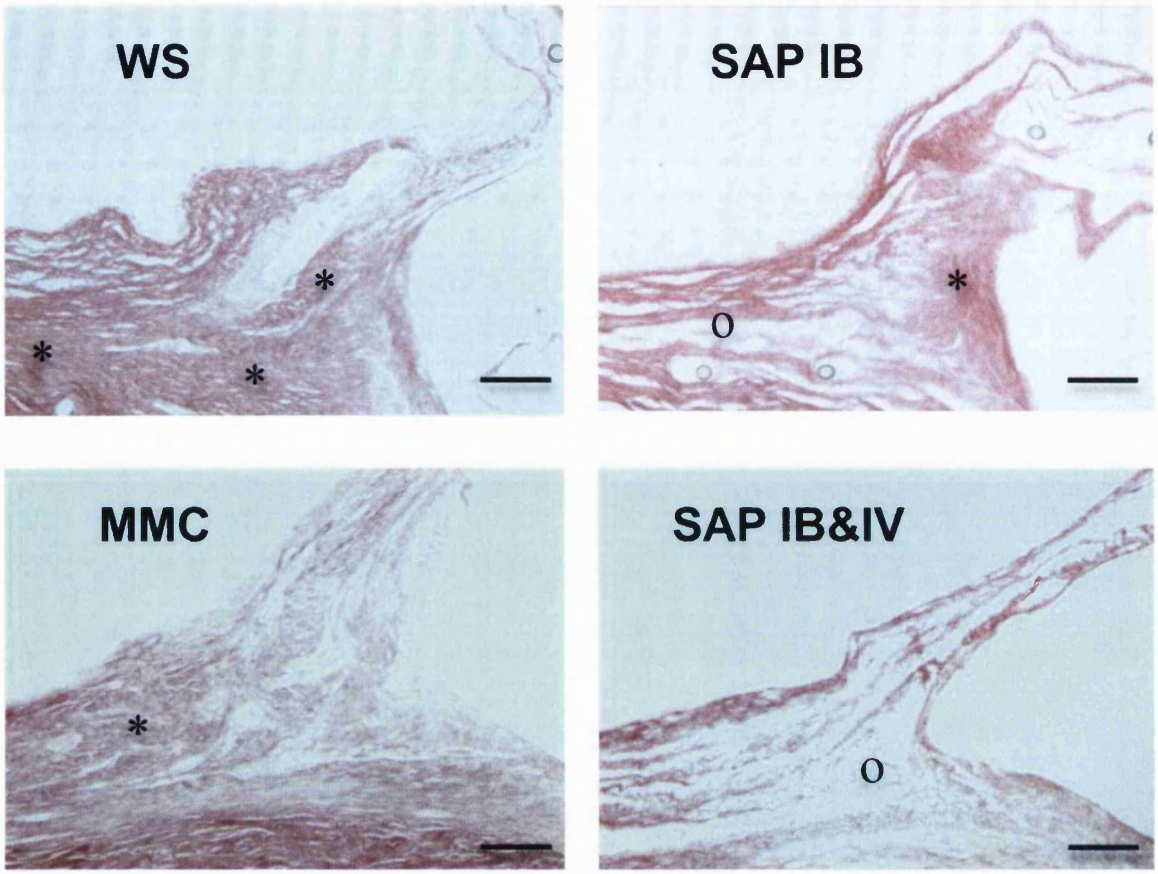

Figure 29: Representative images of bleb sections stained with Picrosirius Red from the four treatment groups. In the WS and the MMC images deposition of dense collagen can be observed in the blebs. Almost no scarring-free areas can be seen in the bleb areas of the WS and MMC sections that could indicate that aqueous outflow takes place through the bleb area in these rabbits. In the SAP IB and in the SAP IB & IV sections a higher percentage of the blebs is covered by scarring-free areas compared to MMC and WS treated blebs, which indicates that aqueous outflow may take place in these eyes through the blebs. Scale 1 mm.

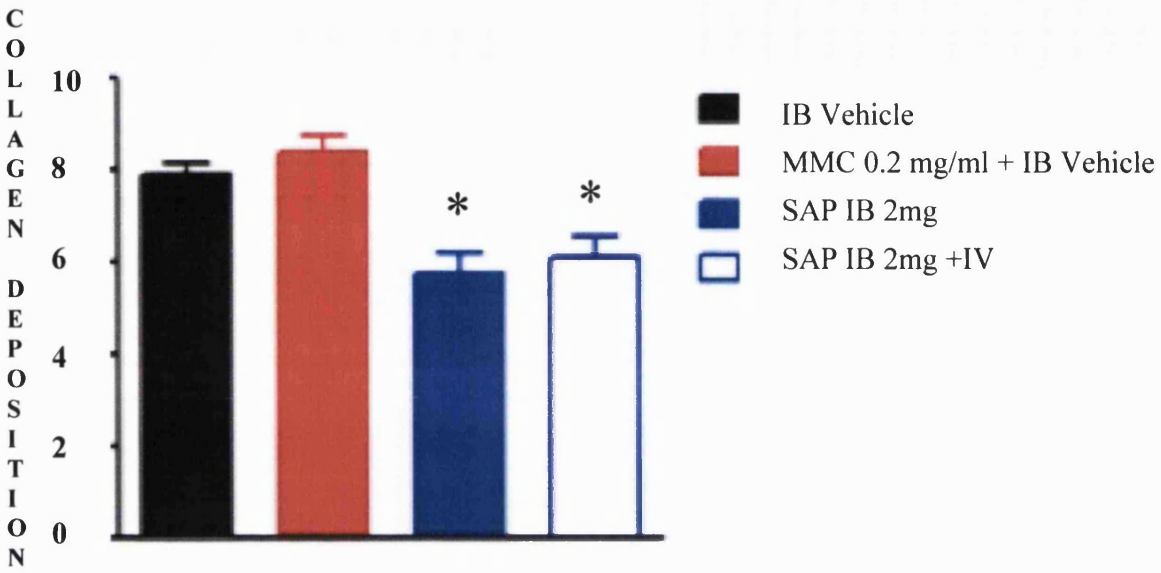

Figure 30: Graphical representation of the grading of collagen deposition in the blebs of the four treatment groups. The symbol * indicates that the collagen deposition in the SAP IB and the SAP IB & IV is significantly lower ($P < 0.05$, t test) compared to the WS and MMC samples.

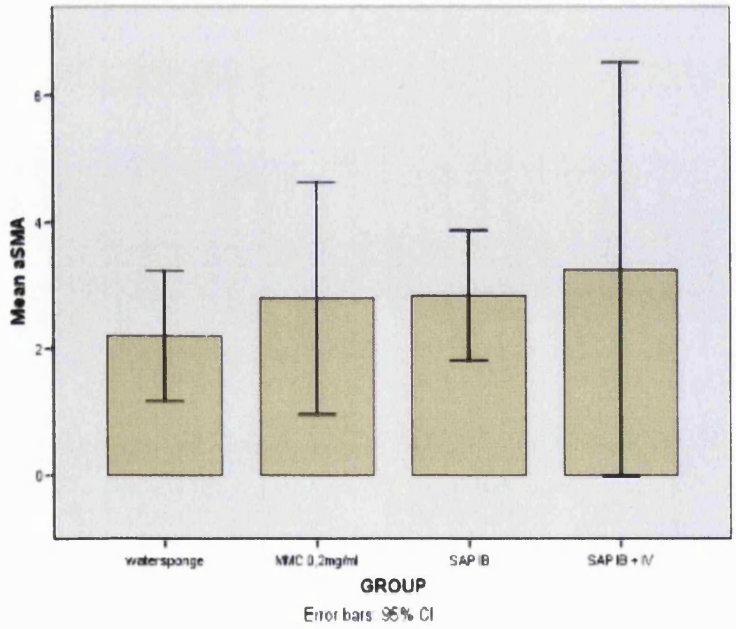

Figure 31: Graphical representation of the grading of the αSMA positive cells in the bleb area of the four treatment groups. No statistical differences were detected between the groups. It is worth mentioning that significant diversity in the number of αSMA positive cells was observed in the blebs treated with SAP IB & IV.

As previously mentioned, one rabbit died on day 7 post surgery immediately after the fifth SAP IV injection, possibly because of anaphylactic shock. The operated eye was harvested and the histological images and findings are shown in Figure 32. The histology indicates the existence of spindle shaped cells in the bleb area, as well as, interestingly, the existence of areas inside the bleb and around the tube that are characterised by decreased collagen deposition.

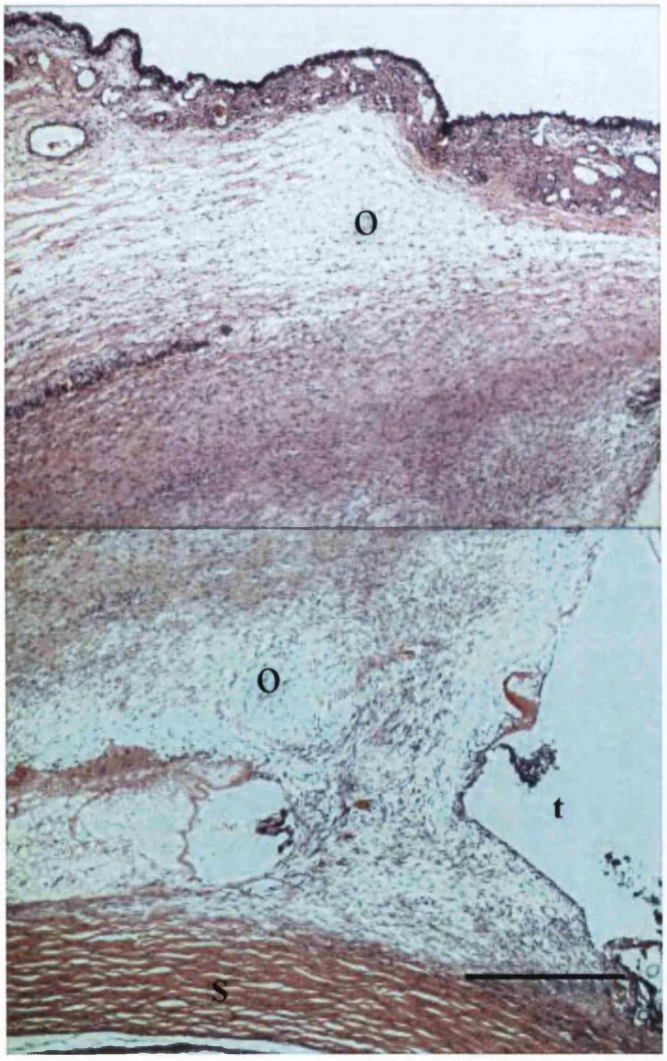

Areas with decreased collagen deposition (o)

Figure 32: Eosin and haematoxylin section of a rabbit, 7 days post glaucoma filtration surgery, treated with SAP IV + IB. The letter S indicates the sclera of the rabbit eye and the letter t indicates the tube that is placed in the rabbit eye during glaucoma filtration surgery. The arrows indicate areas with decreased collagen deposition. Scale 1 mm.

3.2. Ilomastat tissue-tablet

3.2.1. Fabrication and analysis of the ilomastat tissue tablet

3.2.1.1. Ilomastat Callibration curve

A UV calibration curve (280 nm) for Ilomastat dissolution at 7.6 pH in aqueous solution without DMSO is shown in Table 10 and in Table 11 as well as in Figure 33 and in Figure 34. The curve was generated by measurement of the ilomastat peak using two different double beam UV spectrometers (Perkin Elmer). A calibration curve was also made by HPLC (Table 12 and Figure 35).

.

Ilomastat Calibration Curve UV 1 (Perkin Elmer)	
Concentration (μM)	**AUC**
100	0.49
80	0.39
60	0.28
40	0.18
20	0.08
0	0

Table 10: Ilomastat calibration curve obtained by UV using 1 ml cuvets and a Perkin Elmer UV spectrometer.

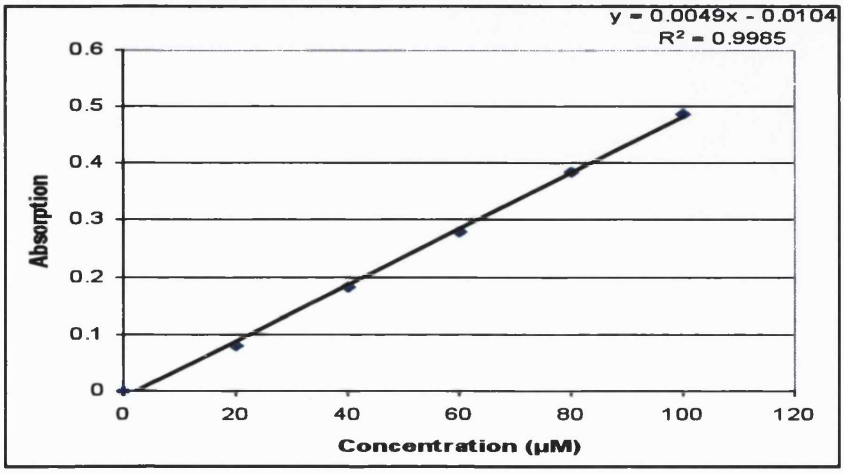

Figure 33: Ilomastat calibration curve constructed with the UV detector 1.

Ilomastat (Galardin) Calibration Curve UV 2	
Concentration (μM)	**AUC**
100	0.5366
80	0.4331
60	0.3239
40	0.2177
20	0.1359
0	0

Table 11: Ilomastat calibration curve obtained by UV using 1 ml cuvets and a second Perkin Elmer UV spectometer.

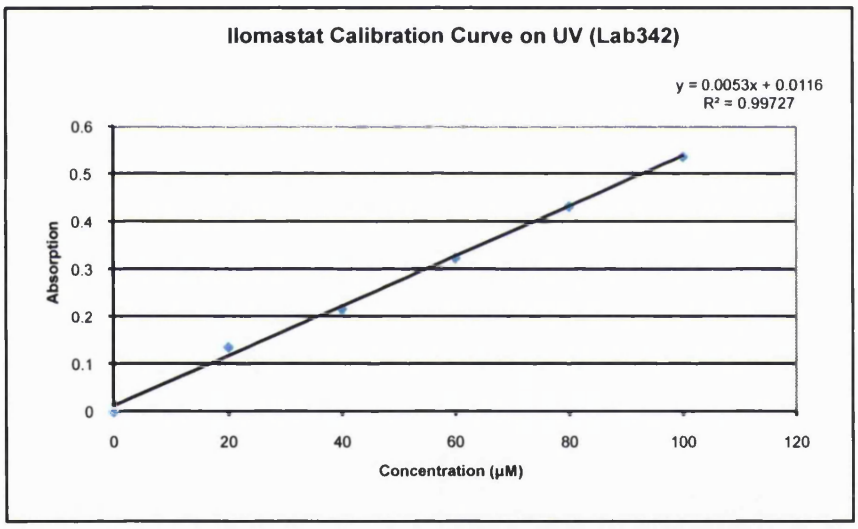

Figure 34: Ilomastat calibration curve constructed with the UV detector 2.

In the initial stages of the ilomastat tablet experiments, before the set up of the HPLC method, the concentration of the samples of ilomastat powder dissolved in aqueous solution was decided using both UV methods for accuracy. This was important because the dissolution of ilomastat powder in a pH 7.6 solution was not facilitated by DMSO, and for that reason, by testing the samples with two methods, we reduced the possibility of making a significant mistake in the recorded concentration of the samples. These initial experiments were very critical as, through these, we gained important understanding on the direct dissolution of ilomastat in aqueous solution, not previously described in the bibliography.

Ilomastat Calibration Curve on HPLC 27-11-06				
Concentration (μM)	AUC			Mean AUC
100	130.99	133.08	132.26	132.1
80	106.73	107.87	101.46	105.35
60	79.21	79.08	80.26	79.51
40	52.48	47.35	52.88	50.9
20	24.51	25.2	24.86	24.85
10	12.43	12.51	12.5	12.48
5	6.73	6.84	6.71	6.76
0	0	0	0	0

Table 12: HPLC measurements for the construction of the calibration curve. The method was repeated three times for greater accuracy.

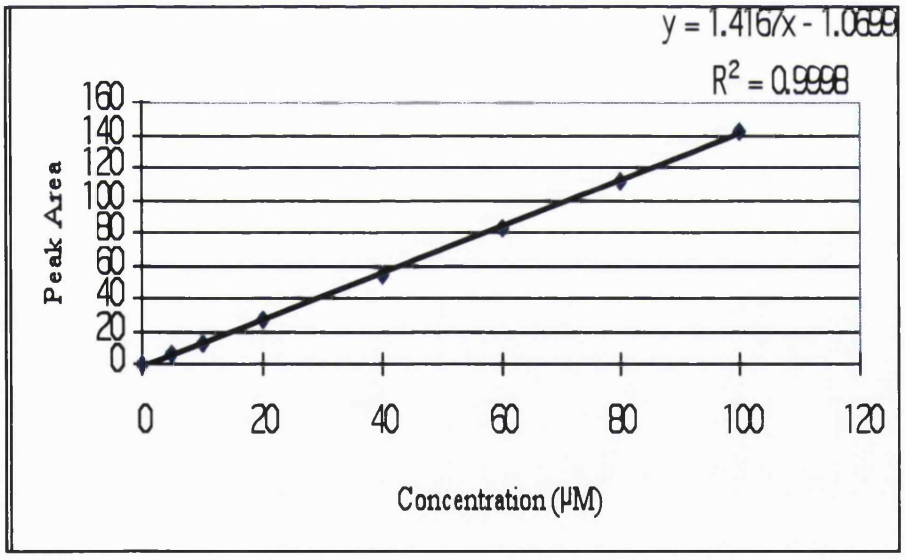

Figure 35: Callibration curve of solubility of ilomastat in pH 7.6 aqueous solution constructed by HPLC.

3.2.1.2. HPLC characterization of ilomastat

A C18 column was used as the stationary phase. Using a 25% acetonitrile aqueous mobile phase (flow 1 ml/min), ilomastat was detected at approximately 6-8 min after the injection (Figure 36). Just before the ilomastat peak, an additional peak was detected (Figure 37). This peak possibly represents one or more trace impurities since our Ilomastat from Caldiochem was 95% pure.

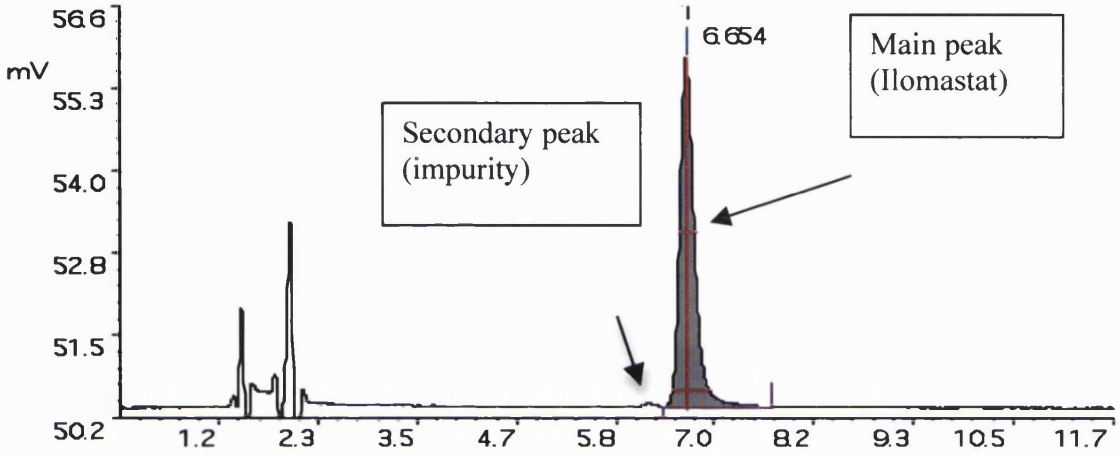

Figure 36: Ilomastat peak detection with HPLC. The elution time of ilomastat with the method we developed was 6.5 – 8.0 min. The peaks shown at 1.5 – 2.5 elution time are indicating a signal produced when the sample reaches the stationary phase.

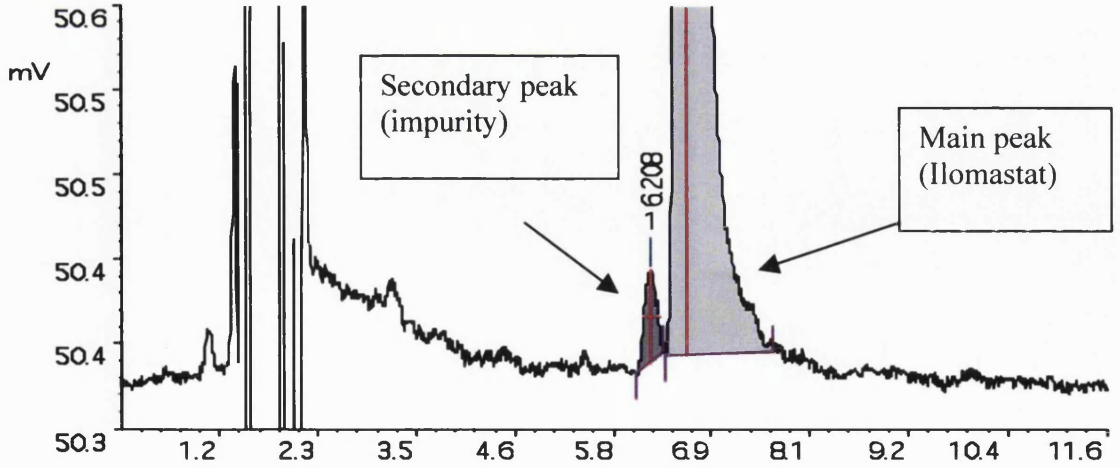

Figure 37: Main and secondary ilomastat peak. The elution time of the secondary peak with the HPLC method we developed was 6.0 – 6.5 min and was counting for less than 2 % of the main ilomastat peak. This image is magnified several times from its normal size in order the surface area of the secondary peak to be easily calculated.

3.2.1.3. Fabrication of the ilomastat tissue-tablet

Our aim was to determine if placing a small tablet made of compressed pure ilomastat in the subconjunctival space after glaucoma filtration surgery could result in slow release of a therapeutic concentration of ilomastat in the aqueous humor. Because ilomastat is a very expensive compound, we had first to gain experience in small tablet fabrication using other compounds such as 5-fthorioruracil (FU) prior to the formation of the ilomastat tablets. From both pharmaceutical and physicochemical perspectives, 5-FU is very different from ilomastat. However, it was important to develop the processes for formulating an ocular tissue tablet-to gain important information regarding the compression pressure, the use of the punch and die, the amount of powder needed to create a prolonged release tissue tablet-. This forms part of Qian Ru's thesis.

Once the methodology for the tablet fabrication had been established using 5-FU Two excipientless ilomastat tablets were made initially. These tablets are denoted A and B and were made using 6.5 mg and 5.6 mg of ilomastat powder respectively. For the formulation of tablets A and B, the application of pressure by a punch and dye mechanism to the ilomastat powder was necessary (a pressure of five bars was applied to the powder in order to fabricate the tablets). The first tablet had a diameter of 3 mm, thickness of 0.87 mm and a weight of 4.8 mg. The second tablet had the same diameter, thickness of 0.62 mm and weight of 4.1 mg. Some of the ilomastat was lost during the tablet fabrication, as it remained inside the die cylinder. At this point it is worth mentioning that the quantity of the ilomastat that was initially used for tablet fabrication was based on the hypothesis that throughout the thirty days, ilomastat would dissolve to reach what was considered to be its maximum concentration (Cmax) in aqueous solution (approximately 100 μM).

After determination of the release profiles of tablets A and B, smaller tablets were fabricated. In these smaller tablets, 3 mg of ilomastat powder was used to give a tablet weighing 2.3 mg with a diameter of 3 mm and a thickness of about 0.4 mm. These smaller tablets were then evaluated for their efficiency in releasing ilomastat at a therapeutic concentration for 30 days. These smaller 2.3 mg tablets were fabricated to determine if there were processing correlations (e.g. compression pressure) or differences in the release profile due to temperature variation and artifacts in tablet placement in the rig. It was also necessary to fabricate several tablets, so they could be sterilised and evaluated for degradation.

3.2.1.4. Ilomastat tablet release profile

After the placement of each tablet into the rig, 7.6 pH aqueous solution was pumped into the rig. The flow rate was set in 5 μl/min for tablet A and 2 μl/min. Only tablet A was tested with the 5 μl/min flow rate and in a 50 μl rig. For all the other tablets, a 200 μl rig was used with a 2 μl/min flow rate. This flow rate is similar to the flow rate of aqueous humour through the trabecular meshwork. Liquid samples were collected after exiting the rig. The samples were filtered and then analysed by HPLC and the concentration of ilomastat was determined using the calibration curve.

The release profiles for tablets A and B are graphically shown below in Figure 38, Figure 39, Figure 40 and Figure 41 respectively. The issue of reproducibility of the release profiles of ilomastat tablets is discussed in detail in section 3.2.1.6.

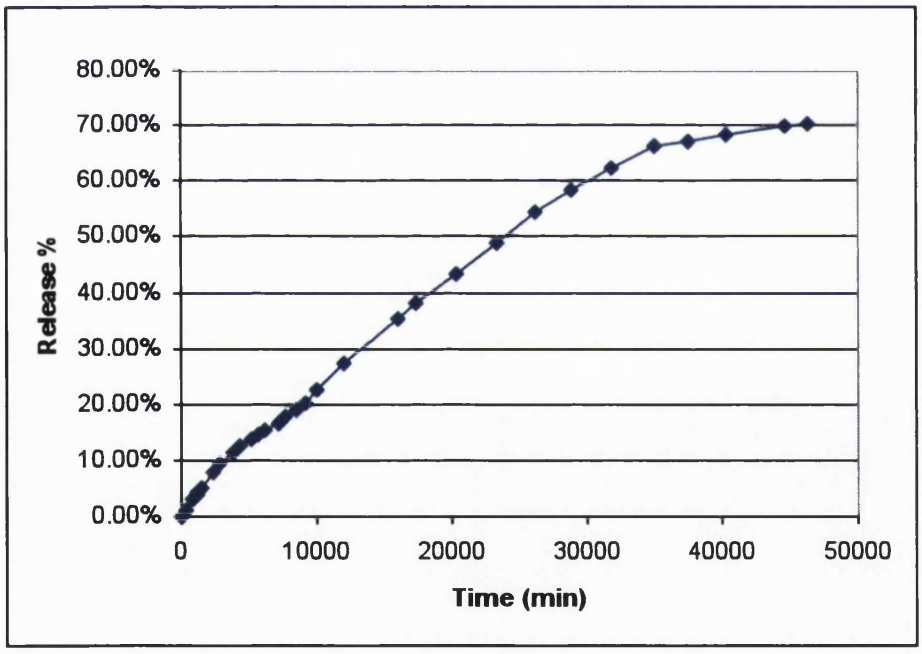

Figure 38: Percent release of Ilomastat by the Ilomastat tablet A (Weight: 4.8 mg, pressure 5 bar). After 30 days with the tablet in the 37°C aqueous environment of the 50 μl rig, about 70 % of the tablet was dissolved. The aqueous outflow was set at 5 μl/min.

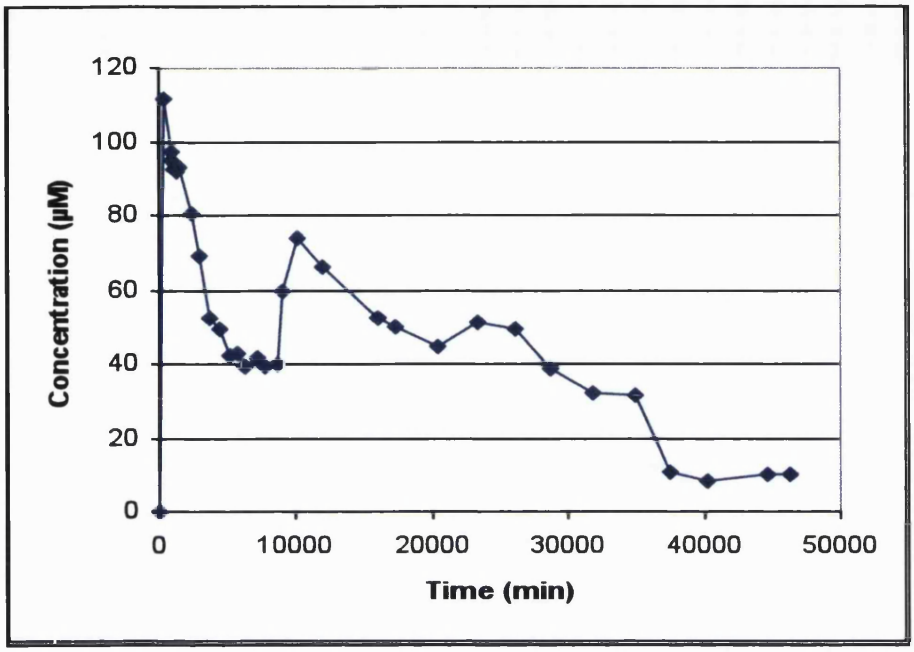

Figure 39: Concentration of ilomastat in the samples collected from the rig with tablet A. Throughout the experiment the ilomastat concentration released from tablet A was higher than 10 µM, indicative of the slow release of ilomastat from tablet A for a period of at least 30 days.

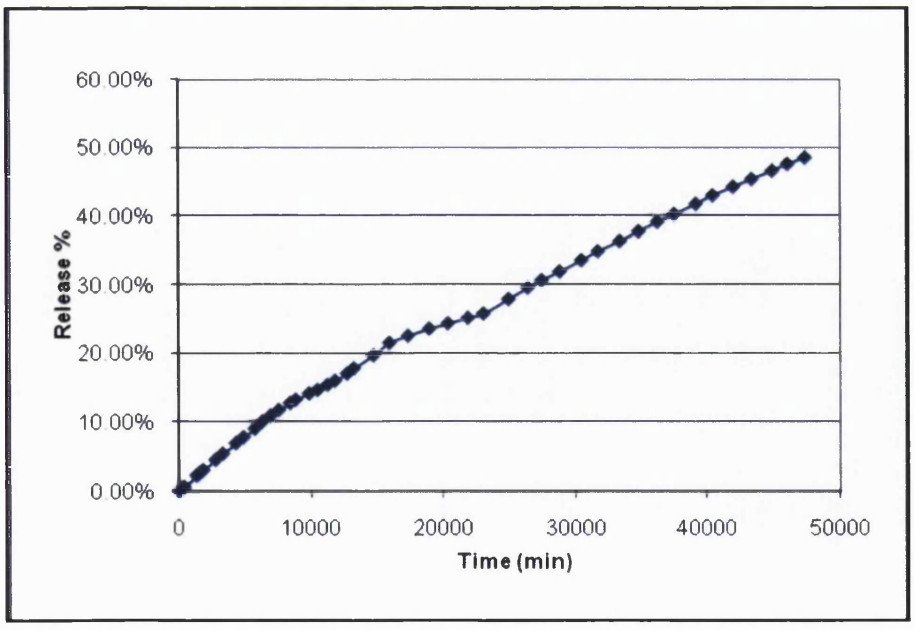

Figure 40: Percent release of ilomastat by the Ilomastat tablet B (Weight: 4.1 mg, pressure 5 bar). After 30 days of presence of tablet B in the 37°C aqueous environment of the rig, about 50 % of the tablet was released. The aqueous outflow was set at 2 µl/min (less than in the case of tablet A). The capacity of the flow rig that was used for the testing of the release profile of the tablet B was 200 µl, significantly larger than the 50 µl rig used in the case of tablet A.

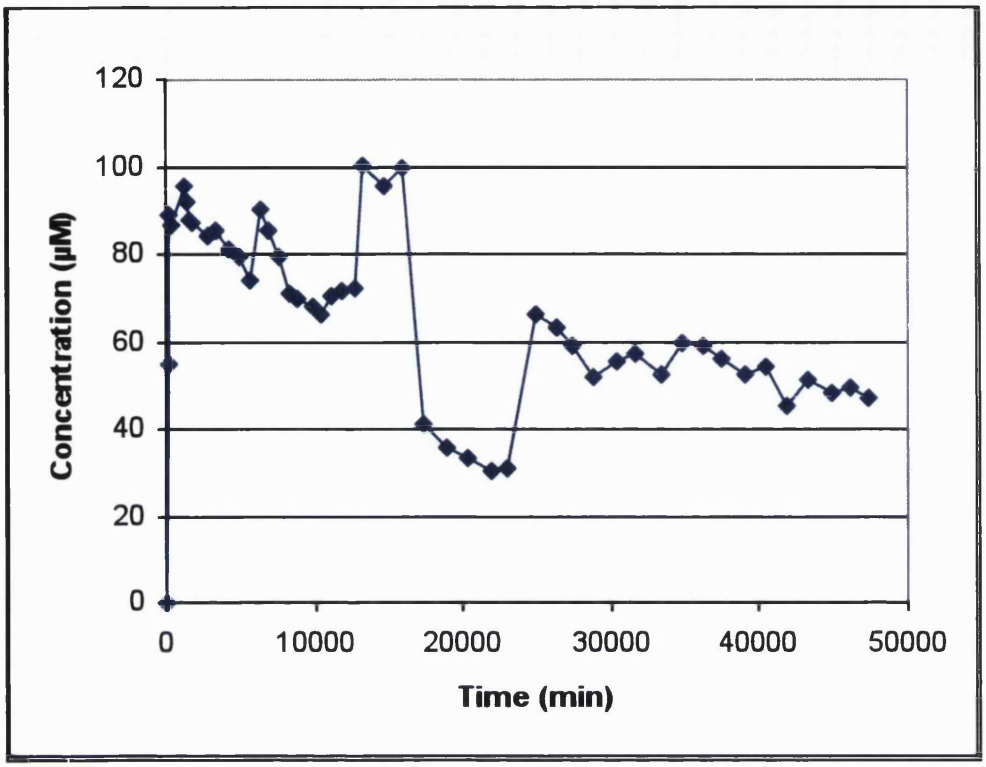

Figure 41: Concentration of ilomastat in the samples collected from the rig with tablet B. From the time point ~ 17000 min to the time point ~ 23000 min a bubble that occupied part of the rig decreased the quantity of the aqueous solution in the rig and its contact time with the tablet, which resulted in the decrease of the concentration shown in the graph. Throughout the experiment the ilomastat concentration released from tablet B was higher than 20 μM, indicative of the slow release of ilomastat from tablet B for a period of at least 30 days.

These preliminary results indicate that a small ilomastat tablet can slowly dissolve over a 30 day period to release ilomastat in what is considered a therapeutic concentration. The therapeutic concentration of ilomastat for scarring inhibition has not been defined *in vivo*, but is considered to be the concentration of ilomastat that is effective *in vitro* against HTF populated collagen I gels (<10 μM) (Daniels *et al.* 2003). The results indicate that the aim of formulating a slow release ilomastat mechanism has been met. Additionally, it is obvious that only part of the tablet had dissolved for 30 days. Subsequently, the next aim was to formulate a tablet of appropriate size that releases ilomastat in therapeutic concentration for 30 days, with only a small part of the tablet remaining at the rig after 30 days. After testing many tablets we found that 3 mg of ilomastat, which after compression give excipientless ilomastat tablets of about 2.1-2.3 mg, are enough for a therapeutic

ilomastat release (Figure 43) for about thirty days and less than 1/3 of the tablet remains in the rig after 30 days (Figure 42). It was expected that the 2.1 – 2.3 mg tablet size would be good for *in vivo* testing in order to achieve a therapeutic concentration of ilomastat for about 30 days without a large proportion of the tablet remaining in the bleb area at the end of the 30 day period. We believed that the release of several enzymes in the bleb area, the movement of the rabbit eye and several other factors could speed up the dissolution of the tablet in the bleb area (faster than in the rig).

We applied three different pressures, two, five and ten bars to the ilomastat powder in order to fabricate tablets. Some of the compound was lost during the tablet fabrication, as it remained inside the cylinder. The release profile of the 2.3mg tablet is graphically shown below in (Figure 42) and (Figure 43).

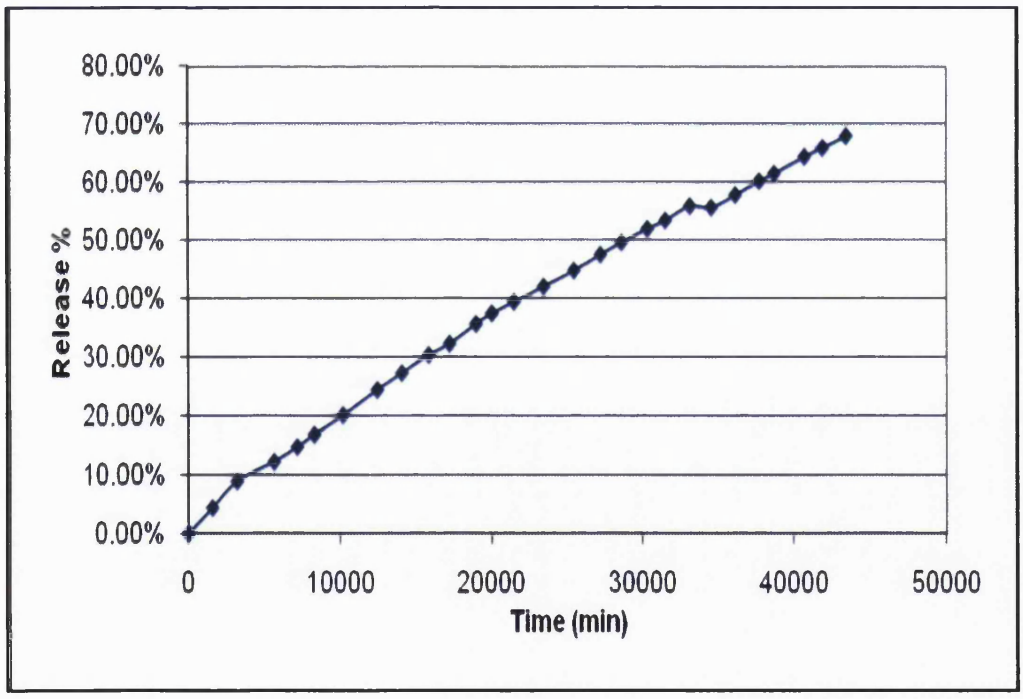

Figure 42: Percent release of ilomastat from the 2.3 mg ilomastat tablet (pressure used during fabrication: 5 bar). After 30 days of presence of a 2.3 mg tablet in the 37°C aqueous environment of the 2rig, about 70 % of the tablet was released. The aqueous outflow was set at 2 µl/min.

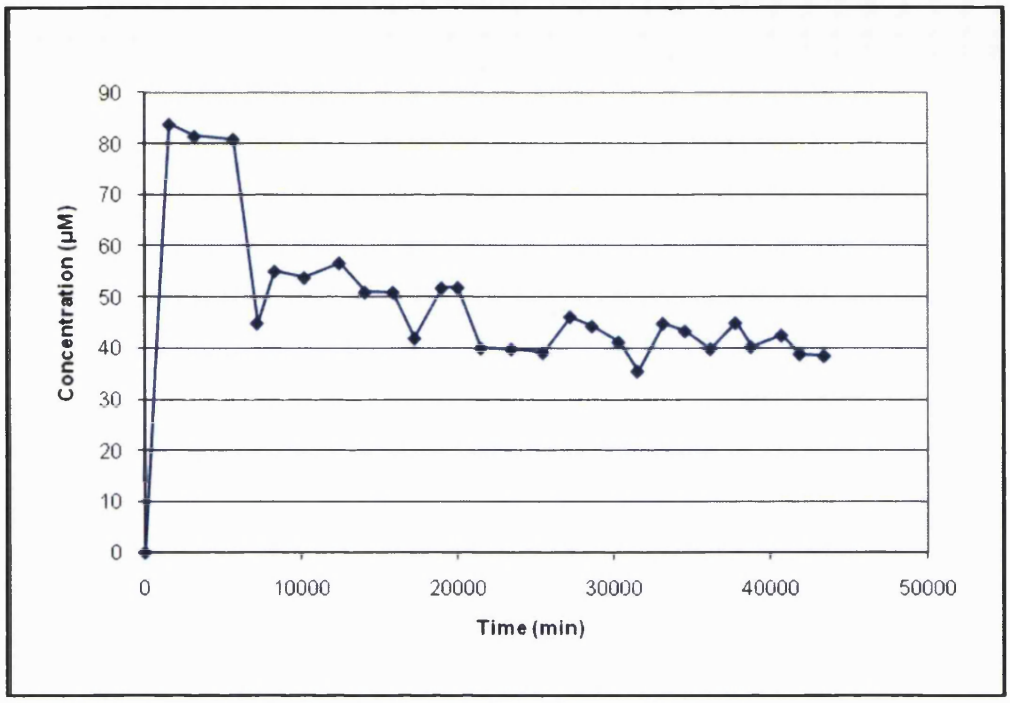

Figure 43: Concentration of ilomastat in the samples collected from the 2.3 mg ilomastat tablet. Throughout the experiment the ilomastat concentration released from tablet B was higher than 30 µM, indicative of the slow release of ilomastat from a 2.3 mg tablet for a period of at least 30 days.

It is worth mentioning to mention that the rig is at best just a crude model of aqueous flow in the eye and that what we were looking at are gross, overall trends of the release of ilomastat from excipientless tablets placed in an aqueous 37°C environment for 30 days. With the use of this model we reached some important conclusions in pharmacokinetics, which facilitated the further testing of the effectiveness of the ilomastat slow release excipientless tablets against scarring.

3.2.1.5. Role of pressure in the formulation of the ilomastat tablet

The effect of the compression pressure used to fabricate the ilomastat tablet was evaluated to determine if there were any correlations with the release profile of ilomastat. Three tablets of the same weight (2.3 mg) were constructed under 3 different pressures (2, 5 and 10 bars).

TIME (min)	Concentration (μM) tablet D 2 bar	Concentration (μM) tablet E 5 bar	Concentration (μM) tablet F 10 bar
0	0	0	0
1500	63.27	72.21	59.35
3130	65.99	67.75	59.1
6540	70.12	65.27	52.66
9730	65.06	60.78	40.69
11645	55.01	59.01	42.71
15350	49.57	55.22	35.41
19830	57.37	55.12	33.11
22760	60.11	59.88	37.21
26130	61.27	52.11	30.04
29740	55.46	47.34	34.5
33615	52.37	50.23	26.78
37120	47.95	44.22	30.54
39200	50.22	40.05	26.91
42100	44.71	39.01	24.12
43560	44.81	37.19	27.79

Table 13: Released ilomastat concentration by the 2 bar, 5 bar and 10 bar tablet.

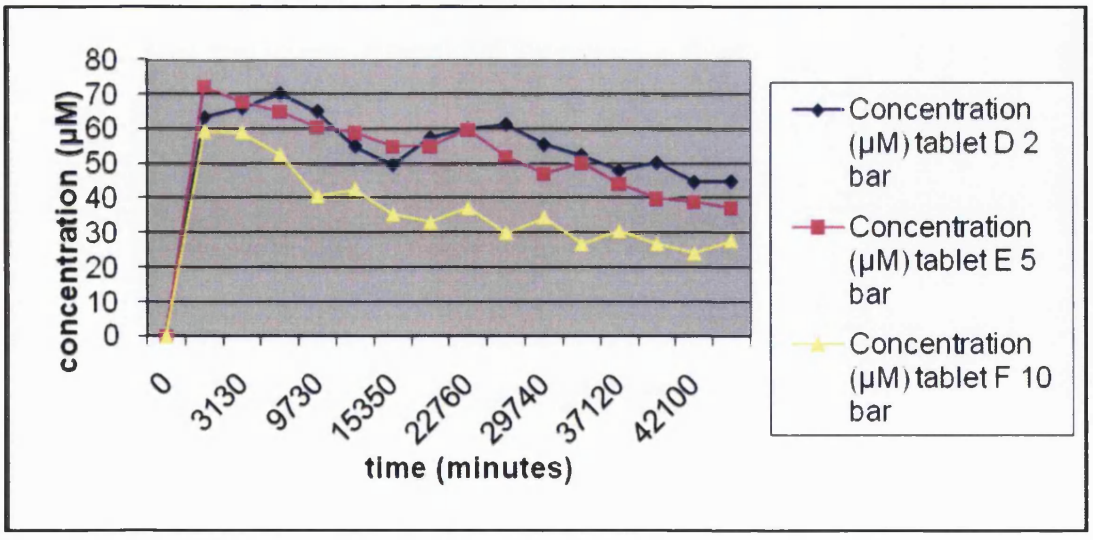

Figure 44: Released ilomastat concentration in the 2 bar, 5 bar and 10 bar tablet. The tablet fabricated under 10 bar pressure releases ilomastat in lower concentration that the tablets fabricated under 2 bar and 5 bar pressure. The release profiles of the 2 bar and the 5 bar tablet are similar.

TIME (min)	Release % Tablet D 2 bar	Release % Tablet E 5 bar	Release % Tablet F 10 bar
0	0.00%	0.00%	0.00%
1500	4.16%	3.34%	2.82%
3130	8.41%	7.08%	5.36%
6540	13.80%	13.73%	10.97%
9730	18.66%	18.93%	14.78%
11645	22.91%	22.90%	16.89%
15350	27.69%	27.27%	20.62%
19830	33.50%	33.65%	24.50%
22760	38.69%	39.83%	26.91%
26130	43.27%	43.08%	29.65%
29740	47.68%	48.70%	35.29%
33615	53.22%	53.23%	39.07%
37120	60.57%	57.24%	42.12%
39200	66.21%	61.19%	46.31%
42100	72.41%	66.02%	49.15%
43560	76.61%	70.33%	51.05%

Table 14: % Release of the 2 bar, 5 bar and 10 bar ilomastat tablet.

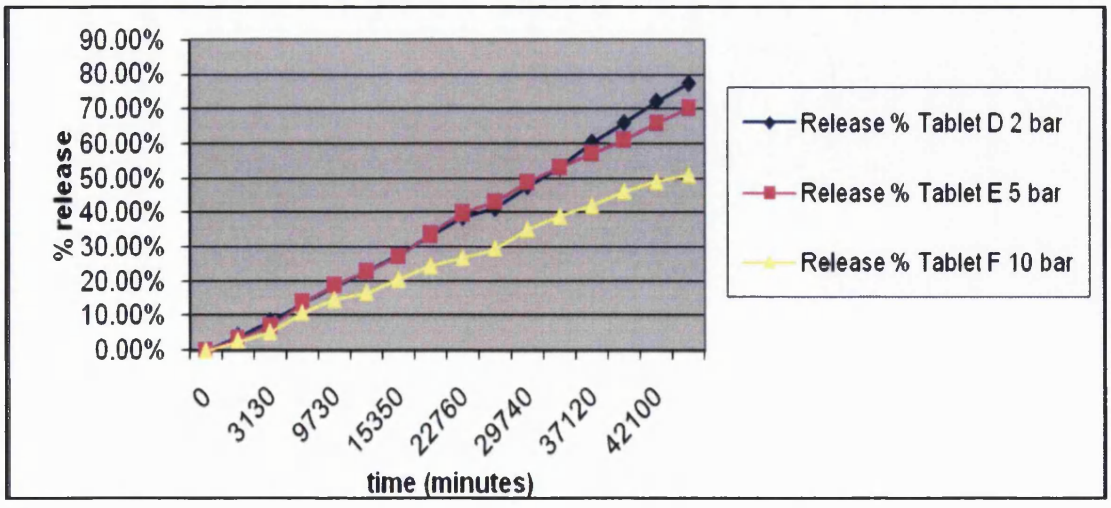

Figure 45: Concentration of ilomastat over a 30-day period from the flow rig. After 30 days, the total release was about 77 % in the 2 bar tablet, 70 % in the 5 bar tablet and 51 % in the 10 bar tablet.

These results suggest that the 10 bar tablet releases less ilomastat over a 30 day period than the 2 bar and the 5 bar tablet. The 2 bar and the 5 bar tablets presented similar release profiles. As the ilomastat tablet constructed under 5 bar pressure is structurally more stable without being significantly inferior in releasing of ilomastat, the decision for further testing of the 5 bar tablet was taken.

3.2.1.6. Reproducibility of results

In the next step, three 2.3 mg ilomastat tablets were fabricated using 5 bar pressure and the release profile of these tablets were compared in order to test if ilomastat tablets created under the same conditions have similar release profiles.

Time Point	Ilomastat tablet G 2.3mg 5 bar	Ilomastat tablet H 2.3mg 5 bar	Ilomastat tablet I 2.3mg 5 bar	Mean	Standard Deviation
0	0	0	0		
1450	80.28	73.02	72.21	75	4.44
2990	75.66	70.68	73.27	73.15	2.49
4320	72.45	67.12	70.77	70.04	2.73
6010	62.33	65.27	62.86	63.46	1.57
7625	56.18	59.47	61.26	58.9	2.58
9315	50.11	56.72	55.33	53.90	3.49
14800	58.2	50.53	54.08	54.09	3.84
16200	59.81	57.73	54.25	57.17	2.81
17630	56.49	51.89	50.06	52.68	3.31
18920	49.61	52.99	53.24	51.9	2.03
20465	50.96	46.21	48.34	48.43	2.38
22045	48.46	48.43	44.18	46.93	2.46
25270	40.54	47.32	42.99	43.44	3.43
28810	44.22	40.69	38.39	40.96	2.94
33590	39.01	40.26	40.89	40.04	0.97
36330	42.39	37.31	43.13	40.77	3.17
39555	40.66	40.98	39.28	40.29	0.90
43790	40.97	36.72	41.85	39.71	2.74

Table 15: Determination of the reproducibility of the *in vitro* release profiles of ilomastat tablets (2.3 mg, 5 bar). The mean and the standard deviation are shown.

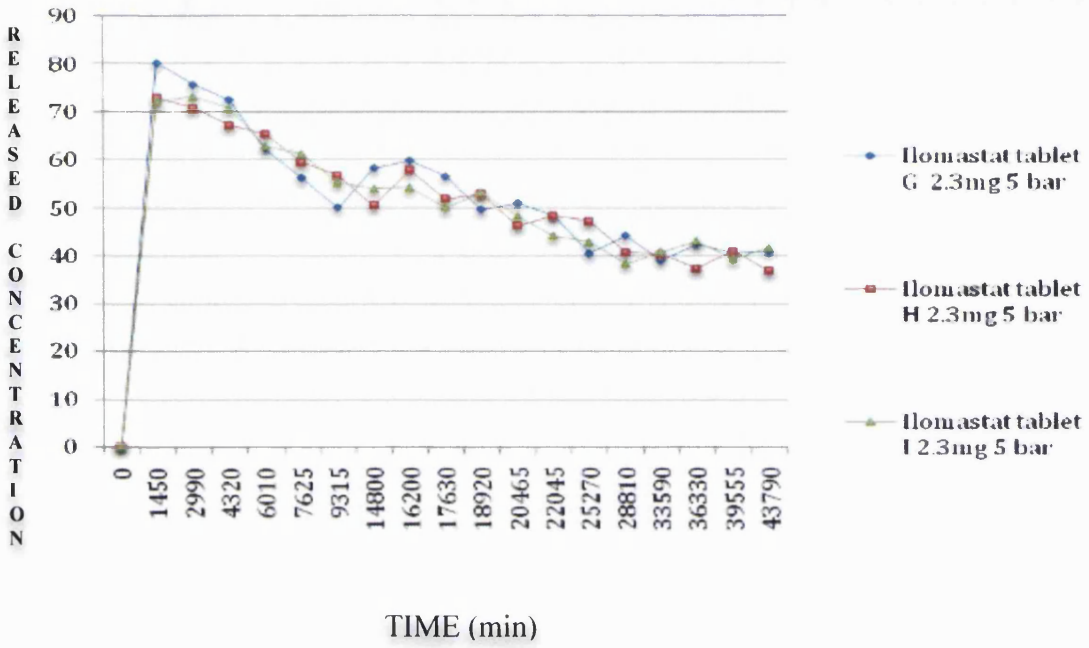

Figure 46: Release profiles of 2.3 mg 5 bar ilomastat tablets. No significant differences were shown, indicative that all three 2.3 mg tablets fabricated using 5 bar pressure produce similar release profiles of ilomastat in a 37oC aqueous environment using a 200 µl rig and 2 µl/min flow rate.

These data indicate that no significant differences in the *in vitro* release profiles were observed for these ilomastat tablets, which were fabricated at the same weight and pressure.

3.2.1.7. Comparison of irradiated and non irradiated ilomastat with HPLC

Implantation of the ilomastat tablet during glaucoma filtration surgery will require that the tablet is sterile. 25 kGys of gamma radiation were applied to ilomastat tablets in order to sterilise them as it is suggested by the European and the US pharmacopoeias. No data had previously been published that we are aware of to indicate the stability of ilomastat in the solid form when irradiated with gamma radiation. The International Conference on Harmonization (ICH) recommends the use of HPLC, mass spectrometry, or gas chromatography to characterize and compare different analytical aspects of an irradiated product versus non-irradiated product. Following these guidelines, we dissolved irradiated ilomastat in pH 7.6 aqueous solution and evaluated it by HPLC. The

chromatogram for the irradiated ilomastat is shown in Figure 47 and the overlay of the non-irradiated and irradiated ilomastat are shown in Figure 48. From the chromatogram of the irradiated ilomastat it can be seen that a new peak has been detected at approximately 8.5 minutes. This peak represents one or more ilomastat products after irradiation and accounts for about 0.25 % of the total ilomastat concentration. This finding meets the criteria of American and European Pharmacopoeia for less than 1% of degradation after irradiation.

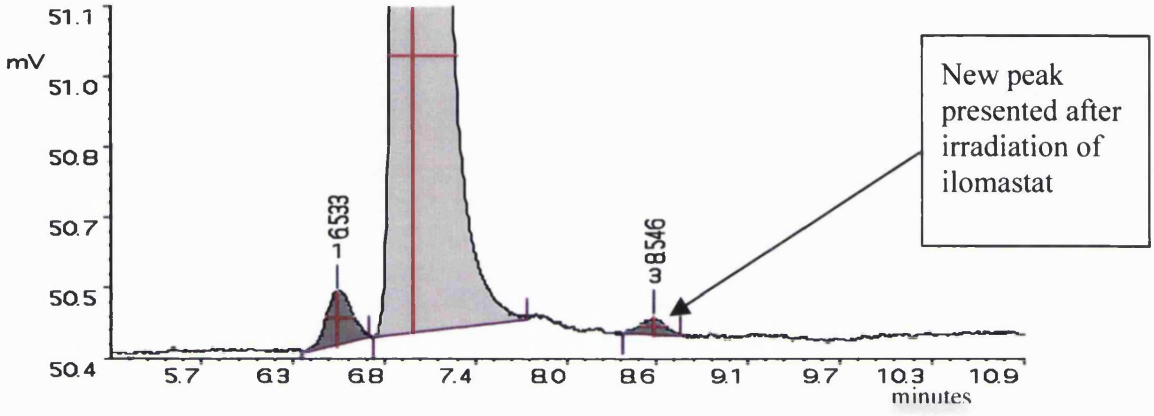

Figure 47: HPLC peak pattern of irradiated ilomastat. The new peak presented after gamma radiation at about 8.5 -9 min elution time accounts for <0.25 % degradation.

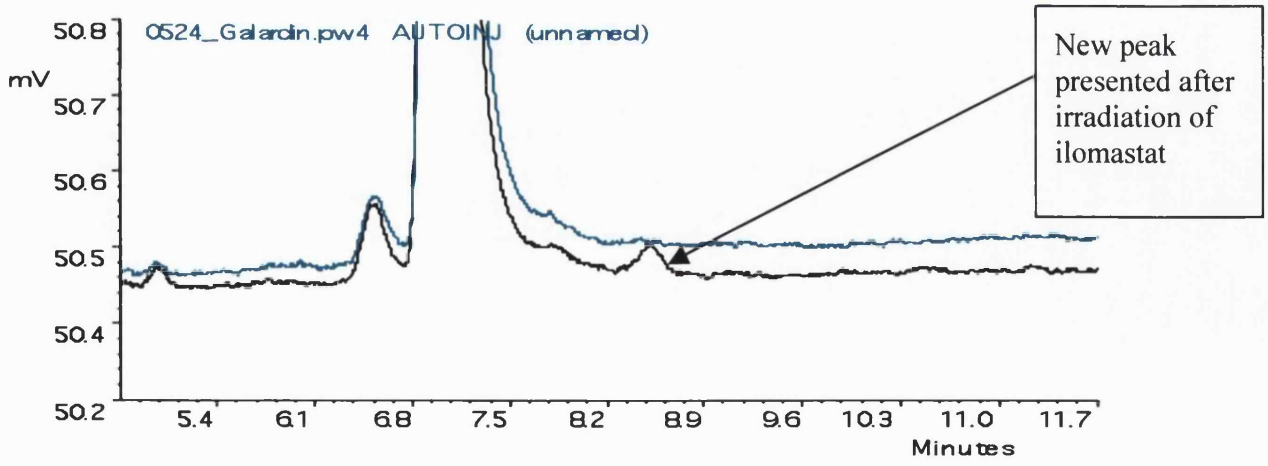

Figure 48: Overlay of chromatograms of irradiated (black) and non-irradiated (green) ilomastat. The changes in the structure of the irradiated ilomastat are insignificant and meet the criteria of the EUP and the USP.

3.2.1.8. Stability of ilomastat tablets

Ilomastat in DMSO or in water at a concentration of 0.1mM decomposes 1% per month at 4°C. At 37°C, this increases to 1% per day (Caldiochem). No data have been published that we are aware of that indicates the stability of ilomastat in the solid form when left in 37°C in a moist environment for several days. A key concern was to ensure that the ilomastat released at each time point was the same throughout the release period. We evaluated the ilomastat tablet for possible decomposition while in an aqueous environment in 37°C for 30 days. After collecting samples from a 2.3 mg 5 bar tablet, we removed the remaining solid from the rig and dissolved it in aqueous solution (pH 7.6). The overlay of the chromatograms of the aqueous solution with the remaining ilomastat compound on day 30 and of the aqueous solution collected from the rig at the first time point are shown in Figure 49. As shown in this figure, both chromatograms were very similar suggesting that no decomposition had occurred during the 30-day period.

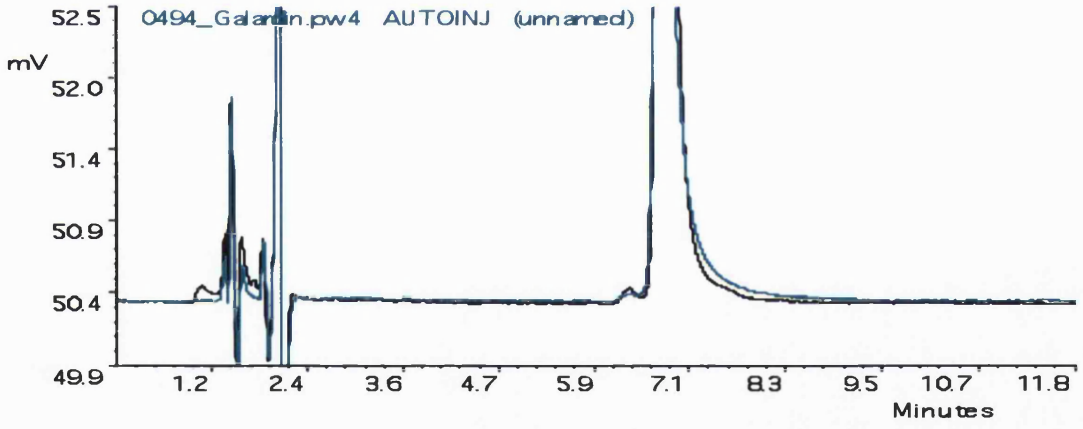

Figure 49: Overlay of chromatograms indicative of the stability of ilomastat at t=0 and t=30 days. The green line represents the chromatogram of the sample released from the tablet on t=0 and the black line the chromatogram of the sample release from the tablet on t=30. Released ilomastat was structurally the same throughout the experiment.

3.2.2. *In vitro* biological evaluation

3.2.2.1. Dissolving of ilomastat in normal media

As we previously mentioned, we attempted the dissolution of ilomastat in normal media without DMSO. The chromatogram below indicates that ilomastat can be dissolved directly in media. The maximum concentration that can be achieved is 297 μM, which is about three times higher than the reported concentration in aqueous solution. The green line represents the media with ilomastat and the black line the media without ilomastat (Figure 50). The molecule that eluted at approximately 4 min after the injection possibly represents L-glutamine, which is in high concentration in the media.

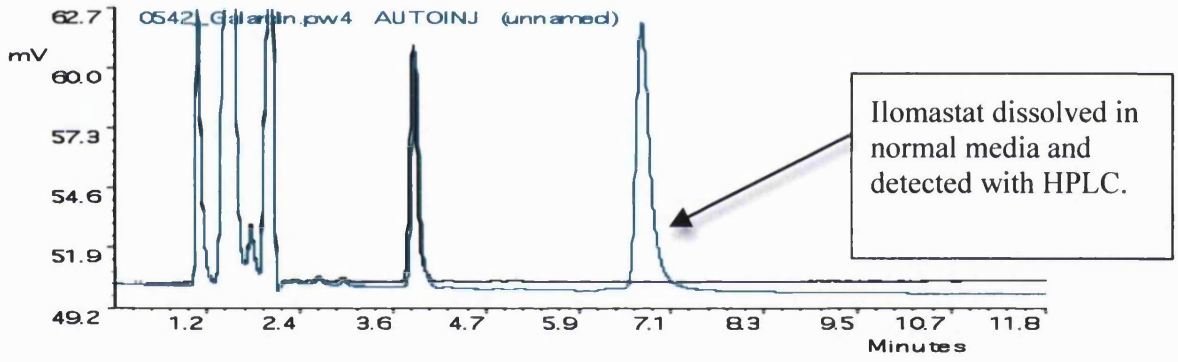

Figure 50: Overlay of chromatograms of media without ilomastat (black) and media with ilomastat (green). This figure indicates that ilomastat can be dissolved in cell culture media without the use of DMSO.

3.2.2.2. Inhibition of HTF populated collagen I GEL contraction (*in vitro* contraction model) by irradiated ilomastat.

Ilomastat released from the tablets at each time point is active and inhibited the contraction of HTF collagen I gels ($p<0.01$) vs control over a standard 7 day period. The inhibitory contraction effect of the ilomastat released from the irradiated tablet was similar to the positive control (non-irradiated ilomastat powder) (Figure 51 and 52).

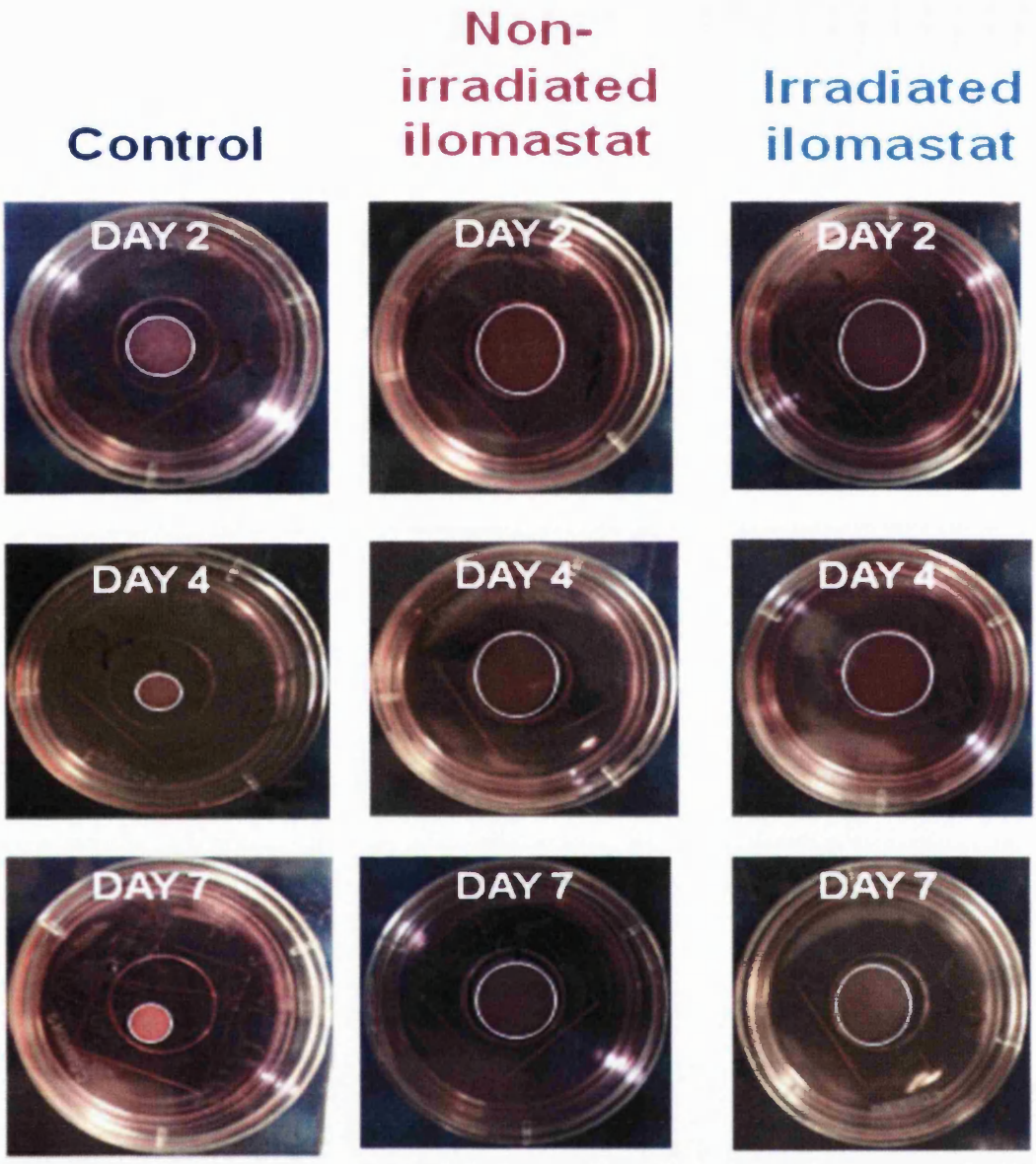

Figure 51: HTF populated collagen I gels treated with normal media without ilomastat (negative control), media in which non-irradiated ilomastat powder was dissolved without DMSO (positive control) and media in which irradiated ilomastat tablet was dissolved without DMSO. The concentration of ilomastat in the positive control and the media in which the ilomastat tablet was dissolved was tested with HPLC and was adjusted to be at the same level (65 μM).

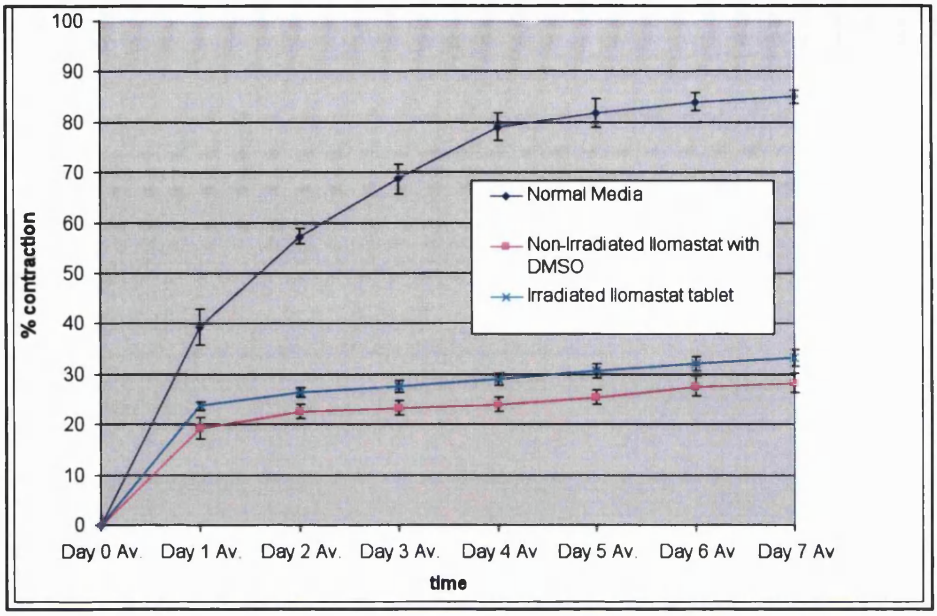

Figure 52: Percent contraction of HTF collagen I gels over a 7 days period. Normal media without any anti-scarring agent was used as negative control. Non – irradiated ilomastat dissolved in DMSO before adding it in the media was used as positive control. This experiment, which was repeated three times showed that irradiated ilomastat released from the tablets significantly inhibited the contraction of HTF collagen I gels compared to the negative control. No significant differences were detected with the anti-contraction effect of the non – irradiated ilomastat.

3.2.3. *In vivo* results

3.2.3.1. Preliminary *in vivo* experiment to evaluate the anti-scarring effect of the ilomastat tissue tablet

A preliminary *in vivo* experiment was designed with four rabbits. This study comprised one bleb treated with an ethylcellulose tablet (negative control tablet that does not get dissolved) and three blebs treated with a 2.3 mg 5 bar ilomastat tablet. The aim of the study was to test the effect of the ilomastat tablet on the bleb survival compared to the effect of a tablet with the same dimensions made with an inactive undissolved compound. It was observed that the bleb of the rabbit treated with an ethylcellulose tablet after GFS failed on day 10. The blebs treated with the ilomastat tablet post glaucoma filtration surgery appeared to be fully functional after 30 days.

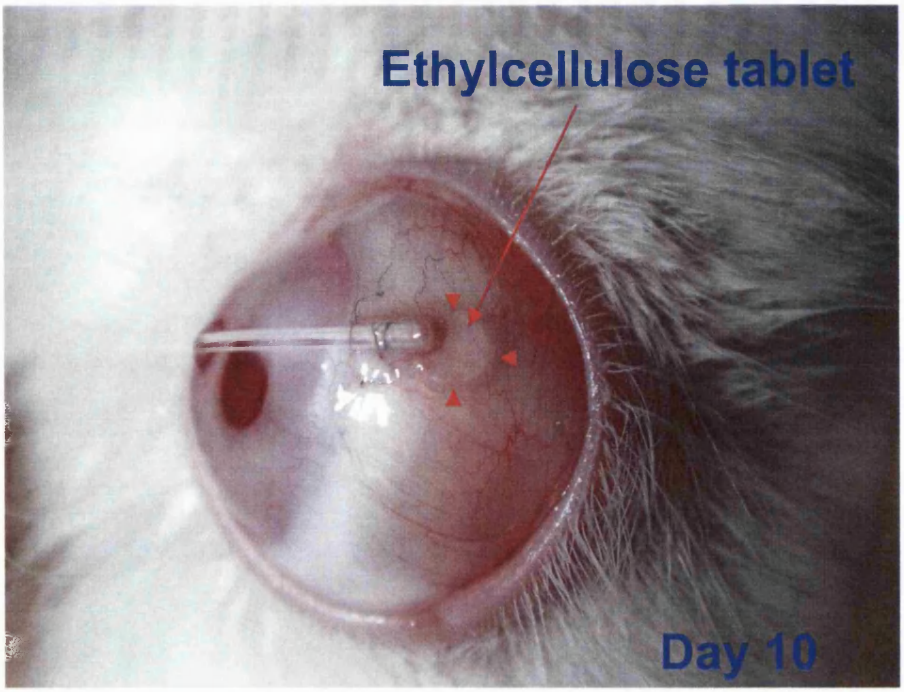

Figure 53: Appearance of bleb on day 30 in which an ethylcellulose tablet after glaucoma filtration surgery. The bleb failed on day 10. In this image it is shown that the conjunctiva surrounded the tablet and the tip of the tube, not possibly allowing aqueous outflow from the tube.

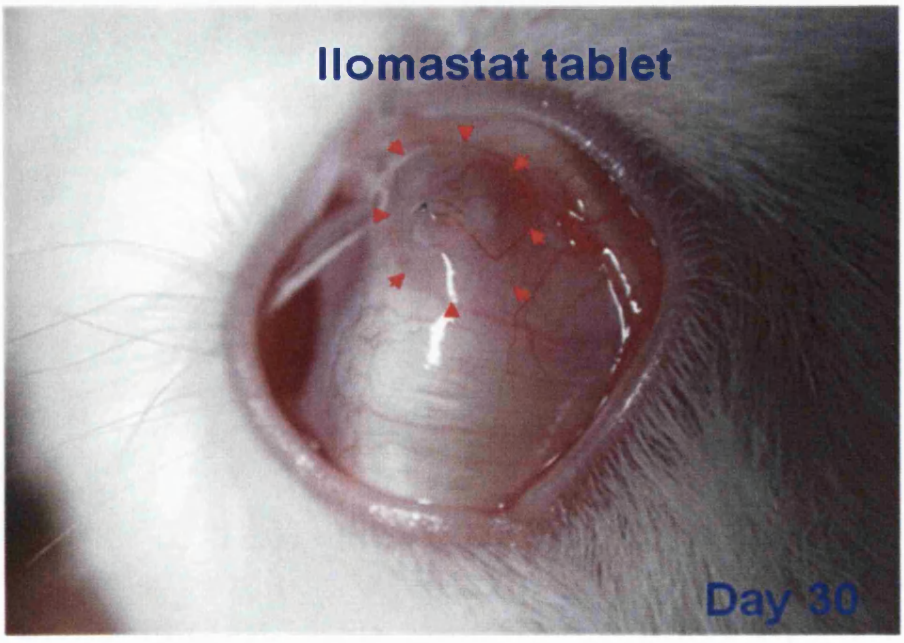

Figure 54: Appearance of bleb on day 30 after glaucoma filtration surgery in which an ilomastat tablet was placed. The bleb remained elevated and functional throughout the experiment and it indicated that the ilomastat tablet may be effective *in vivo* in the inhibition of scarring.

3.2.3.2. Second *in vivo* study of the evaluation of the anti-scarring effect of the ilomastat tissue tablet

3.2.3.2.1. Bleb survival

Since the effect of the ilomastat tablet was evaluated as successful in the preliminary study, a second study was designed in which 24 rabbits were used. Eight rabbits were treated with water sponges for 3 minutes during the glaucoma filtration surgery just before the closure of the conjunctiva (negative control), 8 rabbits were treated with a MMC 0.2 mg/ml sponge for 3 minutes during the glaucoma filtration surgery just before the closure of the conjunctiva (positive control), and finally 8 rabbits were treated with the ilomastat tablet which was placed in the subconjunctival space during the glaucoma filtration surgery just before the closure of the conjunctiva. The tablet was left in the subconjunctival space after the conjunctiva closure; it was not removed as was the case with the water and the MMC sponges. Blebs treated with the tablet (Figure 57) were larger than the blebs treated with MMC 0.2 mg/ml sponges for 3 minutes (Figure 56). A representative failed bleb is shown in Figure 55Figure 55. All of the blebs in the ilomastat tablet group were functional throughout the 30-day period of the experiment. Bleb success and failure was determined macroscopically, by differences in IOP and by histology.

Figure 55: Representative failed bleb from the water sponge negative control group. The bleb is shown to be flat and to block the tip of the tube due to the development of scarring, inhibiting possibly the aqueous outflow through the tube.

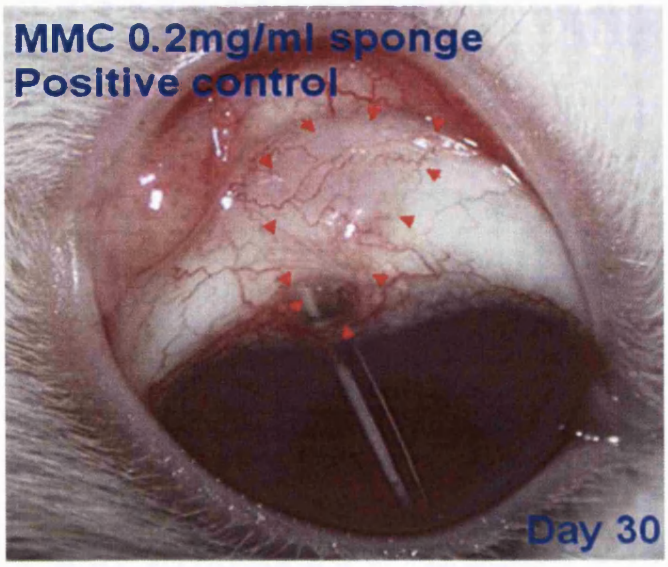

Figure 56: Representative functional bleb from the positive control group (MMC 0.2 mg/ml) sponge for 3 minutes). Two out of eight blebs treated with MMC remained functional throughout the experiment.

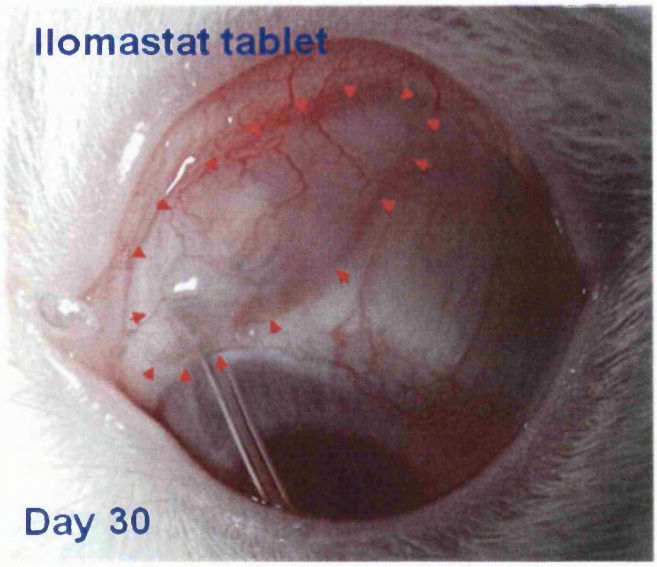

Figure 57: Representative functional bleb from the ilomastat tablet group. The bleb area of all rabbits treated with the ilomastat tablet remained functional and significantly elevated throughout the experiment. This outcome was significantly superior not only compared to the negative control (water sponge) but also compared to the positive control (MMC).

The tested 2.3 mg ilomastat tablet was found significantly more effective in inhibiting failure of the bleb than the currently used MMC anti-scarring treatment.

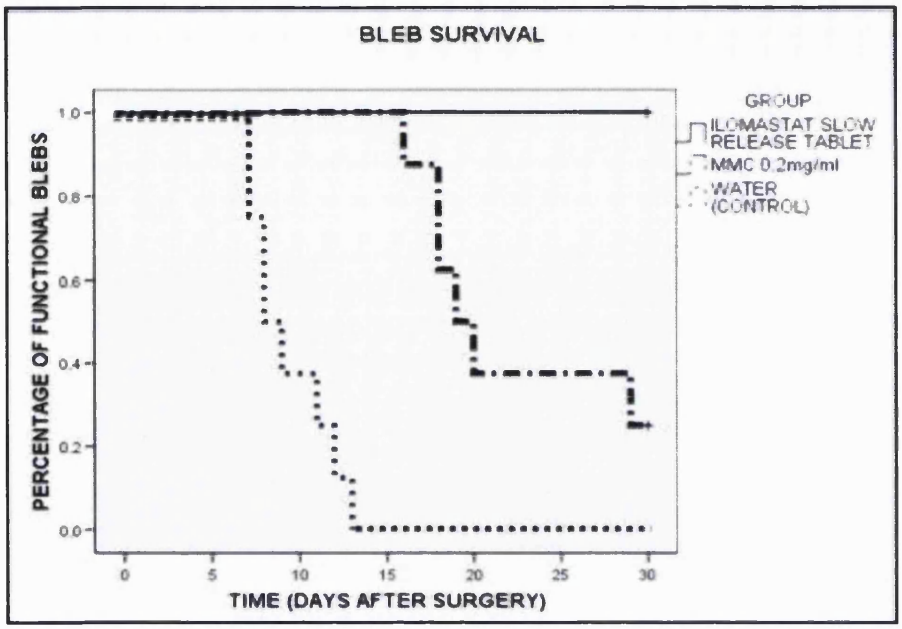

Figure 58: Bleb survival in the ilomastat tablet group was found significantly superior to the sterile water (negative control) ($P<0.001$) and the MMC (positive control – current clinical anti-scarring treatment applied during glaucoma filtration surgery) ($P<0.01$ Log Rank) groups.

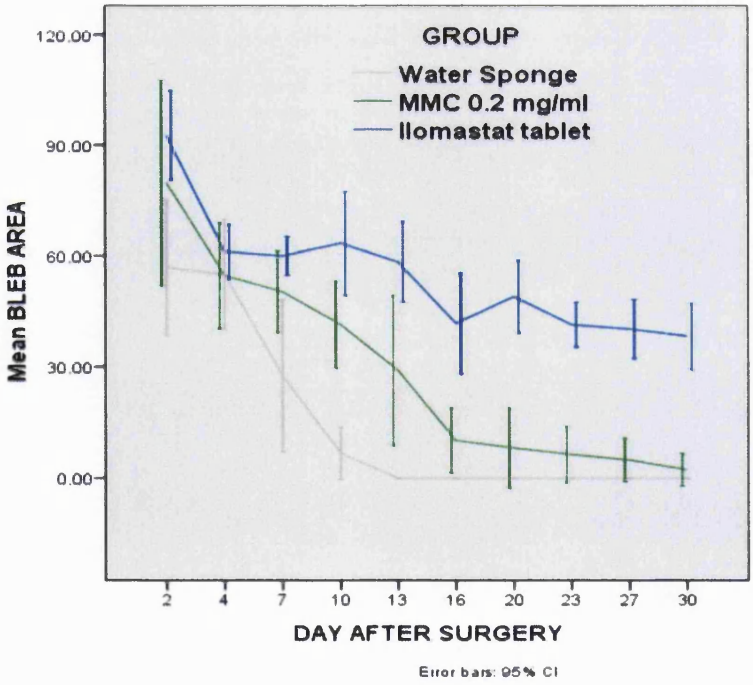

Figure 59: Comparison of the surface area of the blebs between the negative control, the positive control and the ilomastat tablet groups. The surface area of the bleb was calculated by multiplying the length and the width of the bleb. The bleb surface area of the ilomastat tablet group was significantly higher than the bleb surface area of the negative as well as the positive control.

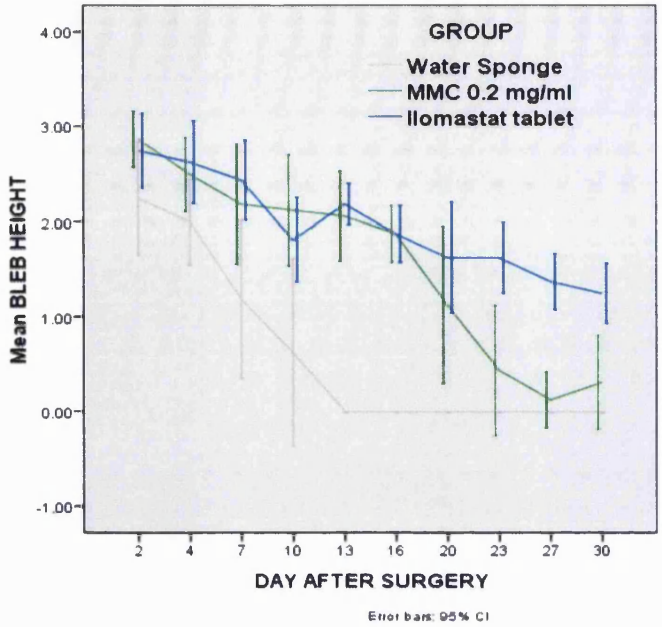

Figure 60: Comparison of the height of the blebs between the negative control, the positive control and the ilomastat tablet groups. The bleb height of the ilomastat tablet group was significantly larger compared to the negative control throughout the experiment as well as after day 20 post glaucoma filtration surgery compared to the positive control (most of the positive control blebs had failed).

3.2.3.2.2. The effect of ilomastat tablet in the IOP

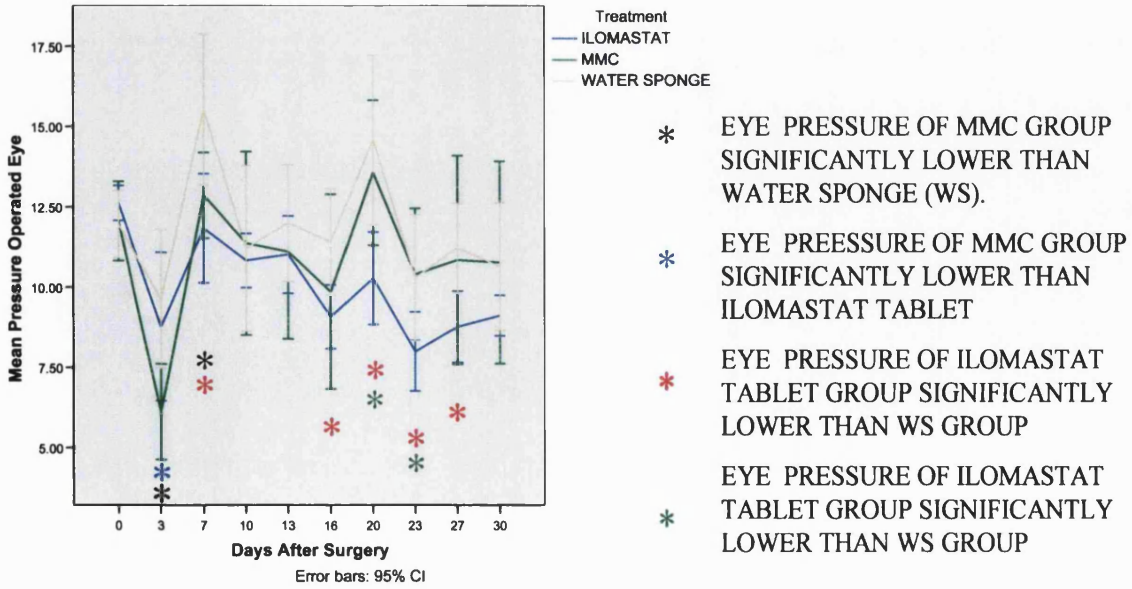

Figure 61: Ilomastat tablet significantly reduced IOP compared to positive and negative controls.

The rabbit eyes treated with ilomastat tablet maintained a normal IOP throughout the experiment. Additionally, the mean IOP of the ilomastat tablet group was found significantly lower than the negative control at the time points day 7, day 16, day 20, day 23 and day 27. Additionally, the ilomastat tablet treated group had significantly lower IOP than the positive control at the time points day 20 and day 23. No hypotony was observed in the ilomastat tablet group at any time points. Hypotony, though, was observed in the MMC treatment group at the time point day 3.

3.2.3.2.3. Detection of ilomastat in the aqueous humor, vitreous body and blood serum of the rabbits treated with the ilomastat tablet

Ilomastat was not detected with our HPLC method in the blood serum (Figure 62), vitreous body (Figure 63) or aqueous humor (Figure 64) of any of the rabbits treated with the ilomastat tissue tablet.

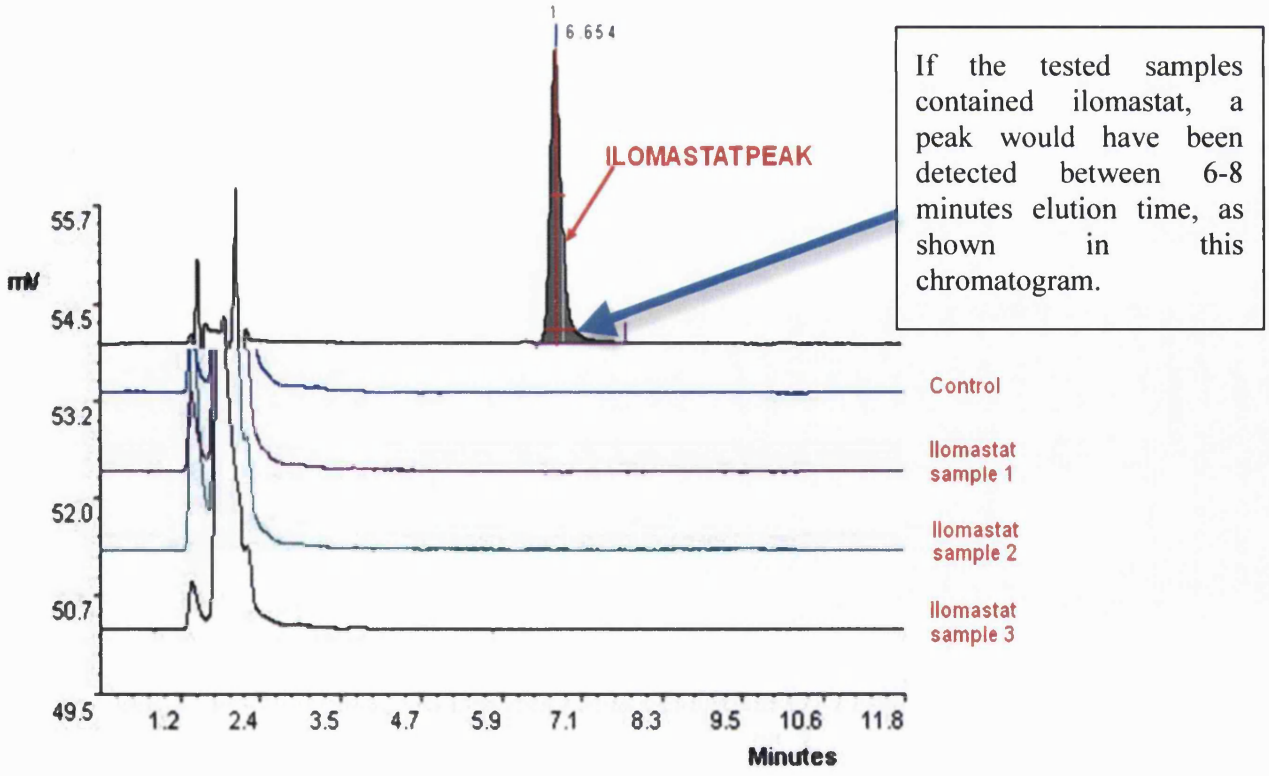

Figure 62: Ilomastat was not detected in the systemic blood circulation, indicating that the constant dose released locally in the bleb would potentially not pose a safety risk in humans.

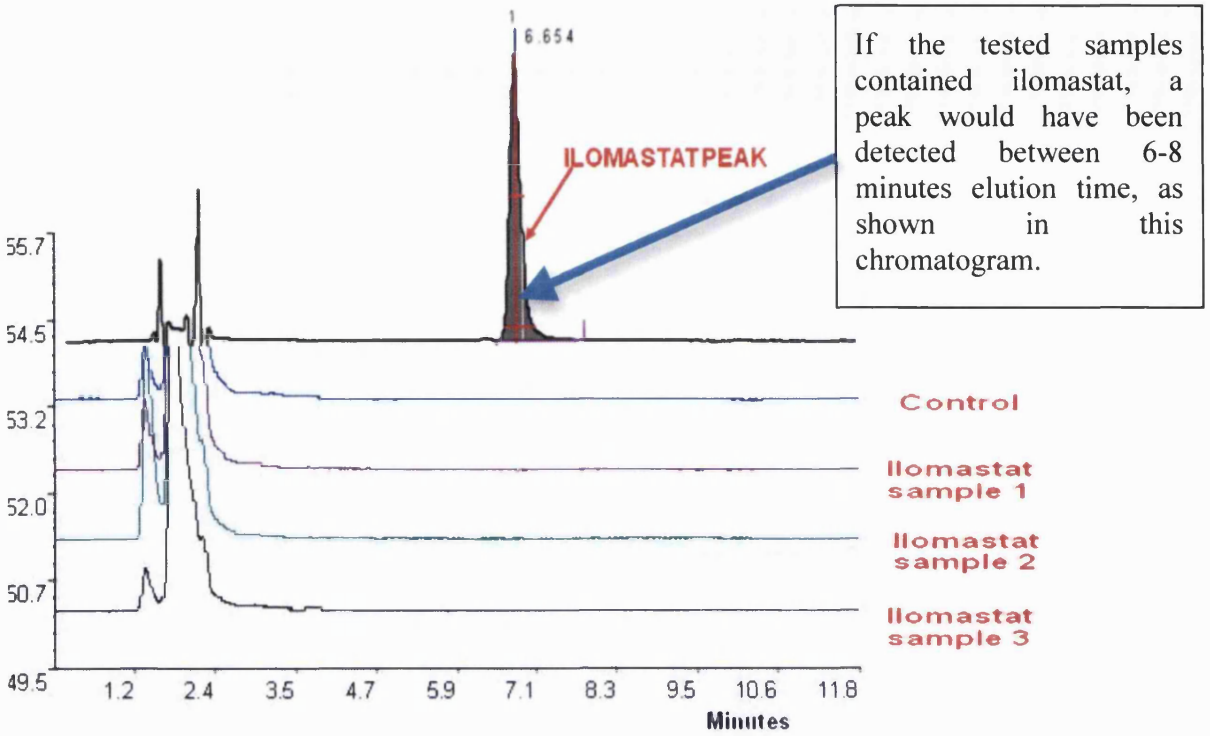

Figure 63: Ilomastat was not detected in the vitreous body, indicating that the low constant dose released locally would potentially not cause toxicity or changes in general in the retina and other parts of the human eye.

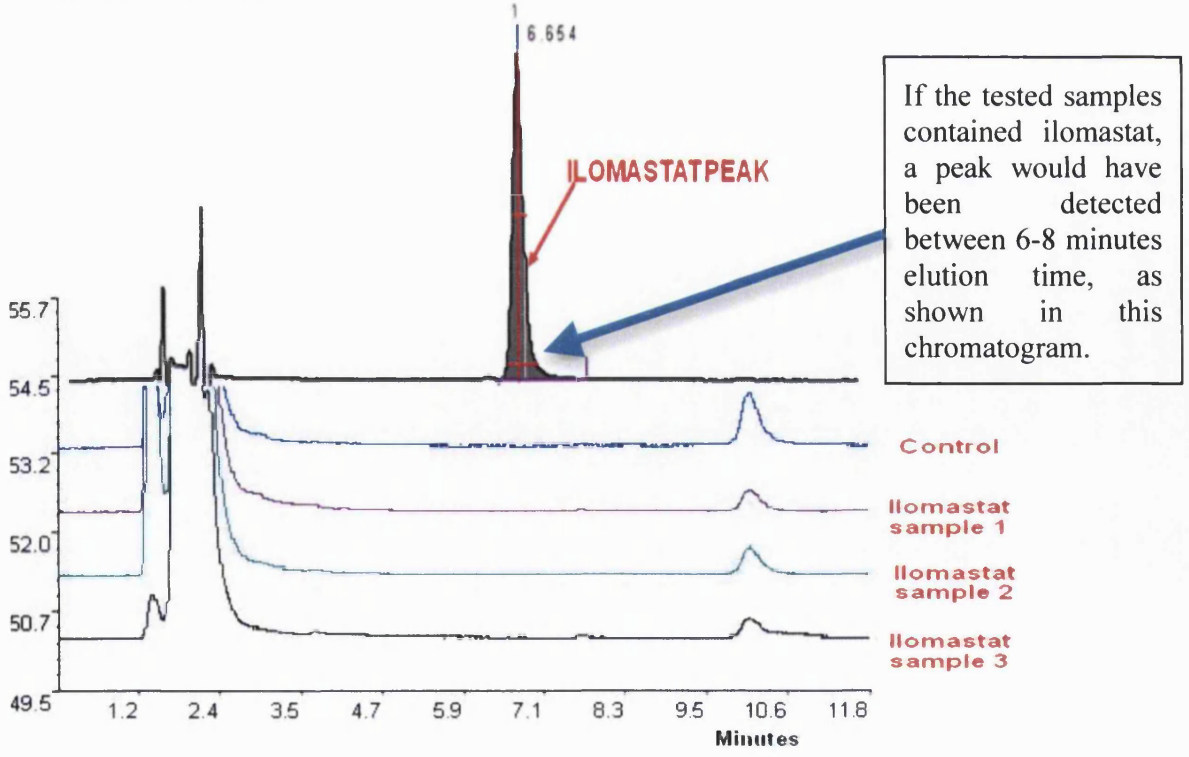

Figure 64: Ilomastat was not detected in the aqueous humor, indicating that the low constant dose released locally would potentially not cause toxicity or changes in general in the structure of the human eye in contact with the aqueous humor.

3.2.3.3. Histological evaluation of scarring deposition and cellularity

Sections of the operated rabbit eyes treated with MMC, water sponge or ilomastat tablet were stained with Eosin and Haematoxylin (H & E) and with Sirius Red. The cellularity in the bleb area was evaluated from the H&E sections and the scarring deposition was evaluated based on the Sirius Red sections. Five eyes from each group were analysed histologically. The tissue from the remaining three rabbit eyes per group was used for the development of tissue specific methods of in situ zymography and microarray analysis for future experiments.

3.2.3.3.1. Descriptive Histology

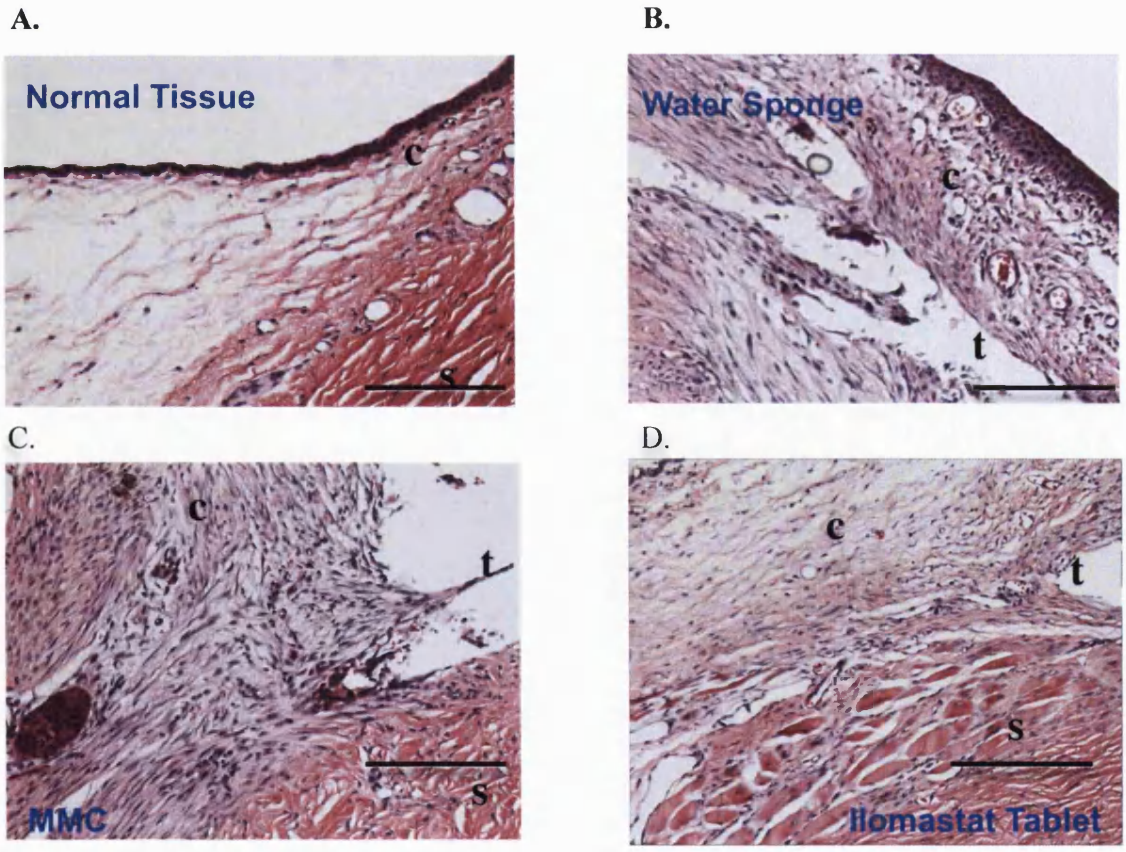

Figure 65: Picture A, B, C and D from sections stained with eosin and hematoxylin. Picture A: Normal tissue; A few round fibrocytes are shown in the subconjunctival space. Pictures B and C: Enhanced presence of elongated fibroblasts in the bleb area (bleb area indicated with the letter c). Picture D: In the bleb area of the ilomastat tablet treatment group, elongated and non-elongated fibroblasts were observed in lower numbers than in the positive and negative control treated rabbits. Scale 1 mm.

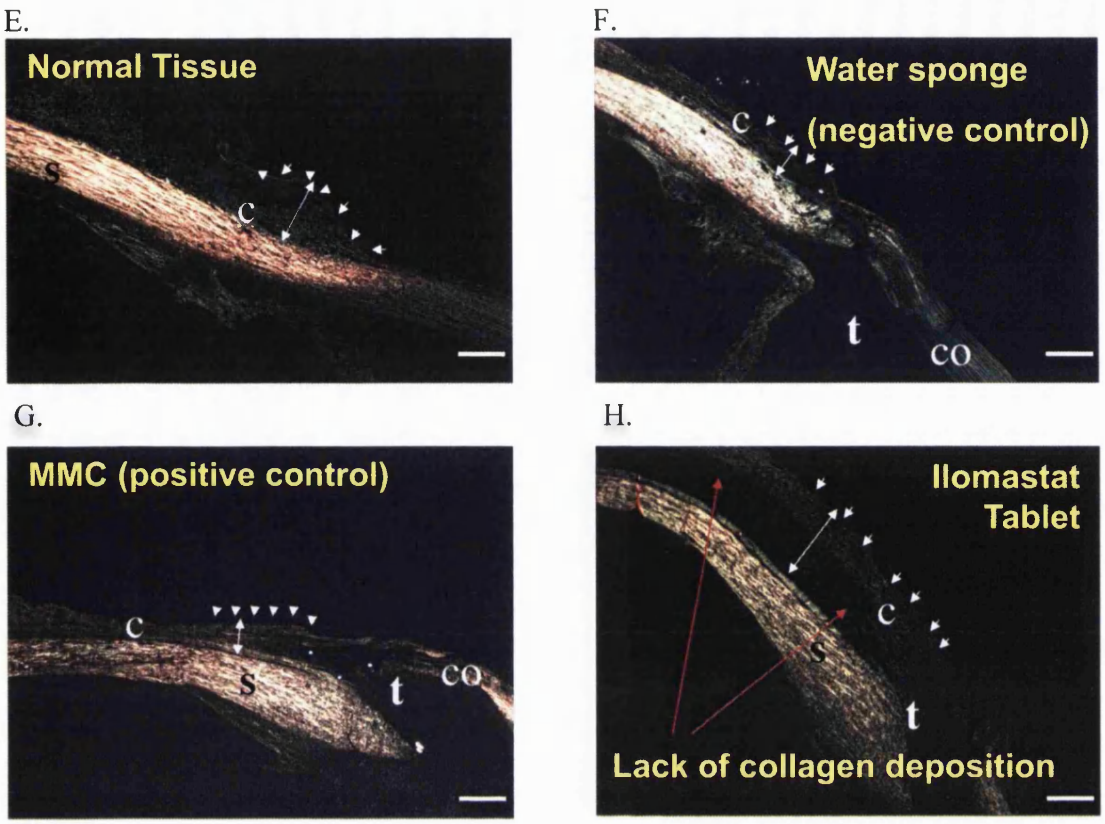

Figure 66: Photos E, F, G and H from sections stained with picrosirius red. Legend: c: conjunctiva, s: sclera, co: cornea, t: drainage tube. The upper margins of the conjunctiva are indicated with white small arrows. Photos F and G: Dense collagen deposition is deposited in the bleb area. Photo H: An extensive area of decreased deposition of collagen was observed in the subconjunctival space of the ilomastat tablet treated bleb. Scale 1 mm.

The histological analysis revealed some interesting findings. First of all, increased fibrosis was shown in the negative control treated blebs. Strands of collagen deposition were found in the bleb area. Areas of established and active fibrosis were detected and significant number of fibroblasts was located in the bleb area. Active fibrosis was detected closer to the tube and more established fibrosis was found in the area 2 – 4 mm posterior to the tip of the tube. Active fibrosis areas are characterised by the presence of large number of fibroblasts and established fibrosis areas are characterised by the presence of densely packed collagen fibres with fewer fibroblasts. In the Picrosirius Red staining images obtained from negative control sections, strong green/yellow signal is observed in the area 2 – 4 mm posterior the tube and slightly less strong signal is observed in the area just 1 mm posterior to the tube which is populated by increased number of fibroblasts. Normal scleral collagen is also stained clearly. No more inflammatory cells were observed in the negative

control treated blebs than in the normal unoperated tissue. It is worth mentioning that in almost all the sections of the operated and non operated rabbits a very limited number (1-5) of inflammatory cells was observed. No signs of active inflammation were observed in the bleb area.

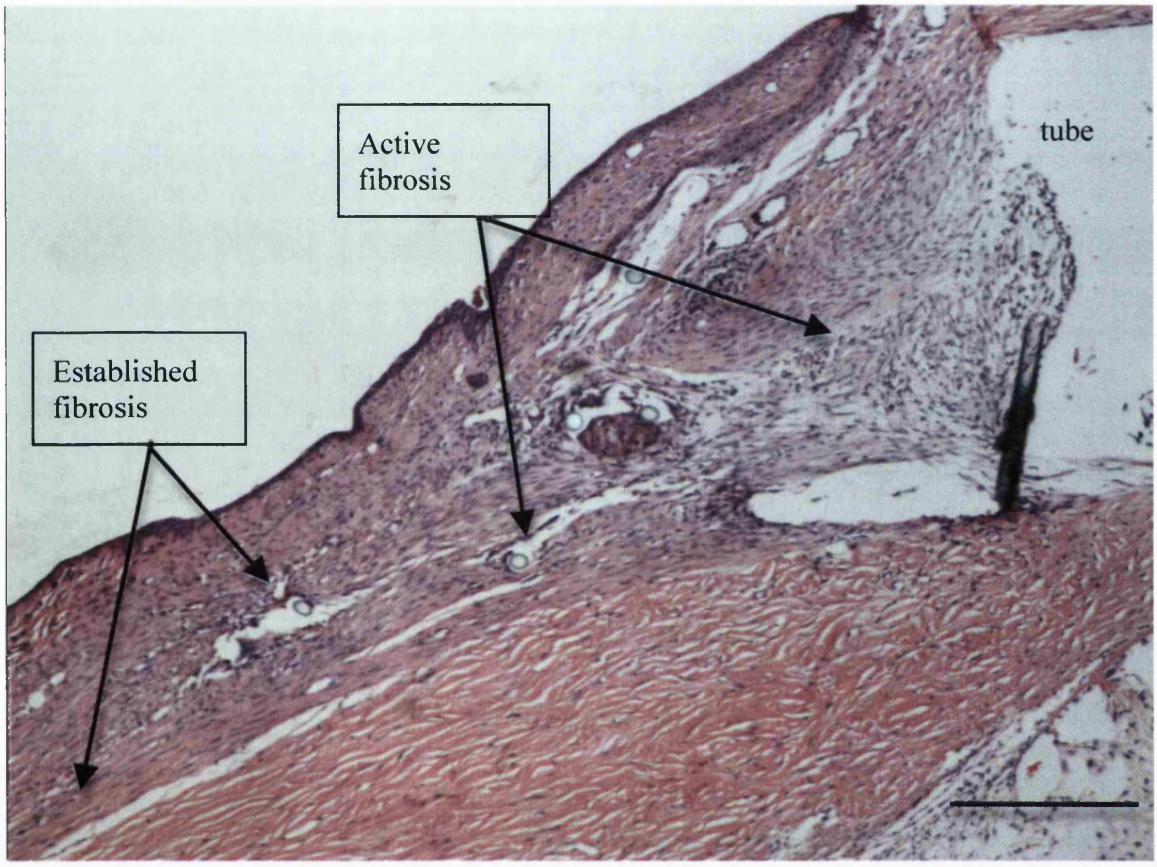

Figure 67: Negative control bleb. Dense collagen deposition and established fibrosis was observed in the area 2-4 mm posterior to the tube, which may inhibit the aqueous humor outflow and may result in the failure of the bleb. In the bleb area closer to the tube, extensive active fibrosis was observed. Scale 1 mm.

In the MMC treated eyes, established fibrosis was detected in the entire bleb area. Active fibrosis was observed in the area in contact with the tube. The established fibrosis areas were more extended in the MMC treated sections compared to the negative control sections and the active fibrosis was limited compared to the negative control samples. The characteristic of the MMC treated eyes was that the area 2 – 4 mm posterior to the tube

(where the treatment was administered) was characterised by thick collagen deposition and hypocellularity (few elongated fibroblasts located among the densely packed collagen fibres), indicative of chronic – established scarring. This is also confirmed by the strong yellow/ green signal shown in the Picrosirius Red images. As in the negative control images, a very limited number of inflammatory cells (no more than the inflammatory cells detected in the normal tissue) were observed.

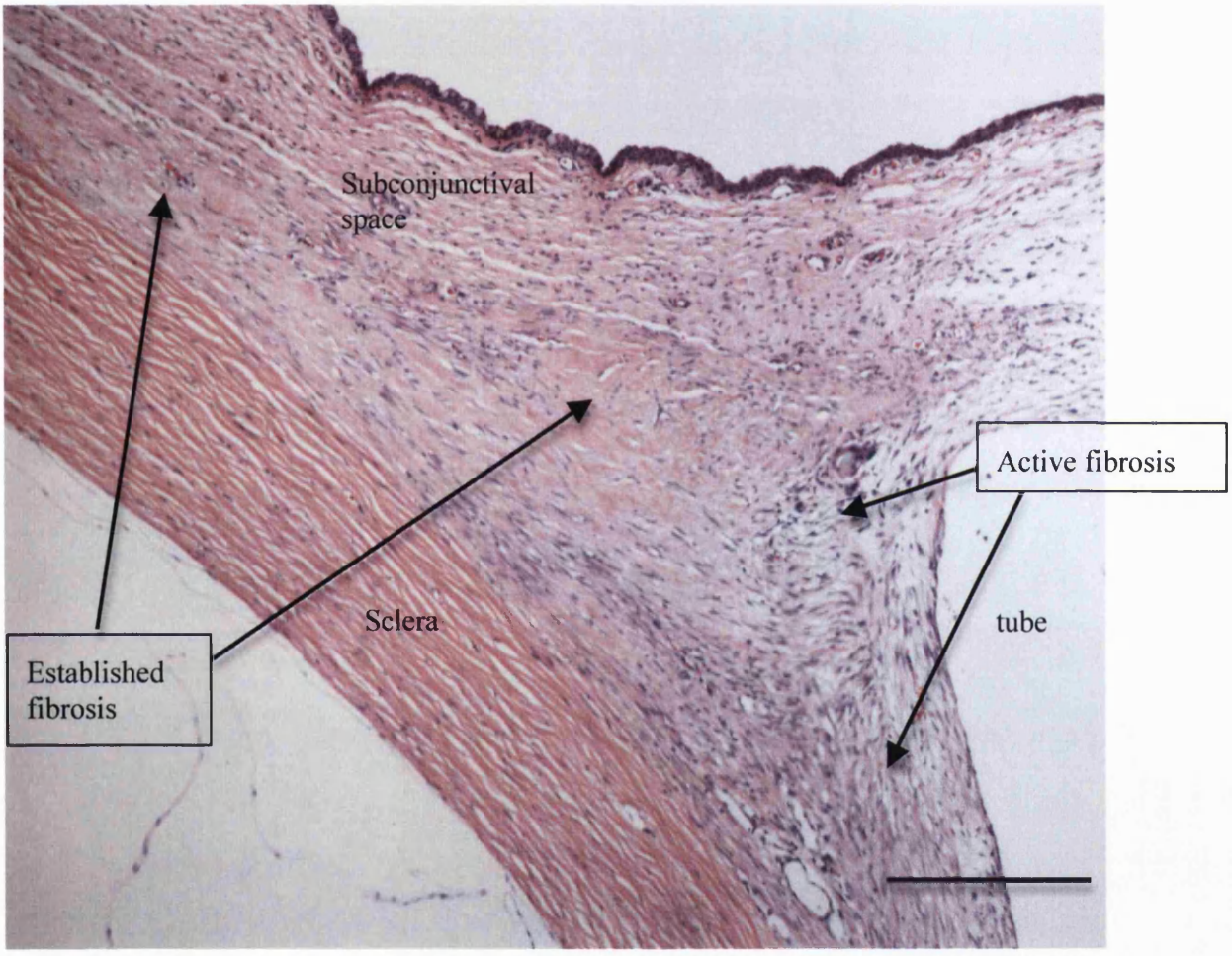

Figure 68: MMC treated bleb. Signs of established fibrosis are apparent in the area 2-5 mm posterior to the tube. Limited number of fibroblasts is also observed in the areas of established fibrosis. Extensive fibroblastic population is observed, similar to the negative control group, in the bleb area in contact with the tube. Scale 1 mm.

A key issue that was investigated in the ilomastat tablet treated blebs was whether the placement of the tablet had caused the development of a capsule formation around the tablet. If a capsule had formed, there would have been extensive scarring in the bleb, as well as signs of inflammation, and there would be signs of undissolved material in the subconjunctival area (most likely, big gaps in the subconjunctival area would have been detected and fibroblasts and inflammatory cells would have created a wall around them). These findings were also confirmed by two ocular pathologists (PL and CT), who suggested in their review of the histological images that no capsule formation took place in the bleb area. In addition, the analysis of the structure of the subconjunctival space indicated that the ilomastat tablet was completely dissolved at the end of the 30-day period. There is a possibility that small parts of the tablet may have remained at the end of the 30 day *in vivo* period and these could have been dissolved during the fixation process, but there were no histological signs to suggest this.

In three out of the five rabbits treated with the ilomastat tablet, limited deposition of collagen was observed and no significant signs of established scarring were shown. Analysis of picrosirius red polarised images from the blebs of these rabbits confirms these findings; low yellow/ green signals observed in an extensive area in the subconjunctival space indicated decreased deposition of collagen. It is worth noting that the green/yellow signal was diminished compared to the positive and negative control samples. In addition, no hypercellularity was observed in the blebs of the ilomastat treatment blebs. Again, a very limited number of inflammatory cells, no more than in the normal tissue were observed. With the remaining two out of the five rabbits in the ilomastat tablet treatment group, the histology findings were slightly different. Although in these blebs limited collagen deposition was detected, signs of active scarring were observed in the bleb. In one of the two rabbits, this was more apparent than in the other and covered a larger area. Our interpretation of these results are corroborated by two ocular pathologists and indicate that the ilomastat tissue-tablet treatment administered in these blebs has delayed the scarring process, and that the positive and negative control samples, on day 30 after the experiment, had more progressed-mature scarring, even when compared to these two rabbits treated with the ilomastat tablet.

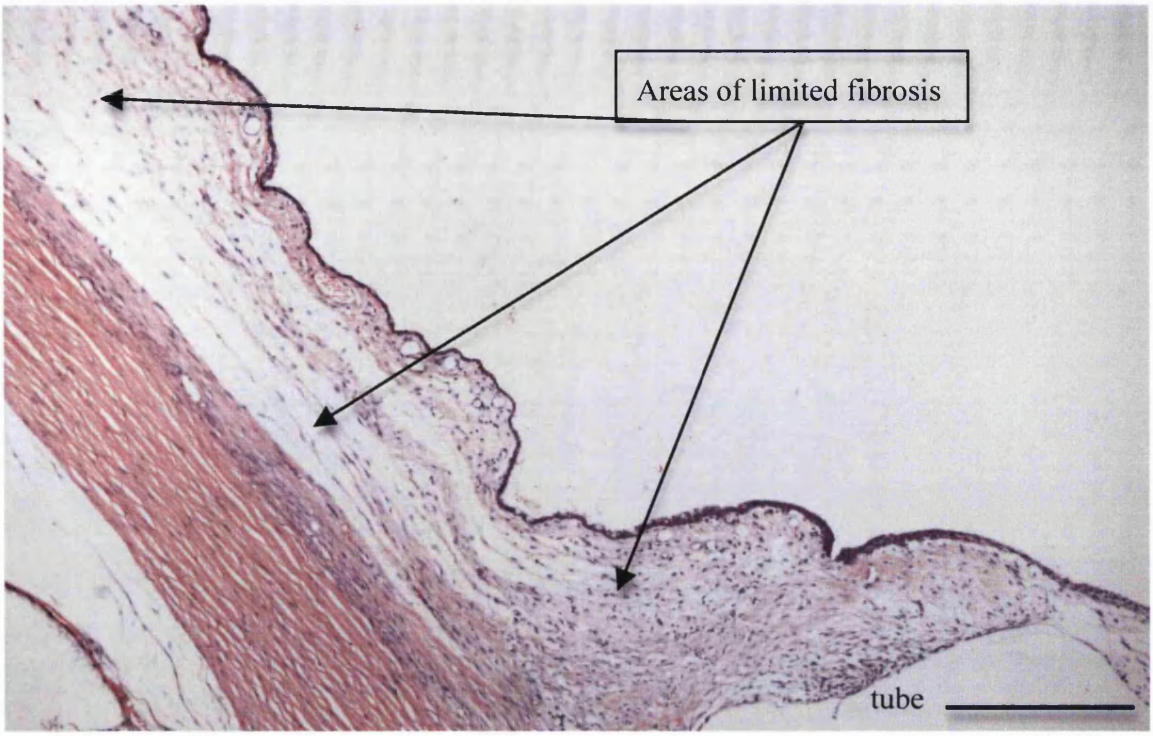

Figure 69: Ilomastat tablet treated bleb. Signs of active fibrosis were observed in the area close to the tube as in the positive and negative control although the fibroblastic population in this case is smaller. Few small or no areas of established fibrosis were observed 2-4 mm posterior to the tube and the bleb area was characterised by the presence of extended areas of limited fibrosis, which could facilitate the aqueous outflow. Scale 1 mm.

3.2.3.3.2. Comparative histology

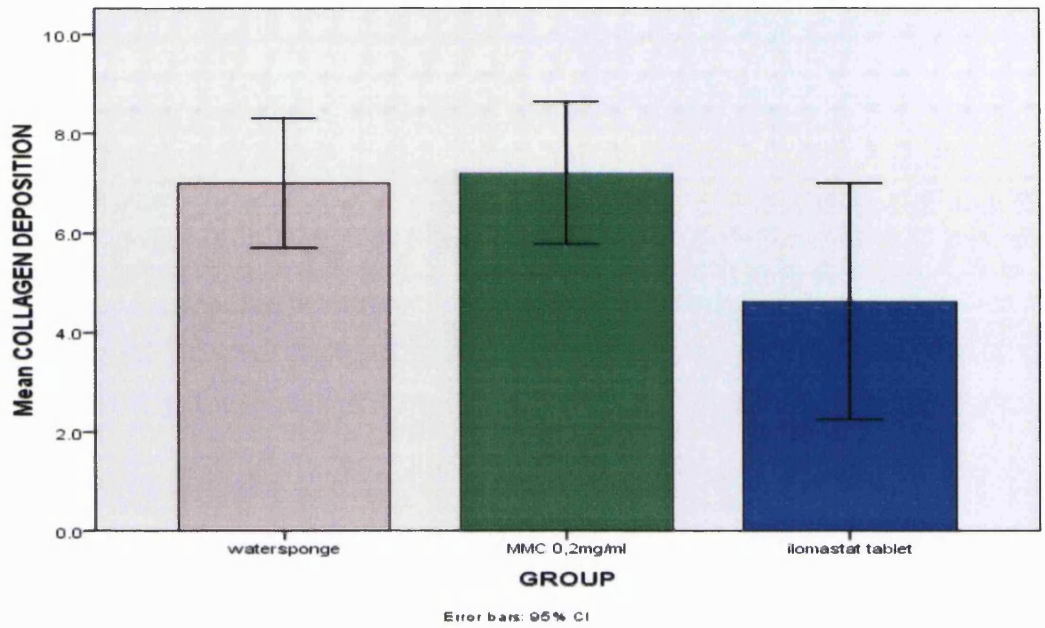

Figure 70: Comparative histology regarding the collagen deposition in the bleb area between the different groups. Blebs treated with ilomastat tablet to have significantly less collagen deposition ($P<0.05$) than the positive and negative control groups. Another interesting finding was that the positive and negative control groups had about the same mean collagen deposition in their blebs.

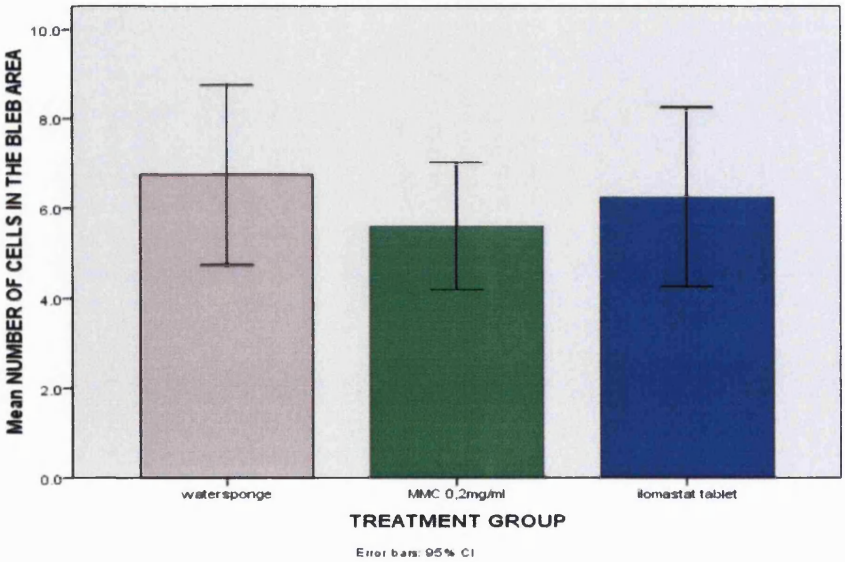

Figure 71: Comparative histology regarding the number of cells found in the bleb area between the different groups. No significant differences were found although the cell number in the ilomastat tablet group was smaller.

3.3. Evaluation of novel compounds to inhibit fibrosis

3.3.1. *In vitro* gel contraction

Four novel MMP inhibitors were tested for first time for their effectiveness against contraction in our in the HTF populated collagen I gels *in vitro* contraction model. Three different concentrations for each compound were evaluated for their effectiveness in inhibiting *in vitro* contraction (their maximum achieved concentration in normal media, 30% of their maximum achieved concentration in normal media and 10% of their maximum achieved concentration in normal media). DMSO was used for easier dissolution of the compounds in normal media. Normal media with DMSO was used as negative control. Normal media with ilomastat (maximum reported concentration, 30% of maximum reported concentration and 10 % of maximum reported concentration) dissolved in DMSO was used as positive control. The effect of the Compounds 1,2,3 and 4 on gel contraction compared to the positive and negative controls are shown in Figure 72, Figure 73, Figure 74 and Figure 75.

Statistical analysis (ANOVA) showed that the effect of all compound (in all three concentrations) in inhibiting gel contraction was significantly higher than the negative control ($P<0.001$).

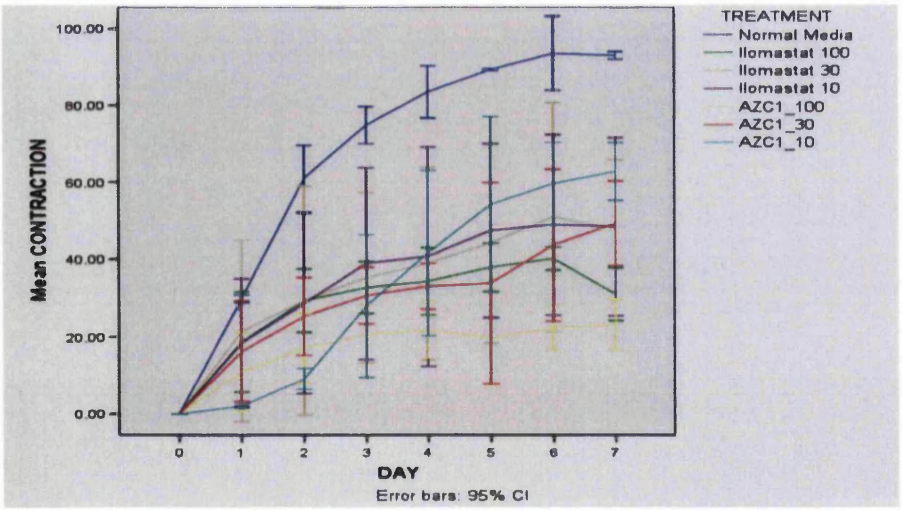

Figure 72: The effect of three different concentrations of Compound 1 in the HTF populated collagen I gels *in vitro* contraction model. Three concentrations of ilomastat were used as positive controls and media without any anti-scarring agent was used as negative control. The effect of three different concentrations of Compound 1 was tested. Compound 1 had a significant inhibitory effect in the contraction of the gels compared to the negative control in all three tested concentrations. The higher the concentration of Compound 1 the more significant the anti-contraction effect was.

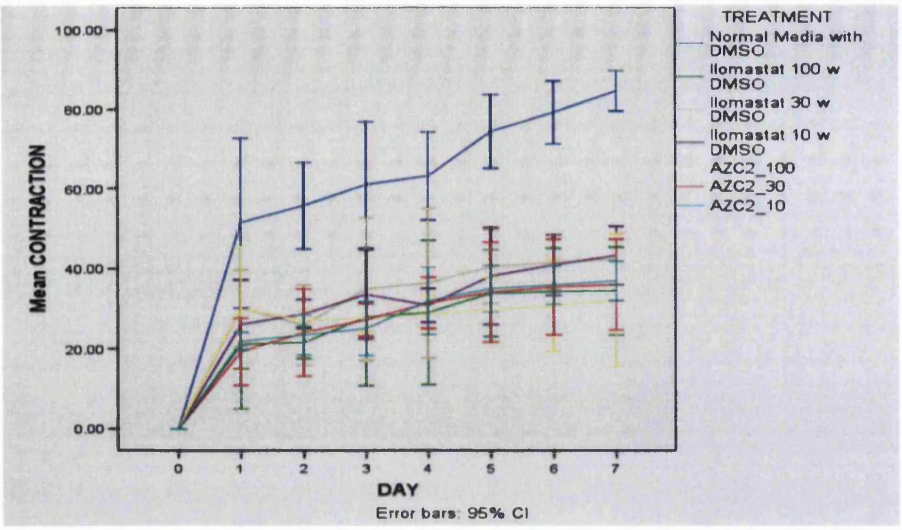

Figure 73: The effect of three different concentrations of Compound 2 in the HTF populated collagen I gels *in vitro* contraction model. Three concentrations of ilomastat were used as positive controls and media without any anti-scarring agent was used as negative control. The effect of three different concentrations of Compound 2 was tested. Compound 2 had a significant inhibitory effect in the contraction of the gels compared to the negative control in all three tested concentrations. The different tested concentrations of Compound 2 had similar anti-contraction effect.

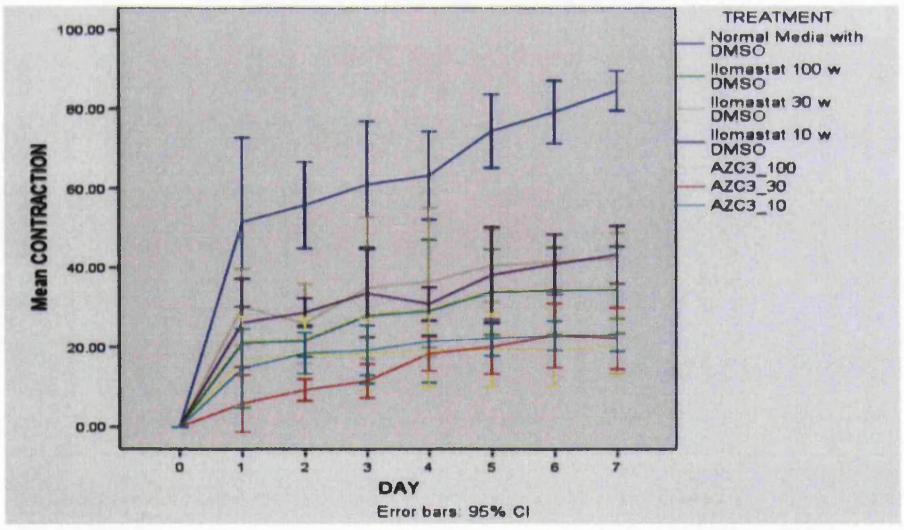

Figure 74: The effect of three different concentrations of Compound 3 in the HTF populated collagen I gels *in vitro* contraction model. Three concentrations of ilomastat were used as positive controls and media without any anti-scarring agent was used as negative control. Compound 3 had a significant inhibitory effect in the contraction of the gels compared to the negative control in all three tested concentrations. All Compound 3 concentrations also had a significantly superior effect compared to ilomastat ($P<0.01$, ANOVA).

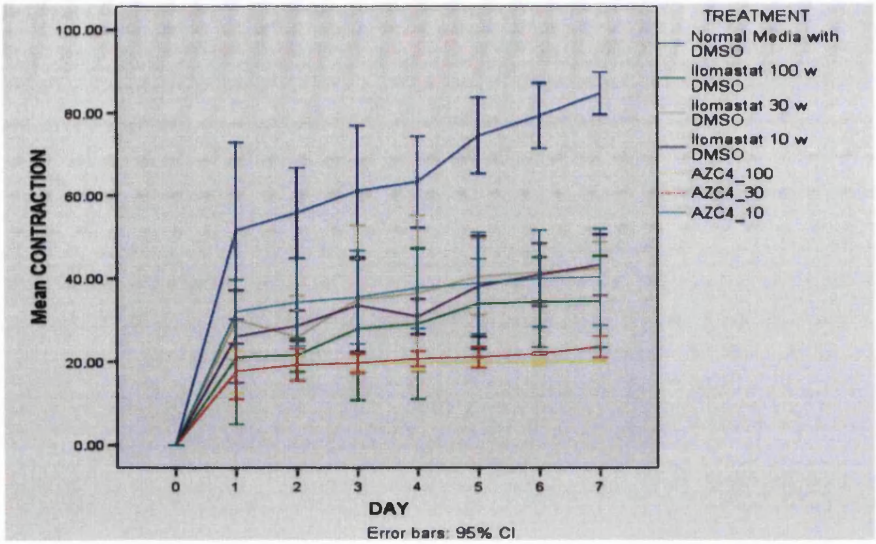

Figure 75: The effect of three different concentrations of Compound 4 in the HTF populated collagen I gels *in vitro* contraction model. Three concentrations of ilomastat were used as positive controls and media without any anti-scarring agent was used as negative control. Compound 4 had a significant inhibitory effect in the contraction of the gels compared to the negative control in all three tested concentrations. Compound 4, also had a significantly superior effect compared to ilomastat (Maximum and 30% of maximum Compound 4 concentrations vs Ilomastat concentrations $P<0.01$, ANOVA).

3.3.2. Morphology of Human Tenon's Fibroblastasts in the different treatment groups

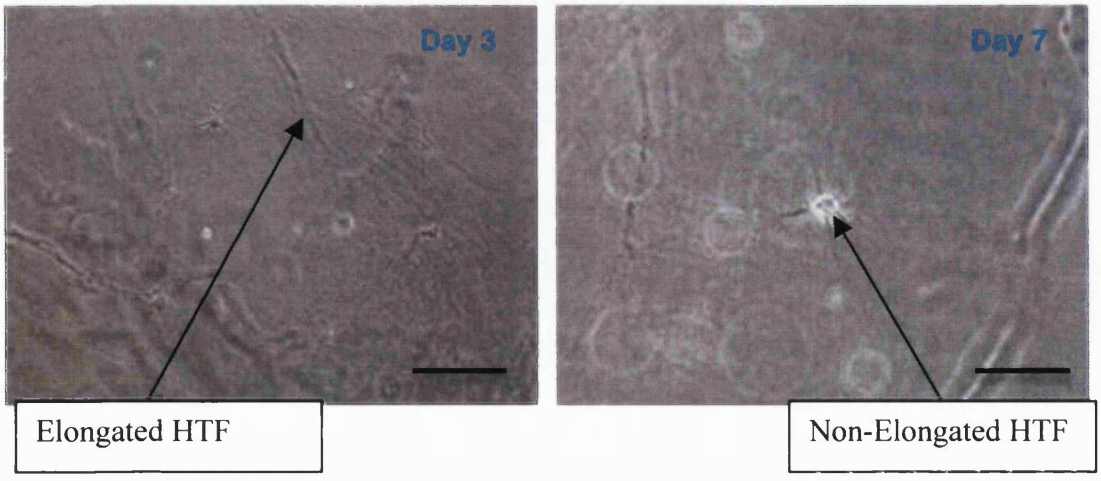

Figure 76: Morphology of HTFs located in collagen I gels treated with Ilomastat (in maximum concentration). The percentage of non-elongated /elongated cells was about 70 / 30 % respectively. Magnification 10 X. Scale 50 μM.

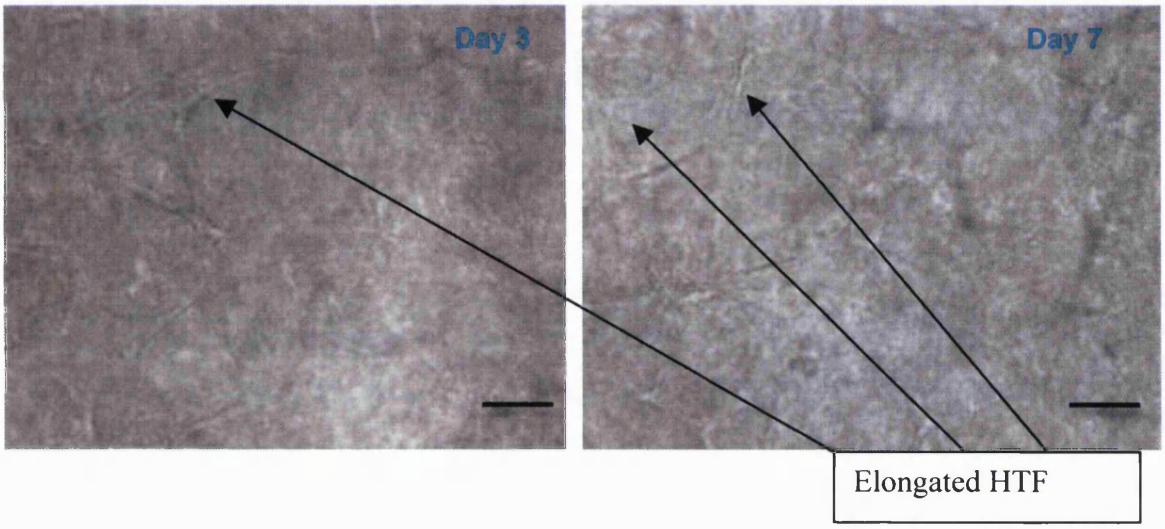

Figure 77: Morphology of HTFs located in collagen I gels treated with normal media without any MMP inhibitor (negative control). More than 95% of the cells with which the gels were populated were elongated. Magnification 10 X. Scale 50 μM.

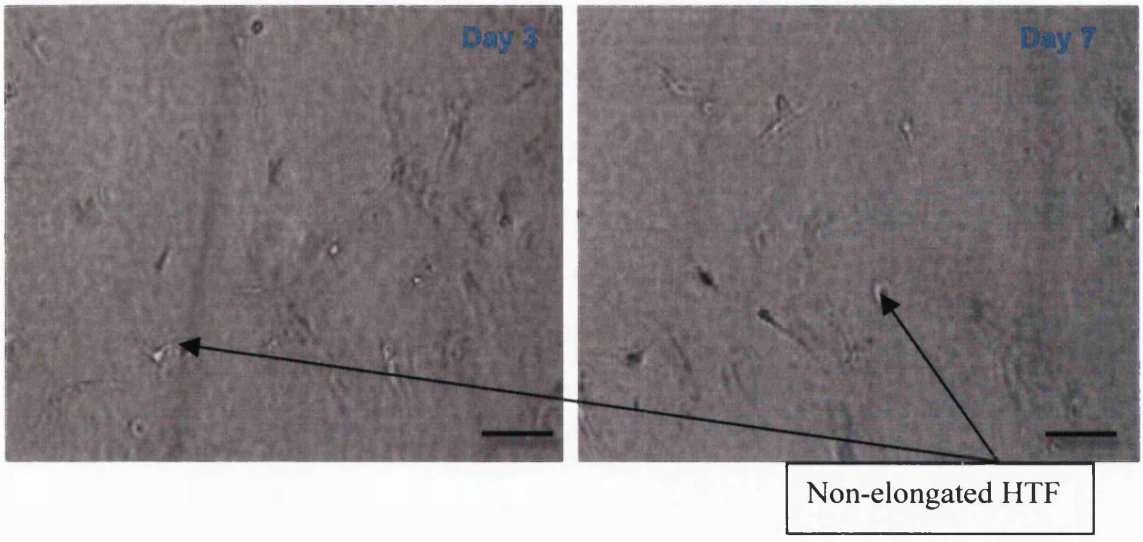

Figure 78: Morphology of HTFs located in collagen I gels treated with Compound 1 (maximum concentration). More than 80% of the cells in the gels of this treatment group did not elongate. Magnification 10 X. Scale 50 μM.

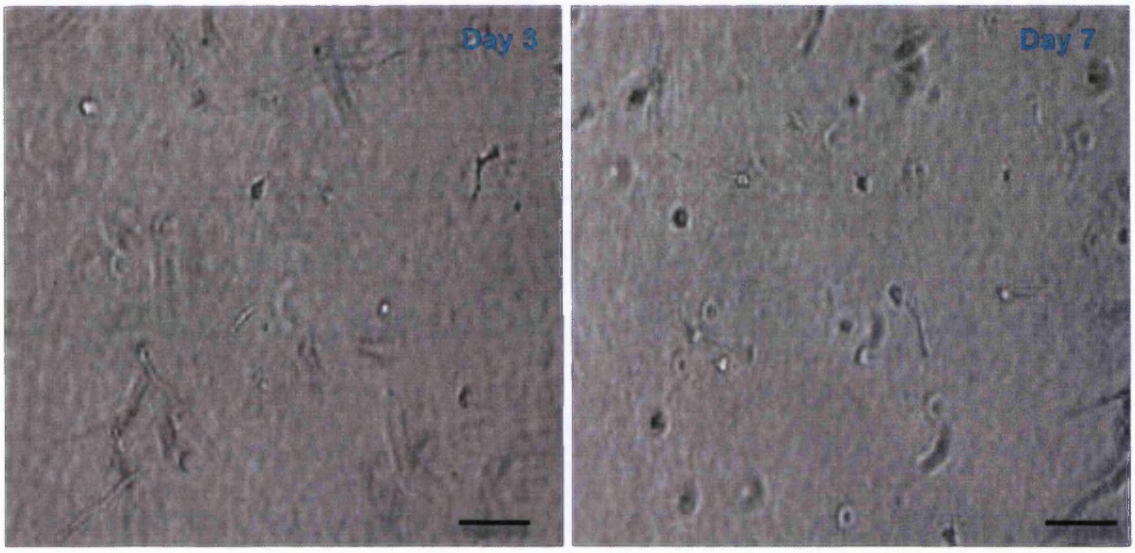

Figure 79: Morphology of HTFs located in collagen I gels treated with AZ Compound 2 (maximum concentration). About 75% of the cells in the gels of this treatment group were not elongated. Magnification 10 X. Scale 50 μM.

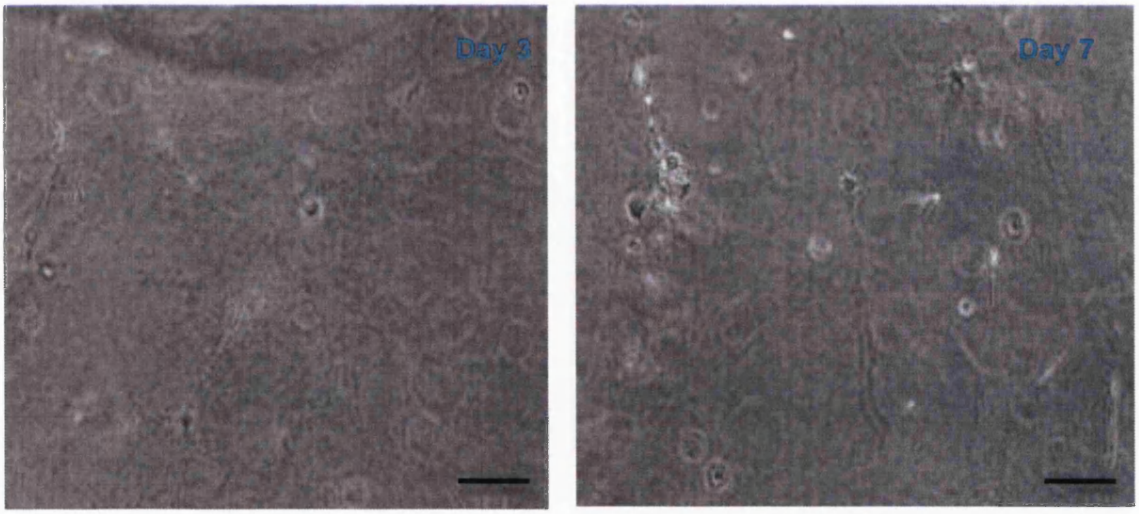

Figure 80: Morphology of HTFs located in collagen I gels treated with Compound 3 (in maximum concentration). As in the Compound 2, about 75% of the cells in the gels of this treatment group were not elongated. Magnification 10 X. Scale 50 μM.

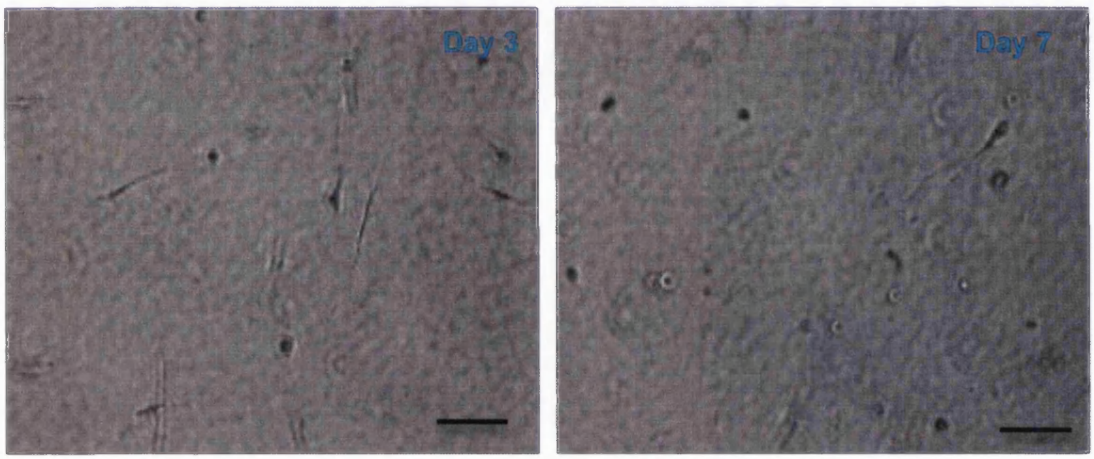

Figure 81: Morphology of HTFs located in collagen I gels treated with Compound 4 (in maximum concentration). More than 80% of the cells in the gels of this treatment group were not elongated. Magnification 20 X. Scale 50 μM.

In the negative control gels (gels treated with media without ilomastat or any of the Compounds), the Tenon's fibroblasts gradually became elongated and took on a spindle-shaped appearance. They developed a long and extended morphology into the matrix without any sign of cytotoxicity (Figure 77). In the ilomastat treated gels (positive control, (Figure 76) as well as in the gels treated with the AZ compounds (Figure 78, Figure 79, Figure 80 and Figure 81) a high percentage of Tenon's fibroblasts remained round or slightly elongated until the end of the experiment. The applied monotherapy (MMP inhibition by ilomastat or one novel MMP inhibitor) delayed or even stopped the elongation of the fibroblasts and the development of the characteristic cytoplasmic processes. The cells did not stretch in the positive control group as well as in the gels treated with the novel MMP inhibitors group, unlike those in the negative control group. No development of vacuoles or other signs of cytotoxicity were developed. Additionally, after day 7, in 2 gels per group, the treatment was replaced with normal media without any anti-contraction treatment. This was performed in order to test in the novel MMP inhibitors or the positive control had caused cell death. After 5-7 days, the vast majority of the cells populating the gels previously treated with ilomastat (positive control) or with the novel MMP inhibitors were elongated.

3.4. SiRNA to inhibit MMP formation

3.4.1. *In vitro* results

3.4.1.1. Contraction assay

Gel contraction assays were conducted in order to test the *in vitro* effectiveness of siRNAs against MMPS. Three different concentrations were tested (100 nM, 30 nM and 10 nM) with the use or not of lipofectamine. Ilomastat 100 μM (ILO) and Media with no treatment (marked as HTF) served as positive and negative control respectively. The cells used in this essay had been pre-incubated with the treatments for 24 h (Figure 82 or 48 h (Figure 83) and were placed in the gels for 7 days.

The following graphs indicate the effect of different concentrations of MMP SiRNAs against contraction in the HTF populated Collagen I gels.

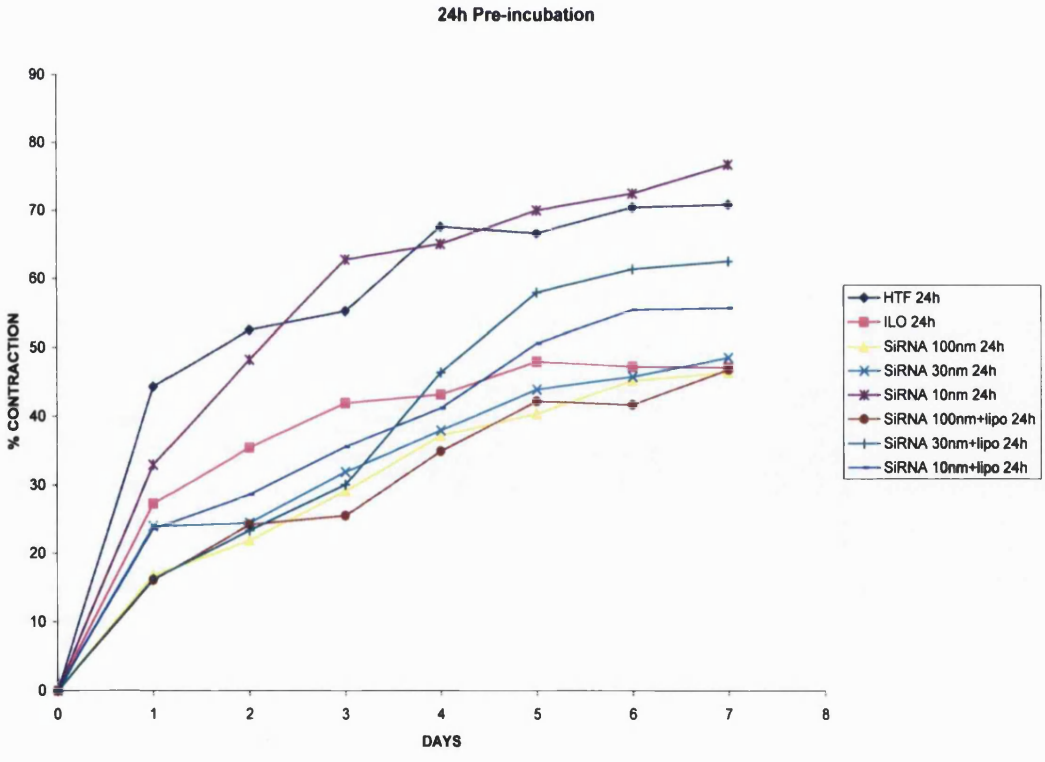

Figure 82: *In vitro* experiments with 24h pre-incubation of HTFs with the siRNA treatments. Axe Y represents the % *in vitro* contraction and axe X the time points of the experiment. SiRNA with lipofectamine and SiRNA without lipofectamine in the two out of the three concentrations (100 nM and 30 nM) inhibited significantly the contraction of the gels.

The SiRNA 10 nM group (without lipofectamine) had about the same effect in the contraction model as the negative control with slight differences over the 7 days period (Figure 82). All the other groups displayed a greater inhibition for contraction of the HTF collagen gels which was statistical significant. It is worthwhile that some of the SiRNA groups managed overall to inhibit contraction even more than the positive control (the SiRNA 100 nM with and without lipofectamine and the SiRNA 30 nM groups inhibited the contraction more than the positive control from day 1-day 6, although the end point was the same with the positive control (ilomastat). These outcomes though were not statistical significant. The SiRNA 30 nM + lipo and the 10nM+lipo group inhibited contraction from day1-day3 more than the positive control but after day 5 the gels contracted more than the positive control.

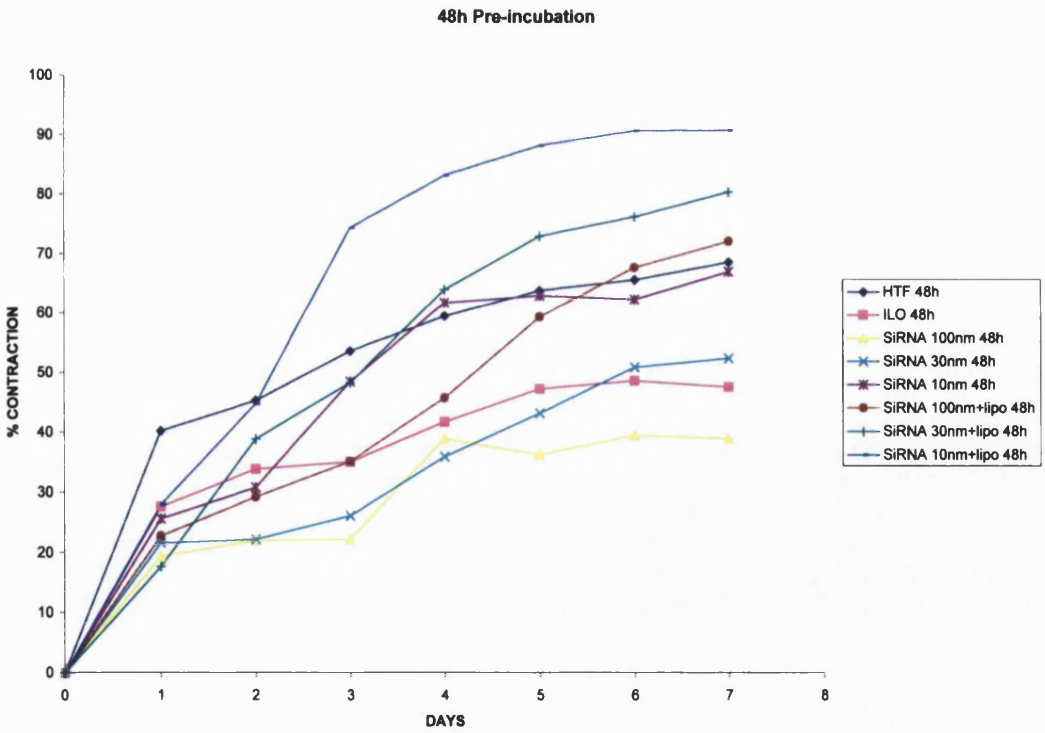

Figure 83: *In vitro* gel contraction experiments with 48h preincubation of HTFs with the treatments. Axe Y represents the % *in vitro* contraction and axe X the time points of the experiment.

Significant differences from the 24h Pre-incubation experiment were observed in the 48h preincubation *in vitro* experiment (Figure 83). It is interesting to notice that all the lipofectamine treated groups end up with higher percentage of gel contraction than the

negative control. It is additionally noteworthy that the SiRNA 100 nM group had until the end of the experiment higher inhibitory effect than the positive control group; the SiRNA 30 nM group had also better results than ilomastat from day1-day 5.

3.4.1.2. Morphology of the HTFs used for the *in vitro* experiments

The cell morphology described below indicates the morphology of the HTFs pre-incubated with media containing no treatment or ilomastat or SiRNA with lipofectamine or SiRNA without lipofectamine. Based on our observations, the pre-incubation time (24 or 48 h) of the cells or the concentration of the treatment did not play a significant role in the morphology of the cells treated with the same treatment. For this reason, in the morphology described below, the only parameter that is used for describing the morphology of the cells is the treatment and not the concentration or the pre-incubation time.

Normal media treated groups: Tenon's Fibroblasts elongated at the pre-incubation period without the development of vacuoles in their cytoplasm. They gradually became elongated and obtained a spindle-shaped appearance in the gels. The fibroblasts extended into the collagen matrix without the development of vacuoles (Figure 84)

Ilomastat treated groups: A high percentage (~ 70 %) of Tenon's fibroblasts remained round and did not elongate. Ilomastat as a MMPi is thought to delay or even stop the elongation of the fibroblasts and the development of the characteristic cytoplasmic processes of fibroblast activation without being cytotoxic (Daniels *et al* 2003). SiRNA treated groups without lipofectamine: Cellular morphology was similar to the ilomastat groups. Again, a high percentage (~ 70 - 80 %) of Tenon's fibroblasts did not elongate until the end of the experiment or developed only small cytoplasmic processes. Some elongated cells were observed however. During the pre-incubation period, vacuoles were observed in the cytoplasm of the cells in both of the 24 and in 48 h and in all the different siRNA concentrations tested (100 nM, 30 nM and 10 nM), indicative of cytotoxicity (Figure 88, Figure 89)

SiRNA treated groups with lipofectamine: Severe cytotoxicity was observed in all the groups during pre-incubation, especially in the 48 h groups. When the cells were placed onto the gels, they appeared to recover, as we did not observe vacuoles after the day 2. It is most likely that removal of lipofectamine when the cells were placed in the gels allowed the fibroblasts to recover.

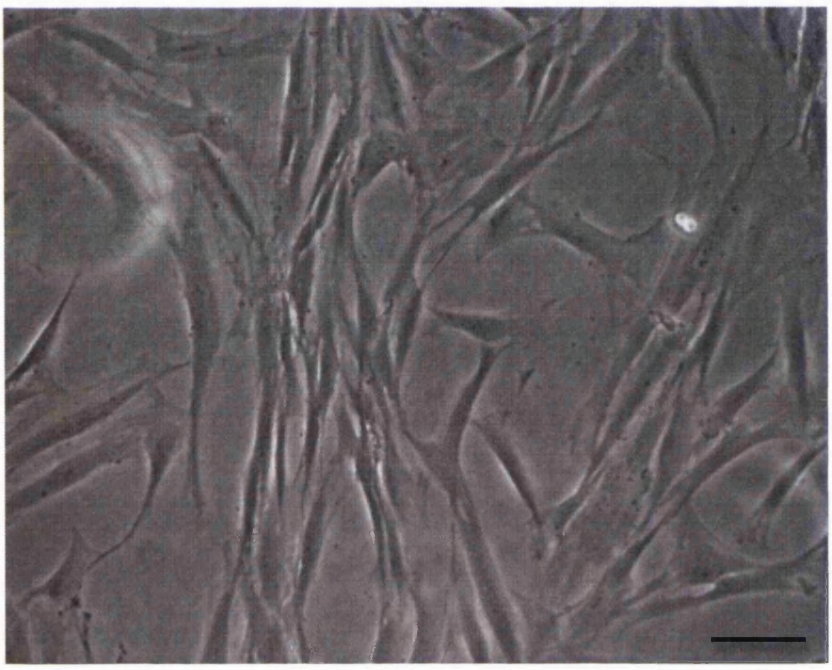

Figure 84: Negative Control (HTFs incubated with media without treatment). All fibroblasts elongated. Magnification 20 X. Scale 50 μM.

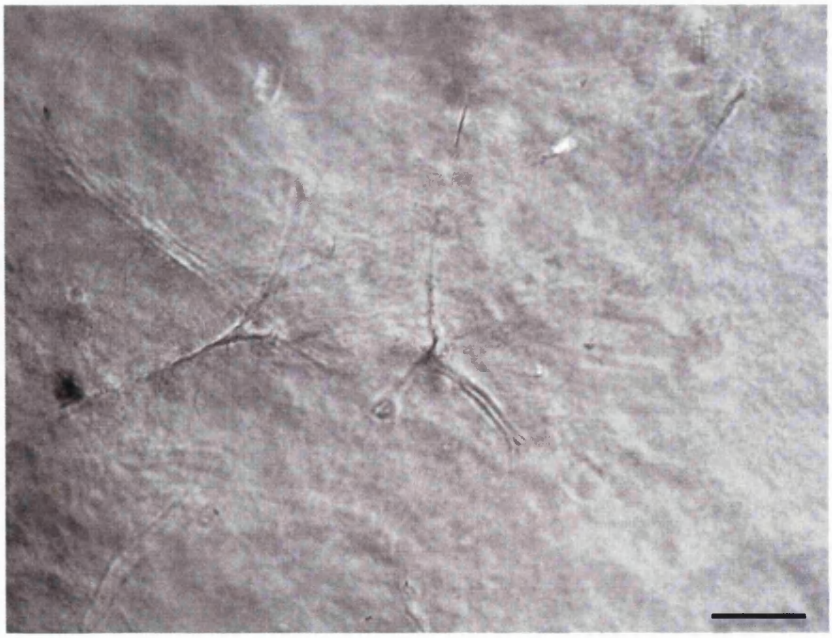

Figure 85: Morphology of HTFs that populated collagen I gels and were treated with media without anti-scarring treatment. Picture taken on the last day of the 7-days *in vitro* experiment. More than 95% of the HTFs were elongated. Magnification 20 X. Scale 25 μM.

Figure 86: Morphology of HTFs incubated for 48 h with Ilomastat (concentration 100 μM). No signs of cytotoxicity were observed. Magnification 20 X. Scale 50 μM.

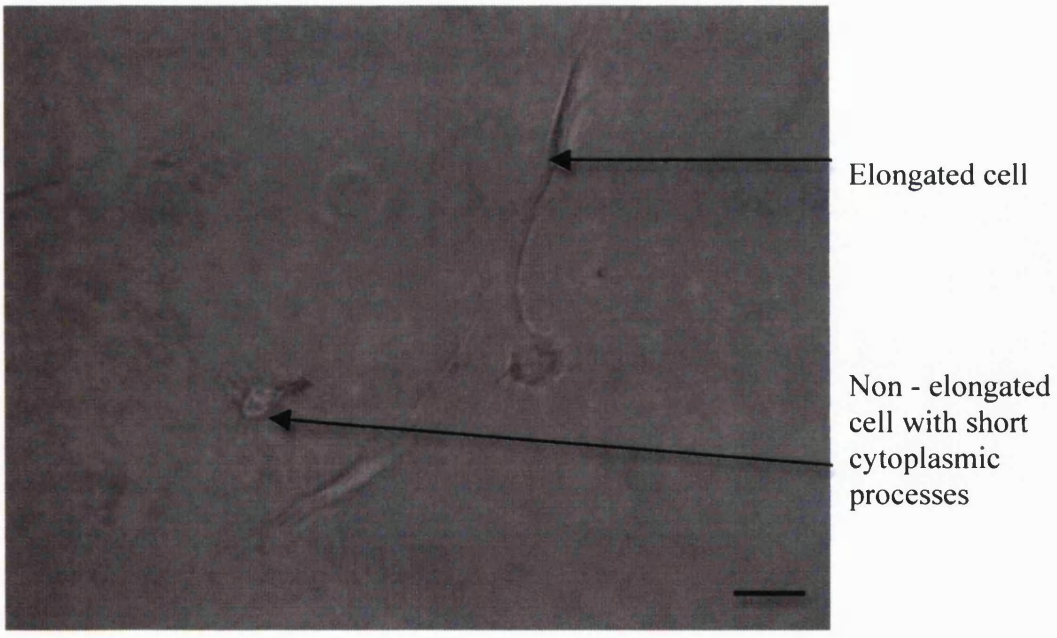

Figure 87: Gels treated with Ilomastat (concentration 100 μM) and populated with HTFs pre incubated with Ilomastat 100 μM for 48h (positive control group). More than 70% of the HTFs in these gels remained round (as the non activated fibrocytes) or developed only short cytoplasmic processes. Magnification 20 X. Scale 25 μM.

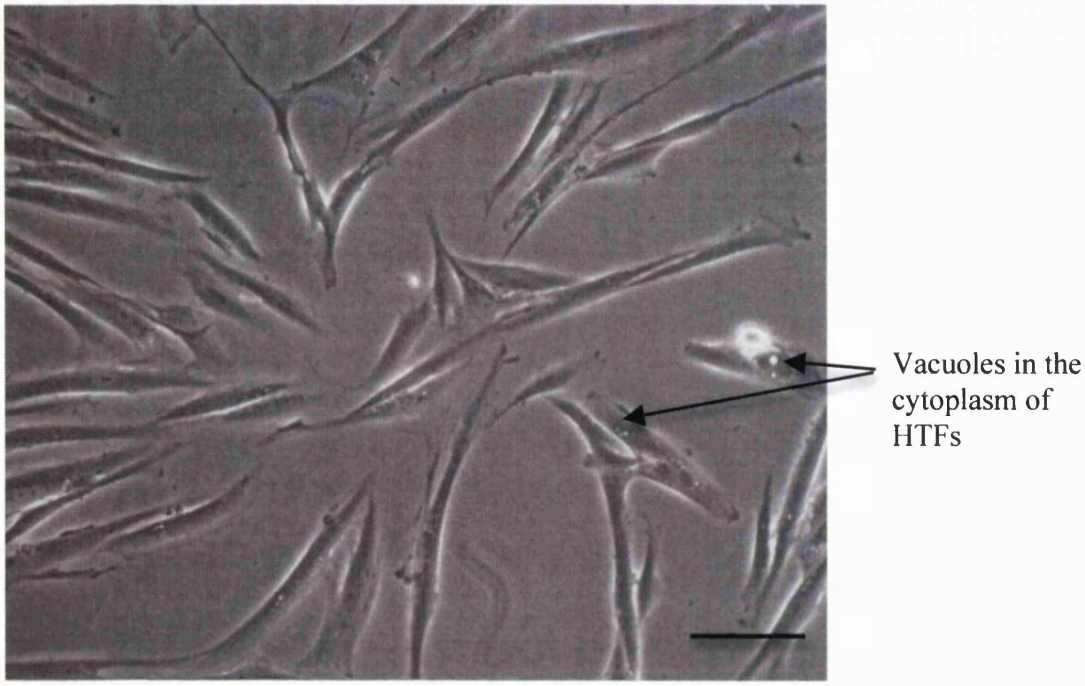

Figure 88: HTFs incubated with SiRNA (100 μM) without lipofectamine for 48h. Few vacuoles were observed, which is a sign of cytotoxicity. Magnification 20 X. Scale 50 μM

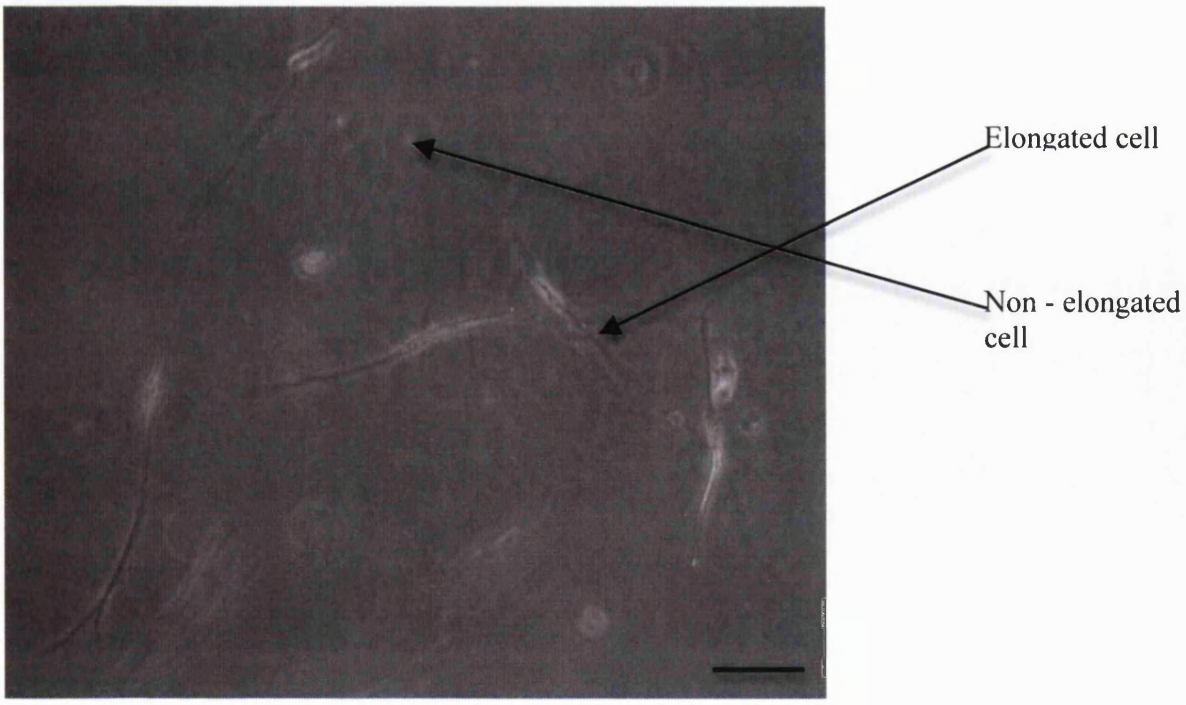

Figure 89: Gels treated with SiRNA (100 μM) without lipofectamine. Only 20 – 25 % of the HTFs became fully elongated. The rest either remained round or obtained small cytoplasmic processes, similar to the morphology of the HTFs treated with ilomastat. Magnification 20 X. Scale 25 μM

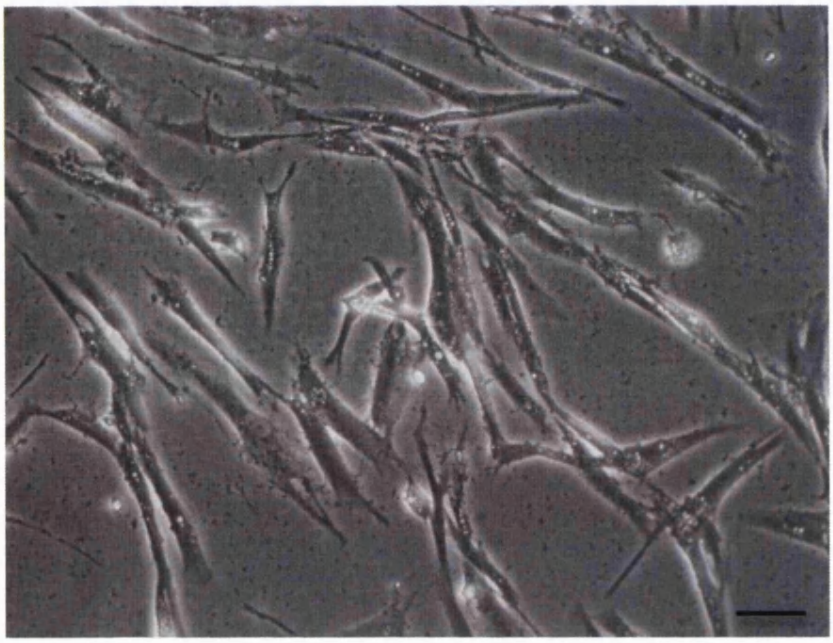

Figure 90: HTFs pre-incubated with MMP SiRNA (100 μM) with lipofectamine for 48h. Increased number of vacuoles was observed in the cytoplasm of HTFs, indicative of cytotoxicity. The number of vacuoles observed in the cells treated with lipofectamine was significantly increased than in the cells treated without lipofectamine. Magnification 20X. Scale 50 μM

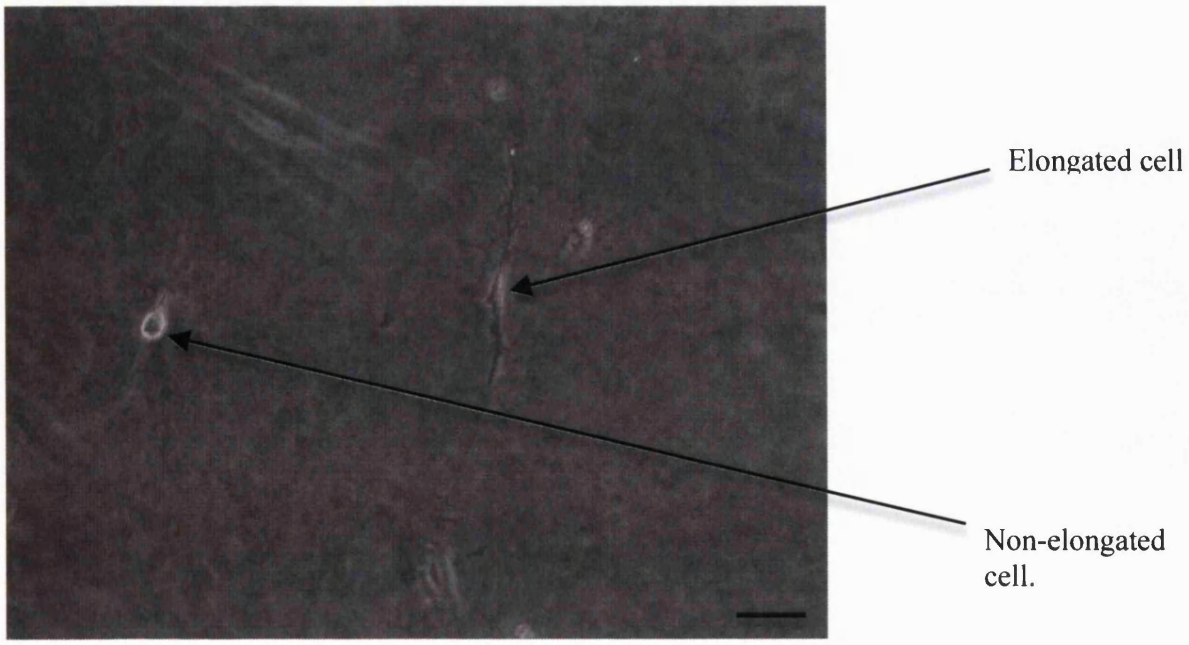

Figure 91: Gels treated with SiRNA (100 μM) with lipofectamine. Only 15 - 20 % of the HTFs became fully elongated. The rest either remained round or obtained small cytoplasmic processes, similar to the morphology of the HTFs treated with ilomastat. Magnification 20 X. Scale 25 μM

3.4.2. First *in vivo* experiment

We used the rabbit GFS model (Wong *et al* 2003; 2005; Cordeiro *et al* 1999) to compare bleb survival and morphology for three treatment groups (siRNAs against MMP-1, -2, -3, -8 and -9 – concentration 20 mM; antibody against Transglutaminase II – concentration 2 mg/ injection and PBS (negative control). In the survival curve below, the blue line represents the group A (rabbits treated with SiRNAs against MMPs), the green line represents the group B (rabbits treated with the antibody against TGase II) and the red line represents the group C (rabbits treated with PBS). One rabbit in group B had to be euthanized, as on the day one after surgery was found to suffer from endophthalmitis, so the starting point for group B is 7 instead of 8).

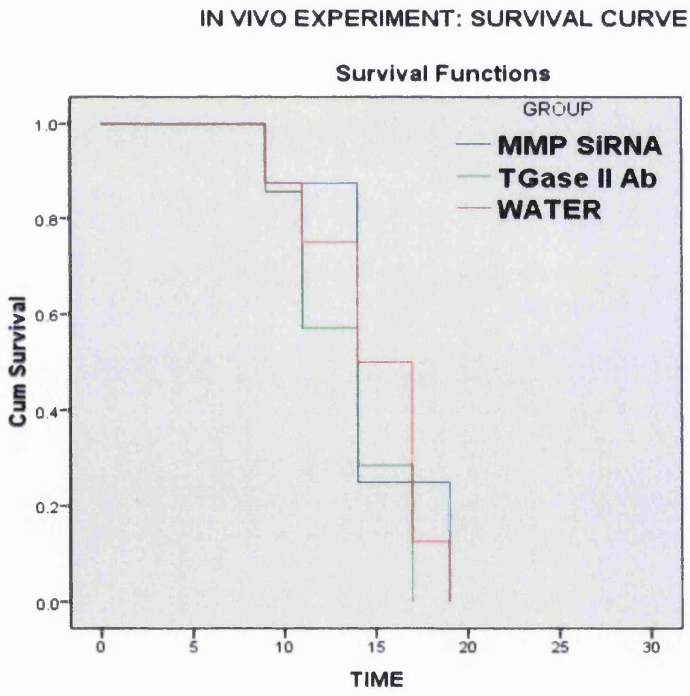

Figure 92: Survival curve. Statistical analysis indicated that there are no significant differences in the survival of the bleb between the three groups (P=0.492 Log Rank). The Y Axe represents the % of functional blebs in each treatment group and the X axe represents the days after GFS.

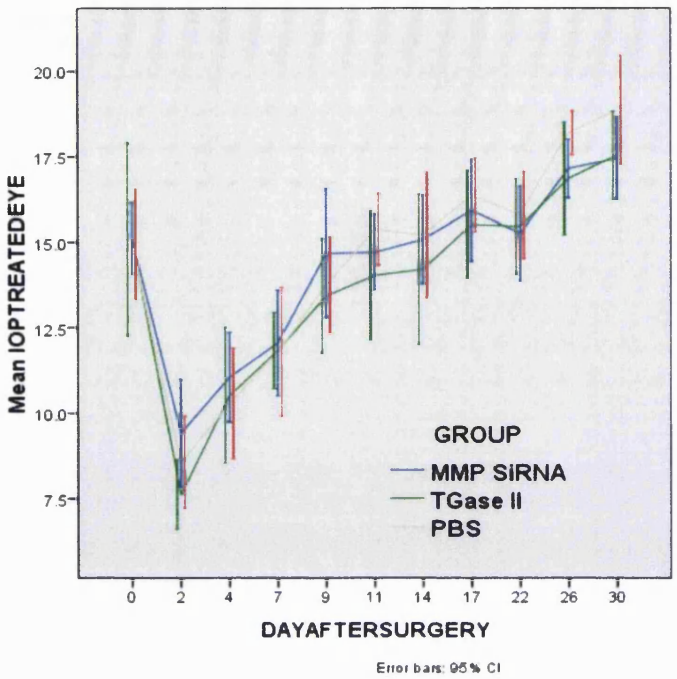

Figure 93: Analysis of the IOP in the treated eye. Statistical analysis indicated that no significant differences were detected between the three groups.

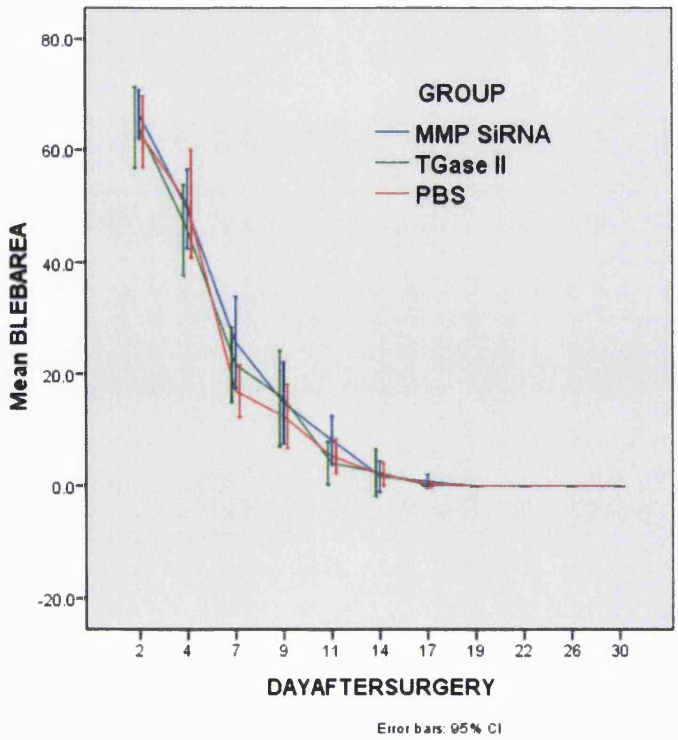

Figure 94: Comparison of the bleb area between the three different groups. Statistical analysis (ANOVA) indicated that no significant differences were detected between the three treatment groups.

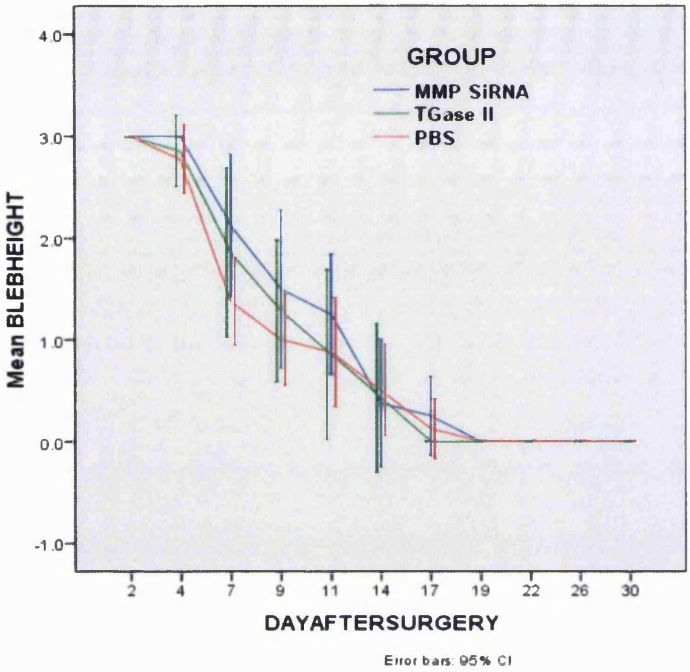

Figure 95: Comparison of the bleb height between the three groups. Statistical analysis (ANOVA) indicated that no significant differences were observed in the bleb height of the three different groups.

It was found that there were no significant differences in the three groups as regards the bleb survival, intraocular pressure and bleb size (bleb surface area and height). The siRNA treatment against MMPs was found not to have better results against scarring compared to the negative control (injections with PBS) and to the positive control (TGase II ab). Although the industrial sponsors of this work, Quark PLC, assured us that TGase was a suitable positive control in our model, it was found that this treatment was no better than the negative control and the siRNA treatment. Ideally MMC could have been used as positive control, but in this case the choice of the positive control was beyond our control. This is one of the reasons that this study had significant limitations.

3.4.3. Second *in vivo* experiment

Since the initial *in vivo* study indicated that the siRNA treatment against MMPs was not successful and did not inhibit scarring in our GFS model, we then examined the extent of siRNA cellular uptake by subconjunctival fibroblasts in a second *in vivo* experiment. As the siRNAs against MMPs were found *in vitro* to be successful against contraction, one of

the main reasons that siRNAs could have been unsuccessful in inhibiting scarring *in vitro* could have been a potential non-uptake of the siRNAs by the cells located in the subconjunctival space.

A second *in vivo* study with six rabbits was performed in order to assess the uptake of an siRNA molecule by cells in the subconjunctival space. Confocal microscopy was used in these uptake experiments. This study was designed as a qualitative experiment, attempting to assess if any uptake is achieved and not a quantitative experiment aiming to investigate the percentage of cells in the subconjunctival space that uptake the siRNAs. An siRNA against PTEN mRNA was tagged for observation by confocal microscopy. As described in the materials and methods section, an 100 μl injection of CY3 PTEN was administered in the subconjunctival space of the left eye in rabbits. Two rabbits were sacrificed 6 hours after the injection, two rabbits were sacrificed 24 h after the injection and the remaining two rabbits were sacrificed 7 days after the injection. After sacrifice, subconjunctival and subconjunctival tissue was dissected from the harvested eyes and analysed with confocal microscopy. In the images presented below (Figure 95, Figure 96 and Figure 97), it is obvious that there is uptake of the CY3PTEN siRNA from the cells. The difference we see in the three categories is that in the group of rabbits that were injected 7 days before sacrifice there was no fluorescent background and in the group of 1 day before sacrifice there is less fluorescent background than in the group of 6 hours before sacrifice.

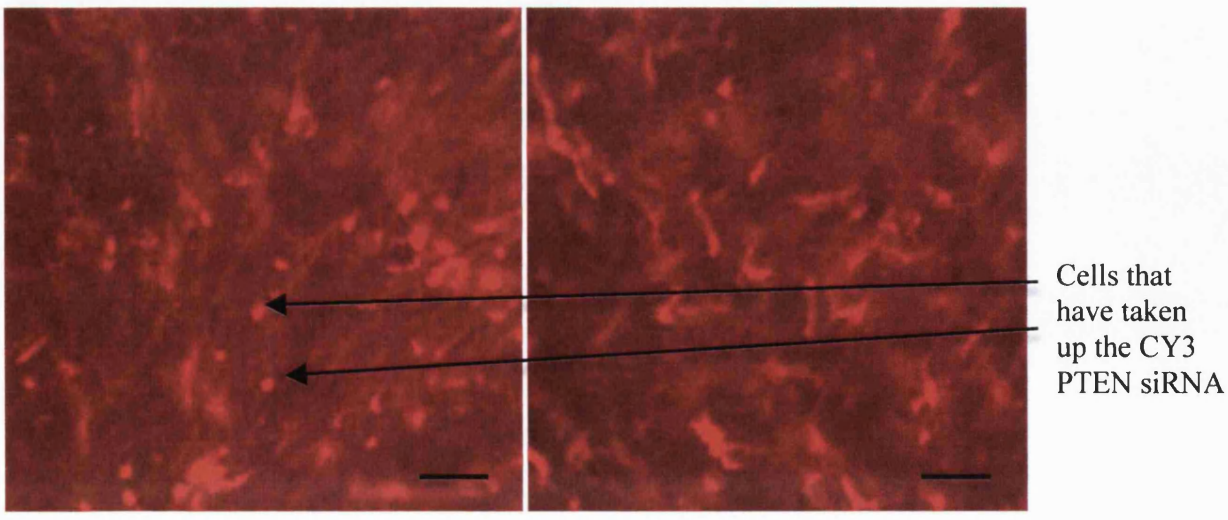

Figure 96: Group 1 – 100 μl CY3PTEN subconjunctival injection 6 hours before euthanasia. Uptake of the siRNA by the cells in the subconjunctival space was shown. Strong fluorescent background is also detected. Magnification 20 X. Scale 50 μM

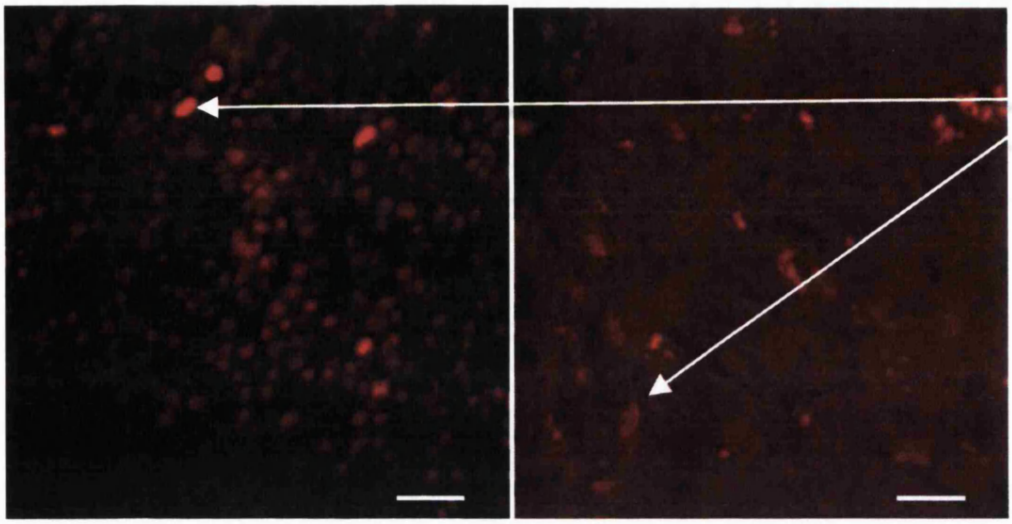

Figure 97: Group 2 – 100 µl CY3PTEN subconjunctival injection 24 h before euthanasia in both eyes. Uptake of the siRNA by the cells in the subconjunctival space was shown. Fluorescent background is reduced compared to the images obtained from the eyes harvested 6h post injection. The fluorescent intracellular signal though remains strong, indicative of the uptake of the siRNA by the cells. Magnification 20 X. Scale 50 µM.

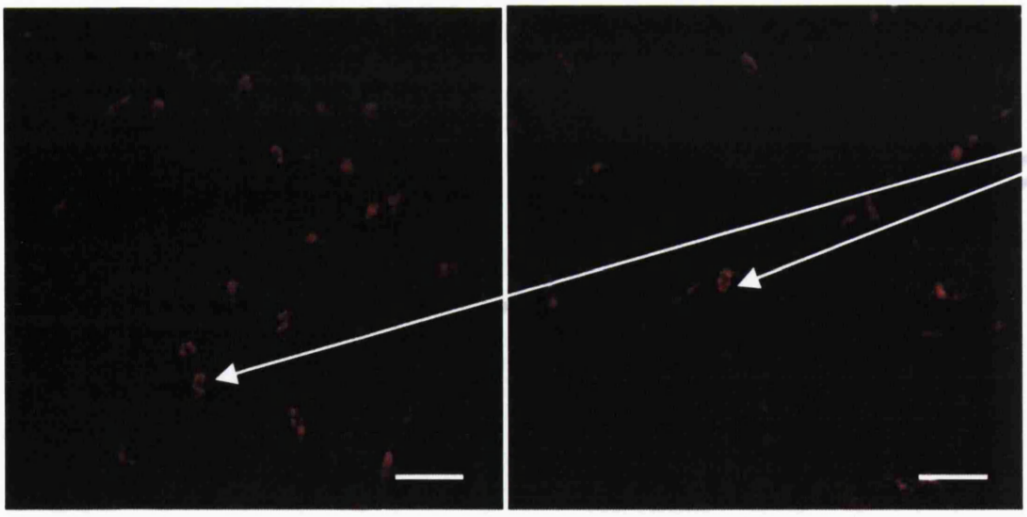

Figure 98: Group 3 – 100 µl CY3-PTEN subconjunctival injection, 7 days before euthanasia in both eyes. Uptake of the siRNA by the cells in the subconjunctival space was shown. No fluorescent background was detected. Magnification 20 X. Scale 50 µM.

The key ambiguity of this experiment was that we did not unequivocally know the nature of the cells responsible for the uptake of siRNA. The morphology of the observed

cells with siRNA was consistent for fibroblasts. However confirmation would require that a specific marker for fibroblasts be used. Upon uptake, we also need to confirm the cellular trafficking of the siRNA to determine the extent and distribution of uptake into the cytoplasm. Cellular fractionation would confirm the proportion of siRNA remaining in the endocytic pathway (i.e. within endosomes and lysosomes). Lastly, we do not know if the interaction between MMP siRNA and the cells will be the same as in the CY3PTEN siRNA and if the CY3 fluorescent radical is covalently bound with the siRNA (so we are not in place to know if only the CY3 went into the cells or the siRNA went as well).

4. DISCUSSION

4.1. Serum Amyloid P

The work that has been done during the last decade by the Ocular Repair and Regeneration Biology Unit at the UCL Institute of Ophthalmology has focused on examining scarring as a function in which the local fibrocytes, transformed into myofibroblasts, play the dominant role. By testing the effects of Serum Amyloid P in the inhibition of scarring, a broader picture of the mechanisms of wound healing after glaucoma filtration surgery was examined. Many scientific groups have suggested that non-activated fibroblasts (fibrocytes) circulating in the blood participate in the mechanism of scarring (Bucala *et al* 1994). As it was previously discussed in the introduction of this thesis, several studies provided evidence that myofibroblasts do not originate from tissue fibroblasts, but from a bone-marrow-derived precursor (Brittan *et al.* 2002; Direkze *et al.* 2003). It was suggested that these cells enter the wound area after tissue damage and, by expressing cytokines and chemokines, cleave the existing ECM and promote angiogenesis, to produce new ECM and to promote contraction (Pilling *et al* 2003). These cells were found to be involved in the promotion of fibrosis in an *in vivo* pulmonary fibrosis model (Phillips *et al* 2004), in several fibrotic disorders, such as liver cirrhosis (Friedman *et al.* 2003; Bataller & Brennen, 2005), and in autoimmune diseases (Johnson *et al.* 2002).

Human Serum Amyloid P (SAP) was shown to reduce the fibrotic reaction in many *in vivo* models and for that reason testing the effects of SAP in a local scarring model, such as the glaucoma filtration surgery scarring model in rabbits, was considered to be an interesting approach. Scarring, and subsequently the effects of SAP, is easier to be evaluated in the glaucoma filtration surgery *in vivo* scarring model, in which local administration of SAP can take place. Local administration cannot take place in other models of fibrosis, such as the pulmonary and the kidney fibrosis as well as the liver cirrhosis model in which systemic administration in much higher doses is necessary.

It is not known yet if the fibroblasts that participate in the wound healing after glaucoma filtration surgery come from local fibrocytes or from circulating monocytes or from both. The *in vitro* scarring model that is used in the Ocular Repair and Regeneration Biology Unit is based only on fibrocytes isolated from the Tenon's capsule. We tested the effect of SAP in the HTF populated collagen I gels, as this had not been tested previously. As expected, SAP did not manage to inhibit the contraction of the collagen I gels. SAP inhibits the transformation of circulating monocytes to fibroblasts, but it does not inhibit

the transformation of fibrocytes located in the Tenon's fibrocytes to myofibroblasts. In all the SAP treated groups, the HTFs located in the collagen I gels became gradually elongated and obtained a spindle-shaped appearance. They developed long processes and extended into the matrix causing contraction at the same possibly manner as the negative control group. In the ilomastat treated group (positive control), as shown in many other *in vitro* experiments, the elongation of the fibroblasts and the development of the characteristic cytoplasmic processes were delayed or even stopped.

Regarding the results from the *in vivo* experiment, our observations indicate that SAP has managed to inhibit macroscopically the scarring of the bleb significantly more compared to the negative, but also the positive control. The positive control used in this experiment is the currently used treatment in humans for scarring inhibition after glaucoma filtration surgery, which is the reason why this finding is very important. The bleb height and area were significantly increased compared to the positive and negative control groups in most of the evaluated time points. This result presents similarities with the study performed by Naik-Mathuria *et al.* (2008) in skin wounds. As described in the introduction of this thesis, many studies have indicated the structural and wound healing similarities between the conjunctiva and skin; for this reason the comparison of the effect of the SAP administration in the wound healing of the conjunctiva and the skin is important. Naik-Mathuria *et al* (2008) found that SAP treated mice with intraperitoneal or intradermal injections had slower dermal wound closure than control, which is similar to our bleb finding.

Regarding the differences in the subconjunctival scarring between rabbits treated with SAP intrableb injections only and rabbits treated with intrableb and intravenous injections, the group that was treated only with SAP intrableb injections had better results in bleb survival than the group treated with SAP intrableb and intravenous injections, although the difference was not significant. The opposite result was expected, as the monocytes transformed into fibroblasts are located in the main circulation before approaching the wound, and with the intravenous injections of SAP, blockage of this transformation was achieved not only locally but also systemically. Possibly, the introduction of human Serum Amyloid P into the rabbit circulation caused an immune reaction, which may have slightly inhibited the antiscarring inhibitory activity of Serum Amyloid P. This suggestion is also supported by the sudden death of a rabbit just after the administration of the fifth intravenous injection of Serum Amyloid P, which possibly happened due to anaphylactic shock. Blood was collected after the death of this rabbit and

from the other rabbits at the end of the experiment so that antibody levels against SAP could be measured. Promedior PLC reported to us that the antibody levels were found normal.

Furthermore, that IOP results also indicate that the administration of SAP may have been effective in inhibiting scarring after glaucoma filtration surgery in our *in vivo* model. The intraocular pressure was kept at normal levels in the SAP groups and, at many time points, the IOP was significantly lower than the negative control, but also (in fewer points) than the positive control. Additionally, the SAP treated groups showed no hypotony, as was the case with the MMC treated groups. We understand the limitations of this model regarding the measurement of the effect of potential treatment in the IOP, as the surgeries take place in normotensive rabbits and not in rabbits with high IOP. Although the significantly lower IOP of the SAP treated groups compared to the controls is a favourable finding, the effect of the SAP in eyes with high IOP may be different and was not tested.

Regarding the new histology method that was developed in order to evaluate more precisely the histological findings, this thesis suggests that this method allows the generation of more accurate results than the method previously used that grades the level of scarring on a scale of 0-4. By measuring the percentage of the bleb space covered by collagen and by comparing it between the different groups, a clearer picture can be obtained regarding the level of scarring and the effectiveness of the tested treatments. Moreover, this method recognises as an important parameter the population of the bleb by cells and for that reason the number of cells are calculated and compared.

Histological analysis of the treated eyes of the *in vivo* experiment revealed lower collagen deposition in the SAP treated groups compared to the controls. Lower collagen deposition in SAP treated animals has also been reported by Kisseleva *et al* (2006), who found that Serum amyloid P reduces scarring deposition in a bile duct ligation model. Additionally, Pilling *et al* (2007) found that Serum amyloid P inhibits bleomycin induced increase in lung collagen. As regards to the number of fibroblasts found in the bleb area, histological sections stained with Eosin and Haematoxylin showed that the SAP treated rabbits had reduced number of fibroblasts in the bleb area compared to both the positive and negative control groups. This result agrees with previously published studies that examined the administration of the SAP against fibrosis in other parts of the body. Haudek *et al* (2006) found decreased number of fibroblasts after SAP treatment in an *in vivo* cardiac fibrosis model.

Regarding the immunohistochemistry results, the results from our *in vivo* study are contradictory compared to other published studies that examined fibrosis in other tissues. It was found in our studies that the +αSMA fibroblasts in the rabbit bleb area were slightly increased in the SAP treatment groups compared to the negative control group and reduced compared to the positive control group. In contradiction to our findings, Haudek *et al* (2006) reported decreased number of +aSMA fibroblasts as an effect of the application of SAP in a cardiac fibrosis model. Additionally, Kisseleva *et al* (2006) found decreased number of +aSMA fibroblasts in an *in vivo* bile duct ligation fibrosis model. In our results there were significant differences regarding the number of the +aSMA fibroblastst between the rabbits belonging at the same groups and treated with SAP. For that reason, repetition of the experiment is suggested.

Future plan

As a future plan the following steps are suggested. First of all, as the BRU Unit of the UCL Institute of Ophthalmology has limited capacity of hosting experiments with rabbits, and because we have used only 24 rabbits for this experiment (6 in each group), repetition of the experiment is suggested in order to test reproducibility of the results. Furthermore, in collaboration with Promedior PLC we may try in the future to label the circulating monocytes of rabbits that are transformed into fibroblasts and which populate wounds. If this is achieved, we will be able to evaluate the percentage of the circulating monocytes that are transformed into fibroblasts and populate the bleb after glaucoma filtration surgery in SAP treated rabbits and in controls, as well as what is the proportion of these cells in scarring after GFS compared to the local fibrocytes.

Finally, significant amounts of research have been performed during the last decade on the role that bone marrow (BM) cells play on fibrosis. Many scientific groups have suggested, based on extensive and multiple experiments that BM cells can be transformed into fibroblasts, myofibroblasts and epithelial cells that participate in fibrosis (Brittan *et al* 2002; 2005; Direkze *et al* 2003; 2004; Lin *et al* 2008). By techniques of mitochondrial DNA (mtDNA) sequencing, it has been found that cells of the same origin also participate in the pathological mechanisms of severe fibrotic diseases. The ability of bone marrow cells to generate collagen-expressing myofibroblasts and endothelial cells has broad implications for epithelial regeneration, fibrosis and end-stage fibrotic disease (e.g. in cirrhosis). Our future aim is to study the link between the circulating monocytes that are

transformed into fibroblasts and the BM cells that participate in fibrotic processes, as well as to establish what percentage of the post glaucoma surgery fibrosis occurs because of the BM cells. Undertaking experiments on the effect of SAP, if any, on the transformation of BM cells into fibroblasts and myofibroblasts in the case of ocular fibrosis and other fibrotic conditions in the human body would be also of great interest.

4.2. Formation, characterisation and experimental evaluation of an excipientless slow release ilomastat tablet

We have observed a prolonged release of ilomastat from all the tablets we have tested. These tablets were fabricated without use of any excipients. During the release period (at least 30 days), at least 100 times higher concentration than the dose of ilomastat required to block MMPs (Ki values: Human MMP-1 (Fibroblast collagenase): 0.4 nM, Human MMP-3 (Stromelysin): 27 nM, Human MMP-2 (72 kDa gelatinase): 0.5 nM, Human MMP-8 (Neutrophil collagenase): 0.1 nM, Human MMP-9 (92 kDa gelatinase): 0.2 nM (Galardy *et al.* 1994c) was achieved throughout the experiment, as the concentration of ilomastat release from the tablet was 30 – 80 μM. This was an initial encouraging finding for the continuation of our attempts to formulate ilomastat in a way that will not require multiple injections. In previous experiments (Wong *et al.* 2003; 2005), ilomastat was administered with many subconjunctival injections; ten 100 μl injections in a 30 days bleb scarring *in vivo* study (Wong *et al.* 2003) and 15 injections in a 60 days bleb scarring *in vivo* study (Wong *et al* 2005). There are two significant disadvantages to the subconjunctival administration of the drugs in the subconjunctival space by injections. First, injections are painful and can cause eye infections. Second, it is known that the aqueous outflow from the human eye is 2μl/min. The aqueous humor is released by the ciliary body, and from the posterior chamber of the eye it goes to the anterior chamber and then, through the trabecular meshwork, it is directed to the subconjunctival space and onwards, through the scleral veins and the conjunctiva vessels to the main circulation. Aqueous outflow also takes place through the uveosleral pathway but in limited quantity compared to the trabecular meshwork pathway. Subsequently, because of the aqueous outflow, the administered drug, if it is in a liquid form, is cleared from the subconjunctival space soon after the injection and additional administrations are needed in order to re-attain again a therapeutic concentration of the drug in the subconjunctival space. For these reasons, a slow release formulation placed in the subconjunctival space at the time of glaucoma filtration surgery with which a therapeutic concentration is maintained without the need of multiple injections may offer significant advantages compared to less effective methods which also are of high risk.

In contrast to previous *in vitro* and *in vivo* experiments (Daniels *et al* 2003, Wong *et al*. 2003; 2005) we avoided the use of DMSO throughout our experiments, as it has not been approved for ocular clinical use.

Although more tablets will require evaluation in the future and additional experiments need to be performed, based on our experiments to date we have reached some important conclusions.

Regarding the findings of the tablet characteristics and the *in vitro* experiments, our results showed that the size of the rig and the flow rate used *in vitro* play a significant role in the release profile of the tablet. The detected concentration of ilomastat in the collected samples from the tablet B (4.1 mg, Figure 41), where the flow rate used was 2μl/min, was higher than in the tablet A (4.8 mg, Figure 39) which was tested with flow rate 5μl/min. Additionally, tablet B was tested in a larger rig (200μl volume), which was 4 times bigger than the rig that tablet A was tested (50μl). The lower flow rate and the larger rig in the case of tablet B extended the time that the aqueous solution interacted with the tablet, which is possibly the reason for the higher concentrations in the samples of tablet B. Indicative especially of the role that the rig size plays in the concentration of ilomastat was that when a bubble coming from the PBS 7.6 pH solution was captured into the rig as was the case with tablet B from the time point ~17000 - ~23000 minutes (Figure 41), reducing subsequently the capacity of the rig in aqueous solution and the time that the solution interacted with the tablet, the concentration was dramatically reduced. This possibly indicates that if a tablet is placed in small blebs, the dissolution rate of the tablet may be reduced compared to bigger blebs. For that reason it is suggested that the creation of large blebs and wide dissection of subconjunctival space during glaucoma filtration surgery may have an enhancing effect in the concentration of ilomastat achieved in the subconjunctival space. We understand of course that this suggestion is based on an *in vitro* model that only mimics some of the mechanical aspects of the bleb and none of the functional ones.

One of the issues that must be resolved is the minimum size of the tablet needed to achieve a therapeutic concentration for 30 days and whether a 30-day dose is required. The selected conditions used for tablet B are thought to be closer to that in the human bleb (the volume in the bleb is expected to be close to 200μl and the flow rate about 2μl/min). The initial weight of the tablet B was 4.1mg. At the end of the experiment approximately half of the tablet remained in the rig (Figure 40). For that reason, the size of the subsequent tablets was further reduced. The next ilomastat tablet that was fabricated was a 2.1 mg – 2.3 mg tablet for which 3 mg of ilomastat were used during its fabrication. It appears that 0.7 mg

of ilomastat was lost in the punch and die during the tablet fabrication process. It was expected that this reduction of the tablet size may result in a reduction of the tablet surface area, thus decreasing the release rate if dissolution rate was rate limiting. The release profile of this tablet showed that prolonged release of ilomastat can be achieved at much higher levels than the therapeutic dose (Table 18, Appendix 5.1.1.), as shown also in the tablets A and B (Table 16 and Table 17, Appendix 5.1.1.). About 60-70 % of the tablet was released by the end of day 30 in the rig. The surface areas of the cylindrical tablet in the rig that are in touch with the aqueous solution are the top and the side ones and not the bottom surface, which is in touch with the bottom of the rig, and we assume that the bottom area does not contribute to the increase of ilomastat concentration. *In vivo*, this could possibly be different, as the eye and body movements will not keep the tablet in the same one position as in the rig. Additionally, the surface of the eye where the tablet will be placed in *in vivo* experiments is not completely flat as is the rig surface. This means that possibly a very thin stroma of aqueous humor will be in touch with the bottom of the tablet as well, which can possibly lead to faster dissolution of ilomastat resulting in a higher concentration of ilomastat in the bleb. These unpredictable parameters make it difficult to accurately calculate the amount of ilomastat that we need to achieve therapeutic concentration in real life for 30 days. As the 2.1–2.3 mg tablet was more easily placed in the subconjunctival space than the larger tablets tested (tablet A and tablet B) and managed to achieve a release of ilomastat in therapeutic levels for more than 30 days, it was tested for *in vitro* and *in vivo* efficacy and we did not further reduce the size of the tablet. Further experiments in the future need to determine the dose of ilomastat that is needed in order therapeutic concentration of ilomastat in the subconjunctival space to be achieved for about 30 days. It is difficult though to accurately calculate the dose of ilomastat that is needed for antiscarring treatment after trabeculectomy. Some of the reasons are the following; although the rabbit eye and the human eye share many similarities, the aqueous outflow may present differences, which may influence the dissolution rate of the tablet. Furthermore, the aqueous outflow from normal rabbit eyes having undergone tube filtration surgery may be different from post trabeculectomy human glaucomatous eyes; the presence of enzymes in the bleb area may also influence the dissolution rate of the tablet. As the rig is only a mechanical representation of the bleb area mimicking the aqueous outflow in the subconjunctival space, the role of enzymes in the dissolution rate of the tablet cannot be tested in the rig; moreover, the bleb size does not remain stable *in vivo* but it gradually decreases. Finally, the rigs that we used for the *in vivo* experiments have a fixed size, which

is an extra reason why the dissolution rate *in vitro* and *in vivo* are different, and the ideal size dose of the tablet that should be placed in the subconjunctival space after glaucoma filtration surgery difficult to predict accurately.

As mentioned in the results section, before starting the formulation of the ilomastat tablet, we experimented with other much cheaper compounds in order to get some useful knowledge on how to fabricate powder into tablets. The compression pressure that was used to fabricate the ilomastat tablets was initially 5 bar, based on previous experience with other compounds, but as a parameter that may affect the ilomastat release from the tablet we had to assess the release profile of ilomastat tablets using different pressures. Also we had to assess whether the pressure used for the tablet fabrication results in the loss of ilomastat function. In order to test these parameters we fabricated three 2.1 mg ilomastat tablets under three different pressures: 2 bar, 5 bar and 10 bar. The release profiles of the three tablets were assessed and it was found that the tablets that were fabricated using pressures of 2 and 5 bar released ilomastat in higher concentration than the 10 bar tablet in almost all the measured time points (Table 13 and Figure 43). Additionally, the comparison between the release profiles of the 2 bar and the 5 bar tablet showed that the 2 bar tablet released ilomastat at marginally higher levels compared to the 5 bar tablet without providing any significant advantage. Because the 5 bar tablet is more firm and does not break as easily as the 2 bar tablet, we decided to continue the rest of the experiments with the 5 bar 2.1 mg ilomastat tablet.

The chromatograms of the three tablets were also compared with the chromatogram of the starting ilomastat powder in order to detect if there were potential changes in the structure of the released ilomastat. It was possible that over time the ilomastat may have undergone chemical degradation. No differences in the chromatograms were found between the three tablets. This means that the pressure that is applied to the ilomastat powder for tablet fabrication did not cause any structural changes to the chemical structure of ilomastat. Further future experiments utilising Nuclear Magnetic Resonance Spectroscopy and Differential Scanning Calorimetry could increase our understanding about different phases of ilomastat that exist in the tablet

To evaluate the reproducibility of the release profile of the 2.1 mg tablet that was fabricated at 5 bar, three similar tablets were fabricated and their release profiles were evaluated with HPLC. No significant differences were detected in the release profiles of these three tablets (Figure 46), indicating that tablets created under the same conditions displayed the same release profiles. This is very important because it established that it

should be possible to prepare a tablet that could deliver a reproducible dose. Also it means that tablets created under these conditions could release ilomastat at higher concentration than the therapeutic levels for more than 30 days.

A key need was to sterilise the tablet. There are a few ways to sterilise pharmaceutical dosage forms for parenteral administration or implants. These include aseptic preparation, the use of ethylene oxide and gamma irradiation. Preparation of ilomastat tablets under aseptic conditions is possible, but can only happen if, in the future, mass production of tablets takes place. Irradiation was thought to be the most practical method for sterilisation because all that was needed was to prepare the tablets and then put them into a vial for irradiation. No change in our fabrication process would be needed, unlike for example, if we were to use aseptic techniques. If ethylene oxide was to be used, we would have needed to have an extra process step to remove the ethylene oxide. The potential disadvantage of gamma irradiation is that it is a chemically harsh technique that can result in chemical degradation.

The effects of irradiation on other metalloproteinase inhibitors such as captopril (Volpert *et al.* 1996) have been evaluated (Engalytcheff *et al.* 2004; Engalytcheff, Vanhelleputte, & Tilquin 2004). Degradation of captopril caused from irradiation was not significant. The main peak that was appeared after the 25kGys gamma radiation of captopril counted for only 0.001% of the captopril peak (Engalytcheff *et al.* 2004). Furthermore, the same scientific group found that administration of gamma radiation to beta-blockers leads to about 0.1% degradation. With our HPLC method, we also found that the degradation of ilomastat caused by the 25KGys gamma radiation dose was not significant (0.25%) and is within the acceptable limits as defined by the European and US Pharmacopoeias (1%). It is worth mentioning that gamma irradiation offers a significant advantage for ilomastat tablet sterilization in its package, which is very important as it means that no further process are needed between gamma irradiation and the opening of the package and the placement of the tablet in the subconjunctival space during GFS.

Furthermore, we confirmed that ilomastat can be dissolved in normal media without the need to use DMSO. It is a time consuming process, as ilomastat powder needs to remain in the cell culture media for more than 12 hours to be completely dissolved in maximum concentration. In previous experiments (Daniels *et al* 2003; Wong *et al* 2003; 2005) DMSO was used *in vitro* (ilomastat dissolved initially in DMSO and added to gels) and *in vivo* (ilomastat dissolved in DMSO and administered in the subconjunctival space as 100μl injections). In previous experiments, as DMSO was used in the *in vivo* application of

the drug, the use of DMSO *in vitro* too was acceptable. As the ilomastat tablet does not contain DMSO, the dissolution of ilomastat powder in the normal media without the use of DMSO was an important step in our experimental methodology in order to test the direct effect of ilomastat *in vitro* without DMSO. We also tested the effectiveness of irradiated ilomastat in inhibiting collagen I gel contraction and we observed significant inhibition compared to the negative control and inhibition at about the same levels as the positive control. Although irradiated ilomastat seems to be slightly more potent in inhibiting gel contraction than the non-irradiated ilomastat, this difference was not statistically significant. We repeated this *in vitro* experiment three times and we believe that gamma radiation does not affect the functionality of ilomastat.

Another issue that had to be examined was the stability of the ilomastat tablet in an aqueous environment in 37 °C over the prolonged periods that would be needed. The 2.1 – 2.3 mg 5 bar ilomastat tablet was designed to stay in the bleb for about 30 days and an experiment was undertaken to evaluate if the released ilomastat from the tablet after 30 days presents any structural (and subsequently functional) differences compared to the ilomastat released from the tablet on day 1 (Figure 49). The results of all the tested tablets showed that no differences could be detected with HPLC between day 1 and day 30, which is indicative that ilomastat is not degraded by staying in an aqueous environment for 30 days. This result, although it is very encouraging, does not guarantee that ilomastat will stay stable in an animal or in a human bleb. The main reason for this is that in a living organism, there is a plethora of enzymes (e.g. endopeptidases) that can potentially cause the degradation of ilomastat.

Following these positive results, we decided to test the 2.1 – 2.3 mg ilomastat tablet that had been fabricated at 5 bar in a small scale *in vivo* experiment. We fabricated a control tablet in order to evaluate the effect of the ilomastat tablet against scarring. In order to fabricate this negative control tablet, ethylcellulose was used as a control to determine if there was any effect due simply to the physical presence of the tablet. Ethylcellulose was chosen because it does not dissolve or swell in an aqueous environment. Before the *in vivo* experiment, we made three 2.1 mg 5 bar tablets and placed them in the rig for 30 days. At the end of the 30-day period we measured the dimensions of the tablet and we found that the size of the tablet was exactly the same as before it had been placed in the rig. One ethylcellulose tablet and 3 ilomastat tablets were then sterilised. Only four rabbits were used in the first *in vivo* experiment. This limited number of rabbits was used because we did not know what would be the effects of the ilomastat tablet in the rabbit eye. We did not

want to waste rabbits if it was observed that the tablet had deleterious effects. Encouragingly, as shown in the results of the preliminary *in vivo* study, the blebs of the rabbits treated with the ilomastat tablet remained significantly elevated until the end of the 30-day period. In contrast, the bleb treated with the ethylcellulose tablet became flat after the day 10 and fibrotic tissue was observed to have formed around the bleb.

Following these encouraging results we then conducted a larger study with three treatment groups; after observing in the preliminary study that the ilomastat tablet does not cause harm to the rabbit eyes, the aim of the second study was to compare the antiscarring effect of the ilomastat tablet with MMC, the currently used treatment in clinics. As the work of this PhD is focused in developing and evaluating potentially effective anti-scarring treatments, MMC serves as the golden standard with which the potential treatments are compared. MMC application, though, is known for not being effective in all patients. The bleb often leaks and there are lots of other effects including hypotony, endophthalmitis and excessive ocular cell apoptosis that can cause irreversible vision loss (Doyle *et al.* 1993; Khaw *et al.* 1992; Khaw *et al.* 1994); these are some of the reasons that a more effective and less toxic treatment is sought. But although it is associated with severe side effects, it is possibly the most effective anti-scarring treatment used in trabeculectomies to date and for this reason it was used as the positive control in our studies. Regarding the dose of MMC, we used a moderate (2 mg/ml) and not a very high dose (5 mg/ml of MMC) in order to avoid severe side effects in the MMC treated rabbits. The same concentration is widely used in trabeculectomies in humans and was also used in former *in vivo* studies in our lab (Wong *et al* 2003; 2005). Water sponge treatment was used as the negative control. A sponge with sterile water was placed in the subconjunctival space just before the suturing of the conjunctiva at the end of the trabeculectomy. The sponge was kept in the subconjunctival space for 3 minutes (as with MMC), then removed and the conjunctiva sutured. We did not use an ethylcellulose tablet in this larger study as negative control, because the bleb size and the histological evaluation would have been very difficult. If an ethylcellulose tablet had been used, in the sections of the negative control sample a 0.4 mm high x 3 mm wide gap would have been present, as ethylcellulose is inactive and not dissolvable. This was confirmed in the sectioning of the treated eye with an ethylcellulose tablet in the preliminary *in vivo* study. The ilomastat tablet is different, because ilomastat does dissolved in an aqueous environment (in this case in the aqueous humor that reaches the subconjunctival space through mainly the tube that connects the anterior chamber with the subconjunctival space). The results were again very encouraging, as the ilomastat

tablet group had significantly better bleb survival compared not only with the negative control group but also with the positive control group (Figure 58). None of the rabbits treated with ilomastat tablets had flat blebs at the end of the experiment (Figure 57). On the other hand, all the negative control rabbits and most of the positive control ones had failed blebs at the end of the experiment. This result is superior to studies done in the past in which multiple ilomastat injections were used as treatment anti-scarring method (Wong *et al* 2003; 2005). Additionally, the size of the bleb in the ilomastat tablet treated group was significantly larger compared to the positive and negative control groups as shown in Figure 59 and Figure 60.

Histological analysis of the positive control, negative control and ilomastat tablet treated blebs indicated that in the ilomastat tablet treated blebs limited collagen was deposited compared to the positive and negative control. In both the negative and positive control groups, the fibrosis was more established throughout the bleb area and the development of scar tissue was more apparent compared to the ilomastat bleb treated rabbits. These results agree with the findings of the study performed by Wong *et al.* (2003), which found limited deposition of scar tissue in the eyes treated with multiple ilomastat injections after trabeculectomy compared to negative control (PBS injections) treated rabbit eyes. In a following study, Wong *et al* (2005) tested the effects against scarring of multiple ilomastat injections compared to PPBS injections (negative control) and intraoperative application of MMC (positive control). Reduced scarring was observed in the blebs treated with multiple ilomastat injections. In the MMC treated blebs reduced loose subconjunctival tissue was observed in the centre of the blebs and dense scarring tissue in the periphery of the bleb. The MMC treated blebs in our *in vivo* study had dense scarring tissue in the periphery, which agrees with the results of the Wong *et al.* (2005) study, but also had dense scarring tissue in the centre of the bleb, which disagrees with the Wong *et al* (2005) study. Deposition of dense scarring tissue in the MMC treated blebs was also observed in our *in vivo* study in which we tested the antiscarring effect of the serum amyloid P. It is also worth noting that deposition of dense scarring was found in every single rabbit treated with MMC in these two *in vivo* studies. This difference cannot be attributed to the dose of the MMC used, as in Wong *et al* (2005) and in our *in vivo* studies the same MMC dose (0.2 mg/ml) was used. Wong *et al* (2005) does not mention if the finding of loose subconjunctival tissue in the MMC treated blebs was observed in all the treated rabbits with MMC or in some of them.

The effect of the treatments on IOP was tested, too. It was found that the IOP in the ilomastat tablet treated blebs was maintained at normal levels and at many time points was significantly lower than the negative control group (Figure 61). There were also two time points where the IOP was significantly lower compared to the positive control. This result is also very encouraging, as it further confirms the outflow of the aqueous humor from the rabbit eye and the functionality of the bleb. This result agrees with the findings of the Wong *et al* (2005) study, which indicated that rabbit eyes treated with multiple ilomastat injections against scarring after GFS maintained normal IOP for significantly longer period after GFS compared to the negative control (PBS injections). Additionally, the hypotony observed in the MMC group in our study was not observed in the ilomastat tablet group. We understand the limitation of this experiment, as the treatments were tested in normotensive rabbits. Unfortunately there are no rabbit *in vivo* glaucoma models with high IOP in which we could test the tablets. Our *in vivo* model has been developed to evaluate the inflammatory, fibrotic and healing responses to the GFS procedure. Attempts to develop a high IOP rabbit *in vivo* model using steroids resulted in high mortality rate (personal communication). The glaucoma filtration surgery model in rabbit offers the advantage that rabbits scar very quickly and the potential success of an anti-scarring treatment in rabbits for 30 days suggests that the treatment would be successful in humans for an extended period of time.

Aqueous humor, vitreous body and blood samples were collected on the day that the experiment was terminated to test if ilomastat could be detected in aqueous humor, vitreous body and blood serum. Analysis of the samples with HPLC showed that no ilomastat was detected in any of the samples of the treated rabbits with the ilomastat tablets, which indicates that side effects linked to the tablet treatment are unlikely. Our HPLC ilomastat method though detects ilomastat in concentration as low as 0.125 μM. We understand that a more sensitive method is necessary in order to detect traces of ilomastat in the tissues, as ilomastat inhibits MMPs in the nanomolar range. A new method is developed at the moment in the Ocular Repair and Regeneration Biology Unit using mass spectrometry for the detection of ilomastat in the range of nM.

The limited risk of side effects was further suggested by no detection of signs of conjunctival or corneal tocixity, inflammation, atrophy of the conjunctiva or structural changes in the anatomical structures of the eye. The assessment was done both macroscopically and by histological evaluation of the structures of the treated eyes compared to controls. Regarding inflammation, the limited number of eosinophils found in

almost all the specimens indicates that the presence of eosinophils is not linked with a specific treatment. The blebs of all the rabbits looked healthy throughout the experiment and no signs of macroscopical hypervascularisation were observed in any of the treated eyes with the ilomastat tablet.

This innovative project constitutes to the best of our knowledge the first attempt to develop a prolonged release formulation against scarring after glaucoma filtration surgery. The sterile (after gamma radiation) ilomastat tablet meets the criteria of the European and the US pharmacopoeia for the lack of degradation after radiation and significantly inhibited scarring and enhanced bleb survival compared to the positive and negative controls as shown in the *in vitro* and *in vivo* results. As the positive control (MMC) used in this experiment is the currently used anti-scarring treatment after glaucoma filtration surgery, this work indicates that the ilomastat tablet may offer enhanced therapeutic effect in the attempts to inhibit scarring after glaucoma filtration surgery, and subsequently the increase in IOP and potential blindness.

Future plan

Our future plan includes the fabrication of tablets that release ilomastat for 10, 20, 30, 45, 60-days in order to increase our understanding about the release profile of excipientless tablets in non sink conditions. Additionally, we aim to develop an ilomastat detection method significantly more sensitive than the one that was used for the aforementioned experiments. This will be important in order to detect traces of ilomastat in tissues. We aim to perform experiments in order to establish the amount of drug that is needed for a therapeutic outcome *in vivo*. Further studies are planned that will perform physicochemical characterisation of the tablet during and post *in vivo* studies in order to detect potential physicochemical changes that happen to the tablet in the aqueous *in vivo* environment. To assess the decomposition issue of ilomastat *in vivo*, we are planning to sacrifice rabbits at several time points during and after the standard 30-day period. Aqueous humor from the bleb as well as the remaining tablet will be collected and HPLC analysis and *in vitro* experiments (dissolving the tablet remaining in the bleb) will be performed, in order to determine the functionality of the remaining in the bleb ilomastat (if the remaining ilomastat in the bleb would have been degraded or not). We also plan to harvest the eyes and perform ocular histology in order to evaluate with higher numbers the anti-scarring effect of the tablet and determine local ocular toxicity. This can also happen at different

time points. An *in vivo* evaluation-dose escalation study using 45 and 60-day doses needs to be performed for safety and toxicity reasons. Furthermore, ocular and systemic distribution of ilomastat using HPLC needs to be determined. If all the steps are successfully performed and the encouraging findings presented in this thesis are confirmed, the plan is to source GMP grade ilomastat, fabricate and characterise GMP tablets and evaluate optimised dose reproducibility *in vivo* using GMP ilomastat tablets.

4.3. Novel matrix inhibitors for MMPs

As the inhibition of Matrix Metalloproteinase inhibitors has been found to be a vital process in order to inhibit scarring after glaucoma filtration surgery, during the three years of work that is presented in this thesis, we sought new matrix mettaloproteinase inhibitors in order to test their effectiveness against scarring. This included a collaboration with AstraZeneca was created, which had developed many MMP inhibitors, which have never been tested against ocular scarring.

All four MMPis from AstraZeneca were found to be effective against contraction in our *in vitro* model of scarring (collagen I gels populated with HTFs) over seven days. The compounds were also observed to inhibit the elongation of HTFs. In particular, compound 4 was shown to be more effective than ilomastat, which is known to effectively inhibit MMPs and contraction *in vitro* and *in vivo* (Wong *et al* 2003; 2005). Based on these preliminary results, we believe that these compounds warrant further study. Compounds 1 and 3, due to their high solubility – 11 fold and 30 fold respectively higher than ilomastat- are not suitable for the formulation of slow release mechanisms to be placed in the subconjunctival space after glaucoma filtration surgery. The reason is that the quantity needed in order to keep the concentration of the compounds high in the bleb area would be significantly more and the size of the slow release formulation significantly larger, which could potentially create problems in the aqueous outflow from the eye after the glaucoma filtration surgery. However, these inhibitors are effective against MMPs and can potentially be used therapeutically in other scarring conditions. On the other hand, the limited solubility of compounds 2 and 4 make them ideal for slow release formulations, as we had observed in previous experiments with ilomastat. No development of vacuoles (which is a sign of cytotoxicity) was observed in any of the groups.

Future plan

Future experiments should focus on these and other compounds which have similar ability to reduce contraction and which are of similar solubility to ilomastat. In order to test the applicability of one or more of the AstraZeneca compounds for further development as an anti-scarring treatment, further information about the physical and chemical properties of the compounds will be needed for subsequent *in vitro and vivo* studies. This would allow the development of an HPLC method that will allow accurate measurement of the concentration of the molecule.

The formulations can be tested in the *in vivo* glaucoma filtration surgery scarring model. Bleb survival and size as well as intraocular pressure should be evaluated. Histological analysis, in situ zymography and microarray analysis can provide important information regarding the effectiveness of the compound(s) to inhibit scarring *in vivo*.

If these results are successfully completed and the reproducibility of favourable *in vivo* results is achieved, the slow release formulations could potentially be tested in humans for scarring inhibition after glaucoma filtration surgery and other scarring situations in the human body.

4.4. Small interfering RNAs (siRNAs) against MMPs

Based on the observations of the *in vitro* experiments, it is suggested by this thesis that SiRNAs against MMP-1,-2,-3,-8 and -9 may manage to inhibit contraction. The *in vitro* results indicate that some of the siRNA treatment groups (the siRNA 100nM with and without lipofectamine and the siRNA 30nM groups) inhibit the contraction of Human Tenon's Fibroblasts populated collagen I gels significantly more than the negative control. The same treatment groups were found to be also more effective in inhibiting contraction of the collagen I gels (*in vitro* contraction model) than the positive control (ilomastat 100uM), although the end result between these groups and the ilomastat group was not different. This thesis did not test how the inhibition of contraction was achieved, because the work done for the siRNA project was based on a contract agreement reached between UCL and Quark PLC and the aim was to test the effectiveness of the SiRNAs in our *in vitro* and *in vivo* contraction models and not the mechanisms of function. So although the *in vitro* results indicate that the five siRNA molecules against MMPs may be effective against scarring, it is not known if this was achieved because the siRNAs indeed managed to inhibit the production of MMPs, or because of the cytotoxicity caused to the HTFs.

As presented in the 'Results' section, cytotoxicity was found in the siRNA treatment groups, especially the ones in which lipofectamine was used as a transfection agent. Based on the *in vitro* results, the siRNAs with lipofectamine were no more effective in inhibiting contraction than the siRNAs without lipofectamine. This can possibly be explained by the mention in the patent of the siRNA molecules: the siRNAs used in the preparation of the pharmaceutical composition (as used in our *in vitro* and *in vivo* experiments) were admixed with a carrier in a pharmaceutical effective dose and were conjugated to a steroid or to a lipid or to another suitable molecule e.g. cholesterol. This means that the mechanism of endocytosis, a major cellular mechanism that facilitates the uptake by the cells of macromolecules, was used for these molecules to enter the cells. This mechanism has been suggested as a tool for effective RNA interference by many scientists (Sioud, 2006)

Should an extra transfection agent be needed to facilitate the endocytosis of the siRNAs, lipofectamine is possibly not the best option because of the resulting cytotoxicity, as shown in our case and by others (Clemens *et al.* 2007). Many research groups around the world that have achieved excellent *in vitro* results with different siRNAs do not use

lipofectamine due to the cytotoxicity and there are better transfection agents in the market specialized for SiRNA transfection.

MMPs play a significant role in wound contraction (Occleston N. *et al* 1995, Scott KA *et al* 1998, Porter RA *et al* 1998). A potential knock out of the MMP 1,2,3,8 and 9 genes by the siRNA molecules would have caused prevention of scarring and subsequently prolonged bleb survival (Wong *et al.* 2003; 2005), which did not happen in this siRNA *in vivo* experiment. There are three main the siRNA molecules may have been ineffective in inhibiting contraction. First, the MMP siRNAs may not be effective in the first place in inhibiting MMPs efficiently, meaning that their function may not or may only partially destroy the mRNAs that are translated to the five MMPs. Secondly, no previous studies have been performed regarding effective dosing patterns and subsequently the concentration and the number of injections for effective RNAi is not known. Lastly, the siRNAs may not manage to enter the HTFs, which are the main cells that participate in the wound healing after glaucoma filtration surgery and are the target cells for the inhibition of the expression of MMPs.

Several questions emerged from the second *in vivo* experiment. We do not know the nature of the cells that uptake the siRNA (although the cell shape is indicative for fibroblasts), so we cannot know if fibroblasts uptake the siRNA; a specific marker for fibroblasts may be needed for any future experiments. However, there are no reliable markers on the market for fibroblasts only. Also, we do not know if the siRNA spread into the cytoplasm or was captured from lysosomes that degrade it, making it ineffective. Lastly, we do not know if the interaction between the MMP siRNAs and the cells will be the same as in the CY3PTEN siRNA and if the CY3 fluorescent radical is covalently bound with the siRNA (so we cannot know if only the CY3 went into the cells or the siRNA went as well).

Future plan

As a future guide for the testing of the effectiveness of the Quark PLC siRNAs against MMP-1, -2, -3, -8 and -9, the following experimental steps are suggested.

Firstly, repetition of the *in vitro* experiments would give us more information of the effect of the MMP siRNAs against the contraction function of fibroblasts. Apart from the inhibition of contraction, measurements, zymography, western blotting or ELISA should be performed in order to test if the SiRNA managed to knock out the specific MMPs in the

media from the cultures of fibroblasts. RTPCR and QTRTPCR can also be very helpful, as they will facilitate the testing of the existence and the levels of the MMP-1, -2, -3, -8 and -9 mRNA, which is the direct target of the SiRNAs. In addition, labeling of the siRNAs with a fluorescent radical will allow the percentage of the cells that are transfected in *in vitro* cultures to be determined. Studies about tissue penetration are also suggested before a new *in vivo* study. If a good transfection percentage as well as knock out of MMPs is achieved, then these two parameters could be good indicators for *in vivo* testing of the molecules. The *in vivo* effectiveness of the siRNAs can be tested in our *in vivo* scarring model and in addition to macroscopical evaluation of the function of the bleb, histological evaluation of the inhibition of scarring should also be done.

CONCLUSIONS

It is known that scarring plays a vital role in the failure of the glaucoma filtration surgery. Scarring develops as the result of pathological mechanisms of eye diseases and affects vision. Our work was focused on two main goals. Firstly, to develop and test methods and molecules that could inhibit the activity of Matrix Metalloproteinases. Second, to study the role of Serum Amyloid P (SAP) in fibrosis after experimental glaucoma filtration surgery. To achieve the first goal, we developed a slow release ilomastat tablet, which is effective against our well-established *in vitro* and *in vivo* fibrosis models. Novel MMP inhibitors were tested for first time in a HTF contraction model, and had a significant anti-contraction effect *in vitro*. SiRNA treatment was unsuccessful in our *in vivo* model but it is worthwhile that the experiments on the anti-scarring effects of siRNAs had several limitations. Regarding our second goal, SAP was successful in prolonging the survival of the bleb in our in vivo model. The results of our work are very encouraging and indicate that the aforementioned molecules/formulations have a significant potential against fibrosis *in vitro* and *in vivo* (post experimental glaucoma filtration surgery). Further experiments and clinical trials stemming from this initial work may lead soon to potential treatments against scarring after glaucoma filtration surgery as well as against fibrosis in other parts of the human eye and body.

5. APPENDICES

5.1. Appendix 1

5.1.1. Release data of the tested ilomastat tablets

	Ilomastat Tablet A without excipient (W=4.8mg) started on 14-12-2006 HPLC results									
Collect point	No.	Time point	Peak Area			AVR PA	Volumn(ml)	Concentration (μM)	Released Amount (mg)	Release %
19.00 14-12-06	0	0						0	0	0.00%
23.40 14-12-06	1	280	157.488	155.957	156.809	156.7513333	1.2001	114.7491472	0.05350051	1.11%
9.30 15-12-06	N1	870	137.229	135.642	136.502	136.4576667	2.592	99.91459552	0.100613198	3.21%
11.40 15-12-06	2	1000	134.968	132.079	133.747	133.598	0.629	97.82419591	0.023904956	3.71%
13.30 15-12-06	3	1110	129.648	130.721	130.331	130.2333333	0.5332	95.36464425	0.019754614	4.12%
15.30 15-12-06	4	1230	129.561	128.325	129.147	129.011	0.5724	94.47112573	0.021008243	4.56%
19.30 15-12-06	5	1470	131.138	132.783	129.365	131.0953333	0.9864	95.99476121	0.036786767	5.32%
9.35 16-12-06	6	2315	112.444	113.384	113.338	113.0553333	4.1481	82.80762671	0.133447542	8.10%
19.30 16-12-06	7	2910	97.03	97.095	98.225	97.45	2.9284	71.4002193	0.081230844	9.80%
9.45 17-12-06	8	3765	73.847	73.202	72.517	73.18866667	4.7233	53.66532651	0.098475984	11.85%
19.30 17-12-06	9	4350	69.816	67.342	69.007	68.72166667	2.6526	50.39997563	0.051938944	12.93%
9.30 18-12-06	10	5190	59.512	59.458	58.878	59.28266667	3.89	43.50012183	0.065740212	14.30%
17.45 18-12-06	11	5685	58.327	60.744	59.668	59.57966667	2.4366	43.7172271	0.041383562	15.16%
17.45 19-12-06	13	6180	55.1	54.563	54.488	54.717	2.0125	40.1626462	0.031401416	15.82%
9.40 20-12-06	14	7135	58.549	57.778	58.256	58.19433333	4.264	42.70455653	0.070742831	17.29%
19.10 20-12-06	15	7705	54.922	55.193	54.477	54.864	2.7983	40.27010234	0.043779221	18.20%
9.40 21-12-06	16	8575	55.348	55.694	55.868	55.63666667	4.151	40.83491715	0.06585298	19.57%
18.15 21-12-06	17	9090	83.965	83.557	83.618	83.71333333	2.1473	61.3587963	0.051187106	20.64%
10.15 22-12-06	18	10050	103.506	104.524	103.178	103.736	4.1123	75.99524854	0.121412179	23.17%
18.15 23-12-06	19	11970	94.154	93.2	91.605	92.98633333	8.7515	68.13730507	0.231663958	28.00%
12.15 26-12-06	20	15930	72.826	73.267	72.786	72.95966667	18.8311	53.49792885	0.391384553	36.15%
11.45 27-12-06	21	17340	69.403	70.947	69.854	70.068	6.7603	51.38413743	0.134954094	38.96%
13.30 29-12-06	22	20325	62.785	62.415	63.097	62.76566667	14.4484	46.04617446	0.258466543	44.35%
14.55 31-12-06	23	23290	71.743	71.822	71.599	71.72133333	14.0847	52.59271442	0.287782387	50.34%
14.00 02-01-07	24	26115	68.958	69.033	69.623	69.20466667	13.4965	50.75304581	0.266118026	55.89%
9.55 04-01-07	25	28750	54.295	54.414	53.755	54.15466667	12.9323	39.75158382	0.19971985	60.05%
13.00 06-01-07	26	31815	44.125	44.864	45.289	44.75933333	15.0127	32.8836501	0.191791717	64.04%
18.00 08-01-07	27	34995	43.208	43.358	43.558	43.37466667	15.2311	31.87146686	0.188592468	67.97%
12.15 10-01-07	28	37530	14.723	14	14.022	14.24833333	11.4824	10.58028752	0.047197736	68.95%
10.25 12-01-07	29	40300	10.038	10.702	10.739	10.493	12.6964	7.835160819	0.038647333	69.76%
10.00 15-01-07	30	44595	12.813	13.096	13.132	13.01366667	20.0826	9.677753411	0.075506704	71.33%
14.40 16-01-07	31	46315	12.744	12.918	13.31	12.99066667	8.0509	9.660940546	0.030217245	71.96%

Table 16: Release profile of the Ilomastat tablet A (4.8mg).

	Ilomastat Tablet B without excipient (W=4.1mg) started on 17-1-2006 HPLC results									
Collection point	No.	time point	Peak Area			AVR PA	Volumn(ml)	Concentration (μM)	Released Amount (mg)	Release %
17/01/2007 14:15	1	125	76.724	76.738	77.774	77.07866667	0.2353	55.16239618	0.005042618	0.12%
17/01/2007 16:20	2	250	124.471	124.647	124.983	124.7003333	0.2453	88.77689937	0.008460354	0.33%
17/01/2007 18:40	3	390	121.179	121.461	121.376	121.3386667	0.2683	86.40401402	0.009006284	0.55%
18/01/2007 10:15	4	1325	134.017	134.277	134.948	134.414	1.8601	95.63344392	0.069109398	2.23%
18/01/2007 12:20	5	1450	128.249	128.879	129.151	128.7596667	0.241	91.64224371	0.008580326	2.44%
18/01/2007 14:55	6	1605	122.177	123.375	123.525	123.0256667	0.318	87.59480953	0.010821726	2.71%
18/01/2007 18:10	7	1800	121.623	122.639	122.078	122.1133333	0.3767	86.95082469	0.012725075	3.02%
19/01/2007 10:00	8	2750	118.387	117.594	118.36	118.1136667	1.897	84.127597	0.062000735	4.53%
19/01/2007 19:10	9	3300	118.88	120.321	120.56	119.9203333	1.0905	85.40286111	0.036181712	5.41%
20/01/2007 11:40	10	4286	113.81	114.048	114.532	114.13	1.9651	81.31566316	0.06207974	6.93%
20/01/2007 21:20	11	4866	111.149	111.503	111.717	111.4563333	1.1597	79.42841345	0.035785951	7.80%
21/01/2007 11:45	12	5726	104.638	104.145	103.55	104.111	1.7169	74.24359427	0.049521639	9.01%
21/01/2007 23:05	13	6286	126.784	126.61	127.319	126.9043333	1.1772	90.33262747	0.041312923	10.02%
22/01/2007 09:40	14	6921	119.29	120.395	120.544	120.0763333	1.096	85.51297617	0.036411083	10.90%
22/01/2007 20:05	15	7526	111.619	111.656	111.987	111.754	1.0547	79.63852615	0.032631962	11.70%
23/01/2007 10:30	16	8387	99.59	98.474	99.683	99.249	1.5183	70.81167502	0.041768943	12.72%
23/01/2007 17:30	17	8807	97.844	97.385	98.147	97.792	0.7384	69.78322863	0.020018603	13.21%
24/01/2007 10:25	18	9822	95.043	95.341	95.806	95.39666667	1.396	68.09244488	0.036929665	14.11%
24/01/2007 21:00	19	10454	92.692	92.532	92.841	92.68833333	0.8332	66.18072516	0.021422582	14.63%
25/01/2007 09:29	20	11203	99.118	99.057	99.257	99.144	1.0931	70.73755912	0.030040073	15.36%
25/01/2007 19:05	21	11779	100.226	100.796	100.72	100.5806667	0.8713	71.7516529	0.024287938	15.95%
26/01/2007 10:20	22	12694	101.087	101.081	100.8	100.9893333	1.5272	72.0401167	0.04274264	17.00%
26/01/2007 18:50	23	13204	140.128	140.666	141.232	140.6753333	0.8061	100.0531046	0.031333616	17.76%
27/01/2007 19:10	24	14664	133.228	133.705	136.782	134.5716667	2.0833	95.74473542	0.077492155	19.65%
28/01/2007 15:20	25	15874	139.667	139.716	140.24	139.8743333	1.9183	99.48770617	0.074144163	21.46%
29/01/2007 15:00	26	17294	57.499	57.445	57.715	57.553	2.6583	41.37989694	0.04273507	22.50%
30/01/2007 18:00	27	18914	49.137	49.309	49.563	49.33633333	3.0499	35.58003341	0.042158289	23.53%
31/01/2007 17:30	28	20324	46.969	46.287	45.8	46.352	2.4316	33.47349474	0.031621627	24.30%
01/02/2007 18:45	29	21841	41.858	42.031	41.797	41.89533333	2.7759	30.32768641	0.032706504	25.10%
02/02/2007 14:15	30	23011	42.755	42.323	42.551	42.543	2.2261	30.78485212	0.026623967	25.75%
03/02/2007 21:45	31	24901	93.056	92.924	92.431	92.80366667	3.3564	66.26213501	0.086403266	27.86%
04/02/2007 21:50	32	26346	88.894	88.676	88.447	88.67233333	2.776	63.34596833	0.068317107	29.52%
05/02/2007 15:25	33	27401	82.583	82.637	82.669	82.62966667	1.9655	59.08065693	0.045113798	30.62%
06/02/2007 14:02	34	28758	72.349	72.755	72.87	72.658	2.5736	52.04199901	0.05203386	31.89%
07/02/2007 17:45	35	30421	77.961	77.421	78.448	77.94333333	3.1176	55.77273476	0.067551245	33.54%
08/02/2007 16:25	36	31661	79.964	79.743	79.56	79.75566667	2.4373	57.05199878	0.054022027	34.86%
09/02/2007 20:12	37	33328	73.109	73.59	72.785	73.16133333	2.9739	52.39728477	0.060537735	36.33%
10/02/2007 20:02	38	34758	83.51	82.953	82.943	83.13533333	2.5168	59.4375897	0.058116696	37.75%
11/02/2007 19:39	39	36175	82.228	82.482	82.312	82.34066667	2.4738	58.87666173	0.05658467	39.13%
12/02/2007 15:24	40	37460	78.173	78.153	78.111	78.14566667	2.1196	55.91555493	0.04604448	40.25%
13/02/2007 19:00	41	39110	73.434	73.821	73.954	73.73633333	2.9937	52.80315757	0.061412842	41.75%
14/02/2007 16:18	42	40388	75.344	75.714	75.904	75.654	2.4126	54.15677278	0.050760878	42.99%
15/02/2007 18:15	43	41945	63.16	63.386	63.451	63.33233333	2.9028	45.45933037	0.051266205	44.24%
16/02/2007 17:40	44	43342	71.482	71.508	71.743	71.57766667	2.2821	51.27942872	0.045464129	45.35%
17/02/2007 19:20	45	44882	67.218	67.43	67.623	67.42366667	2.664	48.34726242	0.050037676	46.57%
18/02/2007 14:30	46	46032	68.866	68.951	69.157	68.99133333	2.0982	49.45382462	0.04031232	47.55%
19/02/2007 11:25	47	47347	65.282	65.489	65.722	65.49766667	2.106	46.98776499	0.038444497	48.49%

Table 17: Release profile of the Ilomastat tablet B (4.1 mg).

	Ilomastat Tablet without excipient (W=2.3mg) started on 17-1-2006 HPLC results										
Collection point	No.	time point	Peak Area				AVR PA	Volume (ml)	Concentration (μM)	Released Amount (mg)	Release %
27/05/2007 11:25	0	0							0	0	0.00%
28/05/2007 13:35	1	1570	118.017	117.66	117.746	117.466	117.72225	3.1243	83.85130938	0.101777927	4.43%
29/05/2007 16:50	2	3205	114.342	114.49	114.053	114.761	114.4115	3.2863	81.51436437	0.104071635	8.95%
30/05/2007 13:15	3	5655	113.414	113.822	113.69	113.546	113.618	2.4501	80.9542599	0.077057434	12.30%
31/05/2007 14:30	4	7170	62.568	62.567	62.588	62.633	62.589	3.302	44.93463683	0.057643365	14.81%
01/06/2007 09:20	5	8300	77.02	77.173	76.899	76.791	76.97075	2.2374	55.0862215	0.047882591	16.89%
02/06/2007 16:55	6	10195	75.027	75.15	75.409	75.137	75.18075	3.6196	53.82272182	0.075686297	20.18%
04/06/2007 08:10	7	12430	79.74	78.995	79.474	78.903	79.278	4.4702	56.71483024	0.098495097	24.46%
05/06/2007 11:25	8	14065	71.271	71.165	71.17	71.141	71.18675	3.3518	51.00349404	0.066415439	27.35%
06/06/2007 17:10	9	15850	71.049	71.059	71.301	71.187	71.149	3.5702	50.9768476	0.070706045	30.42%
07/06/2007 16:15	10	17235	57.555	58.416	58.827	58.799	58.39925	2.7007	41.97723583	0.044043437	32.34%
08/06/2007 19:20	11	18980	72.262	72.248	72.361	72.499	72.3425	3.839	51.81929837	0.07728597	35.70%
09/06/2007 12:45	12	20025	73.139	72.187	72.203	72.141	72.4175	2.0691	51.8722383	0.041697258	37.51%
10/06/2007 13:05	13	21485	55.137	56.024	55.776	55.777	55.6785	2.92	40.05675161	0.04544118	39.49%
11/06/2007 21:40	14	23440	58.535	53.968	54.773	54.357	55.40825	3.9206	39.86599139	0.060722008	42.13%
13/06/2007 07:05	15	25445	54.524	54.362	54.123	54.705	54.4285	4.1503	39.17441943	0.063164503	44.87%
14/06/2007 12:30	16	27210	63.931	64.116	64.717	64.678	64.3605	3.5123	46.185078	0.063020858	47.61%
15/06/2007 11:35	17	28605	62.099	61.387	62.312	61.232	61.7575	2.79	44.34770947	0.048069148	49.70%
17/06/2007 16:05	18	30315	57.275	57.316	57.37	57.441	57.3505	3.4029	41.23695913	0.054516359	52.07%
18/06/2007 12:00	19	31510	49.415	49.415	49.325	48.939	49.2735	2.4139	35.53568151	0.033325367	53.52%
19/06/2007 15:15	20	33145	62.381	62.381	62.764	62.493	62.50475	3.3062	44.87516764	0.057640299	56.03%
20/06/2007 15:00	21	34570	60.181	60.377	60.525	60.411	60.3735	2.8471	43.37079128	0.047972361	55.77%
21/06/2007 17:35	22	36165	55.417	55.455	55.412	55.499	55.44575	3.2075	39.89246135	0.049710545	57.93%
22/06/2007 19:55	23	37745	62.733	62.54	62.635	62.639	62.63675	3.16	44.96834192	0.055205835	60.33%
23/06/2007 12:25	24	38735	56.011	56.075	55.891	56.001	55.9945	1.9503	40.27980518	0.030519668	61.66%
24/06/2007 21:30	25	40720	59.344	59.301	59.117	59.132	59.2235	4.0196	42.55904567	0.066460827	64.55%
25/06/2007 16:10	26	41880	53.976	53.999	54.054	54.012	54.01025	2.2968	38.87919108	0.034692167	66.06%
26/06/2007 17:55	27	43425	53.478	53.5	53.499	53.519	53.499	3.1055	38.51831722	0.046471839	68.08%

Table 18: Release profile of the Ilomastat tablet C (2.3 mg).

5.2. Appendix 2

5.2.1. Novel anti-steroid anti-glaucoma drops

During the course of this PhD we worked on a project regarding the effect of hypotensive agents that could potentially be used in the management of glaucoma patients. For this reason this work has been included in the thesis, but because it is not linked with wound healing which is the main focus of this thesis, the work is presented in the appendices.

5.2.1.1. Introduction - Steroid-induced glaucoma

Corticosteroid therapy can result in raised intraocular pressure (IOP). If the duration and level of this increase is significant, it can lead to the development of glaucoma and subsequently to apoptosis of optic neurons resulting in visual field loss and eventually blindness. Several studies, like (Gordon *et al.* 1951), have described the role of corticosteroids in the elevation of IOP. Moreover, it is known that the diurnal fluctuation of IOP may happen because of cortisol levels. This normal condition is absent in patients with removed adrenals (Smith 1966), raised IOP is observed in adrenal adenomas (excessive cortisol production) (Haas & Nootens 1974). In 5% of normal eyes, 92% of primary open angle glaucoma (POAG) patients and 30% of their relatives increased IOP develops after about 6-8 weeks after the application of steroid drops. This elevated IOP declines several weeks after stopping the steroid treatment (Phillips *et al.* 1984).

Mifepristone (or RU-486) is a steroid with similar structure to the natural hormone progesterone. Being a competitive inhibitor of the progesterone receptor, it is categorized as a progesterone antagonist. In pregnancy, the secretion of progesterone by the mother is important to maintenance a healthy pregnancy and the nutrition of the embryo. RU-486 has a structural similarity with progesterone but it is also effective for abortions, as it sends a stop signal to the production of progesterone, due to total occupation of the progesterone receptors in the uterus and dilation of the cervix resulting in abortion.

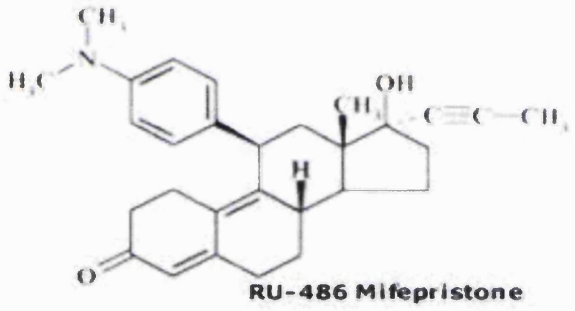

Figure 99: Stereochemical structure of Mifepristone.

The effect of the compound RU486-6 which is similar to Mifepristone (RU-486) on IOP has been tested in rabbit eyes by (Phillips *et al* 1984). During the study, which lasted 13 weeks with RU 486-6 drops three times per day, the authors observed a lowering effect on IOP which they suggested could be either because of steroid blockage leading to an increase of the aqueous outflow through trabecular meshwork, or a decrease of the aqueous production from the ciliary body, or because of reasons irrelevant to steroid blockage action, such as corneo-scleral softening or thinning. Our lab, in a joint project with DanioLabs (subsequently Summit plc), aimed to develop further these exciting findings. We decided to test the effectiveness in IOP reduction of three newly created compounds with structures close to the RU-486, namely RU-42633, RU-42848 and RU-42698.

DanioLabs-Summit plc provided three steroid antagonist molecules, RU 42698, the RU 42848 and the RU 42633 to be tested for their effectiveness in decreasing IOP.

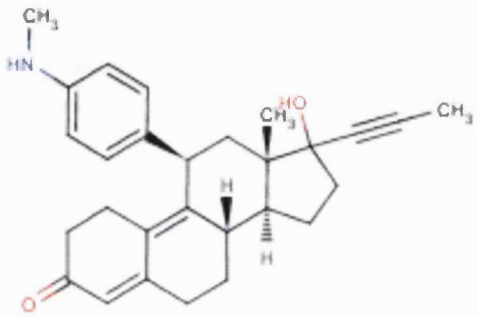

Figure 100: Stereochemical structure of RU - 42633.

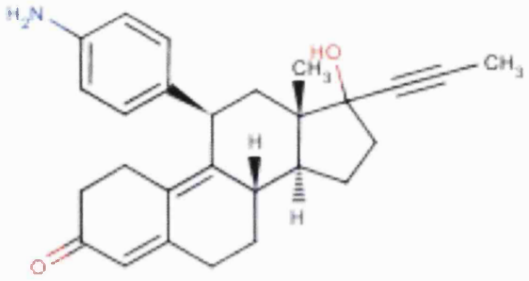

Figure 101: Stereochemical structure of RU – 42848.

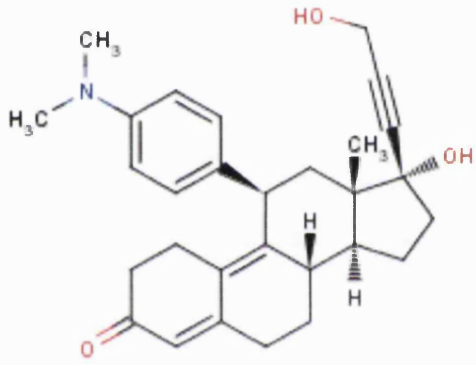

Figure 102: Stereochemical structure of RU - 42698.

Three studies were designed in order to test the efficacy of the compounds.

5.2.1.2. Materials and Methods

5.2.1.2.1. Study I

As the capacity at the UCL Institute of Ophthalmology is for 24 rabbits to be housed, and this study required 48 rabbits, Study I was run in two blocks. The initial batch of 24 rabbits with 8 groups of three rabbits in each group was followed by another batch of 24 rabbits with the same 8 groups of three. In total 48 rabbits (New Zealand female white rabbits from Harlan, UK) with n=6 were used for this study.

Animals were randomly assigned to selected groups. A latin square design randomisation was used to minimize the effects of any variation through the period of the study.

Group 1: RU486 1% suspension in hypromellose eye drops
Group 2: RU486 (3 mg/ml) in reformulated vehicle
Group 3: RU42633 (3 mg/ml) in reformulated vehicle
Group 4: RU42848 (2 mg/ml) in reformulated vehicle
Group 5: RU42698 (3 mg/ml) in reformulated vehicle
Group 6: Abbott compound 19C (3 mg/ml) in reformulated vehicle (positive control)
Group 7: Latanaprost (0.005%) (positive control)
Group 8: Control carrier/vehicle for groups 2, 3, 4 and 5

Method of drug administration

Part A of Study I

A total of six rabbits were assigned to each group. The left eye was treated and the right eye was used as an untreated control. The rabbits in each group as shown in the table below were given one drop in the left eye on Day 0. The intraocular pressure in both eyes was measured before the drop was administered. The IOP was measured again at 0.5, 1, 2, 3, 4 and 8 hours after instillation on day 0, and once a day thereafter for the next two days. No further drops or other agents were administered at the same time. The contralateral right eye remained untreated and acted as a control.

Part B of Study I

On each of days 5, 6, 7, 8 and 9, one drop per rabbit was administered, three times a day, with an interval of approximately 5 hours between drops – the schedule for dosing was 8am, 1pm and 6pm. The control eye remained untreated. Intraocular pressure was measured on each of days 5 to 9 before the drops were administered. In addition, intraocular pressure was measured at 0.5, 1, 2, 3, 4 and 8 hours after instillation on day 5 (Table 18).

Aqueous and blood samples

At the end of the last dose, a sample of aqueous from the anterior chamber and venous blood were taken one hour after instillation and were both stored at -70°C for future analysis.

Endpoints and examination performed

Baseline

At the beginning of the study the ophthalmological examination included:

- intraocular pressure measurement
- corneal and conjunctival appearance

Assessments were made daily from Day 0 to Day 2 and from Day 5 to Day 9 until sacrifice. Both eyes were examined. The contralateral untreated eye acted as control.

Measurement of intraocular pressure

Measurements of intraocular pressure in both eyes were made by using the Mentor tonopen. This was performed after topical installation of 0.5% of Proxymetacaine HCl local anaesthetic. The tonopen was lowered perpendicularly on to the corneal surface and a recording was made. Three recordings per eye were made per time point and a mean reading was documented.

Toxicity

The cornea and conjunctiva were examined daily for abnormality including corneal epithelial damage (fluorescein and blue light) or opacification. The conjunctiva was examined and photographed digitally and graded for inflammation.

Sacrifice

All animals were sacrificed after the experiment was completed with a lethal injection of pentobarbitone intravenously under a general anaesthetic.

Group (Six rabbits per group)	Contents of eye drops	Dose	Schedule of eye drops	Schedule of examinations	Study End
1	RU486 1% suspension in hypromellose eye drops	tbc	Day 0 : 1 drop; Day 5,6,7,8,9: 3 drops/day	Daily examination of cornea/conjunctiva & IOP measurement. In addition, IOP at 0.5, 1, 2, 3, 4 and 8 hours after first drop on days 0 and 5.	Day 9 – rabbits sacrificed
2	RU 486 (3 mg/ml)	~150 µg and ~450 µg/day	Day 0 : 1 drop; Day 5,6,7,8,9: 3 drops/day	Daily examination of cornea/conjunctiva & IOP measurement. In addition, IOP at 0.5, 1, 2, 3, 4 and 8 hours after first drop on days 0 and 5.	Day 9 – rabbits sacrificed
3	RU 42633 (3 mg/ml)	~150 µg and ~450 µg/day	Day 0 : 1 drop; Day 5,6,7,8,9: 3 drops/day	Daily examination of cornea/conjunctiva & IOP measurement. In addition, IOP at 0.5, 1, 2, 3, 4 and 8 hours after first drop on days 0 and 5.	Day 9 – rabbits sacrificed
4	RU42848 (2 mg/ml)	~100 µg and ~300 µg/day	Day 0 : 1 drop; Day 5,6,7,8,9: 3 drops/day	Daily examination of cornea/conjunctiva & IOP measurement. In addition, IOP at 0.5, 1, 2, 3, 4 and 8 hours after first drop on days 0 and 5.	Day 9 – rabbits sacrificed
5	RU42698 (3 mg/ml)	~150 µg and ~450 µg/day	Day 0 : 1 drop; Day 5,6,7,8,9: 3 drops/day	Daily examination of cornea/conjunctiva & IOP measurement. In addition, IOP at 0.5, 1, 2, 3, 4 and 8 hours after first drop on days 0 and 5.	Day 9 – rabbits sacrificed
6	Abbott compound 19C (3 mg/ml)	~150 µg and ~450 µg/day	Day 0 : 1 drop; Day 5,6,7,8,9: 3 drops/day	Daily examination of cornea/conjunctiva & IOP measurement. In addition, IOP at 0.5, 1, 2, 3, 4 and 8 hours after first drop on days 0 and 5.	Day 9 – rabbits sacrificed
7	Latanaprost (0.005%)	Tbc	Day 0 : 1 drop; Day 5,6,7,8,9: 3 drops/day	Daily examination of cornea/conjunctiva & IOP measurement. In addition, IOP at 0.5, 1, 2, 3, 4 and 8 hours after first drop on days 0 and 5.	Day 9 – rabbits sacrificed
8	Control vehicle for Groups 2, 3, 4 and 5	NA	Day 0 : 1 drop; Day 5,6,7,8,9: 3 drops/day	Daily examination of cornea/conjunctiva & IOP measurement. In addition, IOP at 0.5, 1, 2, 3, 4 and 8 hours after first drop on days 0 and 5.	Day 9 – rabbits sacrificed

Table 19: Description and treatment plan for the left eye only of each group in Study I of the anti-steroid drops study. The right eye was untreated and acted as a control.

5.2.1.2.2. Study II

After Study I, further investigation of the efficacy of the RU42698 took place, as in Study I was found that this compound was more effective than RU42848 and RU42633.

The aims of Study II were:

a) To test if one drop of maximal loading of RU 42698 (3 mg/ml) can lower the IOP in rabbit eyes.
b) To determine the concentration of RU 42698 (3 mg/ml) in the aqueous humor of rabbit eyes at several time points after one-drop application (pharmacokinetic analysis).
c) To test if, after a subconjunctival injection of 100 μl maximal loading of RU 42698 (3 mg/ml), there is a lowering effect in the rabbit eye IOP; and to find out if RU 42698 penetrates the sclera and what concentration is achieved in the aqueous humor at several time points after the injection.

The study was designed as follows:

Thirty Female New Zealand White Rabbits (B & K Universal, 3 kg, 14-15 weeks old) were used. Animals were housed in the BRU Unit of the UCL Institute of Ophthalmology and were allowed an acclimatisation period of 7 days. The 30 rabbits were randomly assigned into ten groups (3 rabbits in each group).

Method of drug administration

One drop of RU42698 (3 mg/ml) was administered topically in the left eye of each of the rabbits of the first seven groups (21 rabbits in total). No treatment was applied to the right eyes of the rabbits in groups 1-7. The rabbits in groups 8-10 were treated with one subconjunctival injection of 100 μl of RU 42698 (3 mg/ml). The right eye of the rabbits in groups 8-10 received no treatment.

Rabbits in group 1 were killed 0.5 hour after the administration of the drop of RU42698 (3 mg/ml), rabbits in group 2 were killed 1 hour after the drop, rabbits in group 3 were killed 2 hours after the drop, rabbits in group 4 were killed 4 hours after

the drop, rabbits in group 5 were killed 6 hours after the drop, rabbits in group 6 were killed 8 hours after the drop and rabbits in group 7 were killed 24 hours after the drop. This experiment aimed to facilitate a) the understanding of the pharmacokinetics after the drop application (in particular what percentage of the drug passes the corneal barrier, how many hours after the administration of the drug the peak concentration is detected and how long it takes for RU 42698 to be cleared from the aqueous) and b) the scheduling of a dosing pattern which would achieve a sufficient RU 42698 concentration for the lowering of IOP in the aqueous humor.

Regarding the rabbits treated with injections of RU 42698, rabbits in group 8 were killed 3-4 hours after the injection, rabbits in group 9 were killed between 6 and 8 hours after the injection and rabbits in group 10 were killed after 24 hours. This part of the experiment was important as it would show the concentrations of the RU 42698 in the aqueous humor by the two administration methods, and indicate how prolonged are the effects.

IOP was measured in both eyes of all rabbits before the treatment and at the time points shown in the table below, as well as before the killing. Ophthalmological examination and IOP measurement were performed as described in Study I.

Aqueous humor and blood samples were collected under terminal anesthesia for the detection of the drug levels, as it is described in Study I.

Drug Group	Treated eye	Contralateral Eye	IOP measurements Time Points	Killing & samples
1	1 drop of RU42698 (3mg/ml)	No treatment	0h, 0.5h	0.5h p.t.
2	1 drop of RU42698 (3mg/ml)	No treatment	0h, 0.5h, 1h	1h p.t.
3	1 drop of RU42698 (3mg/ml)	No treatment	0h, 1h, 2h	2h p.t.
4	1 drop of RU42698 (3mg/ml)	No treatment	0h, 2h, 4h	4h p.t.
5	1 drop of RU42698 (3mg/ml)	No treatment	0h, 4h, 6h	6h p.t.
6	1 drop of RU42698 (3mg/ml)	No treatment	0h, 6h, 8h	8h p.t.
7	1 drop of RU42698 (3mg/ml)	No treatment	0h, 8h, 24h	24h p.t.
8	1 subconjunctival injection (100μl) of RU42698 (3mg/ml)	No treatment	0h, 3.5h	3.5h p.t.
9	1 subconjunctival injection (100μl) of RU42698 (3mg/ml)	No treatment	0h, 3.5h, 7h	7h p.t.
10	1 subconjunctival injection (100μl) of RU42698 (3mg/ml)	No treatment	0h, 7h, 24h	24h p.t.

Table 20: Description and treatment plan for the left eye only of each group in Study 1 of the anti-steroid drops study. The right eye was untreated and acted as a control.

5.2.1.2.3. Study III

The third and final study was performed in order to determine:

a) Which of RU486 (3 mg/ml) or RU42698 at different concentrations (1 mg/ml, 3 mg/ml, 6 mg/ml) is the more effective at lowering the IOP after a single or multiple (3 drops/day) drop application. (DanioLabs / Summit PLC were able to make a solution with higher concentration of RU42698 (6 mg/ml and this was also tested in this study).
b) If one drop of RU 42698 at different concentrations (1 mg/ml, 3 mg/ml, 6 mg/ml) can lower the IOP in rabbit eyes and if this reduction is dose dependent.
c) At which time points IOP is found to be significantly decreased after the single drop application of RU 42698 or RU 486.

The study was designed as follows:

24 Female New Zealand White Rabbits (Harlan UK Ltd. c. 2.0-2.5 kg, 12-14 weeks old) were used. Animals were housed in the BRU Unit of the UCL Institute of Ophthalmology, and were allowed an acclimatisation period of 7-10 days. All treatments were applied to the left eye. The right eye did not receive any treatment and served as the control.

To achieve the aims of the study, the experiment was run in two parts.

Method of drug administration

Part A of Study III

The 24 rabbits were randomly assigned into 4 groups (A, B, C and D) (six rabbits in each group) with a Latin square crossover design.

The rabbits in group A received one drop of RU42698 (1 mg/ml) on day 1. On day 7, they received one vehicle drop, on day 13 they received one drop of RU486 (3 mg/ml) and on day 19 they received one drop of RU42698 (3 mg/ml).

The rabbits in group B received one vehicle eye drop on day 1. On day 7 they received one drop of RU 42698 (3 mg/ml), on day 13 they received one drop of RU 42698 (6 mg/ml) and on day 19 they received one drop of RU 486 (3 mg/ml).

The rabbits of the group C received one drop of RU 486 (3 mg/ml) on day 2. On day 8 they received one drop of RU 42698 (6 mg/ml), on day 14 they received one drop of RU 42698 (3 mg/ml) and on day 20 they received one vehicle eye drop.

The rabbits of the group D received one drop of RU 42698 (3 mg/ml) on day 2. On day 8 they will receive one drop of RU 486 (3 mg/ml), on day 14 they received one vehicle eye drop and on day 20 they received one drop of RU 42698 (1 mg/ml).

GROUP	TREATMENT DAY 1	TREATMENT DAY 7	TREATMENT DAY 13	TREATMENT DAY 19
A (6 rabbits) Left eye	One drop of RU42698 (1 mg/ml)	One vehicle drop	One drop of RU486 (3 mg/ml)	One drop of RU42698 (3 mg/ml)
B (6 rabbits) Left eye	One vehicle drop	One drop of RU42698 (3 mg/ml)	One drop of RU42698 (6 mg/ml)	One drop of RU486 (3 mg/ml)

GROUP	TREATMENT DAY 2	TREATMENT DAY 8	TREATMENT DAY 14	TREATMENT DAY 20
C (6 rabbits)	One drop of RU486 (3 mg/ml)	One drop of RU42698 (6 mg/ml)	One drop of RU42698 (3 mg/ml)	One vehicle drop
D (6 rabbits)	One drop of RU42698 (3 mg/ml)	One drop of RU486 (3 mg/ml)	One vehicle drop	One drop of RU42698 (1 mg/ml)

Table 21: Treatment regimen of Part A of Study III.

Intervals of 5-6 days between the drops were believed to be sufficient for the compounds in order to be cleared from the anterior chamber (AC), based on the clearance of the RU 42698 within 24 hours from the AC, as Study II showed.

Using a Mentor tonopen, intraocular pressure (IOP) was measured in both eyes of all rabbits before each treatment and at 1, 2, 4, 6, 8 and 24 hours after each drop application.

Time interval between FIRST and SECOND part of the third study

There was a break of one week to ensure that all the compounds were cleared from the AC and the second study started on day 26.

Part B of Study III

The 24 rabbits were randomly assigned into four groups (E, F, G, H) (six rabbits in each group) with a Latin square crossover design.

- The rabbits of group E received 3 vehicle drops/day for three days.
- The rabbits of group F received 3 drops/day of RU42698 (3 mg/ml) for five days.
- The rabbits of group G received 3 drops/day of RU42698 (6 mg/ml) for five days.
- The rabbits of group H received 3 drops/day of RU486 (3 mg/ml) for five days.

During the five-day period of drug administration, the IOP was measured in both eyes of all rabbits twice per day. The first IOP measurement each day was taken just before the administration of the first drop.

GROUP	TREATMENT DAY26	TREATMENT DAY 27	TREATMENT DAY 28	TREATMENT DAY 29	TREATMENT DAY 30
E (6 rabbits) Left eye	Three vehicle Drops	Three vehicle Drops	Three vehicle drops	Three vehicle Drops	Three vehicle drops
F (6 rabbits) Left eye	Three drops of RU42698 (3mg/ml)	Three drops of RU42698 (3mg/ml)	Three drops of RU42698 (3mg/ml)	Three drops of RU42698 (3mg/ml)	Three drops of RU42698 (3mg/ml)
G (6 rabbits) Left eye	Three drops of RU42698 (6mg/ml)	Three drops of RU42698 (6mg/ml)	Three drops of RU42698 (6mg/ml)	Three drops of RU42698 (6mg/ml)	Three drops of RU42698 (6mg/ml)
H (6 rabbits) Left eye	Three drops of RU486 (3mg/ml)	Three drops of RU486 (3mg/ml)	Three drops of RU486 (3mg/ml)	Three drops of RU486 (3mg/ml)	Three drops of RU486 (3mg/ml)

Table 22: Treatment regimen of the Part B of the Study III

5.2.1.3. Results

5.2.1.3.1. Study I

Part A (One drop application)

Statistical analysis

Significant differences (ANOVA and t tests) were found between the IOP measurements of the treated eyes of groups four (RU 42898) and eight (control) at the 3 and 4 hour time points (Figure 104) and also between groups five (RU 42698) and eight (control) at the 1, 3 and 4 hour time points (Figure 105). The points with statistical differences are identified with green stars in the figures.

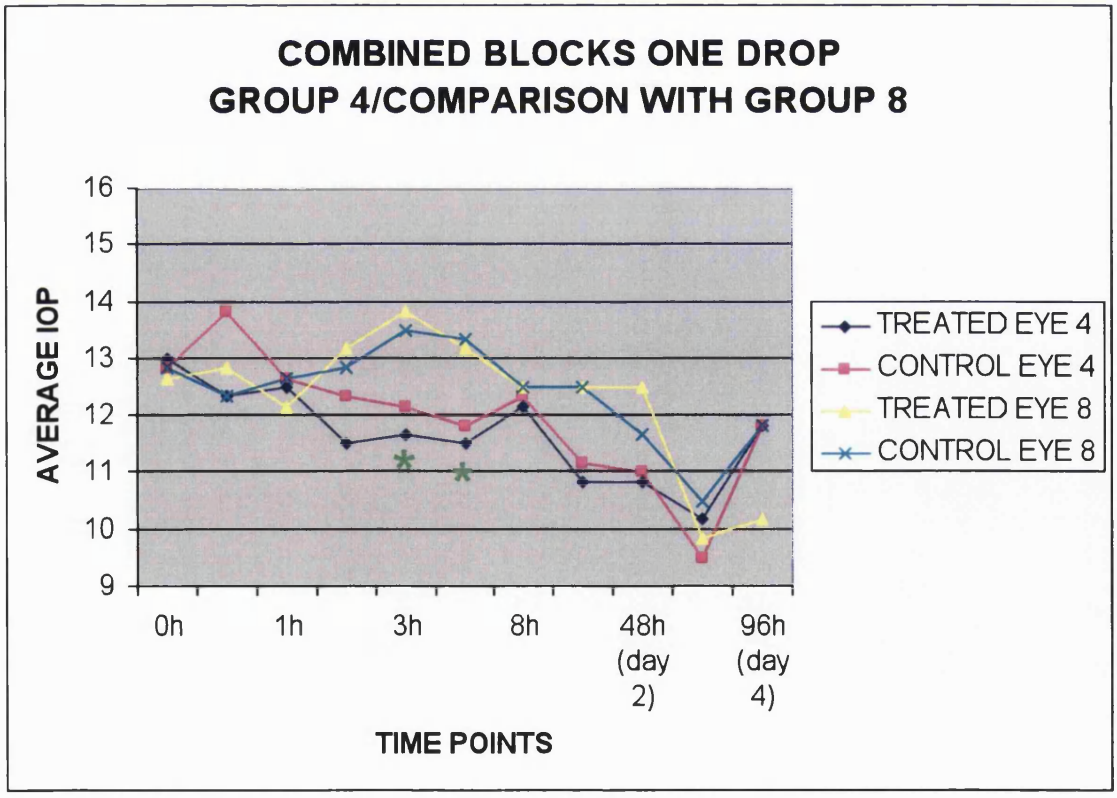

Figure 103: One drop of RU 42898 significantly reduced the intraocular pressure compared to control at time points 3 and 4 hours after the administration of the drop ($P<0.05$ for both time points, t test).

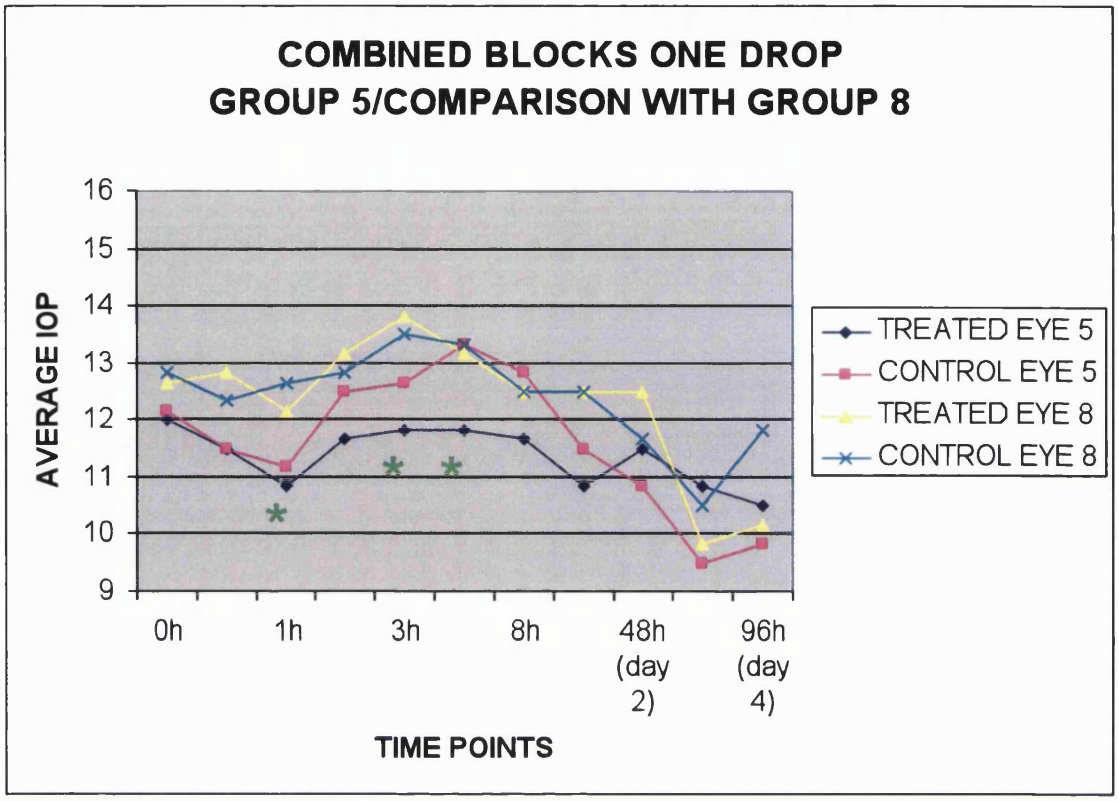

Figure 104: One drop of RU 42698 significantly reduced the intraocular pressure compared to control at the time points 1, 3 and 4 hours after the administration of the drop ($P < 0.05$, t test).

Part B (three drops application)

Significant differences (ANOVA and t tests) were found between the IOP measurements of the treated eyes of groups one (RU 486) and eight (control) at the 4 and 8 hour time points (Figure 106), between groups three (RU 42633) and eight (control) at the 4 hour time point (Figure 107), between group five (RU 42698) and eight (control) at the 3 hour, 4 hour and 4 day time points (Figure 108) and finally between group seven (latanoprost) and eight (control) at the 4 hour time point (graph 6). The points with statistical differences are identified with green stars in the graphs.

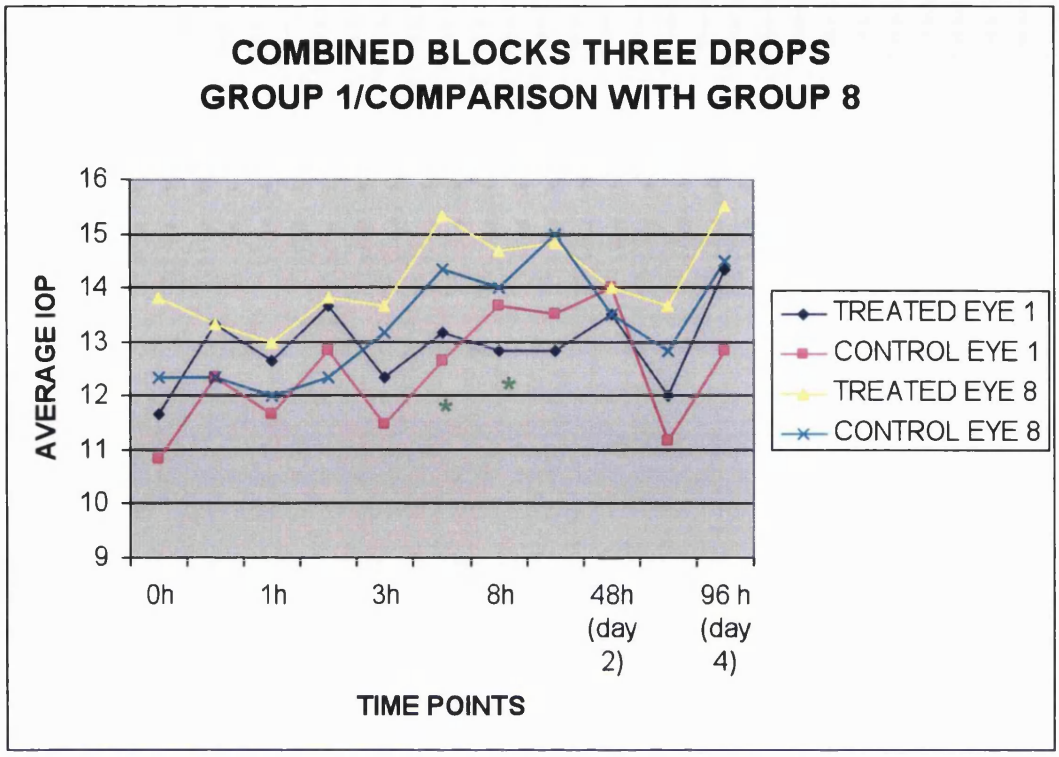

Figure 105: RU 486 significantly reduced the intraocular pressure compared to control at time points 4 and 8 hours after the administration of the first drop.

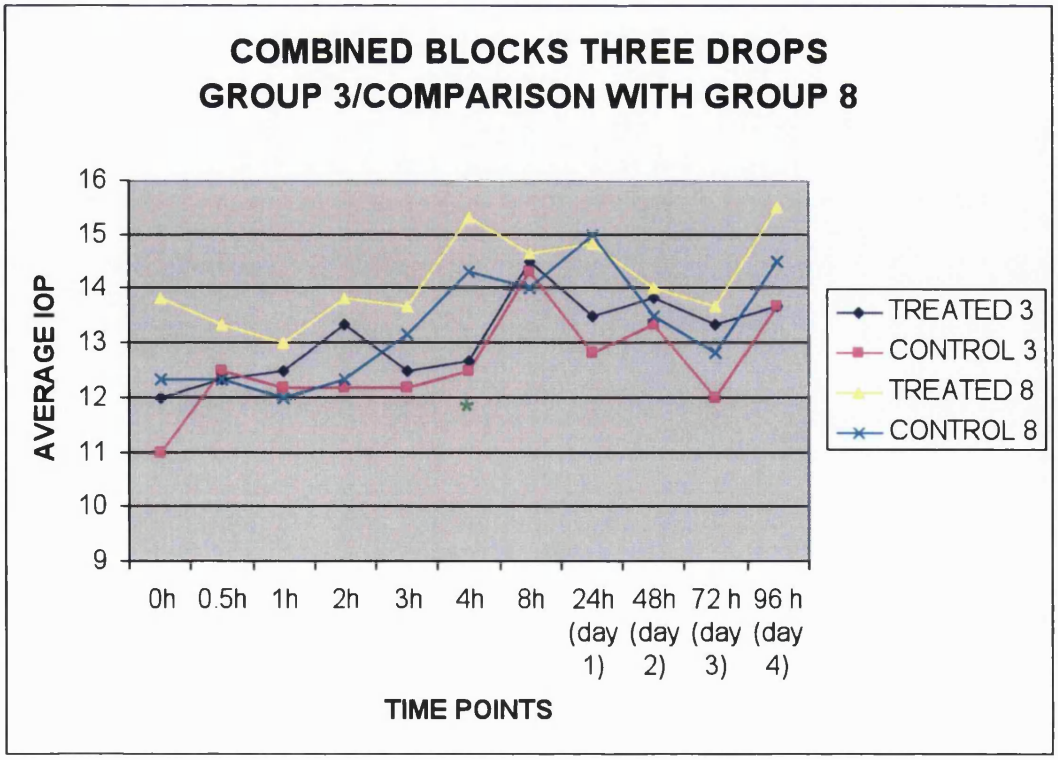

Figure 106: RU42633 significantly reduced the intraocular pressure compared to control at the time points 4 hours after the administration of the first drop.

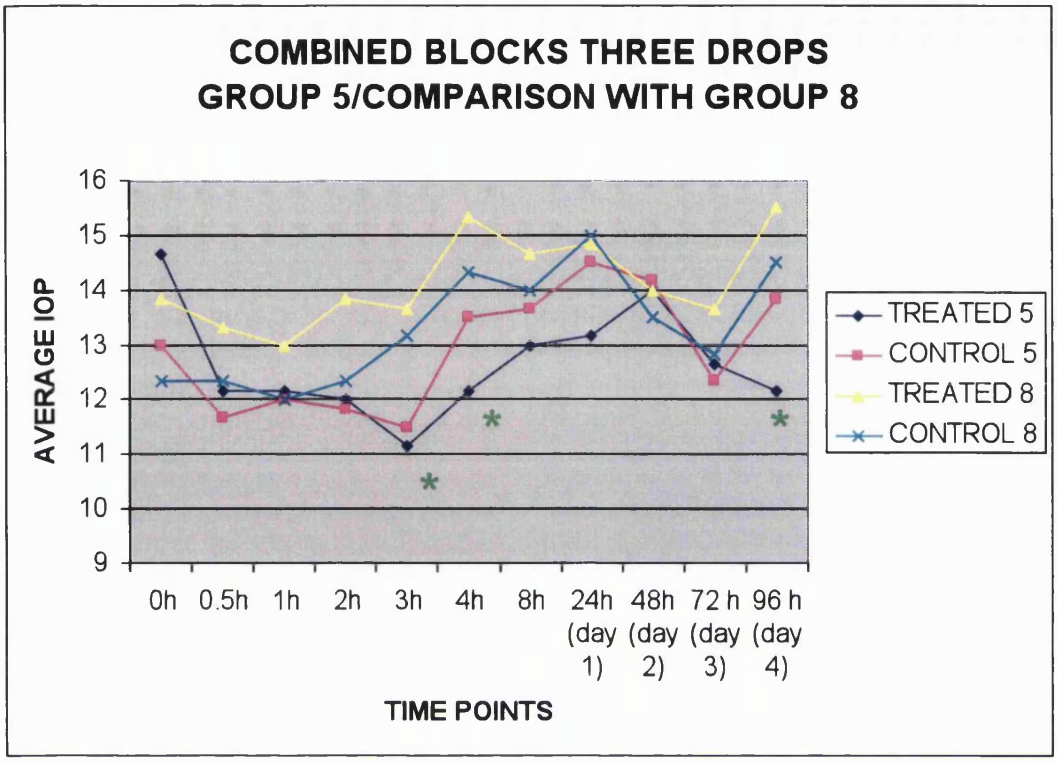

Figure 107: RU 42698 significantly reduced the intraocular pressure compared to control at time points 4, 8 and 96 hours after the administration of the first drop.

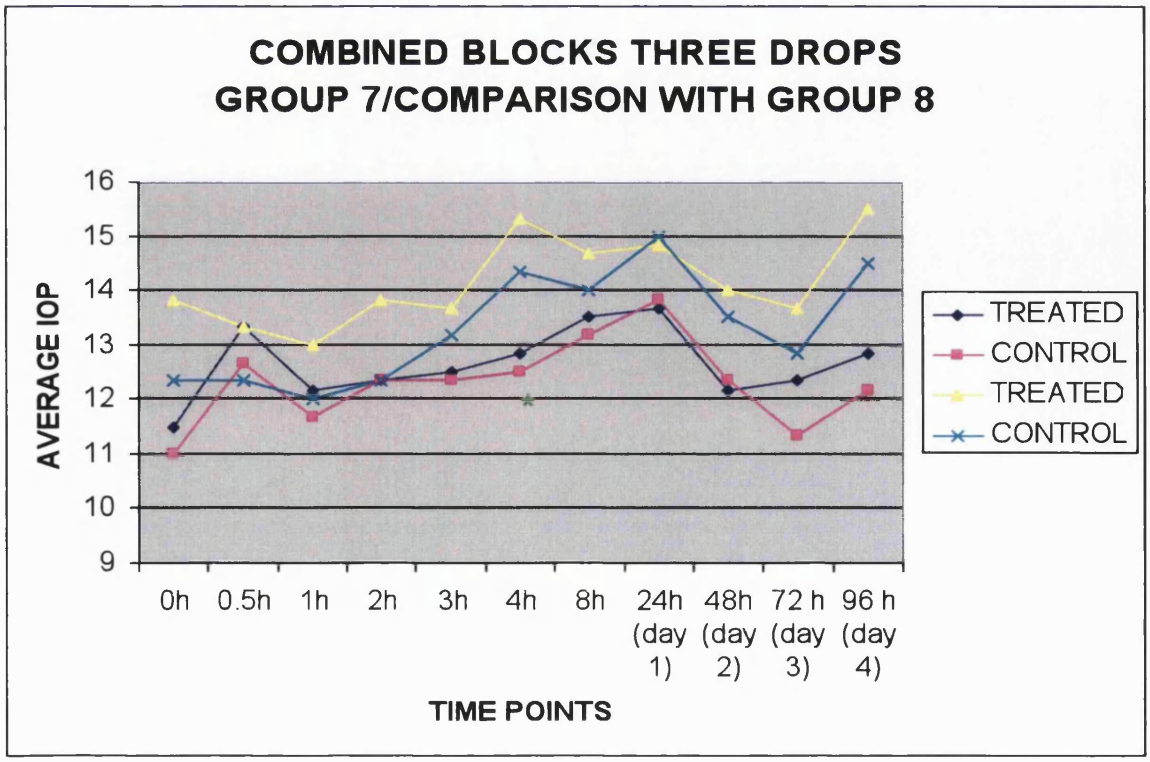

Figure 108: Latanoprost significantly reduced the intraocular pressure compared to control at the time point 4 hours after the administration of the first drop.

From the statistical analysis and the graphs, it is clear that compound RU42698 (3 mg/ml) in group 5 was the most effective in lowering IOP compared to the control group in both the one drop and three drops/day application.

5.2.1.3.2. Study II

One drop application

The aim of the second experiment was to re-examine the IOP lowering effect of RU42698 and to test whether the compound passes through the cornea to reach the aqueous humor and, if so, for how long it can be detected in the aqueous humor.

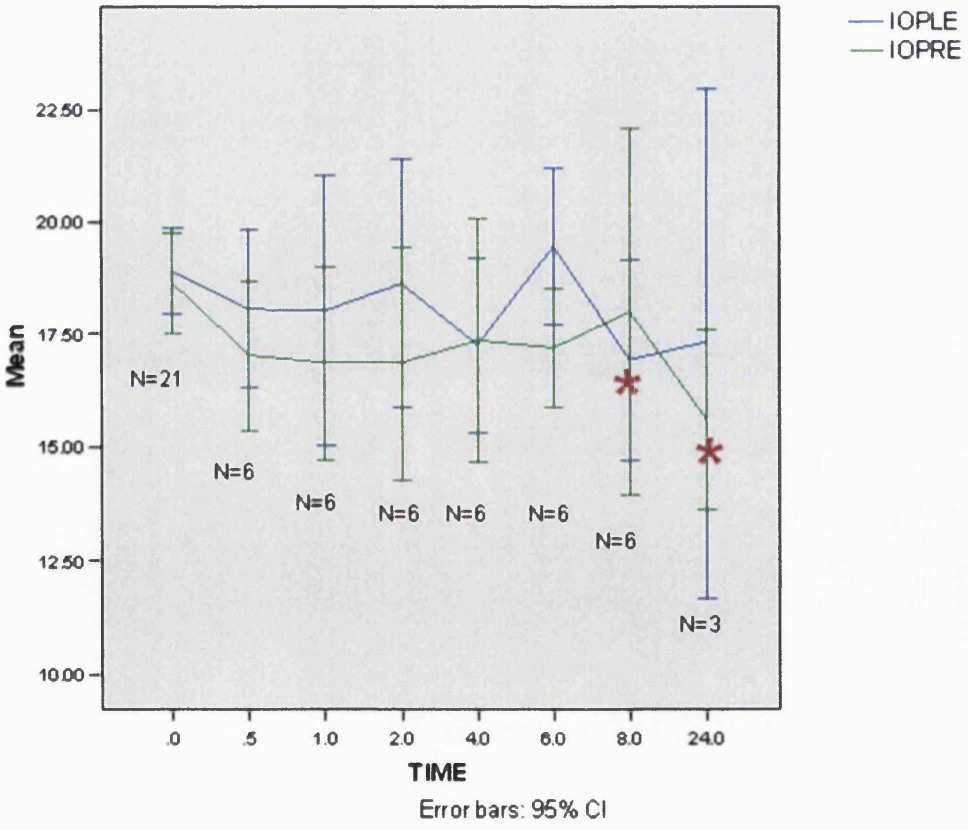

Figure 109: IOP changes at several time points after the application of one drop of RU42698 (3 mg/ml). The red stars * indicate significantly lower IOP in the left eye (treated eye) at the 8 hour and 24 hour time points compared to the initial IOP at time points 0h ($P < 0.05$ for both time points, t test).

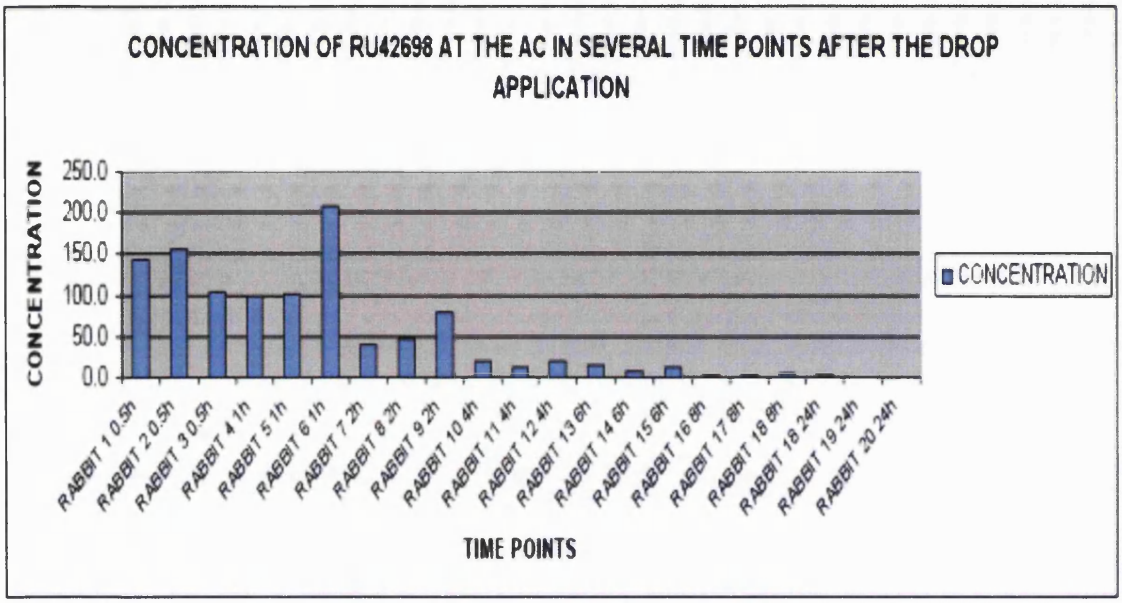

Figure 110: This graph shows the concentration of RU42698 in the aqueous humor at several time points after the administration of one drop administration into the left eye of the rabbit. RU42698 can be detected in the aqueous humor for at least 8 hours after the drop administration.

Administration of one subconjunctival injection

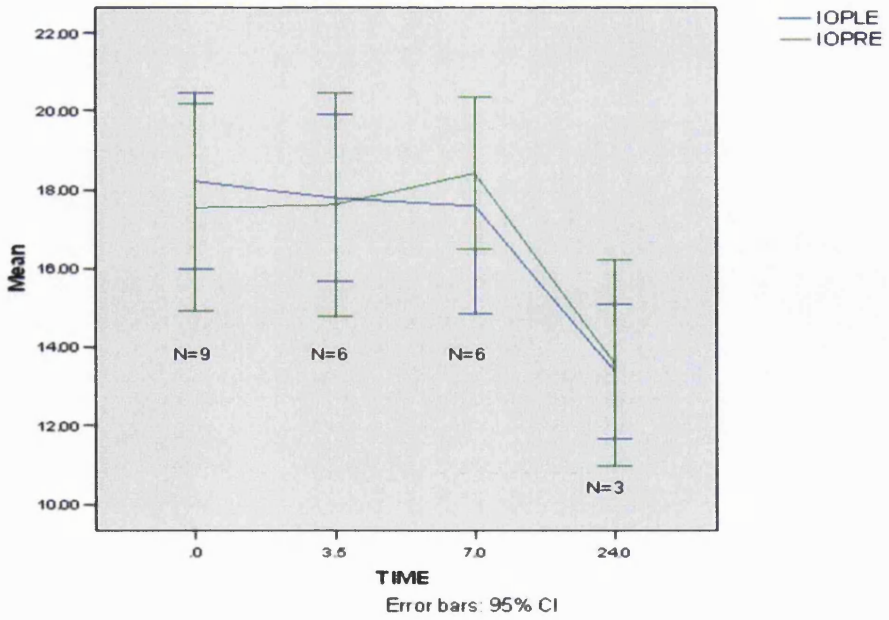

Figure 111: Changes in the IOP after the administration of one RU42698 3mg/ml 100 µl subconjunctival injection in the left eye. No significant changes were detected at the three tested time points (3.5h, 7h and 24h)

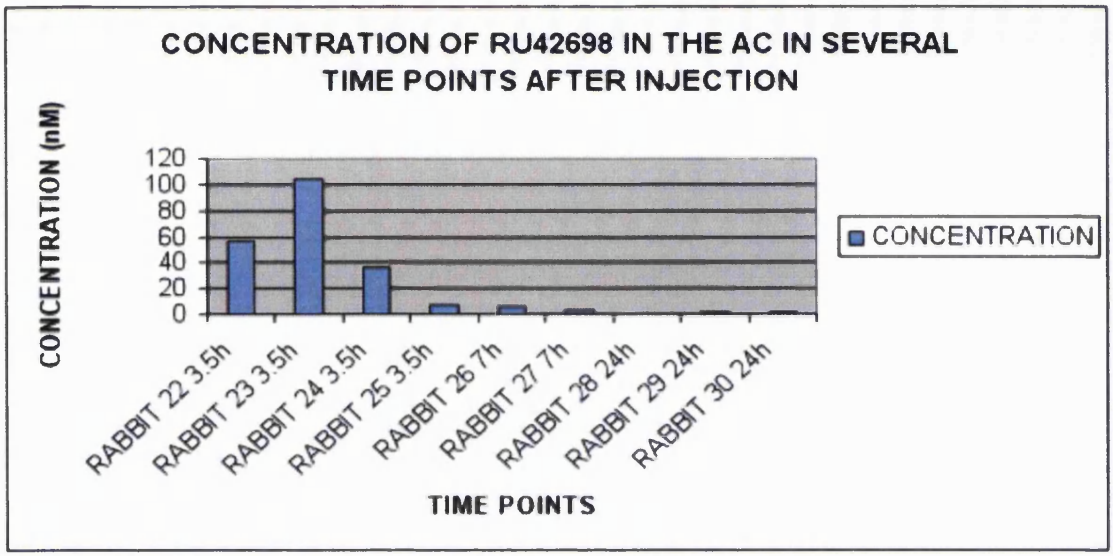

Figure 112: This graph shows the concentration of RU 42698 in the aqueous humor in several time points after the one drop administration at the rabbit eye. RU 42698 can be detected in the aqueous humor for at least 8 hours after the drop administration.

This experiment showed that RU 42698 reduced significantly the IOP in rabbits. One drop of RU 42698 3 mg/ml was more effective in lowering the IOP than the subconjunctival injection of the same compound. RU42698 can be detected in the anterior chamber after a single drop application for more than 8 hours and for more than 7 hours after the administration of a single subconjunctival injection respectively. The concentration of the RU 42698 in the anterior chamber the first four hours was higher in the subconjunctival injection treated rabbits than the drop treated rabbits.

5.2.1.3.3. Study III

Part A

As described in the Materials and Methods section, the effect on IOP reduction of four different treatments plus one control was tested in this study. In study A, the effect of one drop of each treatment was tested. The IOP was measured at several time points after the application of the drop. The results from the five

different groups and the statistical analysis are presented in the graph and the table below.

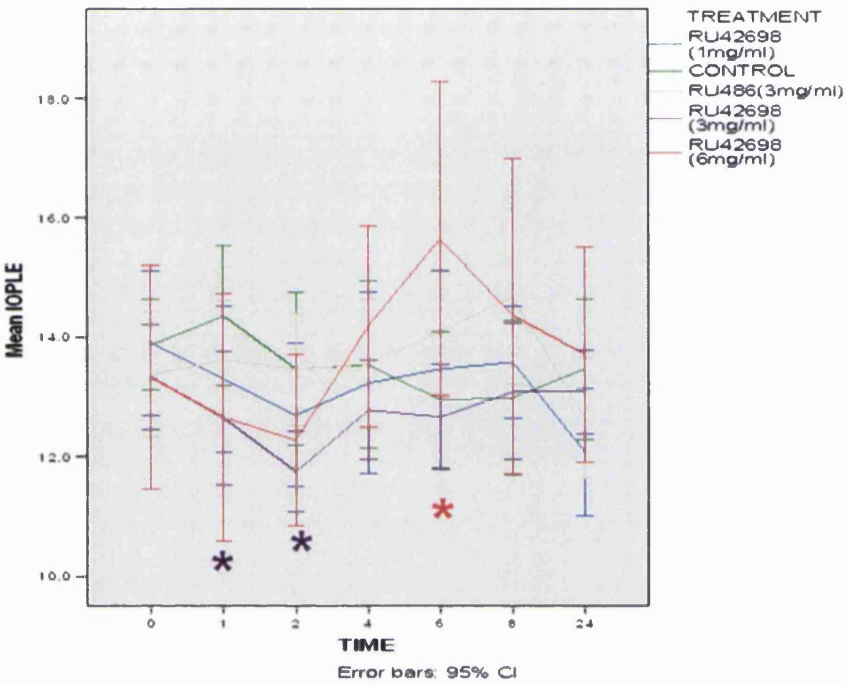

Figure 113: Graph of IOP changes in the five treatment groups. The statistical analysis (AVOVA) indicated that IOP readings in the left eye (treated eye) of the RU 42698 3 mg/ml treatment group at the 1 hour and 2 hour time points were significantly lower compared to control. Additionally, IOP in the left eye of the RU 42698 6 mg/ml treatment group at the 6 hour time point was found to be significantly higher compared to control.

Statistical comparison	**Time point 0h**	**Time point 1h**	**Time point 2h**	**Time point 4h**	**Time point 6h**	**Time point 8h**	**Time point 24h**
RU42698 (1 mg/ml) v control	Not significant	Not significant	Not significant	Not Significant	Not significant	Not significant	Not significant
RU486 (3 mg/ml) v control	Not significant	Not significant	Not significant	Not Significant	Not significant	Not significant	Not Significant
RU42698 (3 mg/ml) v control	Not significant	Significantly lower	Significantly lower	Not Significant	Not significant	Not significant	Not Significant
RU42698 (6mg/ml) v control	Not significant	Not significant	Not significant	Not Significant	Significantly higher	Not significant	Not Significant

Table 23: Statistical analysis of the effect of the four tested treatments in the IOP compared to control.

Part B

In part B of study III, the effect of IOP reduction of three different treatments plus one control was tested in this study. RU42698 1 mg/ml was excluded from this study, due to the poor results shown by this treatment in part A of Study III. In this study, 3 drops per day was applied to the left eye of the rabbits for 5 days in all the treatment groups, as it is described in the Materials and Methods section. The IOP was measured at several time points during the 5 days of the treatment and the graphical representation of the IOP in the three treatment groups as well as the statistical analysis of the results are presented in the graph and the table below.

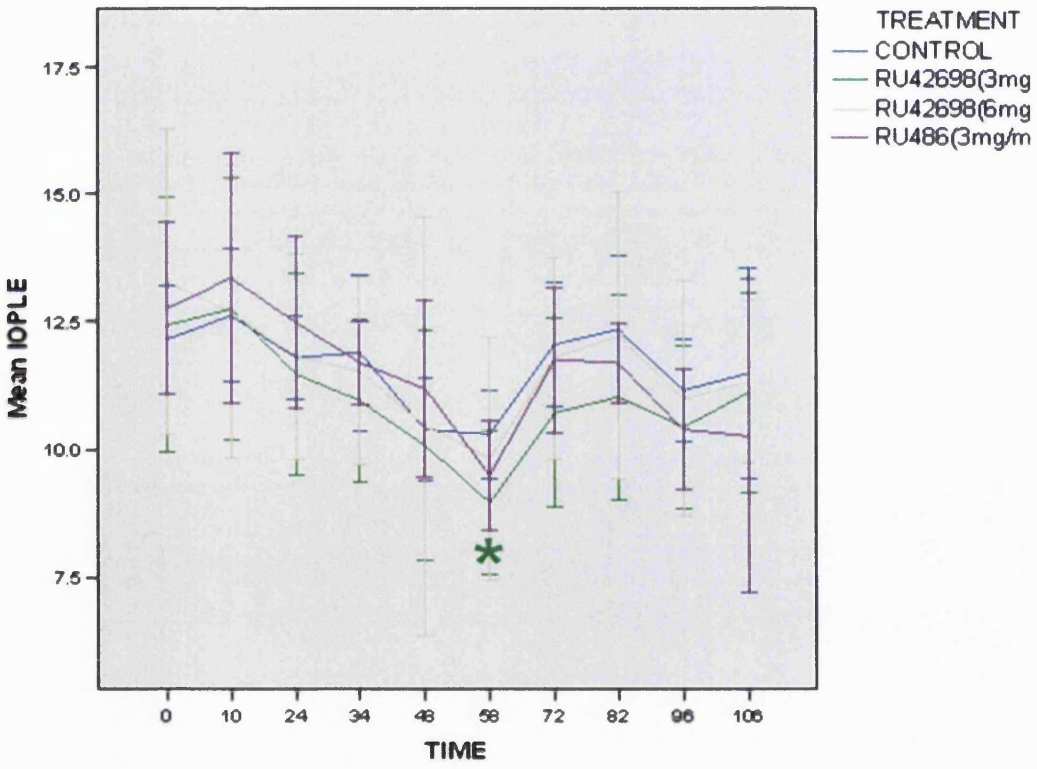

Figure 114: IOP in the LE of the RU42698 3mg/ml treatment group was found lower and close to significance at the time point 58h compared to control. No other significant points were found.

Statistical comparison	Time point 0h	Time point 10h	Time point 24h	Time point 34h	Time point 48h	Time point 58h	Time point 72h	Time point 82h	Time point 96h	Time point 106h
RU42698 (3mg/ml) v control	Not significant	Not significant	Not significant	Not significant	Not significant	Not Significant But close to significant	Not significant	Not significant	Not significant	Not significant
RU42698 (6mg/ml) v control	Not significant	Not significant	Not significant	Not significant	Not significant	Not significant	Not significant	Not significant	Not significant	Not significant
RU486 (3mg/ml) v control	Not significant	Not significant	Not significant	Not significant	Not significant	Not significant	Not significant	Not significant	Not significant	Not significant

Table 24: Statistical analysis of the effect of the three tested treatments in the IOP compared to control.

5.2.1.4. Discussion

5.2.1.4.1. Findings from the one drop studies

In the initial experiment performed in the Ocular Repair and Regeneration Biology Unit at the UCL Institute of Ophthalmology in co-operation with DanioLabs plc (later Summit plc), compounds developed by Summit were tested for their effectiveness in reducing intraocular pressure in normotensive rabbits. Other compounds (Abbott compound 19C and Latanoprost 0.005%.) were used in this study as controls.

In study I, one drop of RU42698 significantly reduced the intraocular pressure compared to negative control at the 1, 3 and 4 hour time points after the administration of the drop. One drop of RU42898 also significantly reduced the intraocular pressure compared to control at the time points 3 and 4 hour time points after the administration of the drop. The compound RU 42848 did not have any significant effect in IOP reduction compared to the negative control group. The compounds RU 42698 and RU 42848 were more effective in reducing IOP than the positive controls (RU 486 in both concentrations, Abbott 19C and Latanoprost 0.005%).

In this experiment, six rabbits were assigned in each treatment group. The left eye was treated and the right eye was used as control. Because of the capacity

limitations at the BRU Unit at the Institute of Ophthalmology and in order to maximise the number rabbits per treatment group for more reliable results, a decision was taken to test only one of the Summit compounds in the second *in vivo* experiment. The RU 42698 compound was chosen as it had been slightly more effective in lowering IOP compared with RU 42848.

The main purpose of the second experiment was to investigate if the RU 42698 drops penetrate the cornea, what is the concentration that is achieved in the anterior chamber, and for how long the compound can be detected in the anterior chamber. In additional, some of the treatment groups in the second study received a subconjunctival injection of RU 42698 instead of a single drop, and the same parameters (concentration in the anterior chamber and duration of detection of the compound) were measured. The effect of the single drop application and the subconjunctival injection in the reduction of the IOP in normotensive rabbits was tested. In this study, all the left eyes were treated and all the right eyes were used as controls. The rabbits treated with one subconjunctival injection of RU42698 3mg/ml had a higher concentration of RU 42698 in the anterior chamber of their treated eyes that the rabbits treated with one drop. In contrast, the application of one drop of RU 42698 3 mg/ml reduced the IOP of the left eye at the 6 hour and 8 hour time points, but the subconjunctival injection did not reduce the IOP at any time points compared to the baseline pre-treatment pressure. This is an interesting finding as we expected that the groups with higher concentration of RU42698 in their anterior chamber would have a higher reduction of IOP, which was not the case.

As the application of RU 42698 with drops is easier and safer and was found to be more effective than the subconjunctival injection, in the third *in vivo* experiment only drops were used as administration method of the compounds and not injections. Five treatment groups were tested in the third *in vivo* experiment; RU 42698 in three different concentrations (1mg/ml, 3 mg/ml and 6 mg/ml), RU 486 (3 mg/ml) and a negative control (vehicle drop) group. In the RU42698 3mg/ml one drop treatment group, the IOP was found to be lower at the 1 hour and 2 hour time points compared to the negative control. Interestingly, the IOP in the RU 42698 (6 mg/ml) group was found to be significantly raised at the 6 hour time point compared to the control, although the concentration of the compound in this group was the highest. This result has similarities with the second study where, when the concentration of RU 42698 in the anterior chamber was high, the IOP was not significantly reduced; and the lower

concentration of RU 42698 was more effective than higher concentration. However, too low a concentration may not be effective in reducing IOP, as no significant points were found in the RU 42698 1 mg/ml group.

The analysis of the three one-drop studies performed with Summit compounds indicate that RU 42698 is more effective than other compounds tested in reducing the IOP in normotensive rabbits. However, the results from the three studies were not consistent nor reproducible, as the reduction of IOP was not achieved at the same time point in all three studies. Furthermore, is the studies suggested that the 3 mg/ml concentration was the most effective in reducing the IOP. A lower concentration (1 mg/ml) showed no effect and a higher concentration (6 mg/ml) caused a rise in IOP. It is possible that the concentration of RU 42698 up to a certain level reduces IOP, but then raises IOP at higher concentrations.

5.2.1.4.2. Findings from the three drops/day studies

We performed two *in vivo* studies (part of the *in vivo* experiments 1 and 3) in the rabbits were treated with 3 drops per day for five days. In the first 3 drops/day for five days study, only RU 42633 and RU 42698 were found to be effective in reducing IOP. This finding is different the findings from the one drop study: although RU 42698 was effective in reducing IOP in both the 1 drop and 3 drops/day for five days studies, the RU 42633 was effective only in the 3 drops per day for five days study and not in the one drop study. Furthermore, the compound RU 42848 was only effective in the one drop study and not in the three drops per day study. RU 42633 significantly decreased the IOP of the treated (left eye) compared to the control group in one time point (4 hours after the application of the first drop). RU 42698 significantly decreased the IOP of the treated (left eye) compared to the control group at three time points (3 hours, 4 hours and 96 hours).

In the third dtufy, two different concentrations of RU 42698 (3 mg/ml and 6 mg/ml) were tested. No significant IOP reduction compared to controls were found at any time points. Only at the 58 hour time point after the first drop application, the reduction in the IOP in the RU 42698 treatment group was close to significance compared to the control.

In conclusion, as was found with the one drop studies, the effectiveness of the three drops /day for five days regimen was not reliable as no reproducibility was shown in the two studies.

REFERENCES

Abe, R., S. C. Donnelly, T. Peng, R. Bucala, C. N. Metz. 2001. Peripheral blood fibrocytes: differentiation pathway and migration to wound sites. J. Immunol. *166:7556.*

Acott, T. S., Kingsley, P. D., Samples, J. R., Van Buskirk, E. M., 1988. Human trabecular meshwork organ culture: morphology and glycosaminoglycan synthesis. Invest Ophthalmol Vis.Sci. 29, 90-100.

Acott, T. S., Samples, J. R., Bradley, J. M., Bacon, D. R., Bylsma, S. S., Van Buskirk, E. M., 1989. Trabecular repopulation by anterior trabecular meshwork cells after laser trabeculoplasty. Am. J. Ophthalmol. 107, 1-6.

Acott, T. S., Westcott, M., Passo, M. S., Van Buskirk, E. M., 1985. Trabecular meshwork glycosaminoglycans in human and cynomolgus monkey eye. Invest Ophthalmol Vis.Sci.. 26, 1320-1329.

Adamis, A. P., Miller, J. W., Bernal, M. T., D'Amico, D. J., Folkman, J., Yeo, T. K., Yeo, K. T., 1994. Increased vascular endothelial growth factor levels in the vitreous of eyes with proliferative diabetic retinopathy. Am. J. Ophthalmol. 118. 445-450.

Aeschlimann, D., Thomazy, V., 2000.Protein crosslinking in assembly and remodelling of extracellular matrices: the role of transglutaminases. Connect Tissue Res. 41: 1-27.

Agapova, O. A., Kaufman, P. L., Lucarelli, M. J., Gabelt, B. T., Hernandez, M. R., 2003. Differential expression of matrix metalloproteinases in monkey eyes with experimental glaucoma or optic nerve transection. Brain Res. 967, 132-143.

Agapova, O. A., Ricard, C. S., Salvador-Silva, M., & Hernandez, M. R., 2001. Expression of matrix metalloproteinases and tissue inhibitors of metalloproteinases in human optic nerve head astrocytes. Glia. 33. 205-216.

Ahir, A., Guo, L., Hussain, A. A., Marshall, J., 2002Expression of metalloproteinases from human retinal pigment epithelial cells and their effects on the hydraulic conductivity of Bruch's membrane", Invest Ophthalmol Vis.Sci. 43, 458-465.

Ahokas, K., Lohi, J., Lohi, H., Elomaa, O., Karjalainen-Lindsberg, M. L., Kere, J., Saarialho-Kere, U., 2002. Matrix metalloproteinase-21, the human orthologue for XMMP, is expressed during fetal development and in cancer. Gene. 301. 31-41.

Ahokas, K., Skoog, T., Suomela, S., Jeskanen, L., Impola, U., Isaka, K., Saarialho-Kere, U., 2005. Matrilysin-2 (matrix metalloproteinase-26) is upregulated in keratinocytes during wound repair and early skin carcinogenesis. J. Invest Dermatol. 124, 849-856.

Aigner, A. 2006 Gene silencing through RNA interference (RNAi) *in vivo*: Strategies based on the direct application of siRNAs. Journal of Biotechnology 124: 12-25.

Akaishi, T., Takagi, Y., Matsugi, T., Ishida, N., Hara, H., & Kashiwagi, K., 2004. Effects of bunazosin hydrochloride on ciliary muscle constriction and matrix metalloproteinase activities. J. Glaucoma. 13, 312-318.

Alapure BV, Praveen MR, Gajjar D, Vasavada AR, Rajkumar S, Johar K., 2008. Matrix metalloproteinase-9 activity in human lens epithelial cells of cortical, posterior subcapsular, and nuclear cataracts. J Cataract Refract Surg. 34, 2063-7.

Alexander, J. P. Acott, T. S., 2003. Involvement of the Erk-MAP kinase pathway in TNFalpha regulation of trabecular matrix metalloproteinases and TIMPs. Invest Ophthalmol Vis.Sci. 44, 164-169.

Alexander, J. P. Acott, T. S. 2001. Involvement of protein kinase C in TNFalpha regulation of trabecular matrix metalloproteinases and TIMPs. Invest Ophthalmol Vis.Sci. 42, 2831-2838.

Alexander, J. P., Bradley, J. M., Gabourel, J. D., Acott, T. S., 1990. Expression of matrix metalloproteinases and inhibitor by human retinal pigment epithelium. Invest Ophthalmol Vis.Sci., 31, 2520-2528.

Alexander, J. P., Samples, J. R., Van Buskirk, E. M., Acott, T. S., 1991. Expression of matrix metalloproteinases and inhibitor by human trabecular meshwork. Invest Ophthalmol Vis.Sci., 32, 172-180.

Allan, J. A., Docherty, A. J., Barker, P. J., Huskisson, N. S., Reynolds, J. J., & Murphy, G., 1995. Binding of gelatinases A and B to type-I collagen and other matrix components. Biochem.J. 299-306.

Allikmets, R., Shroyer, N. F., Singh, N., Seddon, J. M., Lewis, R. A., Bernstein, P. S., Peiffer, A., Zabriskie, N. A., Li, Y., Hutchinson, A., Dean, M., Lupski, J. R., & Leppert, M., 1997. Mutation of the Stargardt disease gene (ABCR) in age-related macular degeneration. Science. 277,1805-1807.

American Academy of Ophthalmology. 2005. Glaucoma.

Amin, S., Chong, N. H., Bailey, T. A., Zhang, J., Knupp, C., Cheetham, M. E., Greenwood, J., & Luthert, P. J., 2004. Modulation of Sub-RPE deposits *in vitro*: a potential model for age-related macular degeneration. Invest Ophthalmol Vis.Sci. 45, 1281-1288.

Anderson, D. R., 1969. Ultrastructure of human and monkey lamina cribrosa and optic nerve head. Arch.Ophthalmol. 82, 800-814.

Angel, P. & Karin, M., 1991. The role of Jun, Fos and the AP-1 complex in cell-proliferation and transformation. Biochim.Biophys.Acta. 1072, 129-157.

Anthony, T. L., Lindsey, J. D., Weinreb, R. N., 2002. Latanoprost's effects on TIMP-1 and TIMP-2 expression in human ciliary muscle cells. Invest Ophthalmol Vis.Sci., 43, 3705-3711.

Antonetti, D. A., Barber, A. J., Khin, S., Lieth, E., Tarbell, J. M., & Gardner, T. W., 1998. Vascular permeability in experimental diabetes is associated with reduced endothelial occludin content: vascular endothelial growth factor decreases occludin in retinal endothelial cells. Penn State Retina Research Group. Diabetes. 47, 1953-1959.

Apte, S. S., Olsen, B. R., Murphy, G., 1995. The gene structure of tissue inhibitor of metalloproteinases (TIMP)-3 and its inhibitory activities define the distinct TIMP gene family. J.Biol.Chem. 270, 14313-14318.

Asahi, M., Wang, X., Mori, T., Sumii, T., Jung, J. C., Moskowitz, M. A., Fini, M. E., Lo, E. H., 2001. Effects of matrix metalloproteinase-9 gene knock-out on the proteolysis of blood-brain barrier and white matter components after cerebral ischemia. J.Neurosci.. 21, 7724-7732.

Auble, D. T., Sirum-Connolly, K. L., Brinckerhoff, C. E., 1992. Transcriptional regulation of matrix metalloproteinase genes: role of AP-1 sequences. Matrix Suppl. 1, 200.

Azar, D. T., Hahn, T. W., Jain, S., Yeh, Y. C., & Stetler-Stevensen, W. G., 1996. Matrix metalloproteinases are expressed during wound healing after excimer laser keratectomy. Cornea. 15, 18-24.

Azar, D. T., Pluznik, D., Jain, S., & Khoury, J. M., 1998. Gelatinase B and A expression after laser in situ keratomileusis and photorefractive keratectomy. Arch. Ophthalmol. 116, 1206-1208.

Azkur, A. K., Kim, B., Suvas, S., Lee, Y., Kumaraguru, U., Rouse, B. T., 2005. Blocking mouse MMP-9 production in tumor cells and mouse cornea by short hairpin (sh) RNA encoding plasmids. Oligonucleotides., 15, 72-84.

Bailey, T. A., Alexander, R. A., Dubovy, S. R., Luthert, P. J., & Chong, N. H., 2001. Measurement of TIMP-3 expression and Bruch's membrane thickness in human macula. Exp.Eye Res. 73, 851-858.

Baker, A. H., Edwards, D. R., & Murphy, G. 2002. Metalloproteinase inhibitors: biological actions and therapeutic opportunities. J.Cell Sci. 115, 3719-3727.

Baker, A. H., Zaltsman, A. B., George, S. J., Newby, A. C., 1998. Divergent effects of tissue inhibitor of metalloproteinase-1, -2, or -3 overexpression on rat vascular smooth muscle cell invasion, proliferation, and death *in vitro*. TIMP-3 promotes apoptosis. J. Clin. Invest. 101, 1478-1487.

Bannikov, G. A., Karelina, T. V., Collier, I. E., Marmer, B. L., & Goldberg, G. I., 2002. Substrate binding of gelatinase B induces its enzymatic activity in the presence of intact propeptide. J. Biol. Chem. 277, 16022-16027.

Barbazetto, I. A., Hayashi, M., Klais, C. M., Yannuzzi, L. A., & Allikmets, R., 2005. A novel TIMP3 mutation associated with Sorsby fundus dystrophy. Arch. Ophthalmol. 123, 542-543.
Bartel, D.P. 2004. MicroRNAs: genomics, biogenesis, mechanism, and function. *Cell* 116:281–297.

Bataller, R., Brenner, D.A. Liver fibrosis. J. Clin. Invest. 2005 115: 209-18.

Baudouin, C., Fredj-Reygrobellet, D., Jambou, D., Gastaud, P., Lapalus, P., 1990. HLA-DR and -DQ expression on human retinal pigment epithelial cells *in vitro*", Graefes Arch.Clin.Exp.Ophthalmol. 228, 86-89.

Becker, J. W., Marcy, A. I., Rokosz, L. L., Axel, M. G., Burbaum, J. J., Fitzgerald, P. M., Cameron, P. M., Esser, C. K., Hagmann, W. K., Hermes, J. D., 1995. Stromelysin-1: three-dimensional structure of the inhibited catalytic domain and of the C-truncated proenzyme. Protein Sci. 4, 1966-1976.

Beliveau, A., Berube, M., Rousseau, A., Pelletier, G., & Guerin, S. L. 2000. Expression of integrin alpha5beta1 and MMPs associated with epithelioid morphology and malignancy of uveal melanoma. Invest Ophthalmol Vis.Sci. 41, 2363-2372.

Bellezza, A. J., Rintalan, C. J., Thompson, H. W., Downs, J. C., Hart, R. T., Burgoyne, C. F., 2003. Deformation of the lamina cribrosa and anterior scleral canal wall in early experimental glaucoma. Invest Ophthalmol Vis.Sci., 44, 623-637.

Bernstein,E., Caudy, A.A., Hammond, S.M. and Hannon, G.J. 2001. Role for bidentate ribonuclease in the initiation step of RNA interference. Nature 409: 363–366.

Berton, A., Godeau, G., Emonard, H., Baba, K., Bellon, P., Hornebeck, W., & Bellon, G., 2000. Analysis of the ex vivo specificity of human gelatinases A and B towards skin collagen and elastic fibers by computerized morphometry. Matrix Biol.. 19, 139-148.

Berube, M., Deschambeault, A., Boucher, M., Germain, L., Petitclerc, E., & Guerin, S. L., 2005. MMP-2 expression in uveal melanoma: differential activation status dictated by the cellular environment. Mol.Vis. 11, 1101-1111.

Bevans-Nelson, S. E., Lausch, R. N., Oakes, J. E., 2001. Tumor necrosis factor-alpha and not interleukin-1alpha is the dominant inducer of matrix metalloproteinase-9 synthesis in human corneal cells. Exp.Eye Res. 73, 403-407.

Bharadwaj, D., Stein, M.P., Volzer, M., Mold, C., Du Clos, T.W., 1999. The major receptor for C-reactive protein on leukocytes is Fcγ receptor II. J Exp Med 190: 585–590.

Bickerstaff, M.C., Botto, M., Hutchinson, W.L., Herbert, J., Tennent, G.A., Bybee A., *et al.* 1999. Serum amyloid P component controls chromatin degradation and prevents antinuclear autoimmunity. Nat. Med. 1999 5: 694-7.

Billinghurst, R. C., Dahlberg, L., Ionescu, M., Reiner, A., Bourne, R., Rorabeck, C., Mitchell, P., Hambor, J., Diekmann, O., Tschesche, H., Chen, J., van, W. H., Poole, A. R., 1997. Enhanced cleavage of type II collagen by collagenases in osteoarthritic articular cartilage. J.Clin.Invest, 99, 1534-1545.

Bode, W., Fernandez-Catalan, C., Tschesche, H., Grams, F., Nagase, H., & Maskos, K., 1999. Structural properties of matrix metalloproteinase's. Cell Mol.Life Sci., 55, 639-652.

Bode, W., Grams, F., Reinemer, P., Gomis-Ruth, F. X., Baumann, U., McKay, D. B., & Stocker, W., 1996. The metzincin-superfamily of zinc-peptidases. Adv. Exp. Med. Biol. 389, 1-11.

Boire, A., Covic, L., Agarwal, A., Jacques, S., Sherifi, S., & Kuliopulos, A., 2005. PAR1 is a matrix metalloprotease-1 receptor that promotes invasion and tumorigenesis of breast cancer cells. Cell, 120, 303-313.

Bradley, J. M., Anderssohn, A. M., Colvis, C. M., Parshley, D. E., Zhu, X. H., Ruddat, M. S., Samples, J. R., Acott, T. S., 2000. Mediation of laser trabeculoplasty-induced matrix metalloproteinase expression by IL-1beta and TNFalpha. Invest Ophthalmol Vis.Sci., 41, 422-430.

Bradley, J. M., Vranka, J., Colvis, C. M., Conger, D. M., Alexander, J. P., Fisk, A. S., Samples, J. R., Acott, T. S., 1998. Effect of matrix metalloproteinases activity on outflow in perfused human organ culture. Invest Ophthalmol Vis.Sci. 39, 2649-2658.

Bramhall, S. R., Hallissey, M. T., Whiting, J., Scholefield, J., Tierney, G., Stuart, R. C., Hawkins, R. E., McCulloch, P., Maughan, T., Brown, P. D., Baillet, M., & Fielding, J. W., 2002. Marimastat as maintenance therapy for patients with advanced gastric ψancer: a randomised trial. Br.J.Cancer 86, 1864-1870.

Brenneisen, P., Wenk, J., Klotz, L. O., Wlaschek, M., Briviba, K., Krieg, T., Sies, H., Scharffetter-Kochanek, K., 1998. Central role of Ferrous/Ferric iron in the ultraviolet B irradiation-mediated signaling pathway leading to increased interstitial collagenase (matrix-

degrading metalloprotease (MMP)-1) and stromelysin-1 (MMP-3) mRNA levels in cultured human dermal fibroblasts. J.Biol.Chem. 273, 5279-5287.

Brew, K., Dinakarpandian, D., Nagase, H., 2000. Tissue inhibitors of metalloproteinases: evolution, structure and function. Biochim. Biophys. Acta 1477, 267-283.

Briggs, M. C., Grierson, I., Hiscott, P., & Hunt, J. A., 2000. Active scatter factor (HGF/SF) in proliferative vitreoretinal disease. Invest Ophthalmol Vis.Sci., 41, 3085-3094.

Brinckerhoff, C. E., Matrisian, L. M., 2002. Matrix metalloproteinases: a tail of a frog that became a prince. Nat. Rev. Mol. Cell Biol., 3, 207-214.

Brittan, M., Hunt, T., Jeffery, R., Poulsom, R., Forbes, S.J., Hodivala-Dilke, K., *et al.* 2002. Bone marrow derivation of pericryptal myofibroblasts in the mouse and human small intestine and colon. Gut. 50 :752-7.

Bron, A. J., 1988. Keratoconus. Cornea 7, 163-169.

Brooks, A. M., Gillies, W. E., 1983. Fluorescein angiography and fluorophotometry of the iris in pseudoexfoliation of the lens capsule. Br.J.Ophthalmol. 67, 249-254.

Brown, D., Chwa, M. M., Opbroek, A., & Kenney, M. C. 1993, Keratoconus corneas: increased gelatinolytic activity appears after modification of inhibitors. Curr..Eye Res. 12, 571-581.

Brown, D., Hamdi, H., Bahri, S., Kenney, M. C., 1994. Characterization of an endogenous metalloproteinase in human vitreous. Curr.Eye Res. 13, 639-647.

Brown, D. J., Bishop, P., Hamdi, H., Kenney, M. C., 1996. Cleavage of structural components of mammalian vitreous by endogenous matrix metalloproteinase-2. Curr.Eye Res. 15, 435-445.

Brummelkamp, T.R., Bernards, R., Agami, R. 2002. A system for stable expression of short interfering RNAs in mammalian cells. Science *296: 550-3.*

Bu el Asrar, A. M., Maimone, D., Morse, P. H., Gregory, S., Reder, A. T., 1992. Cytokines in the vitreous of patients with proliferative diabetic retinopathy. Am. J. Ophthalmol, 114, 731-736.

Bu El-Asrar, A. M., Dralands, L., Veckeneer, M., Geboes, K., Missotten, L., Van, A. I., Opdenakker, G., 1998. Gelatinase B in proliferative vitreoretinal disorders. Am. J. Ophthalmol. 125, 844-851.

Bucala, R., Spiegel, L. A., Chesney, J., Hogan, M., Cerami, A., 1994. Circulating fibrocytes define a new leukocyte subpopulation that mediates tissue repair. Mol Med. 1, 71-81.

Bugno, M., Graeve, L., Gatsios, P., Koj, A., Heinrich, P. C., Travis, J., Kordula, T., 1995. Identification of the interleukin-6/oncostatin M response element in the rat tissue inhibitor of metalloproteinases-1 (TIMP-1) promoter. Nucleic Acids Res. 23, 5041-5047.

Bylsma, S. S., Samples, J. R., Acott, T. S., Van Buskirk, E. M., 1988. Trabecular cell division after argon laser trabeculoplasty. Arch. Ophthalmol. 106, 544-547.

Canete, S. R., Gui, Y. H., Linask, K. K., & Muschel, R. J., 1995. MMP-9 (gelatinase B) mRNA is expressed during mouse neurogenesis and may be associated with vascularization. Brain Res. 88, 37-52.

Canete-Soler, R., Gui, Y. H., Linask, K. K., & Muschel, R. J., 1995. Developmental expression of MMP-9 (gelatinase B) mRNA in mouse embryos. Dev.Dyn. 204, 30-40.

Capon, M. R., Marshall, J., Krafft, J. I., Alexander, R. A., Hiscott, P. S., & Bird, A. C., 1989. Sorsby's fundus dystrophy. A light and electron microscopic study. Ophthalmology. 96,1769-1777.

Capon, M. R., Polkinghorne, P. J., Fitzke, F. W., Bird, A. C., 1988. Sorsby's pseudoinflammatory macula dystrophy -Sorsby's fundus dystrophies. Eye 2 (Pt 1), 114-122.

Carrero-Valenzuela, R. D., Klein, M.L., Weleber, R.G., Murphey, W.H., Litt, M., 1996. Sorsby fundus dystrophy. A family with the Ser181Cys mutation of the tissue inhibitor of metalloproteinases 3. Arch Ophthalmol. 114, 737-8.

Castaño, A. P., Lin, S. L., Surowy, T., Nowlin, B., Turlapati, S. A., Patel, T., Singh, A., Li, S., Lupher, M. Jr., Duffield, M. J., 2009. Serum Amyloid P Inhibits Fibrosis Through FcγR-Dependent Monocyte-Macrophage Regulation *in Vivo*. Sci. Translational 1, 5-13.

Chandrasekher, G., Kakazu, A. H., & Bazan, H. E. 2001. HGF- and KGF-induced activation of PI-3K/p70 s6 kinase pathway in corneal epithelial cells: its relevance in wound healing. Exp. Eye Res., 73, 191-202.

Chang, C., Werb, Z., 2001. The many faces of metalloproteases: cell growth, invasion, angiogenesis and metastasis. Trends Cell Biol. 11, S37-S43.

Char, D. H., 1978. Metastatic choroidal melanoma. Am. J. Ophthalmol. 86, 76-80.

Check, E. 2005. A crucial test. Nat. Med. 11: 243–244.

Chesney, J., Metz, C., Stavitsky, A.B., Bacher, M., Bucala, R. 1998. Regulated production of type I collagen and inflammatory cytokines by peripheral blood fibrocytes. J Immunol. 160: 419-25.

Chintala, S. K., 2006. The emerging role of proteases in retinal ganglion cell death. Exp. Eye Res. 82, 5-12.

Chintala, S. K., Zhang, X., Austin, J. S., Fini, M. E., 2002. Deficiency in matrix metalloproteinase gelatinase B (MMP-9) protects against retinal ganglion cell death after optic nerve ligation. J.Biol.Chem. 277, 47461-47468.

Chong, N. H., Alexander, R. A., Gin, T., Bird, A. C., Luthert, P. J., 2000. TIMP-3, collagen, and elastin immunohistochemistry and histopathology of Sorsby's fundus dystrophy. Invest Ophthalmol Vis.Sci. 41, 898-902.

Chong, N. H., Kvanta, A., Seregard, S., Bird, A. C., Luthert, P. J., & Steen, B., 2003. TIMP-3 mRNA is not overexpressed in Sorsby fundus dystrophy. Am. J. Ophthalmol. 136, 954-955.

Chwa, M., Kenney, M. C., Khin, H., Brown, D. J., 1996. Altered type VI collagen synthesis by keratoconus keratocytes *in vitro*. Biochem.Biophys.Res.Commun. 224, 760-764.

Clarke, M., Mitchell, K. W., Goodship, J., McDonnell, S., Barker, M. D., Griffiths, I. D. McKie, N. 2001, Clinical features of a novel TIMP-3 mutation causing Sorsby's fundus dystrophy: implications for disease mechanism, Br. J. Ophthalmol. 85, 1429-1431.

Clark, I.M, Swingler, T.E., Sampieri, C.L., Edwards, D.R., 2008. The regulation of Matrix Metalloproteinases and their inhibitors. Int. J. Biochem. Cell Biol. 2008 40, 1362-78.

Clements, B.A., Incani, V., Kucharski, C., Lavasanifar, A., Ritchie, B., Uludağ, H. 2007. A comparative evaluation of poly-L-lysine-palmitic acid and Lipofectamine 2000 for plasmid delivery to bone marrow stromal cells. Biomaterials 28: 4693-704.

Collier, S. A., Madigan, M. C., Penfold, P. L., 2000. Expression of membrane-type 1 matrix metalloproteinase (MT1-MMP) and MMP-2 in normal and keratoconus corneas. Curr. Eye Res., 662-668.

Coumoul, X., Deng, C.X. 2006. RNAi in mice: a promising approach to decipher gene functions *in vivo*. Boichimie 88: 637-43.

Cordeiro, M. F., 2002. Beyond Mitomycin: TGF-beta and wound healing. Prog. Retin. Eye Res., 21, 75-89.

Cordeiro, M. F., Siriwardena, D., Chang, L., Khaw, P. T., 2000. Wound healing modulation after glaucoma surgery. Curr. Opin. Ophthalmol, 11, 121-126.

Cottam, D. W., Rennie, I. G., Woods, K., Parsons, M. A., Bunning, R. A., Rees, R. C., 1992. Gelatinolytic metalloproteinase secretion patterns in ocular melanoma. Invest Ophthalmol Vis.Sci., 33, 1923-1927.

Cuello, C., Wakefield, D., Di, G. N., 2002. Neutrophil accumulation correlates with type IV collagenase/gelatinase activity in endotoxin induced uveitis. Br. J. Ophthalmol. 86, 290-295.

Damas, J. K., Waehre, T., Yndestad, A., Ueland, T., Muller, F., Eiken, H. G., Holm, A. M., Halvorsen, B., Froland, S. S., Gullestad, L., & Aukrust, P., 2002. Stromal cell-derived factor-1alpha in unstable angina: potential antiinflammatory and matrix-stabilizing effects. Circulation. 106, 36-42.

Daniels, J. T., Cambrey, A. D., Occleston, N. L., Garrett, Q., Tarnuzzer, R. W., Schultz, G. S., & Khaw, P. T., 2003a. Matrix metalloproteinase inhibition modulates fibroblast-mediated matrix contraction and collagen production *in vitro*. Invest Ophthalmol Vis.Sci. 44, 1104-1110.

Daniels, J. T., Geerling, G., Alexander, R. A., Murphy, G., Khaw, P. T., Saarialho-Kere, U., 2003b. Temporal and spatial expression of matrix metalloproteinases during wound healing of human corneal tissue. Exp.Eye Res. 77, 653-664.

Daniels, J. T., Limb, G. A., Saarialho-Kere, U., Murphy, G., Khaw, P. T., 2003c. Human corneal epithelial cells require MMP-1 for HGF-mediated migration on collagen I. Invest. Ophthalmol. Vis. Sci. 44, 1048-1055.

Daniels, J. T., Occleston, N. L., Crowston, J. G., Cordeiro, M. F., Alexander, R. A., Wilkins, M., Porter, R., Brown, R., & Khaw, P. T., 1998. Understanding and controlling the scarring response: the contribution of histology and microscopy", Microsc.Res.Tech. 42, 317-333.

Das, A., 1999. Prevention of visual loss in older adults. Clin. Geriatr. Med. 15, 131-144.

De La Paz, M. A., Itoh, Y., Toth, C. A., Nagase, H., 1998. Matrix metalloproteinases and their inhibitors in human vitreous. Invest Ophthalmol Vis. Sci. 39, 1256-1260.

De Paiva, C. S., Corrales, R. M., Villarreal, A. L., Farley, W. J., Li, D. Q., Stern, M. E., Pflugfelder, S. C. 2006. Corticosteroid and doxycycline suppress MMP-9 and inflammatory cytokine expression, MAPK activation in the corneal epithelium in experimental dry eye. Exp.Eye Res. 83, 526-535.

Della, N. G., Campochiaro, P. A., Zack, D. J. 1996. Localization of TIMP-3 mRNA expression to the retinal pigment epithelium", Invest Ophthalmol Vis.Sci., 37, 1921-1924.

Descamps, F. J., Martens, E., Proost, P., Starckx, S., Van den Steen, P. E., Van, D. J., Opdenakker, G., 2005. Gelatinase B/matrix metalloproteinase-9 provokes cataract by cleaving lens betaB1 crystallin. FASEB J., 19, 29-35.

Devaraj S., Du Clos T.W., Jialal I. (2005) Binding and internalization of C-Reactive protein by Fcgamma receptors on human aortic endothelial cells mediates biological effects. Arterioscler Thromb Vasc Biol 26:1359–1363.

Di, G. N., Coroneo, M. T., Wakefield, D., 2003. UVB-elicited induction of MMP-1 expression in human ocular surface epithelial cells is mediated through the ERK1/2 MAPK-dependent pathway. Invest. Ophthalmol. Vis. Sci. 44, 4705-4714.

Di, G. N., Coroneo, M. T., Wakefield, D., 2001. Active matrilysin (MMP-7) in human pterygia: potential role in angiogenesis. Invest. Ophthalmol. Vis.Sci. 42, 1963-1968.

Di, G. N., Verma, M. J., McCluskey, P. J., Lloyd, A., Wakefield, D., 1996. Increased matrix metalloproteinases in the aqueous humor of patients and experimental animals with uveitis. Curr.Eye Res., 15, 1060-1068.

Di, G. N., Wakefield, D., Coroneo, M. T., 2000. Differential expression of matrix metalloproteinases and their tissue inhibitors at the advancing pterygium head. Invest Ophthalmol Vis.Sci. 41, 4142-4149.

Direkze, N.C., Forbes, S.J., Brittan, M., Hunt, T., Jeffery, R., Preston, S.L., *et al.* 2003. Multiple organ engraftment by bone-marrow-derived myofibroblasts and fibroblasts in bone-marrow-transplanted mice. Stem Cells 21: 514-20.

Direkze, N.C., K. Hodivala-Dilke, R. Jeffery, T. Hunt, R. Poulsom, D. Oukrif, M.R. Alison, N.A. Wright (2004) Bone marrow contribution to tumor-associated myofibroblasts and fibroblasts. Cancer Res 64: 8492–8495.

Dong, X., Shi, W., Zeng, Q., & Xie, L., 2005. Roles of adherence and matrix metalloproteinases in growth patterns of fungal pathogens in cornea. Curr. Eye Res. 30, 613-620.

Dong, Z., Ghabrial, M., Katar, M., Fridman, R., Berk, R. S., 2000. Membrane-type matrix metalloproteinases in mice intracorneally infected with Pseudomonas aeruginosa. Invest Ophthalmol Vis.Sci. 41, 4189-4194.

Doyle, J. W., Sherwood, M. B., Khaw, P. T., McGrory, S., & Smith, M. F. 1993, Intraoperative 5-fluorouracil for filtration surgery in the rabbit. Invest. Ophthalmol. Vis. Sci., 34, 3313-3319.

Du Clos, T.W. 1989. C-reactive protein reacts with the U1 small nuclear ribonucleoprotein. J Immunol. 143, 2553-9.

Dua, H. S., Zuara-Blanco, A. 2000. Limbal stem cells of the corneal epithelium. Surv. Ophthalmol, 44, 415-425.

Dursun, D., Wang, M., Monroy, D., Li, D. Q., Lokeshwar, B. L., Stern, M. E., Pflugfelder, S. C., 2002. A mouse model of keratoconjunctivitis sicca. Invest Ophthalmol Vis.Sci., 43, 632-638.

Dushku, N., John, M. K., Schultz, G. S., Reid, T. W., 2001. Pterygia pathogenesis: corneal invasion by matrix metalloproteinase expressing altered limbal epithelial basal cells. Arch.Ophthalmol, 119, 695-706.

Duance, M. L. Baltz, M. B. Pepys. 1980. Amyloid P-component is a constituent of normal human glomerular basement membrane. J. Exp. Med. *152:1162.*[Abstract/Free Full Text]

Dwivedi, D. J., Pino, G., Banh, A., Nathu, Z., Howchin, D., Margetts, P., Sivak, J. G., West-Mays, J. A., 2006. Matrix metalloproteinase inhibitors suppress transforming growth factor-beta-induced subcapsular cataract formation. Am. J. Pathol., 168, 69-79.

Edwards, D. R., Murphy, G., Reynolds, J. J., Whitham, S. E., Docherty, A. J., Angel, P., Heath, J. K., 1987. Transforming growth factor beta modulates the expression of collagenase and metalloproteinase inhibitor. EMBO J., 6, 1899-1904.

Egeblad, M., Werb, Z. 2002. New functions for the matrix metalloproteinases in cancer progression. Nat. Rev. Cancer 2, 161-174.

El-Shabrawi, Y., Ardjomand, N., Radner, H., & Ardjomand, N., 2001. MMP-9 is predominantly expressed in epithelioid and not spindle cell uveal melanoma. J. Pathol. 194, 201-206.

El-Shabrawi, Y., Walch, A., Hermann, J., Egger, G., Foster, C. S., 2004. Inhibition of MMP-dependent chemotaxis and amelioration of experimental autoimmune uveitis with a selective metalloproteinase-2 and -9 inhibitor. J. Neuroimmunol., 155, 13-20.

El-Shabrawi, Y. G., Christen, W. G., Foster, S. C., 2000. Correlation of metalloproteinase-2 and -9 with proinflammatory cytokines interleukin-1b, interleukin-12 and the interleukin-1 receptor antagonist in patients with chronic uveitis. Curr.Eye Res. 20, 211-214.

Ellerbroek, S. M., Wu, Y. I., Overall, C. M., Stack, M. S., 2001. Functional interplay between type I collagen and cell surface matrix metalloproteinase activity. J. Biol. Chem. 276, 24833-24842.

Ellis, V., Whawell, S. A., Werner, F., Deadman, J. J., 1999. Assembly of urokinase receptor-mediated plasminogen activation complexes involves direct, non-active-site interactions between urokinase and plasminogen. Biochemistry, 38, 651-659.

Elshaw, S. R., Sisley, K., Cross, N., Murray, A. K., MacNeil, S. M., Wagner, M., Nichols, C. E., Rennie, I. G., 2001. A comparison of ocular melanocyte and uveal melanoma cell invasion and the implication of alpha1beta1, alpha4beta1 and alpha6beta1 integrins. Br. J. Ophthalmol. 85, 732-738.

English, W. R., Holtz, B., Vogt, G., Knauper, V., Murphy, G., 2001. Characterization of the role of the "MT-loop": an eight-amino acid insertion specific to progelatinase A (MMP2) activating membrane-type matrix metalloproteinases. J. Biol. Chem., 276, 42018-42026.

Epstein, J., Cai, J., Glaser, T., Jepeal, L., Maas, R., 1994. Identification of a Pax paired domain recognition sequence and evidence for DNA-dependent conformational changes. J.Biol.Chem., 269, 8355-8361.

Esquenazi, S., Esquenazi, I., Grunstein, L., He, J., Bazan, H., 2009. Immunohistological evaluation of the healing response at the flap interface in patients with LASIK ectasia requiring penetrating keratoplasty. J. Refract. Surg. 25, 739-46.

Esser, P., Heimann, K., Wiedemann, P., 1993. Macrophages in proliferative vitreoretinopathy and proliferative diabetic retinopathy: differentiation of subpopulations. Br. J. Ophthalmol, 77, 731-733.

European Pharmacopoeia (EUP), 2000. Pharmacopee Europeenne 4eme. Edition, pp. 439-444. Direction Europeenne de la Qualite du Medicament, Strasbourg, 2000.

Evans, J. R., 2006. Antioxidant vitamin and mineral supplements for slowing the progression of age-related macular degeneration. Cochrane.Database.Syst.Rev. 2, CD000254.

Fariss, R. N., Apte, S. S., Olsen, B. R., Iwata, K., Milam, A. H., 1997. Tissue inhibitor of metalloproteinases-3 is a component of Bruch's membrane of the eye. Am. J. Pathol. 150, 323-328.

Felbor, U., Benkwitz, C., Klein, M. L., Greenberg, J., Gregory, C. Y., Weber, B. H. 1997. Sorsby fundus dystrophy: reevaluation of variable expressivity in patients carrying a TIMP3 founder mutation. Arch. Ophthalmol. 115, 1569-1571.

Felbor, U., Stohr, H., Amann, T., Schonherr, U., pfelstedt-Sylla, E., Weber, B. H. 1996. A second independent Tyr168Cys mutation in the tissue inhibitor of metalloproteinases-3 (TIMP3) in Sorsby's fundus dystrophy. J.Med.Genet., 33, 233-236.

Felbor, U., Stohr, H., Amann, T., Schonherr, U., Weber, B. H., 1995. A novel Ser156Cys mutation in the tissue inhibitor of metalloproteinases-3 (TIMP3) in Sorsby's fundus dystrophy with unusual clinical features. Hum. Mol. Genet. 4, 2415-2416.

Feng Y, Wang Y, Pfister F, Hillebrands JL, Deutsch U, Hammes HP., 2009. Decreased hypoxia-induced neovascularization in angiopoietin-2 heterozygous knockout mouse through reduced MMP activity.Cell Physiol Biochem. 23, 277-84.

Filipowicz, W., Jaskiewicz, L, Kolb, F.A., Pillai, R. S., 2005. Post-transcriptional gene silencing by siRNAs and miRNAs. Curr Opin Struct Biol.15: 331-41.

Fini, M. E., Cook, J. R., Mohan, R., 1998. Proteolytic mechanisms in corneal ulceration and repair. Arch. Dermatol. Res. 290, S12-S23.

Fini, M. E., Cui, T. Y., Mouldovan, A., Grobelny, D., Galardy, R. E., Fisher, S. J., 1991. An inhibitor of the matrix metalloproteinase synthesized by rabbit corneal epithelium. Invest. Ophthalmol. Vis. Sci., 32, 2997-3001.

Fini, M. E. & Girard, M. T. 1990a. Expression of collagenolytic/gelatinolytic metalloproteinases by normal cornea. Invest Ophthalmol Vis.Sci., 31, 1779-1788.

Fini, M. E., Girard, M. T., 1990b. The pattern of metalloproteinase expression by corneal fibroblasts is altered by passage in cell culture. J.Cell Sci. 97 (Pt 2), 373-383.

Fini, M. E., Girard, M. T., Matsubara, M., 1992, Collagenolytic/gelatinolytic enzymes in corneal wound healing. Acta Ophthalmol Suppl. 202, 26-33.

Fini, M. E., Parks, W. C., Rinehart, W. B., Girard, M. T., Matsubara, M., Cook, J. R., West-Mays, J. A., Sadow, P. M., Burgeson, R. E., Jeffrey, J. J., Raizman, M. B., Krueger, R. R., Zieske, J. D., 1996. Role of matrix metalloproteinases in failure to re-epithelialize after corneal injury. Am.J.Pathol., 149, 1287-1302.

Fini, M. E, Slaugenhaupt, S. A., 2002. Enzymatic mechanisms in corneal ulceration with specific reference to familial dysautonomia: potential for genetic approaches. Adv.Exp.Med.Biol., 506, Pt A, 629-639.

Fini, M. E., Strissel, K. J., Girard, M. T., Mays, J. W., Rinehart, W. B., 1994. Interleukin 1 alpha mediates collagenase synthesis stimulated by phorbol 12-myristate 13-acetate. J. Biol. Chem. 269, 11291-11298.

Fini, M. E., Yue, B. Y., Sugar, J., 1992. Collagenolytic/gelatinolytic metalloproteinases in normal and keratoconus corneas. Curr.Eye Res. 11, 849-862.

Fiotti, N., Pedio, M., Battaglia, P. M., Altamura, N., Uxa, L., Guarnieri, G., Giansante, C., Ravalico, G., 2005. MMP-9 microsatellite polymorphism and susceptibility to exudative form of age-related macular degeneration. Genet.Med. 7, 272-277.

Forrester, J. V., Shafiee, A., Schroder, S., Knott, R., & McIntosh, L., 1993. The role of growth factors in proliferative diabetic retinopathy. Eye. 7 (Pt 2), 276-287.

Francois, J., 1984. Corticosteroid glaucoma. Ophthalmologica. 188, 76-81.

Frank, R. N., 2004. Diabetic retinopathy. N. Engl. J. Med. 350, 48-58.

Friedman, S.L. 2003. Liver fibrosis -- from bench to bedside. J Hepatol. 38 Suppl 1:S38-S53.

Frisch, S. M., Ruley, H. E., 1987. Transcription from the stromelysin promoter is induced by interleukin-1 and repressed by dexamethasone. J. Biol. Chem., 262, 16300-16304.

Gabelt, B. T., Kaufman, P. L, 1989. Prostaglandin F2 alpha increases uveoscleral outflow in the cynomolgus monkey. Exp. Eye Res. 49, 389-402.

Gabison, E. E., Chastang, P., Menashi, S., Mourah, S., Doan, S., Oster, M., Mauviel, A., & Hoang-Xuan, T., 2003. Late corneal perforation after photorefractive keratectomy associated with topical diclofenac: involvement of matrix metalloproteinase's. Ophthalmology. 110, 1626-1631.

Galardy,R.E, Cassabonne,M.E., Giese,C. Gilbert,J.H. Lapierre,F. Lopez,H. Schaefer,M.E. Stack,R. Sullivan,M. Summers,B. 1994. Low molecular weight inhibitors in corneal ulceration. Ann. N.Y. Acad. Sci. 732, 315-323.

Galis, Z. S., Kranzhofer, R., Fenton, J. W., Libby, P., 1997. Thrombin promotes activation of matrix metalloproteinase-2 produced by cultured vascular smooth muscle cells. Arterioscler. Thromb. Vasc. Biol. 17, 483-489.

Garlanda, C., Bottazzi, B., Bastone, A., Mantovani, A. 2005. Pentraxins at the crossroads between innate immunity, inflammation, matrix deposition, and female fertility. Annu Rev Immunol. 23:337-66.

Garner, A., 1993. Histopathology of diabetic retinopathy in man. Eye 7 (Pt 2), 250-253.

Gartaganis, S. P., Georgakopoulos, C. D., Mela, E. K., Exarchou, A., Ziouti, N., Assouti, M., Vynios, D. H., 2002. Matrix metalloproteinases and their inhibitors in exfoliation syndrome. Ophthalmic Res. 34, 165-171.

Gaton, D. D., Sagara, T., Lindsey, J. D., Gabelt, B. T., Kaufman, P. L., Weinreb, R. N., 2001. Increased matrix metalloproteinases 1, 2, and 3 in the monkey uveoscleral outflow pathway after topical prostaglandin F(2 alpha)-isopropyl ester treatment. Arch.Ophthalmol. 119, 1165-1170.

Giebel, S. J., Menicucci, G., McGuire, P. G., Das, A., 2005. Matrix metalloproteinases in early diabetic retinopathy and their role in alteration of the blood-retinal barrier. Lab Invest. 85, 597-607.

Gilbert, C., Hiscott, P., Unger, W., Grierson, I., McLeod, D., 1988. Inflammation and the formation of epiretinal membranes. Eye 2, S140-S156.

Girard, M. T., Matsubara, M., Kublin, C., Tessier, M. J., Cintron, C., Fini, M. E., 1993. Stromal fibroblasts synthesize collagenase and stromelysin during long-term tissue remodeling. J. Cell Sci. 104 (Pt 4), 1001-1011.

Glaser, T., Jepeal, L., Edwards, J. G., Young, S. R., Favor, J., Maas, R. L., 1994a. PAX6 gene dosage effect in a family with congenital cataracts, aniridia, anophthalmia and central nervous system defects. Nat. Genet. 7, 463-471.

Glaser, T., Ton, C. C., Mueller, R., Petzl-Erler, M. L., Oliver, C., Nevin, N. C., Housman, D. E., Maas, R. L., 1994b. Absence of PAX6 gene mutations in Gillespie syndrome (partial aniridia, cerebellar ataxia, and mental retardation). Genomics. 19, 145-148.

Glasspool, R. M., Twelves, C. J. 2001. Matrix metalloproteinase inhibitors: past lessons and future prospects in breast cancer. Breast. 10, 368-378.

Goldenfeld M, Krupin T, Ruderman JM, et al. 1994. 5-Fluorouracil in initial trabeculectomy: a prospective, randomized, multicenter study. Ophthalmology. 1994;101:1024–1029.

Gopinathan, U., Ramakrishna, T., Willcox, M., Rao, C. M., Balasubramanian, D., Kulkarni, A., Vemuganti, G. K., Rao, G. N., 2001. Enzymatic, clinical and histologic evaluation of corneal tissues in experimental fungal keratitis in rabbits. Exp. Eye Res. 72, 433-442.

Gordon, D.M., McLean, J. M., Koteen, H., Bousquet, F. P., McCusker, W. D., Baras, I., Wetzig, P., Norton, E. W. 1951. The use of ACTH and cortisone in ophthalmology. Am. J. Ophthalmol. 34: 1675-86.

Gragoudas, E. S., Egan, K. M., Seddon, J. M., Glynn, R. J., Walsh, S. M., Finn, S. M., Munzenrider, J. E., Spar, M. D., 1991. Survival of patients with metastases from uveal melanoma. Ophthalmology. 98, 383-389.

Grindley, J. C., Davidson, D. R., Hill, R. E., 1995. The role of Pax-6 in eye and nasal development. Development. 121, 1433-1442.

Grishok, A. *et al.* 2001. Genes and mechanisms related to RNA interference regulate expression of the small temporal RNAs that control *C. elegans* developmental timing. *Cell* 106:23–34

Gross, J., Lapiere, C. M. ,1962. Collagenolytic activity in amphibian tissues: a tissue culture assay. Proc. Natl. Acad. Sci. U.S.A. 48, 1014-1022.

Guggenheim, J. A., McBrien, N. A., 1996. Form-deprivation myopia induces activation of scleral matrix metalloproteinase-2 in tree shrew. Invest. Ophthalmol. Vis.Sci., 37, 1380-1395.

Guo, L., Hussain, A. A., Limb, G. A., Marshall, J., 1999. Age-dependent variation in metalloproteinase activity of isolated human Bruch's membrane and choroid. Invest. Ophthalmol. Vis.Sci. 40, 2676-2682.

Guo, L., Moss, S. E., Alexander, R. A., Ali, R. R., Fitzke, F. W., Cordeiro, M. F., 2005. Retinal ganglion cell apoptosis in glaucoma is related to intraocular pressure and IOP-induced effects on extracellular matrix. Invest. Ophthalmol. Vis. Sci. 46, 175-182.

Haas, J.S., Nootens, R.H. 1974. Glaucoma secondary to benign adrenal adenoma. Am J Ophthalmol. 78: 497-500.

Halder, G., Callaerts, P., Gehring, W. J., 1995. New perspectives on eye evolution. Curr. Opin. Genet. Dev. 5, 602-609.

Hammond, S. 2005. Dicing and slicing; The core machinery of the RNA interference pathway. FEBS Letters 579: 5822-5829.

Hammond, S.M., Bernstein, E., Beach, D. and Hannon, G.J. 2000. An RNA-directed nuclease mediates post-transcriptional gene silencing in Drosophila cells. Nature 404: 293–295.

Han, J., Lee, Y., Yeom, K.H., Kim, Y.K., Jin, H., Kim, V.N. The Drosha-DGCR8 complex in primary microRNA processing. Genes Dev. 18: 3016-27.

Hanna, C., O'Brien, J. E., 1960. Cell production and migration in the epithelial layer of the cornea. Arch. Ophthalmol. 64, 536-539.

Hao, J. L., Nagano, T., Nakamura, M., Kumagai, N., Mishima, H., Nishida, T., 1999. Effect of galardin on collagen degradation by Pseudomonas aeruginosa. Exp. Eye Res. 69, 595-601.

Hargrave, S. L., Jung, J. C., Fini, M. E., Gelender, H., Cather, C., Guidera, A., Udell, I., Fisher, S., Jester, J. V., Bowman, R. W., McCulley, J. P., Cavanagh, H. D., 2002. Possible role of the vitamin E solubilizer in topical diclofenac on matrix metalloproteinase expression in corneal melting: an analysis of postoperative keratolysis. Ophthalmology. 109, 343-350.

Harris, A. K., Stopak, D., Wild, P., 1981. Fibroblast traction as a mechanism for collagen morphogenesis. Nature. 290, 249-251.

Hartlapp, I., Abe, R., Saeed, R. W., Peng, T., Voelter, W., Bucala, R., Metz, C. N., 2001. Fibrocytes induce an angiogenic phenotype in cultured endothelial cells and promote angiogenesis *in vivo*. FASEB J. 15, 2215-2224.

Haudek, S.B., Xia, Y., Huebener, P., Lee, J.M., Carlson, S., Crawford, J.R., Pilling, D., Gomer, R.H., Trial, J., Frangogiannis, N.G., Entman, M.L. 2006. Bone marrow-derived fibroblast precursors mediate ischemic cardiomyopathy in mice. Proc Natl Acad Sci U S A. 2006 Nov 28;103(48):18284-9.

He, C. S., Wilhelm, S. M., Pentland, A. P., Marmer, B. L., Grant, G. A., Eisen, A. Z., Goldberg, G. I., 1989. Tissue cooperation in a proteolytic cascade activating human interstitial collagenase. Proc. Natl. Acad. Sci. U.S.A. 86, 2632-2636.

Heck, L. W., Morihara, K., Abrahamson, D. R., 1986. Degradation of soluble laminin and depletion of tissue-associated basement membrane laminin by Pseudomonas aeruginosa elastase and alkaline protease. Infect. Immun. 54, 149-153.

Heck, L. W., Morihara, K., McRae, W. B., Miller, E. J., 1986. Specific cleavage of human type III and IV collagens by Pseudomonas aeruginosa elastase. Infect. Immun. 51, 115-118.

Heiligenhaus, A., Li, H. F., Yang, Y., Wasmuth, S., Steuhl, K. P., Bauer, D., 2005. Transplantation of amniotic membrane in murine herpes stromal keratitis modulates matrix metalloproteinases in the cornea. Invest. Ophthalmol. Vis. Sci., 46, 4079-4085.

Helbig, H., Schlotzer-Schrehardt, U., Noske, W., Kellner, U., Foerster, M. H., Naumann, G. O., 1994. Anterior-chamber hypoxia and iris vasculopathy in pseudoexfoliation syndrome. Ger J. Ophthalmol. 3, 148-153.

Hernandez, M. R., 1992. Ultrastructural immunocytochemical analysis of elastin in the human lamina cribrosa. Changes in elastic fibers in primary open-angle glaucoma. Invest. Ophthalmol. Vis. Sci. 33, 2891-2903.

Hernandez, M. R., Pena, J. D., 1997. The optic nerve head in glaucomatous optic neuropathy. Arch.Ophthalmol. 115, 389-395.

Hernandez, M. R., Weinstein, B. I., Schwartz, J., Ritch, R., Gordon, G. G., Southren, A. L., 1987. Human trabecular meshwork cells in culture: morphology and extracellular matrix components. Invest. Ophthalmol. Vis. Sci. 28, 1655-1660.

Hernandez, M. R., Weinstein, B. I., Wenk, E. J., Gordon, G. G., Dunn, M. W., Southren, A. L., 1983. The effect of dexamethasone on the *in vitro* incorporation of precursors of extracellular matrix components in the outflow pathway region of the rabbit eye. Invest. Ophthalmol. Vis. Sci. 24, 704-709.

Hernandez-Barrantes, S., Shimura, Y., Soloway, P. D., Sang, Q. A., Fridman, R., 2001. Differential roles of TIMP-4 and TIMP-2 in pro-MMP-2 activation by MT1-MMP. Biochem. Biophys. Res. Commun. 281, 126-130.

Hess, A. R., Seftor, E. A., Seftor, R. E., Hendrix, M. J. 2003. Phosphoinositide 3-kinase regulates membrane Type 1-matrix metalloproteinase (MMP) and MMP-2 activity during melanoma cell vasculogenic mimicry. Cancer Res. 63, 4757-4762.

Heuer, D.K., Parrish, R.K., Gressel, M.G., et al. 1986. 5-Fluorouracil and glaucoma filtering surgery. III. Intermediate follow-up of a pilot study. Ophthalmology. 93:1537–1546.

Hill, R. E., Favor, J., Hogan, B. L., Ton, C. C., Saunders, G. F., Hanson, I. M., Prosser, J., Jordan, T., Hastie, N. D., van, H.V., 1991. Mouse small eye results from mutations in a paired-like homeobox-containing gene. Nature. 354, 522-525.

Hiscott, P., Waller, H. A., Grierson, I., Butler, M. G., Scott, D. L., 1993. The extracellular matrix of reparative tissue in the vitreous: fibronectin production in proliferative diabetic retinopathy membranes. Eye. 7 (Pt 2), 288-292.

Hoekstra, R., Eskens, F. A., Verweij, J., 2001. Matrix metalloproteinase inhibitors: current developments and future perspectives. Oncologist. 6, 415-427.

Hoffmann, S., He, S., Jin, M. L., Masiero, L., Wiedemann, P., Ryan, S. J., Kohn, E. C. 2005. Carboxyamido-triazole modulates retinal pigment epithelial and choroidal endothelial cell attachment, migration, proliferation, and MMP-2 secretion of choroidal endothelial cells. Curr. Eye Res. 30, 103-113.

Hollborn, M., Stathopoulos, C., Steffen, A., Wiedemann, P., Kohen, L., Bringmann, A., 2007. Positive Feedback Regulation between MMP-9 and VEGF in Human RPE Cells. Invest. Ophthalmol. Vis. Sci. 48, 4360-4367.

Holopainen, J. M., Moilanen, J. A., Sorsa, T., Kivela-Rajamaki, M., Tervahartiala, T., Vesaluoma, M. H., Tervo, T. M., 2003. Activation of matrix metalloproteinase-8 by membrane type 1-MMP and their expression in human tears after photorefractive keratectomy. Invest. Ophthalmol. Vis. Sci. 44, 2550-2556.

Hosseini, M., Rose, A. Y., Song, K., Bohan, C., Alexander, J. P., Kelley, M. J., Acott, T. S., 2006. IL-1 and TNF induction of matrix metalloproteinase-3 by c-Jun N-terminal kinase in trabecular meshwork. Invest. Ophthalmol. Vis. Sci. 47, 1469-1476.

Hotary, K. B., Yana, I., Sabeh, F., Li, X. Y., Holmbeck, K., Birkedal-Hansen, H., Allen, E. D., Hiraoka, N., Weiss, S. J., 2002. Matrix metalloproteinases (MMPs) regulate fibrin-invasive activity via MT1-MMP-dependent and -independent processes. J. Exp. Med. 195, 295-308.

Howe, T. R., Iglewski, B. H., 1984. Isolation and characterization of alkaline protease-deficient mutants of Pseudomonas aeruginosa *in vitro* and in a mouse eye model. Infect.Immun. 43, 1058-1063.

Huang, S. H., Adamis, A. P., Wiederschain, D. G., Shima, D. T., Shing, Y., Moses, M. A. 1996. Matrix metalloproteinases and their inhibitors in aqueous humor. Exp. Eye Res. 62, 481-490.

Husain, S., Jafri, F., Crosson, C. E., 2005. Acute effects of PGF2alpha on MMP-2 secretion from human ciliary muscle cells: a PKC- and ERK-dependent process. Invest. Ophthalmol. Vis. Sci. 46, 1706-1713.

Hutvagner, G., McLachlan, J., Pasquinelli, A.E., Balint, E., Tuschl, T., Zamore, P.D. 2001. A cellular function for the RNA-interference enzyme Dicer in the maturation of the let-7 small temporal RNA. Science. 293: 834–838.

Iamaroon, A., Wallon, U. M., Overall, C. M., Diewert, V. M., 1996. Expression of 72-kDa gelatinase (matrix metalloproteinase-2) in the developing mouse craniofacial complex. Arch.Oral Biol. 41, 1109-1119.

Ikema, K., Matsumoto, K., Inomata, Y., Komohara, Y., Miyajima, S., Takeya, M., Tanihara, H., 2006. Induction of matrix metalloproteinases (MMPs) and tissue inhibitors of MMPs correlates with outcome of acute experimental pseudomonal keratitis. Exp. Eye Res. 83, 1396-1404.

Illman, S. A., Keski-Oja, J., Parks, W. C., Lohi, J., 2003. The mouse matrix metalloproteinase, epilysin (MMP-28), is alternatively spliced and processed by a furin-like proprotein convertase. Biochem. J. 375 (Pt 1), 191-197.

Imai, K., Shikata, H., Okada, Y., 1995. Degradation of vitronectin by matrix metalloproteinases-1, -2, -3, -7 and -9. FEBS Lett. 369, 249-251.

Ingram, C.J., Brubaker, R.F. (1999). Effect of brinzolamide and dorzolamide on aqueous humor flow in human eyes. Am J Ophthalmol. 1999 Sep;128(3):292-6. Erratum in: Am J Ophthalmol 1999 Nov;128(5):672.

Iovieno, A. Lambiase, A., Moretti, C., Perrella, E., Bonini, S., 2009. Therapeutic effect of topical 5-fluorouracil in conjunctival squamous carcinoma is associated with changes in matrix metalloproteinases and tissue inhibitor of metalloproteinases expression. Cornea 28, 821-4.

Ishizaki, E., Takai, S., Ueki, M., Maeno, T., Maruichi, M., Sugiyama, T., Oku, H., Ikeda, T., & Miyazaki, M., 2006. Correlation between angiotensin-converting enzyme, vascular endothelial growth factor, and matrix metalloproteinase-9 in the vitreous of eyes with diabetic retinopathy. Am. J. Ophthalmol. 141, 129-134.

Ishizaki, M., Westerhausen-Larson, A., Kino, J., Hayashi, T., Kao, W. W., 1993. Distribution of collagen IV in human ocular tissues. Invest. Ophthalmol. Vis. Sci. 34, 2680-2689.

Itoh, T., Tanioka, M., Yoshida, H., Yoshioka, T., Nishimoto, H., Itohara, S., 1998. Reduced angiogenesis and tumor progression in gelatinase A-deficient mice. Cancer Res. 58, 1048-1051.

Itoh, Y., Kajita, M., Kinoh, H., Mori, H., Okada, A., Seiki, M., 1999. Membrane type 4 matrix metalloproteinase (MT4-MMP, MMP-17) is a glycosylphosphatidylinositol-anchored proteinase. J. Biol. Chem. 274, 34260-34266.

Iwanami, H., Ishizaki, M., Fukuda, Y., Takahashi, H., 2009. Expression of matrix metalloproteinases (MMP)-12 by myofibroblasts during alkali-burned corneal wound healing. Curr. Eye Res. 34, 207-14.

Jacobson, S. G., Cideciyan, A. V., Bennett, J., Kingsley, R. M., Sheffield, V. C., Stone, E. M., 2002. Novel mutation in the TIMP3 gene causes Sorsby fundus dystrophy. Arch.Ophthalmol, 120, 376-379.

James, T. W., Wagner, R., White, L. A., Zwolak, R. M., & Brinckerhoff, C. E., 1993. Induction of collagenase and stromelysin gene expression by mechanical injury in a vascular smooth muscle-derived cell line. J. Cell Physiol. 157, 426-437.

Jeffrey, J., 1998. Interstitial Collagenases. Matrix Metalloproteinases. Park. W. & Mecham, R. eds., San Diego, Academic Press, 15-42.

Jenne, D., Stanley, K. K., 1987. Nucleotide sequence and organization of the human S-protein gene: repeating peptide motifs in the "pexin" family and a model for their evolution. Biochemistry 26, 6735-6742.

Jerdan, J. A., Pepose, J. S., Michels, R. G., Hayashi, H., de, B. S., Sebag, M., & Glaser, B. M., 1989. Proliferative vitreoretinopathy membranes. An immunohistochemical study. Ophthalmology. 96, 801-810.

Jiang, A., Zhang, L., Zhao, C., Yang, F., 2001. Clinical effect of acupuncture treatment in 109 cases of knee osteoarthritis. J. Tradit. Chin. Med. 21, 282-285.

Jimenez, M. J., Balbin, M., Alvarez, J., Komori, T., Bianco, P., Holmbeck, K., Birkedal-Hansen, H., Lopez, J. M., Lopez-Otin, C., 2001. A regulatory cascade involving retinoic acid,

Cbfa1, and matrix metalloproteinases is coupled to the development of a process of perichondrial invasion and osteogenic differentiation during bone formation. J. Cell. Biol.155, 1333-1344.

Jin, M., Kashiwagi, K., Iizuka, Y., Tanaka, Y., Imai, M., Tsukahara, S., 2001. Matrix metalloproteinases in human diabetic and nondiabetic vitreous. Retina. 21, 28-33.

Johansson, N., Ahonen, M., Kahari, V. M., 2000. Matrix metalloproteinases in tumor invasion. Cell. Mol. Life Sci. 57, 5-15.

John, M., Jaworski, C., Chen, Z., Subramanian, S., Ma, W., Sun, F., Li, D., Spector, A., Carper, D., 2004. Matrix metalloproteinases are down-regulated in rat lenses exposed to oxidative stress. Exp. Eye Res. 79, 839-846.

Johnatty, R. N., Taub, D. D., Reeder, S. P., Turcovski-Corrales, S. M., Cottam, D. W., Stephenson, T. J., Rees, R. C., 1997. Cytokine and chemokine regulation of proMMP-9 and TIMP-1 production by human peripheral blood lymphocytes. J. Immunol., 158, 2327-2333.

Johnson, D. H., Bradley, J. M., Acott, T. S., 1990. The effect of dexamethasone on glycosaminoglycans of human trabecular meshwork in perfusion organ culture. Invest. Ophthalmol. Vis. Sci., 31, 12, 2568-2571.

Johnson, E. C., Morrison, J. C., Farrell, S., Deppmeier, L., Moore, C. G., McGinty, M. R., 1996. The effect of chronically elevated intraocular pressure on the rat optic nerve head extracellular matrix. Exp. Eye Res. 62, 663-674.

Johnson, R.W., Tew, M.B., Arnett, F.C. 2002 The genetics of systemic sclerosis. Curr. Rheumatol. Rep. 4: 99-107.

Johnson-Wint, B., 1988. Do keratinocytes regulate fibroblast collagenase activities during morphogenesis? Ann. N.Y. Acad. Sci., 548, 167-173.

Johnson-Wint, B., 1980. Regulation of stromal cell collagenase production in adult rabbit cornea: *in vitro* stimulation and inhibition by epithelial cell products. Proc. Natl. Acad. Sci. U.S.A. 77, 5331-5335.

Jones, B. E., Moshyedi, P., Gallo, S., Tombran-Tink, J., Arand, G., Reid, D. A., Thompson, E. W., Chader, G. J., Waldbillig, R. J., 1994. Characterization and novel activation of 72-kDa metalloproteinase in retinal interphotoreceptor matrix and Y-79 cell culture medium. Exp. Eye Res. 59, 257-269.

Jones, B. E., Thompson, E. W., Hodos, W., Waldbillig, R. J., Chader, G. J., 1996. Scleral matrix metalloproteinases, serine proteinase activity and hydrational capacity are increased in myopia induced by retinal image degradation. Exp. Eye Res. 63, 369-381.

Jones, C. B., Sane, D. C., Herrington, D. M., 2003. Matrix metalloproteinases: a review of their structure and role in acute coronary syndrome. Cardiovasc. Res. 59, 812-823.

Junqueira, L.C., Cossermelli, W., Brentani, R. 1978. Differential staining of collagens type I, II and III by Sirius red and polarization microscopy. Arch. Histol. Japonicum. 41, 267-274.

Kadonosono, K., Yazama, F., Itoh, N., Sawada, H., Ohno, S., 1999. Expression of matrix metalloproteinase-7 in choroidal neovascular membranes in age-related macular degeneration. Am. J. Ophthalmol. 128, 382-384.

Kahari, V. M., Saarialho-Kere, U., 1999. Matrix metalloproteinases and their inhibitors in tumour growth and invasion. Ann. Med. 31, 34-45.

Kanwar, Y. S., Ota, K., Yang, Q., Wada, J., Kashihara, N., Tian, Y., Wallner, E. I., 1999. Role of membrane-type matrix metalloproteinase 1 (MT-1-MMP), MMP-2, and its inhibitor in nephrogenesis. Am. J. Physiol. 277 (Pt 2), F934-F947.

Kawashima, Y., Saika, S., Miyamoto, T., Yamanaka, O., Okada, Y., Tanaka, S., Ohnishi, Y., 2000. Matrix metalloproteinases and tissue inhibitors of metalloproteinases of fibrous humans lens capsules with intraocular lenses. Curr. Eye Res. 21, 962-967.

Katz, G.J., Higginbotham, E.J., Lichter, P.R., et al. 1995. Mitomycin C versus5-fluorouracil in high-risk glaucoma filtering surgery: extended follow-up. Ophthalmology. 102:1263–1269.

Kawashima, Y., Saika, S., Yamanaka, O., Okada, Y., Ohkawa, K., Ohnishi, Y., 1998. Immunolocalization of matrix metalloproteinases and tissue inhibitors of metalloproteinases in human subconjunctival tissues. Curr. Eye Res. 17, 445-451.

Kee, C., Son, S., Ahn, B. H., 1999. The relationship between gelatinase A activity in aqueous humor and glaucoma. J. Glaucoma 8, 51-55.

Kenney, M. C., Chwa, M., Alba, A., Saghizadeh, M., Huang, Z. S., Brown, D. J., 1998. Localization of TIMP-1, TIMP-2, TIMP-3, gelatinase A and gelatinase B in pathological human corneas. Curr. Eye Res., 17, 238-246.

Kenney, M. C., Chwa, M., Atilano, S. R., Tran, A., Carballo, M., Saghizadeh, M., Vasiliou, V., Adachi, W., Brown, D. J., 2005. Increased levels of catalase and cathepsin V/L2 but decreased TIMP-1 in keratoconus corneas: evidence that oxidative stress plays a role in this disorder. Invest. Ophthalmol. Vis. Sci. 46, 823-832.

Kenney, M. C., Chwa, M., Opbroek, A. J., Brown, D. J. 1994. Increased gelatinolytic activity in keratoconus keratocyte cultures. A correlation to an altered matrix metalloproteinase-2/tissue inhibitor of metalloproteinase ratio. Cornea 13, 114-124.

Kernacki, K. A., Chunta, J. L., Barrett, R. P., Hazlett, L. D., 2004. TIMP-1 role in protection against Pseudomonas aeruginosa-induced corneal destruction. Exp. Eye Res. 78, 1155-1162.

Kernacki, K. A., Fridman, R., Hazlett, L. D., Lande, M. A., Berk, R. S., 1997. *In vivo* characterization of host and bacterial protease expression during Pseudomonas aeruginosa corneal infections in naive and immunized mice. Curr. Eye Res., 16, 289-297.

Kernacki, K. A., Hobden, J. A., Hazlett, L. D., Fridman, R., Berk, R. S., 1995. *In vivo* bacterial protease production during Pseudomonas aeruginosa corneal infection. Invest. Ophthalmol. Vis. Sci. 36, 1371-1378.

Kessler, E., Mondino, B. J., Brown, S. I., 1977. The corneal response to Pseudomonas aeruginosa: histopathological and enzymatic characterization. Invest. Ophthalmol. Vis. Sci., 16, 116-125.

Khaw, P. T., Doyle, J. W., Sherwood, M. B., Smith, M. F., McGorray, S., 1993. Effects of intraoperative 5-fluorouracil or mitomycin C on glaucoma filtration surgery in the rabbit. Ophthalmology. 100, 367-372.

Khaw, P. T., Sherwood, M. B., MacKay, S. L., Rossi, M. J., Schultz, G. 1992a. Five-minute treatments with fluorouracil, floxuridine, and mitomycin have long-term effects on human Tenon's capsule fibroblasts. Arch. Ophthalmol. 110, 1150-1154.

Khaw, P. T., Ward, S., Porter, A., Grierson, I., Hitchings, R. A., Rice, N. S., 1992b. The long-term effects of 5-fluorouracil and sodium butyrate on human Tenon's fibroblasts. Invest. Ophthalmol. Vis. Sci. 33, 2043-2052.

Khvorova, A., Reynolds, A., Jayasena, S.D. 2003. Functional siRNAs and miRNAs exhibit strand bias. Cell 115: 209–216.

Kim, H. S., Luo, L., Pflugfelder, S. C., Li, D. Q., 2005. Doxycycline inhibits TGF-beta1-induced MMP-9 via Smad and MAPK pathways in human corneal epithelial cells. Invest. Ophthalmol. Vis. Sci., 46, 840-848.

Kim, J., Yu, W., Kovalski, K., Ossowski, L., 1998. Requirement for specific proteases in cancer cell intravasation as revealed by a novel semiquantitative PCR-based assay. Cell. 94, 353-362.

Kim, J. W., Lindsey, J. D., Wang, N., Weinreb, R. N., 2001. Increased human scleral permeability with prostaglandin exposure. Invest. Ophthalmol. Vis. Sci. 42, 1514-1521.

Kim, V.N. 2005. MicroRNA biogenesis: coordinated cropping and dicing. Nat. Rev. Mol. Cell. Biol. 6: 376–385.

Kimpel, M. W., Johnson, D. H., 1992. Factors influencing *in vivo* trabecular cell replication as determined by 3H-thymidine labeling; an autoradiographic study in cats. Curr. Eye Res. 11, 297-306.

Kisseleva, T., Notas, G., Taura, K., Kodama, Y., De Minicis, S., Kramer, M., Hesson, D., Pelura, T., Brenner, D, 2006. Human Serum Amyloid P (Hsap) Inhibits Bile Duct Ligation Induced Liver Fibrosis in Mice. Gastroenterology 134: 768 – 768.

Kleifeld, O., Van den Steen, P. E., Frenkel, A., Cheng, F., Jiang, H. L., Opdenakker, G., Sagi, I., 2000. Structural characterization of the catalytic active site in the latent and active natural gelatinase B from human neutrophils. J. Biol. Chem. 275, 34335-34343.

Klein, G., Vellenga, E., Fraaije, M. W., Kamps, W. A., de Bont, E. S., 2004a. The possible role of matrix metalloproteinase (MMP)-2 and MMP-9 in cancer, e.g. acute leukemia. Crit. Rev. Oncol. Hematol. 50, 87-100.

Klein, R., Peto, T., Bird, A., Vannewkirk, M. R., 2004b. The epidemiology of age-related macular degeneration. Am. J. Ophthalmol. 137, 486-495.

Kliffen, M., Mooy, C. M., Luider, T. M., Huijmans, J. G., Kerkvliet, S., de Jong, P. T., 1996. Identification of glycosaminoglycans in age-related macular deposits", Arch.Ophthalmol. 114, 1009-1014.

Klisovic, D. D., Klisovic, M. I., Effron, D., Liu, S., Marcucci, G., Katz, S. E., 2005. Depsipeptide inhibits migration of primary and metastatic uveal melanoma cell lines *in vitro*: a potential strategy for uveal melanoma. Melanoma Res. 15, 147-153.

Knauper, V., Bailey, L., Worley, J. R., Soloway, P., Patterson, M. L., & Murphy, G. 2002, "Cellular activation of proMMP-13 by MT1-MMP depends on the C-terminal domain of MMP-13", FEBS Lett., vol. 532, no. 1-2, pp. 127-130.

Knauper, V., Smith, B., Lopez-Otin, C., Murphy, G., 1997. Activation of progelatinase B (proMMP-9) by active collagenase-3 (MMP-13). Eur. J. Biochem., 248, 369-373.

Knauper, V., Will, H., Lopez-Otin, C., Smith, B., Atkinson, S. J., Stanton, H., Hembry, R. M., & Murphy, G. 1996, Cellular mechanisms for human procollagenase-3 (MMP-13) activation. Evidence that MT1-MMP (MMP-14) and gelatinase a (MMP-2) are able to generate active enzyme. J. Biol. Chem., 271, 29, 17124-17131.

Knepper, P. A., Breen, M., Weinstein, H. G., Blacik, J. L., 1978. Intraocular pressure and glycosaminoglycan distribution in the rabbit eye: effect of age and dexamethasone. Exp. Eye Res. 27, 567-575.

Knepper, P. A., McLone, D. G., 1985. Glycosaminoglycans and outflow pathways of the eye and brain. Pediatr. Neurosci. 12, 240-251.

Kohn, E. C., Jacobs, W., Kim, Y. S., Alessandro, R., Stetler-Stevenson, W. G., Liotta, L. A. 1994. Calcium influx modulates expression of matrix metalloproteinase-2 (72-kDa type IV collagenase, gelatinase A). J. Biol. Chem. 269, 21505-21511.

Kohno, T., Sorgente, N., Goodnight, R., Ryan, S. J., 1987. Alterations in the distribution of fibronectin and laminin in the diabetic human eye. Invest. Ophthalmol. Vis. Sci., 28, 515-521.

Kojima, S., Itoh, Y., Matsumoto, S., Masuho, Y., Seiki, M., 2000. Membrane-type 6 matrix metalloproteinase (MT6-MMP, MMP-25) is the second glycosyl-phosphatidyl inositol (GPI)-anchored MMP. FEBS Lett. 480, 142-146.

Kolb, C., Mauch, S., Peter, H. H., Krawinkel, U., Sedlacek, R., 1997. The matrix metalloproteinase RASI-1 is expressed in synovial blood vessels of a rheumatoid arthritis patient. Immunol. Lett. 57, 83-88.

Kon, C. H., Occleston, N. L., Charteris, D., Daniels, J., Aylward, G. W., Khaw, P. T. 1998. A prospective study of matrix metalloproteinases in proliferative vitreoretinopathy. Invest. Ophthalmol. Vis. Sci. 39, 1524-1529.

Kreger, A. S., Gray, L. D., 1978. Purification of Pseudomonas aeruginosa proteases and microscopic characterization of pseudomonal protease-induced rabbit corneal damage. Infect. Immun. 19, 630-648.

Kreger, A. S., Lyerly, D. M., Hazlett, L. D., Berk, R. S., 1986. Immunization against experimental Pseudomonas aeruginosa and Serratia marcescens keratitis. Vaccination with lipopolysaccharide endotoxins and proteases. Invest. Ophthalmol. Vis. Sci. 27, 932-939.

Kumaraguru, U., Davis, I., & Rouse, B. T., 1999. Chemokines and ocular pathology caused by corneal infection with herpes simplex virus. J. Neurovirol. 5, 42-47.

Kure, T., Chang, J. H., Kato, T., Hernandez-Quintela, E., Ye, H., Lu, P. C., Matrisian, L. M., Gatinel, D., Shapiro, S., Gosheh, F., Azar, D. T., 2003. Corneal neovascularization after excimer keratectomy wounds in matrilysin-deficient mice. Invest. Ophthalmol. Vis. Sci., 44, 137-144.

Kvanta, A., Shen, W. Y., Sarman, S., Seregard, S., Steen, B., Rakoczy, E., 2000. Matrix metalloproteinase (MMP) expression in experimental choroidal neovascularization. Curr. Eye Res. 21, 684-690.

Kwan, J. A., Schulze, C. J., Wang, W., Leon, H., Sariahmetoglu, M., Sung, M., Sawicka, J., Sims, D. E., Sawicki, G., Schulz, R., 2004. Matrix metalloproteinase-2 (MMP-2) is present in the nucleus of cardiac myocytes and is capable of cleaving poly (ADP-ribose) polymerase (PARP) *in vitro*. FASEB J. 18, 690-692.

Lambert, V., Wielockx, B., Munaut, C., Galopin, C., Jost, M., Itoh, T., Werb, Z., Baker, A., Libert, C., Krell, H. W., Foidart, J. M., Noel, A., Rakic, J. M., 2003. MMP-2 and MMP-9 synergize in promoting choroidal neovascularization. FASEB J. 17, 2290-2292.

Lamping, K.A., Belkin, J.K.. 1995. 5-Fluorouracil and mitomycin C in pseudophakic patients. Ophthalmology. 102:70–75.

Landthaler, M., Yalcin, A. and Tuschl, A. 2004. The human DiGeorge syndrome critical region gene 8 and its D. melanogaster homolog are required for miRNA biogenesis. Curr Biol 14 : 2162–2167.

Langton, K. P., Barker, M. D., McKie, N., 1998. Localization of the functional domains of human tissue inhibitor of metalloproteinases-3 and the effects of a Sorsby's fundus dystrophy mutation. J.Biol.Chem. 273, 16778-16781.

Langton, K. P., McKie, N., Curtis, A., Goodship, J. A., Bond, P. M., Barker, M. D., Clarke, M., 2000. A novel tissue inhibitor of metalloproteinases-3 mutation reveals a common molecular phenotype in Sorsby's fundus dystrophy. J. Biol. Chem. 275, 27027-27031.

Langton, K. P., McKie, N., Smith, B. M., Brown, N. J., Barker, M. D., 2005. Sorsby's fundus dystrophy mutations impair turnover of TIMP-3 by retinal pigment epithelial cells. Hum. Mol. Genet. 14, 3579-3586.

Lashkari, K., Rahimi, N., Kazlauskas, A., 1999. Hepatocyte growth factor receptor in human RPE cells: implications in proliferative vitreoretinopathy. Invest Ophthalmol Vis.Sci. 40, 149-156.

Lawler, S., Fleming, Y., Goedert, M., Cohen, P., 1998. Synergistic activation of SAPK1/JNK1 by two MAP kinase kinases *in vitro*. Curr. Biol., 8, 1387-1390.

Leco, K. J., Khokha, R., Pavloff, N., Hawkes, S. P., Edwards, D. R., 1994. Tissue inhibitor of metalloproteinases-3 (TIMP-3) is an extracellular matrix-associated protein with a distinctive pattern of expression in mouse cells and tissues. J.Biol.Chem. 269, 9352-9360.

Lee, H. K., Kim, J. K., Kim, E. K., Kim, G. O., Lee, I. S., 2003. Phototherapeutic keratectomy with amniotic membrane for severe subepithelial fibrosis following excimer laser refractive surgery. J. Cataract Refract. Surg., 29, 1430-1435.

Lee, S., Zheng, M., Kim, B., Rouse, B. T. 2002. Role of matrix metalloproteinase-9 in angiogenesis caused by ocular infection with herpes simplex virus. J. Clin. Invest. 110, 1105-1111.

Lee, Y.S., Nakahara, K., Pham, J.W., Kim, K., He, Z., Sontheimer, E.J., Carthew, R.W. 2004. Distinct roles for Drosophila Dicer-1 and Dicer-2 in the siRNA/miRNA silencing pathways, Cell 117: 69–81.

Lein, M., Jung, K., Ortel, B., Stephan, C., Rothaug, W., Juchem, R., Johannsen, M., Deger, S., Schnorr, D., Loening, S., Krell, H. W., 2002. The new synthetic matrix metalloproteinase inhibitor (Roche 28-2653) reduces tumor growth and prolongs survival in a prostate cancer standard rat model. Oncogene, 21, 2089-2096.

Lelongt, B., Trugnan, G., Murphy, G., Ronco, P. M., 1997. Matrix metalloproteinases MMP-2 and MMP-9 are produced in early stages of kidney morphogenesis but only MMP-9 is required for renal organogenesis *in vitro*. J. Cell Biol. 136, 1363-1373.

Lema, I., Duran, J. A., 2005. Inflammatory molecules in the tears of patients with keratoconus. Ophthalmology. 112, 654-659.

Leppert, D., Waubant, E., Galardy, R., Bunnett, N. W., Hauser, S. L. 1995, "T cell gelatinases mediate basement membrane transmigration *in vitro*", J.Immunol., 154, 4379-4389.

Leu, S. T., Batni, S., Radeke, M. J., Johnson, L. V., Anderson, D. H., Clegg, D. O. 2002, Drusen are Cold Spots for Proteolysis: Expression of Matrix Metalloproteinases and Their Tissue Inhibitor Proteins in Age-related Macular Degeneration. Exp. Eye Res. 74, 141-154.

Li, D. Q., Lokeshwar, B. L., Solomon, A., Monroy, D., Ji, Z., Pflugfelder, S. C., 2001a. Regulation of MMP-9 production by human corneal epithelial cells. Exp. Eye Res. 73, 449-459.

Li, D. Q., Meller, D., Liu, Y., Tseng, S. C., 2000. Overexpression of MMP-1 and MMP-3 by cultured conjunctivochalasis fibroblasts. Invest. Ophthalmol. Vis. Sci., 41, 404-410.

Li, D. Q., Shang, T. Y., Kim, H. S., Solomon, A., Lokeshwar, B. L., Pflugfelder, S. C., 2003. Regulated expression of collagenases MMP-1, -8, and -13 and stromelysins MMP-3, -10, and -11 by human corneal epithelial cells. Invest. Ophthalmol. Vis.Sci. 44, 2928-2936.

Li, Q., Weng, J., Mohan, R. R., Bennett, G. L., Schwall, R., Wang, Z. F., Tabor, K., Kim, J., Hargrave, S., Cuevas, K. H., Wilson, S. E., 1996. Hepatocyte growth factor and hepatocyte growth factor receptor in the lacrimal gland, tears, and cornea. Invest. Ophthalmol. Vis. Sci., 37, 727-739.

Li, W., Gibson, C. W., Abrams, W. R., Andrews, D. W., DenBesten, P. K., 2001b. Reduced hydrolysis of amelogenin may result in X-linked amelogenesis imperfecta. Matrix Biol., 19, 755-760.

Lijnen, H. R., 2001. Plasmin and matrix metalloproteinases in vascular remodeling. Thromb. Haemost.. 86, 324-333.

Limb, G. A., Alam, A., Earley, O., Green, W., Chignell, A. H., Dumonde, D. C., 1994. Distribution of cytokine proteins within epiretinal membranes in proliferative vitreoretinopathy. Curr. Eye Res. 13, 791-798.

Limb, G. A., Chignell, A. H., Green, W., LeRoy, F., Dumonde, D. C., 1996. Distribution of TNF alpha and its reactive vascular adhesion molecules in fibrovascular membranes of proliferative diabetic retinopathy. Br. J. Ophthalmol. 80, 168-173.

Limb, G. A., Daniels, J. T., Pleass, R., Charteris, D. G., Luthert, P. J., Khaw, P. T. 2002. Differential expression of matrix metalloproteinases 2 and 9 by glial Muller cells: response to soluble and extracellular matrix-bound tumor necrosis factor-alpha. Am. J. Pathol. 160, 1847-1855.

Limb, G. A., Little, B. C., Meager, A., Ogilvie, J. A., Wolstencroft, R. A., Franks, W. A., Chignell, A. H., Dumonde, D. C., 1991. Cytokines in proliferative vitreoretinopathy. Eye. 5 (Pt 6), 686-693.

Limb, G. A., Matter, K., Murphy, G., Cambrey, A. D., Bishop, P. N., Morris, G. E., Khaw, P. T., 2005. Matrix metalloproteinase-1 associates with intracellular organelles and confers resistance to lamin A/C degradation during apoptosis. Am. J. Pathol. 166, 1555-1563.

Lin, W. R., Brittan, M., Alison, M. R. 2008. The Role of Bone Marrow-Derived Cells in Fibrosis Cells Tissues Organs 2008;188:178–188.

Lindsey, J. D., Kashiwagi, K., Boyle, D., Kashiwagi, F., Firestein, G. S., Weinreb, R. N., 1996. Prostaglandins increase proMMP-1 and proMMP-3 secretion by human ciliary smooth muscle cells. Curr. Eye Res. 15, 869-875.

Lindsey, J. D., Kashiwagi, K., Kashiwagi, F., Weinreb, R. N., 1997. Prostaglandin action on ciliary smooth muscle extracellular matrix metabolism: implications for uveoscleral outflow. Surv. Ophthalmol. 41, S53-S59.

Lindsey, J. D., To, H. D., Weinreb, R. N., 1994. Induction of c-fos by prostaglandin F2 alpha in human ciliary smooth muscle cells. Invest. Ophthalmol. Vis. Sci., 35, 242-250.

Lingel, A., Simon, B., Izaurralde, E., Sattler, M. 2004. Nucleic acid 3′-end recognition by the Argonaute2 PAZ domain, Nat Struct Mol Biol 11: 576–581

Liou, G. I., Pakalnis, V. A., Matragoon, S., Samuel, S., Behzadian, M. A., Baker, J., Khalil, I. E., Roon, P., Caldwell, R. B., Hunt, R. C., Marcus, D. M., 2002. HGF regulation of RPE proliferation in an IL-1beta/retinal hole-induced rabbit model of PVR. Mol.Vis. 8, 494-501.

Liu, J., Carmell, M.A., Rivas, F.V., Marsden, C.G., Thomson, J.M., Song, J. J., Hammond, S. M., Joshua-Tor, L. and Hannon, G. J. 2004. Argonaute2 is the catalytic engine of mammalian RNAi, *Science* 305: 1437–1441.

Lobmann, R., Ambrosch, A., Seewald, M., Dietlein, M., Zink, K., Kullmann, K. H., Lehnert, H., 2004. Antibiotic therapy for diabetic foot infections: comparison of cephalosporines with chinolones. Diabetes Nutr. Metab. 17, 156-162.

Lockhart, A. C., Braun, R. D., Yu, D., Ross, J. R., Dewhirst, M. W., Humphrey, J. S., Thompson, S., Williams, K. M., Klitzman, B., Yuan, F., Grichnik, J. M., Proia, A. D., Conway, D. A., Hurwitz, H. I., 2003. Reduction of wound angiogenesis in patients treated with BMS-275291, a broad spectrum matrix metalloproteinase inhibitor. Clin. Cancer Res. 9, 586-593.

Lohi, J., Wilson, C. L., Roby, J. D., & Parks, W. C., 2001. Epilysin, a novel human matrix metalloproteinase (MMP-28) expressed in testis and keratinocytes and in response to injury. J. Biol. Chem. 276, 10134-10144.

Lotze, M.T., Kost, T.A. 2002. Viruses as gene delivery vectors: application to gene function, target validation, and assay development. Cancer Gene Ther. 9: 692–699.

Lu,J., Marnell, L.L., Marjon, K.D., Mold, C., Du Clos, T.D., Sun, P.D. 2008. Structural recognition and functional activation of FcγR by innate pentraxins. Nature 456(7224): 989 – 992.

Lu, P. C., Ye, H., Maeda, M., Azar, D. T., 1999. Immunolocalization and gene expression of matrilysin during corneal wound healing. Invest. Ophthalmol. Vis. Sci. 40, pp. 20-27.

Luo, D., Mari, B., Stoll, I., Anglard, P., 2002. Alternative splicing and promoter usage generates an intracellular stromelysin 3 isoform directly translated as an active matrix metalloproteinase. J. Biol. Chem. 277, 25527-25536.

Lutjen-Drecoll, E., Tamm, E., 1988. Morphological study of the anterior segment of cynomolgus monkey eyes following treatment with prostaglandin F2 alpha. Exp. Eye Res. 47, 761-769.

Ma, J. B., Ye, K., Patel, D. J. 2004. Structural basis for overhang-specific small interfering RNA recognition by the PAZ domain. Nature 429: 318-22

Maatta, M., Tervahartiala, T., Harju, M., Airaksinen, J., utio-Harmainen, H., & Sorsa, T., 2005. Matrix metalloproteinases and their tissue inhibitors in aqueous humor of patients with primary open-angle glaucoma, exfoliation syndrome, and exfoliation glaucoma. J. Glaucoma., 14, 64-69.

Mach, F., Schonbeck, U., Bonnefoy, J. Y., Pober, J. S., & Libby, P., 1997. Activation of monocyte/macrophage functions related to acute atheroma complication by ligation of CD40: induction of collagenase, stromelysin, and tissue factor. Circulation. 96, 396-399.

Mackiewicz, Z., Maatta, M., Stenman, M., Konttinen, L., Tervo, T., & Konttinen, Y. T., 2006. Collagenolytic proteinases in keratoconus. Cornea. 25, 603-610.

Maeda, M., Vanlandingham, B. D., Ye, H., Lu, P. C., Azar, D. T., 1998. Immunoconfocal localization of gelatinase B expressed by migrating intrastromal epithelial cells after deep annular excimer keratectomy. Curr.Eye Res. 17, 836-843.

Maguen, E., Zorapapel, N. C., Zieske, J. D., Ninomiya, Y., Sado, Y., Kenney, M. C., Ljubimov, A. V., 2002. Extracellular matrix and matrix metalloproteinase changes in human corneas after complicated laser-assisted in situ keratomileusis (LASIK). Cornea. 21, 95-100.

Majid, M. A., Smith, V. A., Easty, D. L., Baker, A. H., Newby, A. C., 2002. Adenovirus mediated gene delivery of tissue inhibitor of metalloproteinases-3 induces death in retinal pigment epithelial cells. Br. J. Ophthalmol. 86, 97-101.

Malecaze, F., Simorre, V., Chollet, P., Tack, J. L., Muraine, M., Le, G. D., Vita, N., Arne, J. L., Darbon, J. M., 1997. Interleukin-6 in tear fluid after photorefractive keratectomy and its effects on keratocytes in culture. Cornea. 16, 580-587.

Manche, L., Green, S.R., Schmedt, C and Mathews, M.B. 1992. Interactions between double-stranded RNA regulators and the protein kinase DAI. Mol. Cell. Biol. 12: 5238–5248.

Mannello, F., Gazzanelli, G., 2004. Tissue inhibitors of metalloproteinases and programmed cell death: conundrums, controversies and potential implications. Apoptosis. 6, 479-482.

Mannello, F., Tonti, G. A., Bagnara, G. P., Papa, S., 2006. Role and function of matrix metalloproteinases in the differentiation and biological characterization of mesenchymal stem cells. Stem Cells. 24, 475-481.

Mantovani, A.; Garlanda, C.; Bottazzi, B.; Peri, G.; Doni, A.; Martinez de la Torre, Y.; Latini, R.; 2006 The long pentraxin PTX3 in vascular pathology. Vascul Pharmacol. 2006 Nov;45(5):326-30.

Marchenko, G. N., Marchenko, N. D., Strongin, A. Y., 2003. The structure and regulation of the human and mouse matrix metalloproteinase-21 gene and protein. Biochem. J. 372 (Pt 2), 503-515.

Marchenko, G. N., Strongin, A. Y., 2001. MMP-28, a new human matrix metalloproteinase with an unusual cysteine-switch sequence is widely expressed in tumors. Gene. 265, 87-93.

Marchenko, N. D., Marchenko, G. N., Weinreb, R. N., Lindsey, J. D., Kyshtoobayeva, A., Crawford, H. C., Strongin, A. Y., 2004. Beta-catenin regulates the gene of MMP-26, a novel metalloproteinase expressed both in carcinomas and normal epithelial cells. Int. J. Biochem. Cell Biol. 36, 942-956.

Marshall, J., Mellerio, J., 1971. Disappearance of retino-epithelial scar tissue from ruby laser photocoagulations. Exp. Eye Res. 12, 173-174.

Marshall, J., Trokel, S. L., Rothery, S.,, Krueger, R. R., 1988. Long-term healing of the central cornea after photorefractive keratectomy using an excimer laser. Ophthalmology. 95, 1411-1421.

Massova, I., Kotra, L. P., Fridman, R., Mobashery, S., 1998. Matrix metalloproteinases: structures, evolution, and diversification. FASEB J. 12, 1075-1095.

Matsubara, M., Girard, M. T., Kublin, C. L., Cintron, C., Fini, M. E. ,1991. Differential roles for two gelatinolytic enzymes of the matrix metalloproteinase family in the remodelling cornea. Dev.Biol. 147, 425-439.

Matsubara, M., Zieske, J. D., Fini, M. E., 1991. Mechanism of basement membrane dissolution preceding corneal ulceration. Invest. Ophthalmol. Vis. Sci.. 32, 3221-3237.

Matsumoto, K., Shams, N. B., Hanninen, L. A., Kenyon, K. R., 1993. Cleavage and activation of corneal matrix metalloproteases by Pseudomonas aeruginosa proteases. Invest. Ophthalmol. Vis. Sci. 34, 1945-1953.

Matsuo, T., Cynader, M. S., 1992. Localisation of prostaglandin F2 alpha and E2 binding sites in the human eye. Br. J. Ophthalmol., 76, 210-213.

McClellan, S. A., Huang, X., Barrett, R. P., Lighvani, S., Zhang, Y., Richiert, D., Hazlett, L. D., 2006. Matrix metalloproteinase-9 amplifies the immune response to Pseudomonas aeruginosa corneal infection. Invest. Ophthalmol. Vis. Sci., 47, 256-264.

McCluskey, P., Molteno, A., Wakefield, D., Di Girolamo, N., 2009. Otago Glaucoma Surgery Outcome Study: the pattern of expression of MMPs and TIMPs in bleb capsules surrounding Molteno implants. Invest Ophthalmol Vis Sci. 50, 2161-4.

McDonald, M. B., Frantz, J. M., Klyce, S. D., Salmeron, B., Beuerman, R. W., Munnerlyn, C. R., Clapham, T. N., Koons, S. J., Kaufman, H. E., 1990. One-year refractive results of central photorefractive keratectomy for myopia in the nonhuman primate cornea. Arch.Ophthalmol, 108, 40-47.

McLean, I. W., 1993. The biology of haematogenous metastasis in human uveal malignant melanoma. Virchows Arch. A Pathol.Anat.Histopathol. 422, 433-437.

Mecham, R. P., Broekelmann, T. J., Fliszar, C. J., Shapiro, S. D., Welgus, H. G., Senior, R. M., 1997. Elastin degradation by matrix metalloproteinases. Cleavage site specificity and mechanisms of elastolysis. J. Biol. Chem. 272, 18071-18076.

Meister, G. and Tuschl, T. 2004. Mechanisms of gene silencing by double-stranded RNA, Nature 431: 343–349.

Meller, D., Li, D. Q., Tseng, S. C., 2000. Regulation of collagenase, stromelysin, and gelatinase B in human conjunctival and conjunctivochalasis fibroblasts by interleukin-1beta and tumor necrosis factor-alpha. Invest. Ophthalmol. Vis. Sci. 41, 2922-2929.

Meller, D., Tseng, S. C., 1998. Conjunctivochalasis: literature review and possible pathophysiology. Surv. Ophthalmol, 43, 225-232.

Mietz, H., Esser, J. M., Welsandt, G., Kociok, N., Hueber, A., Joussen, A., Esser, P., Krieglstein, G. K., 2003. Latanoprost stimulates secretion of matrix metalloproteinases in tenon fibroblasts both *in vitro* and *in vivo*. Invest. Ophthalmol. Vis. Sci. 44, 5182-5188.

Migdal, C., Gregory, W., Hitchings, R. 1994. Long-term functional outcome after early surgery compared with laser and medicine in open-angle glaucoma. Ophthalmology.

101(10):1651-6

Miles, L. A., Dahlberg, C. M., Plescia, J., Felez, J., Kato, K., Plow, E. F., 1991. Role of cell-surface lysines in plasminogen binding to cells: identification of alpha-enolase as a candidate plasminogen receptor. Biochemistry. 30, 1682-1691.

Mimura, T., Han, K.Y., Onguchi, T., Chang, J. H., Kim, T.I., Kojima, T., Zhou, Z., Azar, D.T., 2009. MT1-MMP-mediated cleavage of decorin in corneal angiogenesis. J. Vasc. Res. 46, 541-50.

Miralles, F., Battelino, T., Czernichow, P., Scharfmann, R., 1998. TGF-beta plays a key role in morphogenesis of the pancreatic islets of Langerhans by controlling the activity of the matrix metalloproteinase MMP-2. J. Cell Biol. 143, 827-836.

Miyajima, S., Akaike, T., Matsumoto, K., Okamoto, T., Yoshitake, J., Hayashida, K., Negi, A., Maeda, H., 2001. Matrix metalloproteinases induction by pseudomonal virulence factors and inflammatory cytokines *in vitro*. Microb. Pathog. 31, 271-281.

Mohan, R., Chintala, S. K., Jung, J. C., Villar, W. V., McCabe, F., Russo, L. A., Lee, Y., McCarthy, B. E., Wollenberg, K. R., Jester, J. V., Wang, M., Welgus, H. G., Shipley, J. M., Senior, R. M., Fini, M. E., 2002. Matrix metalloproteinase gelatinase B (MMP-9) coordinates and effects epithelial regeneration. J. Biol. Chem. 277, 2065-2072.

Mohan, R., Rinehart, W. B., Bargagna-Mohan, P., Fini, M. E., 1998. Gelatinase B/lacZ transgenic mice, a model for mapping gelatinase B expression during developmental and injury-related tissue remodeling. J. Biol. Chem. 273, 25903-25914.

Mohtai, M., Smith, R. L., Schurman, D. J., Tsuji, Y., Torti, F. M., Hutchinson, N. I., Stetler-Stevenson, W. G., Goldberg, G. I., 1993. Expression of 92-kD type IV collagenase/gelatinase (gelatinase B) in osteoarthritic cartilage and its induction in normal human articular cartilage by interleukin 1. J. Clin. Invest. 92, 179-185.

Moller-Pedersen, T., Li, H. F., Petroll, W. M., Cavanagh, H. D., Jester, J. V., 1998. Confocal microscopic characterization of wound repair after photorefractive keratectomy. Invest. Ophthalmol. Vis. Sci., 39, 487-501.

Mott, J. D., Thomas, C. L., Rosenbach, M. T., Takahara, K., Greenspan, D. S., Banda, M. J., 2000. Post-translational proteolytic processing of procollagen C-terminal proteinase enhancer releases a metalloproteinase inhibitor. J. Biol. Chem. 275, 1384-1390.

Mott, J. D., Werb, Z., 2004. Regulation of matrix biology by matrix metalloproteinases. Curr. Opin. Cell Biol., 16, 558-564.

Moulin, V., Castilloux, G., Auger, F. A., Garrel, D., O'Connor-McCourt, M. D., Germain, L., 1998. Modulated response to cytokines of human wound healing myofibroblasts compared to dermal fibroblasts. Exp. Cell Res., 238, 283-293.

Mulholland, B., Tuft, S. J., Khaw, P. T., 2005. Matrix metalloproteinase distribution during early corneal wound healing. Eye. 19, 584-588.

Murphy, G., Bretz, U., Baggiolini, M., Reynolds, J. J., 1980. The latent collagenase and gelatinase of human polymorphonuclear neutrophil leucocytes. Biochem.J., 192, 517-525.

Murphy, G., Houbrechts, A., Cockett, M. I., Williamson, R. A., O'Shea, M., Docherty, A. J.,1991. The N-terminal domain of tissue inhibitor of metalloproteinases retains metalloproteinase inhibitory activity. Biochemistry. 30, 8097-8102.

Myint, E., Brown, D. J., Ljubimov, A. V., Kyaw, M., Kenney, M. C., 1996. Cleavage of human corneal type VI collagen alpha 3 chain by matrix metalloproteinase-2. Cornea. 15, 490-496.

Nagase, H., 1998. Stromelysins 1 and 2. In Matrix Metalloproteinases, W. Park & R. Mecham, eds., San Diego, Academic Press.

Nagase, H. 1997. Activation mechanisms of matrix metalloproteinase's. Biol.Chem. 378, 151-160.

Nagase, H., Suzuki, K., Enghild, J. J., Salvesen, G., 1991. Stepwise activation mechanisms of the precursors of matrix metalloproteinases 1 (tissue collagenase) and 3 (stromelysin). Biomed. Biochim. Acta 50, 749-754.

Nagase, H., Visse, R., Murphy, G., 2006. Structure and function of matrix metalloproteinases and TIMPs. Cardiovasc. Res. 69, 562-573.

Nagase, H., Woessner, J. F., Jr., 1999. Matrix metalloproteinase's. J. Biol. Chem. 274, 21491-21494.

Nakamura, Y., Sato, K., Wakimoto, N., Kimura, F., Okuyama, A., Motoyoshi, K. 2001. A new matrix metalloproteinase inhibitor SI-27 induces apoptosis in several human myeloid leukemia cell lines and enhances sensitivity to TNF alpha-induced apoptosis. Leukemia. 15, 1217-1224.

Nand-Apte, B., Pepper, M. S., Voest, E., Montesano, R., Olsen, B., Murphy, G., Apte, S. S., Zetter, B., 1997. Inhibition of angiogenesis by tissue inhibitor of metalloproteinase-3. Invest. Ophthalmol. Vis. Sci. 38, 817-823.

Naik-Mathuria B, Pilling D, Crawford JR, Gay AN, Smith CW, Gomer RH, Olutoye OO. Serum amyloid P inhibits dermal wound healing. Wound Repair Regen. 2008 Mar-Apr;16(2):266-73.

Nelson, A. R., Fingleton, B., Rothenberg, M. L., Matrisian, L. M., 2000. Matrix metalloproteinases: biologic activity and clinical implications. J. Clin. Oncol. 18, 1135-1149.

Nelson, S.R., Tennent, G.A., Sethi, D., Gower, P.E., Ballardie, F.W., Matayakul-Chantler, S. *et al.* 1991. Serum amyloid P component in chronic renal failure and dialysis. Clin. Chim. Acta 200: 191-9.

Newby, A. C., 2006. Matrix metalloproteinases regulate migration, proliferation, and death of vascular smooth muscle cells by degrading matrix and non-matrix substrates. Cardiovasc. Res. 69, 614-624.

Nishida, K., Sotozono, C., Adachi, W., Yamamoto, S., Yokoi, N., Kinoshita, S., 1995. Transforming growth factor-beta 1, -beta 2 and -beta 3 mRNA expression in human cornea. Curr. Eye Res. 14, 235-241.

Noda, K., Ishida, S., Inoue, M., Obata, K., Oguchi, Y., Okada, Y., Ikeda, E. 2003. Production and activation of matrix metalloproteinase-2 in proliferative diabetic retinopathy. Invest. Ophthalmol. Vis. Sci. 44, 2163-2170.

Ocklind, A., 1998. Effect of latanoprost on the extracellular matrix of the ciliary muscle. A study on cultured cells and tissue sections. Exp. Eye Res. 67, 179-191.

Ocklind, A., Lake, S., Wentzel, P., Nister, M., Stjernschantz, J., 1996. Localization of the prostaglandin F2 alpha receptor messenger RNA and protein in the cynomolgus monkey eye. Invest. Ophthalmol. Vis. Sci. 37, 716-726.

Oh, J., Takahashi, R., Kondo, S., Mizoguchi, A., Adachi, E., Sasahara, R. M., Nishimura, S., Imamura, Y., Kitayama, H., Alexander, D. B., Ide, C., Horan, T. P., Arakawa, T., Yoshida, H., Nishikawa, S., Itoh, Y., Seiki, M., Itohara, S., Takahashi, C., Noda, M. 2001. The membrane-anchored MMP inhibitor RECK is a key regulator of extracellular matrix integrity and angiogenesis. Cell 107, 789-800.

Ohnishi, J., Ohnishi, E., Jin, M., Hirano, W., Nakane, D., Matsui, H., Kimura, A., Sawa, H., Nakayama, K., Shibuya, H., Nagashima, K., Takahashi, T., 2001. Cloning and characterization of a rat ortholog of MMP-23 (matrix metalloproteinase-23), a unique type of membrane-anchored matrix metalloproteinase and conditioned switching of its expression during the ovarian follicular development. Mol. Endocrinol. 15, 747-764.

Onguchi, T., Han, K.Y., Chang, J.H., Azar, D.T., 2009. Membrane type-1 matrix metalloproteinase potentiates basic fibroblast growth factor-induced corneal neovascularization. Am J Pathol. 174,1564-71.

Ooi, Y.H., Oh, D.J., Rhee, D.J., 2009. Effect of bimatoprost, latanoprost, and unoprostone on matrix metalloproteinases and their inhibitors in human ciliary body smooth muscle cells. Invest Ophthalmol Vis Sci. 50, 5259-65.

Opbroek, A., Kenney, M. C., Brown, D., 1993. Characterization of a human corneal metalloproteinase inhibitor (TIMP-1). Curr. Eye Res. 12, 877-883.

Osmand, A.P., Friedenson, B., Gewurz, H., Painter, R.H., Hofmann, T., Shelton, E. 1977. Proc Natl Acad Sci U S A. 74(2):739-43.

Ozerdem, U., Mach-Hofacre, B., Cheng, L., Chaidhawangul, S., Keefe, K., McDermott, C. D., Bergeron-Lynn, G., Appelt, K., Freeman, W. R., 2000. The effect of prinomastat

(AG3340), a potent inhibitor of matrix metalloproteinases, on a subacute model of proliferative vitreoretinopathy. Curr. Eye Res. 20, 447-453.

Ozerdem, U., Mach-Hofacre, B., Varki, N., Folberg, R., Mueller, A. J., Ochabski, R., Pham, T., Appelt, K., & Freeman, W. R. 2002. The effect of prinomastat (AG3340), a synthetic inhibitor of matrix metalloproteinases, on uveal melanoma rabbit model. Curr. Eye Res. 24, 86-91.

Padgett, L. C., Lui, G. M., Werb, Z., & LaVail, M. M., 1997. Matrix metalloproteinase-2 and tissue inhibitor of metalloproteinase-1 in the retinal pigment epithelium and interphotoreceptor matrix: vectorial secretion and regulation. Exp. Eye Res. 64, 927-938.

Pang, I. H., Fleenor, D. L., Hellberg, P. E., Stropki, K., McCartney, M. D., Clark, A. F., 2003. Aqueous outflow-enhancing effect of tert-butylhydroquinone: involvement of AP-1 activation and MMP-3 expression", Invest. Ophthalmol. Vis. Sci. 44, 3502-3510.

Park, J. K., Tripathi, R. C., Tripathi, B. J., Barlow, G. H., 1987. Tissue plasminogen activator in the trabecular endothelium", Invest. Ophthalmol. Vis. Sci. 28, 1341-1345.

Parker, M.H., Lunney, E. A., Ortwine, D. F., Pavlovsky, A.G., Humblet, C., Brouillette, C.G. 1999. Analysis of the binding of hydroxamic acid and carboxylic acid inhibitors to the stromelysin-1 (matrix metalloproteinase-3) catalytic domain by isothermal titration calorimetry. Biochemistry. 38, 13592-601.

Parkin, B. T., Smith, V. A., Easty, D. L., 2000. The control of matrix metalloproteinase-2 expression in normal and keratoconic corneal keratocyte cultures. Eur. J. Ophthalmol. 10, 276-285.

Parshley, D. E., Bradley, J. M., Fisk, A., Hadaegh, A., Samples, J. R., Van Buskirk, E. M., Acott, T. S., 1996. Laser trabeculoplasty induces stromelysin expression by trabecular juxtacanalicular cells. Invest. Ophthalmol. Vis. Sci. 37, 795-804.

Parshley, D. E., Bradley, J. M., Samples, J. R., Van Buskirk, E. M., & Acott, T. S., 1995. Early changes in matrix metalloproteinases and inhibitors after *in vitro* laser treatment to the trabecular meshwork. Curr. Eye Res. 14, 537-544.

Pei, D., Kang, T., Qi, H. 2000. Cysteine array matrix metalloproteinase (CA-MMP)/MMP-23 is a type II transmembrane matrix metalloproteinase regulated by a single cleavage for both secretion and activation. J. Biol. Chem. 275, 33988-33997.

Pei, D., Weiss, S. J., 1995. Furin-dependent intracellular activation of the human stromelysin-3 zymogen. Nature 375, 244-247.

Pena, J. D., Agapova, O., Gabelt, B. T., Levin, L. A., Lucarelli, M. J., Kaufman, P. L., Hernandez, M. R., 2001. Increased elastin expression in astrocytes of the lamina cribrosa in response to elevated intraocular pressure. Invest. Ophthalmol. Vis. Sci. 42, 2303-2314.

Pena, J. D., Mello, P. A., Hernandez, M. R. 2000. Synthesis of elastic microfibrillar components fibrillin-1 and fibrillin-2 by human optic nerve head astrocytes in situ and *in vitro*. Exp. Eye Res. 70, 589-601.

Pena, J. D., Taylor, A. W., Ricard, C. S., Vidal, I., Hernandez, M. R., 1999a. Transforming growth factor beta isoforms in human optic nerve heads. Br. J. Ophthalmol. 83, 209-218.

Pena, J. D., Varela, H. J., Ricard, C. S., Hernandez, M. R., 1999b. Enhanced tenascin expression associated with reactive astrocytes in human optic nerve heads with primary open angle glaucoma. Exp. Eye Res., 68, 29-40.

Pendas, A. M., Knauper, V., Puente, X. S., Llano, E., Mattei, M. G., Apte, S., Murphy, G., & Lopez-Otin, C., 1997. Identification and characterization of a novel human matrix metalloproteinase with unique structural characteristics, chromosomal location, and tissue distribution. J. Biol. Chem. 272, 4281-4286.

Pflugfelder, S. C., Farley, W., Luo, L., Chen, L. Z., De Paiva, C. S., Olmos, L. C., Li, D. Q., Fini, M. E., 2005. Matrix metalloproteinase-9 knockout confers resistance to corneal epithelial barrier disruption in experimental dry eye. Am. J. Pathol. 166, 61-71.

Phillips, C.I., Green, K., Gore, S.M., Cullen, P. M., Campbell, M. 1984. Eye drops of RU 486-6, a peripheral steroid blocker, lower intraocular pressure in rabbits. Lancet 1: 767-8.

Phillips, R.J., Burdick, M.D., Hong, K., Lutz, M.A., Murray, L.A., Xue, Y.Y., *et al.* 2004. Circulating fibrocytes traffic to the lungs in response to CXCL12 and mediate fibrosis. J. Clin. Invest. 114: 438-46.

Pignatelli, M., Vessey, C. J., 1994. Adhesion molecules: novel molecular tools in tumor pathology. Hum. Pathol. 25, 849-856.

Pilcher, B. K., Dumin, J. A., Sudbeck, B. D., Krane, S. M., Welgus, H. G., Parks, W. C., 1997. The activity of collagenase-1 is required for keratinocyte migration on a type I collagen matrix. J. Cell Biol. 137, 1445-1457.

Pilcher, B. K., Sudbeck, B. D., Dumin, J. A., Welgus, H. G., Parks, W. C., 1998. Collagenase-1 and collagen in epidermal repair. Arch. Dermatol. Res. 290, S37-S46.

Pilling, D., Buckley, C.D., Salmon, M., Gomer, R.H. 2003. Inhibition of fibrocyte differentiation by serum amyloid P. J Immunol. 17: 5537-46.

Pilling, D., Roife, D., Wang, M., Ronkainen, S.D., Crawford, J.R., Travis, E.L., Gomer, R.H. 2007. Reduction of bleomycin-induced pulmonary fibrosis by serum amyloid P. J Immunol. 15;179(6):4035-44.

Plantner, J. J., Smine, A., Quinn, T. A., 1998. Matrix metalloproteinases and metalloproteinase inhibitors in human interphotoreceptor matrix and vitreous. Curr. Eye Res. 17, 132-140.

Polansky, J. R., Wood, I. S., Maglio, M. T., Alvarado, J. A., 1984. Trabecular meshwork cell culture in glaucoma research: evaluation of biological activity and structural properties of human trabecular cells *in vitro*. Ophthalmology. 91, 580-595.

Polette, M., Nawrocki-Raby, B., Gilles, C., Clavel, C., Birembaut, P., 2004. Tumour invasion and matrix metalloproteinase's. Crit. Rev. Oncol. Hematol. 49, 179-186.

Polkinghorne, P. J., Capon, M. R., Berninger, T., Lyness, A. L., Sehmi, K., Bird, A. C., 1989. Sorsby's fundus dystrophy. A clinical study. Ophthalmology 96, 1763-1768.

Porter, R. A., Brown, R. A., Eastwood, M., Occleston, N. L., Khaw, P. T., 1998. Ultrastructural changes during contraction of collagen lattices by ocular fibroblasts. Wound. Repair Regen. 6, 157-166.

Puente, X. S., Sanchez, L. M., Overall, C. M., Lopez-Otin, C., 2003. Human and mouse proteases: a comparative genomic approach. Nat. Rev. Genet. 4, 544-558.

Quantin, B., Murphy, G., Breathnach, R., 1989. Pump-1 cDNA codes for a protein with characteristics similar to those of classical collagenase family members. Biochemistry 28, 5327-5334.

Quigley, H. A., Brown, A., Dorman-Pease, M. E., 1991. Alterations in elastin of the optic nerve head in human and experimental glaucoma. Br. J. Ophthalmol, 75, 552-557.

Rada, J. A., Achen, V. R., Rada, K. G., 1998. Proteoglycan turnover in the sclera of normal and experimentally myopic chick eyes. Invest. Ophthalmol. Vis. Sci. 39, 1990-2002.

Rada, J. A., Brenza, H. L., 1995. Increased latent gelatinase activity in the sclera of visually deprived chicks. Invest. Ophthalmol. Vis. Sci. 36, 1555-1565.

Rada, J. A., Perry, C. A., Slover, M. L., Achen, V. R., 1999. Gelatinase A and TIMP-2 expression in the fibrous sclera of myopic and recovering chick eyes. Invest. Ophthalmol. Vis. Sci., 40, 3091-3099.

Rada, J. A., Shelton, S., Norton, T. T., 2006. The sclera and myopia. Exp. Eye Res. 82, 185-200.

Ramaesh, T., Ramaesh, K., Leask, R., Springbett, A., Riley, S. C., Dhillon, B., West, J. D., 2006. Increased apoptosis and abnormal wound-healing responses in the heterozygous Pax6+/- mouse cornea. Invest. Ophthalmol. Vis. Sci. 47, 1911-1917.

Rauch, B. H., Bretschneider, E., Braun, M., Schror, K., 2002. Factor Xa releases matrix metalloproteinase-2 (MMP-2) from human vascular smooth muscle cells and stimulates the conversion of pro-MMP-2 to MMP-2: role of MMP-2 in factor Xa-induced DNA synthesis and matrix invasion. Circ. Res. 90, 1122-1127.

Richiert, D. M., Ireland, M. E., 1999. Matrix metalloproteinase secretion is stimulated by TGF-beta in cultured lens epithelial cells. Curr. Eye Res. 19, 269-275.

Ringvold, A., Davanger, M., 1981. Iris neovascularisation in eyes with pseudoexfoliation syndrome. Br. J. Ophthalmol. 65, 138-141.

Rivas, F.V., Tolia, N.H., Song, J.J., Aragon, J.P., Liu, J., Hannon, G.J., 2005 Purified Argonaute2 and an siRNA form recombinant human RISC. Nat. Struct. Mol. Biol. 12: 340–349.

Ritchie, H., Robbie, L. A., Kinghorn, S., Exley, R., Booth, N. A., 1999. Monocyte plasminogen activator inhibitor 2 (PAI-2) inhibits u-PA-mediated fibrin clot lysis and is cross-linked to fibrin. Thromb. Haemost. 81, 96-103.

Rivera, S., Ogier, C., Jourquin, J., Timsit, S., Szklarczyk, A. W., Miller, K., Gearing, A. J., Kaczmarek, L., Khrestchatisky, M., 2002. Gelatinase B and TIMP-1 are regulated in a cell- and time-dependent manner in association with neuronal death and glial reactivity after global forebrain ischemia. Eur. J. Neurosci. 15, 19-32.

Rohen, J. W., 1983. Why is intraocular pressure elevated in chronic simple glaucoma? Anatomical considerations. Ophthalmology 90, 758-765.

Rohen, J. W., Linner, E., Witmer, R., 1973. Electron microscopic studies on the trabecular meshwork in two cases of corticosteroid-glaucoma. Exp. Eye Res. 17, 19-31.

Rohini, G., Murugeswari, P., Prajna, N. V., Lalitha, P., Muthukkaruppan, V., 2007. Matrix metalloproteinases (MMP-8, MMP-9) and the tissue inhibitors of metalloproteinases (TIMP-1, TIMP-2) in patients with fungal keratitis. Cornea. 26, 207-211.

Rothman, R.F., Liebmann, J.M., Ritch,R. 2000. Low-dose 5-fluorouracil trabeculectomy as initial surgery in uncomplicated glaucoma: longterm followup. Ophthalmology 107 (6): 1184-90.

Ruiz, A., Brett, P., Bok, D., 1996. TIMP-3 is expressed in the human retinal pigment epithelium. Biochem. Biophys. Res. Commun. 226, 467-474.

Russell, S. R., Shepherd, J. D., Hageman, G. S., 1991. Distribution of glycoconjugates in the human retinal internal limiting membrane. Invest. Ophthalmol Vis. Sci. 32, 1986-1995.

Saarialho-Kere, U., Kerkela, E., Jahkola, T., Suomela, S., Keski-Oja, J., Lohi, J., 2002. Epilysin (MMP-28) expression is associated with cell proliferation during epithelial repair. J. Invest Dermatol. 119, 14-21.

Sachdev, N. H., Di, G. N., McCluskey, P. J., Jennings, A. V., McGuinness, R., Wakefield, D., Coroneo, M. T., 2002. Lens dislocation in Marfan syndrome: potential role of matrix metalloproteinases in fibrillin degradation. Arch. Ophthalmol. 120, 833-835.

Sachdev, N. H., Di, G. N., Nolan, T. M., McCluskey, P. J., Wakefield, D., Coroneo, M. T. 2004. Matrix metalloproteinases and tissue inhibitors of matrix metalloproteinases in the human lens: implications for cortical cataract formation. Invest. Ophthalmol. Vis. Sci. 45, 4075-4082.

Sagara, T., Gaton, D. D., Lindsey, J. D., Gabelt, B. T., Kaufman, P. L., Weinreb, R. N. 1999. Topical prostaglandin F2alpha treatment reduces collagen types I, III, and IV in the monkey uveoscleral outflow pathway. Arch. Ophthalmol. 117, 794-801.

Saika, S., Okada, Y., Miyamoto, T., Yamanaka, O., Ohnishi, Y., Ooshima, A., Liu, C. Y., Weng, D., Kao, W. W., 2004. Role of p38 MAP kinase in regulation of cell migration and proliferation in healing corneal epithelium. Invest. Ophthalmol. Vis. Sci. 45, 100-109.

Sakai, T., Gross, J. 1967. Some properties of the products of reaction of tadpole collagenase with collagen. Biochemistry 6, 518-528.

Sakamoto, T., Hinton, D. R., Kimura, H., Spee, C., Gopalakrishna, R., Ryan, S. J. 1996. Vitamin E succinate inhibits proliferation and migration of retinal pigment epithelial cells *in vitro*: therapeutic implication for proliferative vitreoretinopathy. Graefes Arch. Clin. Exp. Ophthalmol. 234, 186-192.

Sakuma, M., Miyachi, S., Sakamoto, T., 2000. The effect of sodium hyaluronate on the expression of gelatinases in rabbit corneal epithelial wound healing. Jpn. J. Ophthalmol. 44, 475-481.

Salzmann, J., Limb, G. A., Khaw, P. T., Gregor, Z. J., Webster, L., Chignell, A. H., Charteris, D. G., 2000. Matrix metalloproteinases and their natural inhibitors in fibrovascular membranes of proliferative diabetic retinopathy. Br. J. Ophthalmol. 84, 1091-1096.

Samples, J. R., Alexander, J. P., Acott, T. S., 1993. Regulation of the levels of human trabecular matrix metalloproteinases and inhibitor by interleukin-1 and dexamethasone. Invest. Ophthalmol. Vis. Sci. 34, 3386-3395.

Santavicca, M., Noel, A., Angliker, H., Stoll, I., Segain, J. P., Anglard, P., Chretien, M., Seidah, N., Basset, P., 1996. Characterization of structural determinants and molecular mechanisms involved in pro-stromelysin-3 activation by 4-aminophenylmercuric acetate and furin-type convertases. Biochem. J. 315 (Pt 3), 953-958.

Sato, H., Kinoshita, T., Takino, T., Nakayama, K., Seiki, M., 1996. Activation of a recombinant membrane type 1-matrix metalloproteinase (MT1-MMP) by furin and its interaction with tissue inhibitor of metalloproteinases (TIMP)-2. FEBS Lett. 393, 101-104.

Schachtschabel, D. O., Rohen, J. W., Wever, J., Sames, K., 1982. Synthesis and composition of glycosaminoglycans by cultured human trabecular meshwork cells. Graefes Arch. Clin. Exp. Ophthalmol. 218, 113-117.

Schachtschabel, U., Lindsey, J. D., Weinreb, R. N., 2000. The mechanism of action of prostaglandins on uveoscleral outflow. Curr. Opin. Ophthalmol. 11, 112-115.

Schlotzer-Schrehardt, U., Lommatzsch, J., Kuchle, M., Konstas, A. G., Naumann, G. O., 2003. Matrix metalloproteinases and their inhibitors in aqueous humor of patients with pseudoexfoliation syndrome/glaucoma and primary open-angle glaucoma. Invest. Ophthalmol. Vis. Sci. 44, 1117-1125.

Schlotzer-Schrehardt, U., Naumann, G. O., 2006. Ocular and systemic pseudoexfoliation syndrome. Am. J. Ophthalmol. 141, 921-937.

Schlotzer-Schrehardt, U. M., Koca, M. R., Naumann, G. O., Volkholz, H., 1992. Pseudoexfoliation syndrome. Ocular manifestation of a systemic disorder? Arch. Ophthalmol. 110, 1752-1756.

Seemayer, C.A., Distler, O., Kuchen, S., Muller-Ladner, U., Michel, B.A., Neidhart M, *et al.* 2001. Rheumatoid arthritis: new developments in the pathogenesis with special reference to synovial fibroblasts. Z Rheumatol. 60: 309-18.

Seftor, R. E., Seftor, E. A., Kirschmann, D. A., Hendrix, M. J., 2002. Targeting the tumor microenvironment with chemically modified tetracyclines: inhibition of laminin 5 gamma2 chain promigratory fragments and vasculogenic mimicry. Mol. Cancer Ther. 13, 1173-1179.

Seiki, M., 1998. Matrilysin. In Handbook of Proteolytic Enymes, A. Barrett, N. Rawlings, J. Woessner, eds. Academic Press, London, 1192-1195.

Seomun, Y., Kim, J., Lee, E. H., Joo, C. K., 2001. Overexpression of matrix metalloproteinase-2 mediates phenotypic transformation of lens epithelial cells. Biochem. J. 358 (Pt 1), 41-48.

Seppala, H. P., Maatta, M., Rautia, M., Mackiewicz, Z., Tuisku, I., Tervo, T., Konttinen, Y. T., 2006. EMMPRIN and MMP-1 in keratoconus. Cornea 25, 325-330.

Shalinsky, D. R., Brekken, J., Zou, H., McDermott, C. D., Forsyth, P., Edwards, D., Margosiak, S., Bender, S., Truitt, G., Wood, A., Varki, N. M., Appelt, K., 1999. Broad antitumor and antiangiogenic activities of AG3340, a potent and selective MMP inhibitor undergoing advanced oncology clinical trials. Ann. N.Y. Acad. Sci. 878, 236-270.

Sharp, P.A. 2001. RNA interference. Genes Dev. 15: 485-490.

Sharrocks, A. D., Brown, A. L., Ling, Y., Yates, P. R., 1997. The ETS-domain transcription factor family. Int. J. Biochem. Cell Biol. 29, 1371-1387.

Shaunak, S., Thomas, S., Gianasi, E., Godwin, A., Jones, E., Teo, I., Mireskandari, K., Luthert, P., Duncan, R., Patterson, S., Khaw, P., Brocchini, S. 2004. Polyvalent dendrimer glucosamine conjugates prevent scar tissue formation. Nat Biotechnol. 22 (8): 977-984

Sheridan, C. M., Occleston, N. L., Hiscott, P., Kon, C. H., Khaw, P. T., Grierson, I., 2001. Matrix metalloproteinases: a role in the contraction of vitreo-retinal scar tissue. Am. J. Pathol. 159, 1555-1566.

Shields, J. A., 1977. Current approaches to the diagnosis and management of choroidal melanomas. Surv. Ophthalmol. 21, 443-463.

Shields, J. A., Shields, C. L., Donoso, L. A., 1991. Management of posterior uveal melanoma. Surv. Ophthalmol. 36, 161-195.

Shields, M. B., 1992. Textbook of Glaucoma. Baltimore, Williams & Wilkins.

Shipley, J. M., Doyle, G. A., Fliszar, C. J., Ye, Q. Z., Johnson, L. L., Shapiro, S. D., Welgus, H. G., Senior, R. M., 1996. The structural basis for the elastolytic activity of the 92-kDa and 72-kDa gelatinases. Role of the fibronectin type II-like repeats. J. Biol. Chem. 271, 4335-4341.

Shuman, M. A., Polansky, J. R., Merkel, C., Alvarado, J. A., 1988. Tissue plasminogen activator in cultured human trabecular meshwork cells. Predominance of enzyme over plasminogen activator inhibitor. Invest. Ophthalmol. Vis. Sci. 29, 401-405.

Siegwart, J. T., Jr., Norton, T. T., 2001. Steady state mRNA levels in tree shrew sclera with form-deprivation myopia and during recovery. Invest. Ophthalmol. Vis. Sci. 42, 1153-1159.

Siegwart, J. T., Jr., Norton, T. T., 2005. Selective regulation of MMP and TIMP mRNA levels in tree shrew sclera during minus lens compensation and recovery. Invest. Ophthalmol. Vis. Sci. 46, 3484-3492.

Siegwart, J. T., Jr., Norton, T. T., 2002. The time course of changes in mRNA levels in tree shrew sclera during induced myopia and recovery. Invest. Ophthalmol. Vis. Sci. 43, 2067-2075.

Sivak, J. M., Mohan, R., Rinehart, W. B., Xu, P. X., Maas, R. L., Fini, M. E., 2000. Pax-6 expression and activity are induced in the re-epithelializing cornea and control activity of the transcriptional promoter for matrix metalloproteinase gelatinase B. Dev. Biol. 222, 41-54.

Sivak, J. M., West-Mays, J. A., Yee, A., Williams, T., Fini, M. E., 2004. Transcription Factors Pax6 and AP-2alpha Interact To Coordinate Corneal Epithelial Repair by Controlling Expression of Matrix Metalloproteinase Gelatinase B. Mol. Cell. Biol. 24, 245-257.

Siwik, D. A., Chang, D. L., Colucci, W. S., 2000. Interleukin-1 beta and tumor necrosis factor-alpha decrease collagen synthesis and increase matrix metalloproteinase activity in cardiac fibroblasts *in vitro*. Circ. Res. 86, 1259-1265.

Skiles, J. W., Gonnella, N. C., Jeng, A. Y., 2001. The design, structure, and therapeutic application of matrix metalloproteinase inhibitors. Curr. Med. Chem. 8, 425-474.

Skuta, G. L., Beeson, C. C., Higginbotham, E. J., Lichter, P. R., Musch, D. C., Bergstrom, T. J., Klein, T. B., Falck, F. Y., Jr., 1992. Intraoperative mitomycin versus postoperative 5-fluorouracil in high-risk glaucoma filtering surgery. Ophthalmology, 99, 438-444.

Smine, A., Plantner, J. J., 1997. Membrane type-1 matrix metalloproteinase in human ocular tissues. Curr. Eye Res. 16, 925-929.

Smith, M. R., Kung, H., Durum, S. K., Colburn, N. H., Sun, Y., 1997. TIMP-3 induces cell death by stabilizing TNF-alpha receptors on the surface of human colon carcinoma cells. Cytokine. 9, 770-780.

Smith, V. A., Easty, D. L., 2000. Matrix metalloproteinase 2: involvement in keratoconus. Eur. J. Ophthalmol. 10, 215-226.

Smith, V. A., El-Rakhawy, A., Easty, D. L., 2001. Matrix metalloproteinase 2 activation in cultured corneas. Ophthalmic Res. 33, 1-6.

Smith, V. A., Hoh, H. B., Littleton, M., Easty, D. L., 1995. Over-expression of a gelatinase A activity in keratoconus. Eye 9 (Pt 4), 429-433.

Smith, V. A., Matthews, F. J., Majid, M. A., Cook, S. D., 2006. Keratoconus: matrix metalloproteinase-2 activation and TIMP modulation. Biochim. Biophys. Acta, 1762, 431-439.

Smith, V. A., Rishmawi, H., Hussein, H., & Easty, D. L., 2001. Tear film MMP accumulation and corneal disease. Br. J. Ophthalmol. 85, 147-153.

Solomon, A., Dursun, D., Liu, Z., Xie, Y., Macri, A., Pflugfelder, S. C., 2001. Pro- and anti-inflammatory forms of interleukin-1 in the tear fluid and conjunctiva of patients with dry-eye disease. Invest. Ophthalmol. Vis.Sci. 42, 2283-2292.

Somerville, R. P., Oblander, S. A., Apte, S. S., 2003. Matrix metalloproteinases: old dogs with new tricks. Genome Biol. 4, 216.

Song, E., Zhu, P., Lee, S. K., Chowdhury, D., Kussman, S., Dykxhoorn, D. M. *et al.* 2005. Antibody mediated *in vivo* delivery of small interfering RNAs via cell-surface receptors. Nat Biotech. 23: 709–717.

Song, X. J., Li, D. Q., Farley, W., Luo, L. H., Heuckeroth, R. O., Milbrandt, J., Pflugfelder, S. C., 2003. Neurturin-deficient mice develop dry eye and keratoconjunctivitis sicca. Invest. Ophthalmol. Vis. Sci. 44, 4223-4229.

Sorsby, A., 1949. Genetically determined ocular lesions simulating inflammatory reactions. Acta Neurol. Psychiatr. Belg. 49, 611.

Sounni, N. E., Noel, A., 2005. Membrane type-matrix metalloproteinases and tumor progression. Biochimie, 87, 329-342.

Spaeth, G. L., Rodrigues, M. M., Weinreb, S., 1977. Steroid-induced glaucoma: A. Persistent elevation of intraocular pressure B. Histopathological aspects. Trans. Am. Ophthalmol. Soc. 75, 353-381.

Springman, E. B., Angleton, E. L., Birkedal-Hansen, H., Van Wart, H. E., 1990. Multiple modes of activation of latent human fibroblast collagenase: evidence for the role of a Cys73 active-site zinc complex in latency and a "cysteine switch mechanism for activation. Proc. Natl. Acad. Sci. U.S.A. 87, 364-368.

Steely, H. T., Browder, S. L., Julian, M. B., Miggans, S. T., Wilson, K. L., Clark, A. F., 1992. The effects of dexamethasone on fibronectin expression in cultured human trabecular meshwork cells. Invest. Ophthalmol. Vis. Sci. 33, 2242-2250.

Steen, B., Sejersen, S., Berglin, L., Seregard, S., Kvanta, A., 1998. Matrix metalloproteinases and metalloproteinase inhibitors in choroidal neovascular membranes. Invest. Ophthalmol. Vis. Sci. 39, 2194-2200.

Steffensen, B., Hakkinen, L., Larjava, H., 2001. Proteolytic events of wound-healing coordinated interactions among matrix metalloproteinases (MMPs), integrins, and extracellular matrix molecules. Crit. Rev. Oral Biol. Med. 12, 373-398.

Stein MP, et al. C-reactive protein binding to FcgammaRIIa on human monocytes and neutrophils is allele-specific. *J Clin Invest.* 2000;105: 369–376.

Sternlicht, M. D., Werb, Z., 2001. How matrix metalloproteinases regulate cell behavior. Annu. Rev. Cell Dev. Biol. 17, 463-516.

Stetler-Stevenson, W. G., Aznavoorian, S., Liotta, L. A., 1993. Tumor cell interactions with the extracellular matrix during invasion and metastasis. Annu. Rev. Cell Biol. 9, 541-573.

Steuhl, K. P., Doring, G., Henni, A., Thiel, H. J., Botzenhart, K., 1987. Relevance of host-derived and bacterial factors in Pseudomonas aeruginosa corneal infections. Invest. Ophthalmol. Vis. Sci. 28, 1559-1568.

Streilein, J. W., Dana, M. R., Ksander, B. R., 1997. Immunity causing blindness: five different paths to herpes stromal keratitis. Immunol. Today. 18, 443-449.

Strissel, K. J., Rinehart, W. B., Fini, M. E., 1995. A corneal epithelial inhibitor of stromal cell collagenase synthesis identified as TGF-beta 2. Invest. Ophthalmol. Vis. Sci. 36, 151-162.

Strissel, K. J., Rinehart, W. B., Fini, M. E., 1997. Regulation of paracrine cytokine balance controlling collagenase synthesis by corneal cells. Invest. Ophthalmol. Vis. Sci. 38, 546-552.

Sun, C. C., Cheng, C. Y., Chien, C. S., Pang, J. H., Ku, W. C., Chen, P. Y., Yang, C. M., 2005. Role of matrix metalloproteinase-9 in ex vivo expansion of human limbal epithelial cells cultured on human amniotic membrane. Invest. Ophthalmol. Vis. Sci. 46, 808-815.

Suzuki, T., Sullivan, D. A., 2005. Estrogen stimulation of pro-inflammatory cytokine and matrix metalloproteinase gene expression in human corneal epithelial cells. Cornea 24, 1004-1009.

Swallow, C. J., Murray, M. P., Guillem, J. G., 1996. Metastatic colorectal cancer cells induce matrix metalloproteinase release by human monocytes Clin. Exp. Metastasis 14, 3-11.

Tabara, H., Sarkissian, M., Kelly, W.G., Fleenor, J., Grishok, A., Timmons, L., *et al* 1999. The rde-1 gene, RNA interference, and transposon silencing in *C. elegans*. *Cell* 99:123–132.

Tabata, Y., Isashiki, Y., Kamimura, K., Nakao, K., Ohba, N., 1998. A novel splice site mutation in the tissue inhibitor of the metalloproteinases-3 gene in Sorsby's fundus dystrophy with unusual clinical features. Hum. Genet. 103, 179-182.

Takahashi, T., Nakamura, T., Hayashi, A., Kamei, M., Nakabayashi, M., Okada, A. A., Tomita, N., Kaneda, Y., Tano, Y., 2000. Inhibition of experimental choroidal

neovascularization by overexpression of tissue inhibitor of metalloproteinases-3 in retinal pigment epithelium cells. Am. J. Ophthalmol. 130, 774-781.

Tamiya, S., Wormstone, I. M., Marcantonio, J. M., Gavrilovic, J., Duncan, G., 2000. Induction of matrix metalloproteinases 2 and 9 following stress to the lens. Exp. Eye Res. 71, 591-597.

Tan, H. K., Heywood, D., Ralph, G. S., Bienemann, A., Baker, A. H., Uney, J. B., 2003. Tissue inhibitor of metalloproteinase 1 inhibits excitotoxic cell death in neurons. Mol. Cell Neurosci. 22, 98-106.

Tang, S., Scheiffarth, O. F., Thurau, S. R., Wildner, G., 1993. Cells of the immune system and their cytokines in epiretinal membranes and in the vitreous of patients with proliferative diabetic retinopathy. Ophthalmic Res. 25, 177-185.

Tang, S., Scheiffarth, O. F., Wildner, G., Thurau, S. R., Lund, O. E., 1992. Lymphocytes, macrophages and HLA-DR expression in vitreal and epiretinal membranes of proliferative vitreoretinopathy. An immunohistochemical study. Ger J. Ophthalmol. 1, 176-179.

Taraboletti, G., Sonzogni, L., Vergani, V., Hosseini, G., Ceruti, R., Ghilardi, C., Bastone, A., Toschi, E., Borsotti, P., Scanziani, E., Giavazzi, R., Pepper, M. S., Stetler-Stevenson, W. G., Bani, M. R., 2000. Posttranscriptional stimulation of endothelial cell matrix metalloproteinases 2 and 1 by endothelioma cells. Exp. Cell Res. 258, 384-394.

Tebes, S.J., Kruk, P.A.. 2005. The genesis of RNA interference, its potential clinical applications, and implications in gynecologic cancer. Gynecol. Oncol. 99: 736-41.

Thakur, A., Xue, M., Stapleton, F., Lloyd, A. R., Wakefield, D., Willcox, M. D., 2002. Balance of pro- and anti-inflammatory cytokines correlates with outcome of acute experimental Pseudomonas aeruginosa keratitis. Infect. Immun. 70, 2187-2197.

The Fluorouracil Filtering Surgery Study Group. Fluorouracil Filtering Surgery Study one-year follow-up. Am J Ophthalmol. 1989; 108:625–635.

Thiel, H. J., Steuhl, K. P., Doring, G., 1987. Therapy of Pseudomonas aeruginosa eye infections. Antibiot. Chemother. 39, 92-101.

Thomas, J., Gangappa, S., Kanangat, S., Rouse, B. T., 1997. On the essential involvement of neutrophils in the immunopathologic disease: herpetic stromal keratitis. J. Immunol. 158, 1383-1391.

Thomas, J., Rouse, B. T., 1997. Immunopathogenesis of herpetic ocular disease. Immunol. Res. 16, 375-386.

Ticho, U., Lahav, M., Berkowitz, S., Yoffe, P., 1979. Ocular changes in rabbits with corticosteroid-induced ocular hypertension. Br. J. Ophthalmol, 63, 646-650.

Tripathi, B. J., Millard, C. B., Tripathi, R. C., 1990. Corticosteroids induce a sialated glycoprotein (Cort-GP) in trabecular cells *in vitro*. Exp. Eye Res. 51, 735-737.

Tripathi, B. J., Tripathi, R. C., Yang, C., Millard, C. B., Dixit, V. M., 1991. Synthesis of a thrombospondin-like cytoadhesion molecule by cells of the trabecular meshwork. Invest. Ophthalmol. Vis. Sci. 32, 181-188.

Tschumper, R. C., Johnson, D. H., 1990. Trabecular meshwork cellularity. Differences between fellow eyes. Invest. Ophthalmol. Vis. Sci. 31, 1327-1331.

Twining, S. S., Kirschner, S. E., Mahnke, L. A., Frank, D. W., 1993. Effect of Pseudomonas aeruginosa elastase, alkaline protease, and exotoxin A on corneal proteinases and proteins. Invest. Ophthalmol. Vis. Sci. 34, 2699-2712.

Uekita, T., Itoh, Y., Yana, I., Ohno, H., Seiki, M., 2001. Cytoplasmic tail-dependent internalization of membrane-type 1 matrix metalloproteinase is important for its invasion-promoting activity. J. Cell. Biol. 155, 1345-1356.

Ullian, E. M., Barkis, W. B., Chen, S., Diamond, J. S., Barres, B. A., 2004. Invulnerability of retinal ganglion cells to NMDA excitotoxicity. Mol. Cell Neurosci. 26, 544-557.

United States Pharmacopoeia (USP) 2000. Sterilization and sterility assurance of compendial articles. In The
United States Pharmacopoeia. Data file released in Pharmacopeial Convention, Rockville, MD.

Unemori, E. N., Hibbs, M. S., Amento, E. P., 1991. Constitutive expression of a 92-kD gelatinase (type V collagenase) by rheumatoid synovial fibroblasts and its induction in normal human fibroblasts by inflammatory cytokines. J. Clin. Invest. 88,1656-1662.

Uprichard, S.L. 2005. The therapeutic potential of RNA interference. FEBS Lett. 579: 5996-6007.

Uzui, H., Harpf, A., Liu, M., Doherty, T. M., Shukla, A., Chai, N. N., Tripathi, P. V., Jovinge, S., Wilkin, D. J., Asotra, K., Shah, P. K., Rajavashisth, T. B., 2002. Increased expression of membrane type 3-matrix metalloproteinase in human atherosclerotic plaque: role of activated macrophages and inflammatory cytokines. Circulation 106, 3024-3030.

Vaisanen, A., Kallioinen, M., von, D. K., Laatikainen, L., Hoyhtya, M., Turpeenniemi-Hujanen, T., 1999. Matrix metalloproteinase-2 (MMP-2) immunoreactive protein - a new prognostic marker in uveal melanoma? J. Pathol. 188, 56-62.

Valtanen, H., Lehti, K., Lohi, J., Keski-Oja, J., 2000. Expression and purification of soluble and inactive mutant forms of membrane type 1 matrix metalloproteinase. Protein Expr. Purif.19, 66-73.

Van Buskirk, E. M., 1989. Pathophysiology of laser trabeculoplasty. Surv. Ophthalmol. 33, 264-272.

Van Ess, H. H., Arts, G. J. 2005. Biology calls the targets: combining RNAi and disease biology. Drug Discov. Today 10: 1385-91.

Van Wart, H. E., Birkedal-Hansen, H., 1990. The cysteine switch: a principle of regulation of metalloproteinase activity with potential applicability to the entire matrix metalloproteinase gene family. Proc. Natl. Acad. Sci. U.S.A 87, 5578-5582.

Varela, H. J., Hernandez, M. R., 1997. Astrocyte responses in human optic nerve head with primary open-angle glaucoma. J. Glaucoma 6, 303-313.

Vassalli, J. D., Sappino, A. P., Belin, D., 1991. The plasminogen activator/plasmin system. J. Clin. Invest. 88, 1067-1072.

Velasco, G., Cal, S., Merlos-Suarez, A., Ferrando, A. A., Alvarez, S., Nakano, A., Arribas, J., Lopez-Otin, C., 2000. Human MT6-matrix metalloproteinase: identification, progelatinase A activation, and expression in brain tumors. Cancer Res. 60, 877-882.

Velasco, G., Pendas, A. M., Fueyo, A., Knauper, V., Murphy, G., Lopez-Otin, C., 1999. Cloning and characterization of human MMP-23, a new matrix metalloproteinase predominantly expressed in reproductive tissues and lacking conserved domains in other family members. J. Biol. Chem. 274, 4570-4576.

Visse, R., Nagase, H., 2003. Matrix metalloproteinases and tissue inhibitors of metalloproteinases: structure, function, and biochemistry. Circ. Res. 92, 827-839.

Vranka, J. A., Johnson, E., Zhu, X., Shepardson, A., Alexander, J. P., Bradley, J. M., Wirtz, M. K., Weleber, R. G., Klein, M. L., Acott, T. S., 1997. Discrete expression and distribution pattern of TIMP-3 in the human retina and choroid. Curr. Eye Res. 16, 102-110.

Vu, T., Werb, Z., 1998. Gelatinase B: Structure, Regulation and Function. In Matrix Metalloproteinases, W. Parks & R. Mecham, eds. San Diego, Academic Press, pp. 15-42.

Vu, T. H., Shipley, J. M., Bergers, G., Berger, J. E., Helms, J. A., Hanahan, D., Shapiro, S. D., Senior, R. M., Werb, Z., 1998. MMP-9/gelatinase B is a key regulator of growth plate angiogenesis and apoptosis of hypertrophic chondrocytes. Cell 93, 411-422.

Vu, T. H., Werb, Z. 2000. Matrix metalloproteinases: effectors of development and normal physiology. Genes Dev. 14, 2123-2133.

Wallace, G. R., Whiston, R. A., Stanford, M. R., Wells, G. M., Gearing, A. J., Clements, J. M., 1999. The matrix metalloproteinase inhibitor BB-1101 prevents experimental autoimmune uveoretinitis (EAU). Clin. Exp. Immunol. 118, 364-370.

Wang, X., Jung, J., Asahi, M., Chwang, W., Russo, L., Moskowitz, M. A., Dixon, C. E., Fini, M. E., Lo, E. H., 2000. Effects of matrix metalloproteinase-9 gene knock-out on morphological and motor outcomes after traumatic brain injury. J. Neurosci., 20, 7037-7042.

Wax, M. B., Tezel, G., Kobayashi, S., Hernandez, M. R., 2000. Responses of different cell lines from ocular tissues to elevated hydrostatic pressure. Br. J. Ophthalmol. 84, 423-428.

Weber, B. H., Vogt, G., Pruett, R. C., Stohr, H., Felbor, U., 1994a. Mutations in the tissue inhibitor of metalloproteinases-3 (TIMP3) in patients with Sorsby's fundus dystrophy. Nat. Genet. 8, 352-356.

Weber, B. H., Vogt, G., Wolz, W., Ives, E. J., Ewing, C. C., 1994b. Sorsby's fundus dystrophy is genetically linked to chromosome 22q13-qter. Nat.Genet. 7, 158-161.

Webster, L., Chignell, A. H., Limb, G. A., 1999. Predominance of MMP-1 and MMP-2 in epiretinal and subretinal membranes of proliferative vitreoretinopathy. Exp. Eye Res. 68, 91-98.

Weinreb, R. N., 2001. Enhancement of scleral macromolecular permeability with prostaglandins. Trans. Am. Ophthalmol. Soc. 99, 319-343.

Weinreb, R. N., Kashiwagi, K., Kashiwagi, F., Tsukahara, S., Lindsey, J. D., 1997. Prostaglandins increase matrix metalloproteinase release from human ciliary smooth muscle cells. Invest Ophthalmol Vis.Sci. 38, 2772-2780.

Weinreb, R. N., Lindsey, J. D. 2002. Metalloproteinase gene transcription in human ciliary muscle cells with latanoprost. Invest Ophthalmol Vis. Sci., 43, 716-722.

Weinreb, R. N., Lindsey, J. D., Marchenko, G., Marchenko, N., Angert, M., Strongin, A., 2004. Prostaglandin FP agonists alter metalloproteinase gene expression in sclera. Invest. Ophthalmol. Vis. Sci. 45, 4368-4377.

Weinreb, R. N., Zangwill, L., 1997. Reproducibility of nerve fiber layer thickness measurements. Ophthalmology 104, 1530-1531.

Welgus, H. G., Jeffrey, J. J., Stricklin, G. P., Eisen, A. Z., 1982. The gelatinolytic activity of human skin fibroblast collagenase. J. Biol. Chem. 257, 11534-11539.

West-Mays, J. A., Sadow, P. M., Tobin, T. W., Strissel, K. J., Cintron, C., Fini, M. E. 1997. Repair phenotype in corneal fibroblasts is controlled by an interleukin-1 alpha autocrine feedback loop. Invest. Ophthalmol. Vis. Sci. 38, 1367-1379.

West-Mays, J. A., Strissel, K. J., Sadow, P. M., Fini, M. E., 1995. Competence for collagenase gene expression by tissue fibroblasts requires activation of an interleukin 1 alpha autocrine loop. Proc. Natl. Acad. Sci. U.S.A. 92, 6768-6772.

Williams, R., Airey, M., Baxter, H., Forrester, J., Kennedy-Martin, T., Girach, A. 2004. Epidemiology of diabetic retinopathy and macular oedema: a systematic review. Eye 18, 963-983.

Williamson, R. A., Marston, F. A., Angal, S., Koklitis, P., Panico, M., Morris, H. R., Carne, A. F., Smith, B. J., Harris, T. J., Freedman, R. B., 1990. Disulphide bond assignment in human tissue inhibitor of metalloproteinases (TIMP) Biochem. J. 268, 267-274.

Witty, J. P., Wright, J. H., Matrisian, L. M., 1995. Matrix metalloproteinases are expressed during ductal and alveolar mammary morphogenesis, and misregulation of stromelysin-1 in transgenic mice induces unscheduled alveolar development. Mol. Biol. Cell. 6, 1287-1303.

Woessner, J., 1998. Matrilysin. In Handbook of Proteolytic Enzymes, A. Barrett, N. Rawlings, J. Woessner, eds. Academic Press, London, 1183-1187.

Woessner, J. F., Jr., 1991. Matrix metalloproteinases and their inhibitors in connective tissue remodeling. FASEB J. 5, 2145-2154.

Wong, T. T., Daniels, J. T., Crowston, J. G., Khaw, P. T., 2004. MMP inhibition prevents human lens epithelial cell migration and contraction of the lens capsule. Br. J. Ophthalmol, 88, 868-872.

Wong, T. T., Mead, A. L., Khaw, P. T., 2003. Matrix metalloproteinase inhibition modulates postoperative scarring after experimental glaucoma filtration surgery. Invest. Ophthalmol. Vis. Sci. 44, 1097-1103.

Wong, T. T., Mead, A. L., Khaw, P. T., 2005. Prolonged antiscarring effects of ilomastat and MMC after experimental glaucoma filtration surgery. Invest. Ophthalmol. Vis. Sci. 46, 2018-2022.

Wong, T. T., Sethi, C., Daniels, J. T., Limb, G. A., Murphy, G., Khaw, P. T., 2002. Matrix metalloproteinases in disease and repair processes in the anterior segment. Surv. Ophthalmol, 47, 239-256.

Wormstone, I. M., Tamiya, S., Anderson, I., Duncan, G., 2002. TGF-beta 2-induced matrix modification and cell transdifferentiation in the human lens capsular bag. Invest. Ophthalmol. Vis. Sci. 43, 2301-2308.

Worthen, D. M., Cleveland, P. H., 1982. Fibronectin production by cultured human trabecular meshwork cells. Invest. Ophthalmol. Vis. Sci. 23, 265-269.

Xu, J., Rodriguez, D., Petitclerc, E., Kim, J. J., Hangai, M., Moon, Y. S., Davis, G. E., Brooks, P. C., 2001. Proteolytic exposure of a cryptic site within collagen type IV is required for angiogenesis and tumor growth *in vivo*. J. Cell Biol., 154, 1069-1079.

Xue, M. L., Wakefield, D., Willcox, M. D., Lloyd, A. R., Di, G. N., Cole, N., Thakur, A., 2003. Regulation of MMPs and TIMPs by IL-1beta during corneal ulceration and infection. Invest. Ophthalmol. Vis. Sci. 44, 2020-2025.

Yamaoka, A., Matsuo, T., Shiraga, F., Ohtsuki, H., 2001. TIMP-1 production by human scleral fibroblast decreases in response to cyclic mechanical stretching. Ophthalmic Res. 33, 98-101.

Yan, X., Tezel, G., Wax, M. B., Edward, D. P., 2000. Matrix metalloproteinases and tumor necrosis factor alpha in glaucomatous optic nerve head. Arch. Ophthalmol, 118, 666-673.

Yang, M., Murray, M. T., Kurkinen, M., 1997. A novel matrix metalloproteinase gene (XMMP) encoding vitronectin-like motifs is transiently expressed in Xenopus laevis early embryo development. J. Biol. Chem. 272, 13527-13533.

Yang, Y. N., Bauer, D., Wasmuth, S., Steuhl, K. P., Heiligenhaus, A., 2003. Matrix metalloproteinases (MMP-2 and 9) and tissue inhibitors of matrix metalloproteinases (TIMP-1 and 2) during the course of experimental necrotizing herpetic keratitis. Exp.Eye Res. 77, 227-237.

Yazama, F., Kadonosono, K., Itoh, N., Ohno, S., 2002. Role of matrix metalloproteinase-7 in angiogenesis associated with age-related macular degeneration. J. Electron Microsc. (Tokyo) 51, 127-131.

Ye, H. Q., Azar, D. T., 1998. Expression of gelatinases A and B, and TIMPs 1 and 2 during corneal wound healing. Invest. Ophthalmol. Vis. Sci. 39, 913-921.

Ye, H. Q., Maeda, M., Yu, F. S., Azar, D. T., 2000. Differential expression of MT1-MMP (MMP-14) and collagenase III (MMP-13) genes in normal and wounded rat corneas. Invest. Ophthalmol. Vis. Sci. 41, 2894-2899.

Yu, W. H., Yu, S., Meng, Q., Brew, K., Woessner, J. F., Jr., 2000. TIMP-3 binds to sulfated glycosaminoglycans of the extracellular matrix. J. Biol. Chem. 275, 31226-31232.

Yue, B. Y., Sugar, J., Benveniste, K., 1984. Heterogeneity in keratoconus: possible biochemical basis. Proc. Soc. Exp. Biol. Med. 175, 336-341.

Yue, B. Y., Sugar, J., Benveniste, K., 1985. RNA metabolism in cultures of corneal stromal cells from patients with keratoconus. Proc. Soc. Exp. Biol. Med. 178, 126-132.

Zahedi, K.. 1996. Characterization of the binding of serum amyloid P to type IV collagen. *J. Biol. Chem. 271:14897.*

Zahedi, K. 1997. Characterization of the binding of serum amyloid P to laminin. *J. Biol. Chem. 272:2143.*

Zeng, Y., Yi, R., Cullen, B.R. 2005. Recognition and cleavage of primary microRNA precursors by the nuclear processing enzyme Drosha. *EMBO J.* 24: 138–148.

Zervos, E. E., Norman, J. G., Gower, W. R., Franz, M. G., Rosemurgy, A. S., 1997. Matrix metalloproteinase inhibition attenuates human pancreatic cancer growth *in vitro* and decreases mortality and tumorigenesis *in vivo*. J. Surg. Res. 69, 367-371.

Zhan, G. L., Camras, C. B., Opere, C., Tang, L., Ohia, S. E., 1998. Effect of prostaglandins on cyclic AMP production in cultured human ciliary muscle cells. J. Ocul. Pharmacol. Ther. 14, 45-55.

Zhang, X., Cheng, M., Chintala, S. K., 2004a. Kainic acid-mediated upregulation of matrix metalloproteinase-9 promotes retinal degeneration. Invest Ophthalmol Vis. Sci. 45, 2374-2383.

Zhang, X., Cheng, M., Chintala, S. K., 2004b. Optic nerve ligation leads to astrocyte-associated matrix metalloproteinase-9 induction in the mouse retina", Neurosci.Lett. 356, 140-144.

Zhao, X., Ramsey, K. E., Stephan, D. A., Russell, P., 2004. Gene and protein expression changes in human trabecular meshwork cells treated with transforming growth factor-beta. Invest. Ophthalmol. Vis. Sci. 45, 4023-4034.

Zheng, M., Deshpande, S., Lee, S., Ferrara, N., Rouse, B. T., 2001. Contribution of vascular endothelial growth factor in the neovascularization process during the pathogenesis of herpetic stromal keratitis. J. Virol. 75, 9828-9835.

Zhou, L., Sawaguchi, S., Twining, S. S., Sugar, J., Feder, R. S., Yue, B. Y., 1998. Expression of degradative enzymes and protease inhibitors in corneas with keratoconus. Invest. Ophthalmol. Vis. Sci. 39, 1117-1124.

Zimmerman, L. E., 1980. Metastatic disease from uveal melanomas. A review of current concepts with comments concerning future research and prevention. Trans. Ophthalmol. Soc. U.K. 100, 34-54.

Zucker, S., Conner, C., DiMassmo, B. I., Ende, H., Drews, M., Seiki, M., Bahou, W. F. 1995. Thrombin induces the activation of progelatinase A in vascular endothelial cells. Physiologic regulation of angiogenesis. J. Biol. Chem., 270, 23730-23738.

Zucker, S., Pei, D., Cao, J., Lopez-Otin, C. 2003. Membrane type-matrix metalloproteinases (MT-MMP). Curr. Top. Dev. Biol. 54, 1-74.